

Use of the model yeast *Saccharomyces cerevisiae* to study the regulation of RNA processing enzyme, Rex1, and as a chassis for the development of biotechnological hosts

Quentin Levicky

*This thesis is submitted to the University of Sheffield for
the degree of Doctor of Philosophy*



**University of
Sheffield**

Faculty of Science
School of Biosciences

September 2023

Abstract

Saccharomyces cerevisiae (*S. cerevisiae*) is the most extensively studied eukaryote. It has been substantially used in research to elucidate many molecular mechanisms and as a host for heterologous genes. In this study, we have used *S. cerevisiae* as a model for studying the regulation of the rRNA processing enzyme, Rex1, in response to stress. Simultaneously we have explored the potential of using *S. cerevisiae* as a host for expression of a fungal glycolipid biosynthetic pathway.

Eukaryotic cells are characterised by their sub-cellular compartmentalisation. This cellular segregation offers opportunities for specialised metabolic pockets as well as for metabolic regulation through altering the sub-cellular localisation of proteins. Additionally, cellular compartmentalisation can be used biotechnologically for targeting specialist metabolism to an organelle for biotechnological production, such as in the peroxisome.

Rex1 is a nuclear 3' exonuclease implicated in the processing of 5S rRNA and numerous species of tRNA. Cells exposed to heat stress temperatures show a pre-tRNA processing phenotype akin to *rex1Δ* cells. The implication of this is that Rex1 activity is downregulated in response to heat stress.

This thesis describes two means of regulating Rex1 activity. In cells exposed to heat stress Rex1 is degraded by proteasome complexes and is delocalised from the nucleus where its substrates are found. Through *in vivo* phospholabelling, we have demonstrated that Rex1 is phosphorylated in response to heat stress and this may be required to regulate Rex1 degradation. Additionally, we have identified a nuclear localisation signal in the N-terminal of Rex1.

Mannosylerythritol lipids (MELs) are fungal glycolipids with promising biosurfactant activity. Native producers are maize pathogens that require specific growth conditions and produce additional undesirable glycolipids. There is industrial demand for pure MELs, incentivising the production of MELs in a heterologous host. *S. cerevisiae* has been a model system for heterologous gene expression and for biotechnological manufacture. Here we have demonstrated an impressive capacity for heterologous gene expression in *S. cerevisiae* through the heterologous expression of the 5-gene MEL biosynthetic cluster. We used nuclear magnetic resonance (NMR) and mass spectrometry to verify expression of the gene cluster and to explore limitations of foreign gene expression.

Acknowledgments

I would like to extend my deepest gratitude to my supervisors, Dr Phil Mitchell and Dr Ewald Hetteema, for their boundless patience and enthusiasm when it came to discussing and encouraging my research. Their immense drive, knowledge and attention to detail has repeatedly allowed me to look deeper at generated data and learn to extract more information from it.

I would additionally like to thank all members of the E28 laboratory, particularly Dr Donald Watts, Dr Vijay Raghavendran, Dr Georgia Hulmes, Dr Sondos Alhajouj and Dr Selva Turkolmez, who greatly facilitated my introduction into full time lab work. Additionally I extend my thanks to Pete, Yousef, Abdullaziz, Tarad, Ibrahim and Hunouf who were there to offer support, discuss science and be great colleagues over many challenging periods.

I would like to thank my mum for her infinite support. I also extend my gratitude to Keir, Ewan and Dennis, our adventures have always channelled my focus.

Over the course of these studies, I have found the scientific community at large to be helpful and interesting. A great many people facilitate research and make it a pleasant place to work. I am thankful to all those who welcomed or facilitated my life at university.

Contents

Contents

Chapter 1 – Introduction.....	14
1.1 RNA Transcription and processing.....	14
1.1.1 Background	14
1.1.2 RNA pol III transcription.....	16
1.1.3 Stress and tRNA processing	20
1.1.3.1 CCA addition and stress response.....	21
1.1.3.2 tRNA modifications and stress response	21
1.1.3.3 tRNA subcellular localisation and stress response	22
1.1.4 Rex1 is a 3' exonuclease which catalyses the maturation of RNA pol III transcripts.....	23
1.1.5 Protein degradation in response to stress.....	24
1.1.6.1 Nuclear localisation of proteins	26
1.1.6.2 Nuclear localisation signals	27
1.1.7.1 Rex1 and ribosome biogenesis	16
1.1.7.2 Ribosome biogenesis in response to stress	29
1.8 Biotechnology	32
1.8.1 Biotechnological chemical manufacture.....	32
1.9 Biosurfactants	32
1.10 Host organisms.....	33
1.11 Biosurfactant gene clusters.....	33
1.12 MEL biosynthetic pathway.....	36
1.13 Heterologous gene expression	39
1.14 The use of promoters/terminators in optimising gene expression	42
1.15 Downstream processes.....	43
1.16 Aims and objectives	44
Chapter 2 - Materials and methods.....	45
2.1 Chemicals and enzymes	45
2.2 Growth media	45
2.2.1 Generic growth media	45
2.2.2 Phosphate depleted YPD.....	48
2.3 Strains and plasmids	49
2.3.1 Strains	49

2.3.2 <i>E. coli</i>	50
2.3.3 Plasmids	50
2.4 Long term storage of organisms	53
2.5 <i>S. cerevisiae</i> molecular biology protocols	53
2.5.1 Growth and maintenance of <i>S. cerevisiae</i> strains.....	53
2.5.2 One-step transformation	53
2.5.3 High efficiency yeast transformation	53
2.5.4 Isolation of yeast genomic DNA.....	54
2.5.5 <i>in vivo</i> ³² P phospholabelling and protein extraction.....	54
2.5.6 SDS-PAGE	55
2.5.7 Alkaline protein lysis	56
2.5.8 Protein analysis by western blot.....	56
2.5.9 Protein extraction for analysis by mass-spectrometry	56
2.5.10 Fluorescence microscopy.....	56
2.5.10 Heat shock assays	57
2.5.11 <i>S. cerevisiae</i> mating	57
2.6 <i>Escherichia coli</i> protocols.....	57
2.6.1 Growth and maintenance of <i>E. coli</i>	57
2.6.2 Transformation of chemically competent <i>E. coli</i>	57
2.6.3 Transformation of electrocompetent <i>E. coli</i>	57
2.6.4 Production of chemically competent <i>E. coli</i>	58
2.6.5 Production of electrocompetent <i>E. coli</i>	58
2.7 DNA procedures.....	59
2.7.1 Polymerase chain reaction.....	59
2.7.2 Primer Design.....	60
2.7.3 Gel electrophoresis	64
2.7.4 DNA gel extraction	65
2.7.5 Plasmid extraction from <i>E. coli</i>	65
2.7.6 Restriction digestion	65
2.7.7 DNA sequencing.....	65
2.7.8 DNA Ligation	65
2.7.9 Assembly of DNA fragments from oligos	65
2.7.10 Homologous recombination based cloning	67
2.7.11 5-FOA counterselection mediated gene integration	67
2.8 MEL analysis.....	69
2.8.1 MEL extraction	69

2.8.2 MEL analysis by nuclear magnetic resonance.....	69
Chapter 3 - Rex1 contains an N-terminal NLS and is phosphorylated and delocalised in response to heat stress.....	70
3.1 Introduction	70
3.2 The NLS of Rex1 is found within amino acid 17-52.....	70
3.3 Rex1 is imported into the nucleus through the action of the yeast importin- α , Srp1.....	73
3.4 Rex1 is depleted in response to heat stress	75
3.5 Rex1 is delocalised from the nucleus in response to heat stress under native regulation	80
3.6 Plasmid vs chromosomal Rex1 expression	82
3.7 Rex1 shows numerous stability associated phosphorylation sites within its NLS.....	86
3.9 Non-phosphorylatable Rex1 resists degradation in response to heat stress	89
3.10 Heat stress associated Rex1 degradation is proteasome mediated.....	91
3.11 Rex1 is phosphorylated in response to heat shock	92
3.12 Phosphorylation-associated degradation of Rex1 is not directly associated with the TOR pathway	93
3.13 Bioinformatic tools do not identify a phosphodegron motif in Rex1 protein sequence.....	97
3.14 Discussion.....	97
Chapter 4 Heterologous expression of the MEL biosynthetic pathway in <i>S. cerevisiae</i>	100
4.1 Introduction	100
4.2 Heterologous expression of <i>U. maydis</i> proteins shows correct sub-cellular localisation in <i>S. cerevisiae</i>	101
4.2.1 Cloning of MEL biosynthesis genes and expressing them as GFP fusion proteins	101
4.2.2 <i>U. maydis</i> MEL biosynthetic proteins localise correctly within <i>S. cerevisiae</i>	102
4.3 Expression of 5 genes simultaneously in <i>S. cerevisiae</i>	107
4.3.1 Development of a modular gene expression system	107
4.3.2 A novel approach to the production strain.....	109
4.4 Cell culture for the production of MELs.....	112
4.4.1 Cells expressing the gene cluster reach higher optical density on lipid-enriched media..	112
4.4.2 NMR analysis of cell supernatant and pellet extracts.....	113
4.5 Proteomics to validate protein expression in production strains.....	118
4.7 Discussion.....	122
Chapter 5 – Discussion.....	123
5.1 Introduction	123
5.2.1 Rex1 is part of nuclear delocalisation heat shock effect	123
5.2.2 Stress induced protein degradation.....	123
5.2.3 Alternative stressors	124

5.2.4 Alternative Rex1 degradation pathways/alternative phosphorylation	125
5.2.5 The role of ubiquitination in Rex1 stability	125
5.2.6 Plasmid vs chromosomally expressed Rex1 stability	126
5.2.7 Rex1 phosphorylation status in response to heat shock	126
5.3 Biosynthetic MEL production.....	126
5.3.1 Alternate enzymes in the cluster required for its function	126
5.3.2 Microscopy data was not representative of genetic context in production strains.....	127
5.3.3 Variations in MEL pathway protein expression level.....	128
5.3.4 Extraction efficiency.....	128
References	129

Abbreviations

5-FOA – 5-Fluoroorotic acid

CHX – Cycloheximide

DNA – Deoxyribonucleic acid

ER –Endoplasmic reticulum

ETS – External transcribed spacer

GFP – Green fluorescent protein

ITS – Internal transcribed spacer

LiAc – Lithium acetate

LSU – Large subunit

LTR – Long tandem repeat

MEL – Mannosylerythritol lipid

mRNA – Messenger ribonucleic acid

NLS – Nuclear localisation signal

NMR – Nuclear magnetic resonance

OD – Optical density

ORF - Open reading frame

PCR – Polymerase chain reaction

Pol – Polymerase

PTM – Post translational modification

PTS1 – Peroxisomal targeting signal 1

rDNA – rRNA gene

RNA – Ribonucleic acid

rRNA – Ribosomal RNA

RNP – Ribonucleoparticle

snRNP – Small nucleolar ribonucleoparticle

snRNA – Small nuclear RNA

SSU – Small subunit

TBP – TATA binding protein

tDNA – Transfer RNA gene

tRNA – Transfer RNA

VIP – Very important primer

YCp – Yeast chromosomal plasmid

YEp – Yeast episomal plasmid

List of figures

Chapter 1

- 1.1 Schematic of 35S rRNA processing in yeast
- 1.2 5S RNP processing by Rex1
- 1.3 tRNA synthesis and processing
- 1.4 tRNA processing in response to stress
- 1.5 Schematic of Rex1 NLS
- 1.6 Mechanisms of protein degradation in yeast
- 1.7 Schematic of Srp1 mediated nuclear import
- 1.8 Regulation of rRNA transcription by TORC1
- 1.9 Schematic of MEL biosynthetic gene cluster
- 1.10 Schematic of MEL biosynthetic pathway in *U. maydis*
- 1.11 Stimulated marker excision through homologous recombination
- 1.12 Schematic of Cre recombinase mediated marker excision

Chapter 2

- 2.1 Schematic detailing assembly of DNA fragments from oligos
- 2.2 Schematic detailing 5-FOA mediated counterselection strategy

Chapter 3

- 3.1 An NLS is found between Rex1 17-52
- 3.2 α -GFP western blot on GFP-rex1 truncations demonstrates intact fusion proteins
- 3.3 Rex1 nuclear import is Srp1 mediated
- 3.4 Rex1 is delocalised from the nucleus and depleted at 39°C
- 3.5 Plasmid expressed GFP-Rex1 is delocalised from the nucleus and depleted at 39°C
- 3.6 Rex1 is depleted in cells at 39°C
- 3.7 Rex1 protein is unstable at 39°C
- 3.8 Plasmid expressed pRRP4:zz-Rex1 is depleted at 39°C
- 3.9 Plasmid expressed zz-Rex1 is unstable in CHX treated heat-stressed cells
- 3.10 Rex1 levels remain constant in cells moved to glycerol media
- 3.11 Plasmid expressed Rex1 is 5x overexpressed compared to integrated allele
- 3.12 Schematic of *REX1* promoters used in this study
- 3.13 p*REX1::GFP-Rex1* is delocalised from the nucleus at 39°C
- 3.14 1kb *REX1* promoter does not upregulate transcription
- 3.15 Phosphomimetic and non-phosphorylatable Rex1 *nls* constructs are imported to the nucleus
- 3.16 Full length phosphomimetic and non-phosphorylatable Rex1 are imported into the nucleus.
- 3.17 Non-phosphorylatable plasmid expressed GFP-Rex1 is more stable under heat stress

- 3.18 Non-phosphorylatable plasmid expressed Rex1 is expressed at higher levels at 30°C
- 3.19 Non-phosphorylatable Rex1 shows resistance to heat stress induced depletion
- 3.20 Integrated non-phosphorylatable Rex1 is expressed at higher levels than phosphomimetic Rex1
- 3.21 Proteasome inhibition stabilises Rex1 in heat-stressed cells
- 3.22 Rex1 is phosphorylated in response to heat stress
- 3.23 Rapamycin treated cultures show faster Rex1 depletion when heat stressed
- 3.24 200nM rapamycin inhibits yeast growth
- 3.25 4hr rapamycin incubation increases speed of Rex1 depletion under heat stress
- 3.26 Model for heat stress induced Rex1 regulation

Chapter 4

- 4.1 *MAC2* cloning without introns
- 4.2 *U. maydis* MEL biosynthesis genes show correct subcellular localisation in *S. cerevisiae*
- 4.3 *MAC1* and *MAC2* colocalise with peroxisomes in *S. cerevisiae*
- 4.4 MEL biosynthetic fusion proteins are correct size in *S. cerevisiae*
- 4.5 Schematic showing modular gene expression system design
- 4.6 Inconsistent gene expression from modular gene expression system
- 4.7 New approach to MEL biosynthetic gene cluster cloning
- 4.8 *EMT1* and *MAC2* gene integration and Cre-lox mediated marker excision
- 4.9 PCR validation of *MMF1* integration
- 4.10 MEL biosynthetic strain reach higher OD on lipid media
- 4.11 NMR analysis of MEL controls
- 4.12 2D NMR shows MEL production in *M. antarcticus*
- 4.13 No detectable MEL production in MEL biosynthetic *S. cerevisiae*
- 4.14 Proteomics detects MEL enzymes in *S. cerevisiae*
- 4.15 *MMF1* is only expressed in 5-gene strain

List of Tables

1.1 Function of gene in MEL biosynthetic pathway	35
1.2 Structure and variation of MELs.....	37
2.1 Media used in this study.....	45
2.2 Yeast strains used in this study.....	49
2.3 <i>E. coli</i> strains used in this study.....	50
2.4 Plasmid vectors used in this study.....	50
2.5 Plasmids used in this study.....	51
2.6 SDS acrylamide gel composition.....	55
2.7 Buffers for making chemically competent <i>E. coli</i>	58
2.8 PCR reaction set up.....	59
2.9 PCR cycling conditions.....	60
2.10 Primers used in this study.....	60
4.1 Heterologous MEL expression regulatory sequences.....	106
4.2 MEL detection through NMR in producing strains.....	112

Preface

It should be noted that the work conducted in this thesis is dichotomous in nature. Due to numerous unforeseen circumstances including the COVID-19 pandemic and changes to staff at the University of Sheffield I ended up working on two projects using the budding yeast *Saccharomyces cerevisiae* (*S. cerevisiae*). One project studying regulatory mechanisms of the RNA pol III transcript-maturing enzyme, Rex1, and one working on reconstituting a 5-gene fungal biosynthetic pathway in *S. cerevisiae*.

Chapter 1 – Introduction

1.1 RNA Transcription and processing

1.1.1 Background

Most stable RNAs in the cell are transcribed as a longer form and are processed through the action of exo- and endonucleases to yield a mature transcript. This occurs in coding mRNAs but as well as in the variety of non-coding RNAs required for functions including ribosome biogenesis, tRNA synthesis intron splicing and RNAi, among an increasing amount of other cellular functions (Yan *et al*, 2019, Suzuki *et al*, 2021, Bergeron *et al*, 2023, Neumeier & Meister, 2021). Eukaryotic transcription is conducted by three RNA polymerase complexes dubbed RNA pol I, II & III, additional polymerases are found in mitochondria and chloroplasts (Hess & Borner, 1999, Tracy & Stern, 1995). Each RNA pol complex is tailored to the transcription of a specific subset of genes (Brown, 2002). In prokaryotic cells, RNA transcription is typically carried out by a single RNA polymerase composed of three subunits, (Myer & Young, 1998, Darst, 2001).

In the model yeast *Saccharomyces cerevisiae* (*S. cerevisiae*) all protein coding genes are transcribed by RNA polymerase II, yielding mRNA. This process involves numerous additional enzymes and enzyme-complexes involved in regulating transcription as well as modifying the mRNA. These include 5' capping enzymes, 3' cleavage and polyadenylation systems (Shatkin & Manley, 2000). 5' capping occurs to the nascent mRNA when as few as 25-30 nucleotides are incorporated into the transcript (Furuichi, 2015). It is known that mRNA capping and adenylation are essential for stability and to enhance translation rates. mRNA can 'circularize' to enhance translation, resulting from interactions between the cap and the poly-A tail, demonstrating the importance of RNA modifications for translation (Wells *et al*, 1998). Links between decapping and deadenylation leading to mRNA degradation demonstrate that these modifications are also used to stimulate mRNA degradation. Factors enhancing capping and polyadenylation are known to interact with RNA pol II, demonstrating that these modifications are integral to the mature mRNA product and that cells have evolved to ensure correct modification occurs promptly post-transcription.

RNA pol I is dedicated solely to the transcription of the 35S ribosomal RNA (rRNA), the processing of which yield three of the four rRNAs (fig. 1.1). 35S rRNA undergoes extensive processing. It is cleaved by both exo- and endonucleases, as well as recruiting snoRNPs for base modification prior to further maturation (Kufel *et al*, 1999). The 35S rDNA gene is encoded up to 200 times on yeast chromosome XII, adjacent to it on the opposing strand is the 5S rDNA gene that is transcribed by RNA pol III. Despite extensive repeats along the chromosome, electron microscopy has demonstrated that it is rare for more than 70 of these genes to be transcribed at a given moment (French *et al*, 2008).

Ribosome biogenesis occurs in yeast at a tremendous rate, rRNA accounts for ~80% of total cellular RNA, while up to 50% of RNA pol II transcription events are thought to initiate the synthesis of proteins associated with ribosome biogenesis (Warner, 1999). Unsurprisingly, this process is tightly regulated. The ribosome is a complex machine, composed of two subunits containing 4 rRNAs and ~79 proteins in eukaryotes. While the specific structure of the ribosome varies between prokaryotes and eukaryotes, many of its features are conserved and ribosomes universally contain a large subunit and a small subunit. The yeast large subunit, or 60S, contains 3 rRNAs, the 5.8S, the 5S and the 25S, whereas the 40S small subunit (SSU), contains only the 18S rRNA (Woolford Jnr & Baserga, 2013). While the exact function of the 5S rRNA in the ribosome has not been elucidated, it is essential and is thought to stabilise the ribosome's structure. The 5S rRNA is found in almost all ribosomes except the mitochondrial ribosomes of some fungi and animals.

35S processing involves numerous enzymes and catalytic steps. Many of these steps show redundancy, being processed by multiple pathways. The more prominent steps are co-transcriptional cleavage of the nascent 35S rRNA, which removes the 5' ETS (fig. 1.1). Utp24 is associated with cleavage in ITS1, liberating the 20S pre-rRNA and the 27S-A₃ pre-rRNA (Wells *et al*, 2016, Bleichert *et al*, 2006). The 20S pre-rRNA is then exported to the cytoplasm where its 3' end is exonucleolytically cleaved by Nob1, yielding the mature transcript. This was shown through co-sedimentation of Nob1-TAP alongside 20S rRNA in fractions associated with the 40S ribosomal subunit. Additionally 20S rRNA was pulled down alongside affinity purified Nob1-TAP (Fatica *et al*, 2003). The excised 27S-A₃ transcript is processed at the 5' end by Rat1 or Rrp17, and 3' end processing is catalysed by Rex1 (Kempers-Veenstra *et al*, 1986). The 27S rRNA is cleaved in the ITS2 by Las1. This was shown through the accumulation of extended 25S rRNA in a time course of cells expressing pGAL-LAS1 shifted from galactose to glucose media (Schillewaert *et al*, 2011). This processing exposes and the 5' end of the 25S rRNA which is processed by Rat1 prior to export of the 60S pre-ribosome to the cytosol where the 3' end of 5.8S rRNA is processed by Ngl2 (Thomson & Tollervey, 2010). This was observed using FISH where fluorescent probes targeting 7S rRNA yielded a cytosolic signal in WT cells that was not apparent in cells incapable of exporting 60S ribosomal subunits. Furthermore, blocking 60S export to the cytoplasm resulted in cells with low levels of mature 5.8S rRNA, indicating that this final maturation is cytosolic (Thomson & Tollervey, 2010).

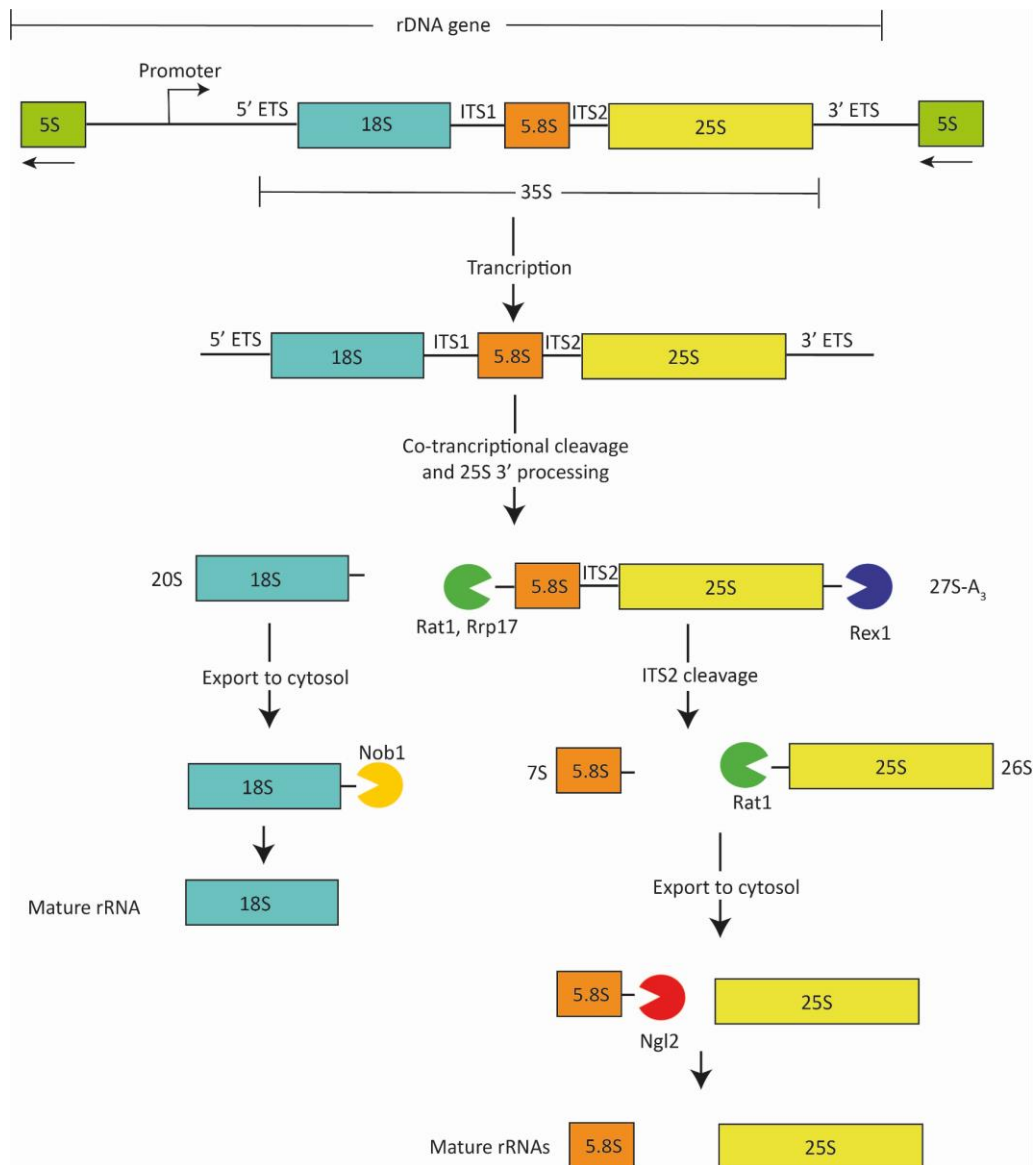


Figure 1.1. Shown is a schematic for an rDNA gene in yeast. The yeast rDNA gene encodes the 5S rRNA and the 35S pre-rRNA which are transcribed from opposing strands. The 35S precursor rRNA is then processed through the action of exo- and endonucleases, as well as snRNP complexes to yield mature 18S, 5.8S and 25S rRNA. The entire gene is duplicated up to 200 times on chromosome XII of yeast. An overview of some of the key 35S processing steps is shown. The 5' ETS is co-transcriptionally cleaved and endonucleolytic cleavage takes place in the ITS1. The 20S is exported to the cytosol where its 3' end is exonucleolytically removed by Nob1. Simultaneously Rat1 and Rrp17 remove the 5' end of the 27S-A₃ rRNA while Rex1 is implicated in removal of the 3' ETS. Subsequently, ITS2 is cleaved. 5.8S rRNA is yielded through 3' exonucleolytic processing of the 7S rRNA in the cytosol by Ngl2. Rat1 removes the 5' end of the 26S rRNA, leaving mature 25S.

1.1.2 Rex1 and ribosome biogenesis

Rex1 is the exonuclease responsible for the 3' maturation of 5S rRNA in yeast; this involves the removal of several nucleotides from the 3' end of the 5S rRNA (Piper *et al*, 1983, van Hoof *et al*, 2000). The synthesis of 5S rRNA is linked to ribosome biogenesis, a process with great energetic demands. Ribosome prevalence is such that the major fraction of total cellular RNA/protein is composed of ribosomal proteins and RNA (Shore & Albert, 2022, Warner, 1999). As Rex1 is involved in the processing of ribosomal components, it is plausible that factors affecting ribosome synthesis would regulate Rex1.

In yeast, the majority of RNA pol III transcripts, including the 5S rRNA, are transcribed and bound to Lhp1, a non-ribosomal protein acting as an RNA chaperone (Pannone *et al*, 1998). Shortly thereafter, Lhp1 is displaced by ribosomal proteins L11 and L5 to form a stable ribonucleoparticle that can be recruited to pre-ribosomes (fig. 1.2). This is the only case of an rRNA binding to ribosomal proteins prior to incorporation into the ribosome (Ciganda & Williams, 2011). The bond between 5S rRNA and L11 forms rapidly after 5S transcription and the ribonucleoparticle is thought to be the actual Rex1 substrate (Daniels *et al*, 2022).

1.1.3 RNA pol III transcription

tRNA, 5S rRNA and some snRNA are products of RNA pol III transcription. RNA pol III transcripts share common multi-subunit transcription factors, TFIIIB and TFIIIC while 5S genes recruit an additional transcription factor TFIIIA. TFIIIA binds to 5S genes through several zinc finger domains (Milne & Segall, 1993). TFIIIA, TFIIIB and TFIIIC bind to the genes transcribed by RNA pol III as well as to nascent RNA pol III transcripts, acting as an RNA chaperone (Rudt & Pieler, 1996, Szymanski *et al*, 2003). Shared transcription factors may indicate synchronised transcriptional regulation. Conditions affecting TFIIIA, B or C recruitment would globally affect RNA pol III transcription. It has been observed that TFIIIB globally downregulates the recruitment of RNA pol III in response to DNA damage through UV irradiation or the addition of methane methylsulfonate (Ghavidel & Schultz, 2001).

Besides shared transcription factors, RNA pol III is globally downregulated by Maf1 in yeast (Pluta *et al*, 2001, Vorlander *et al*, 2018). Inhibition of RNA pol III activity is thought to occur as Maf1 outcompetes TFIIIB in the pre-initiation complex (Vorlander *et al*, 2020). Maf1 is localised to the cytosol but is dephosphorylated to trigger nuclear import where it inhibits RNA pol III transcription. This occurs upon a shift to non-favourable growth conditions as found in stationary phase cells and when shifted to non-fermentable carbon sources (Roberts *et al*, 2006). Yeast grown at 37°C, a heat-stress inducing temperature, do not experience Maf1 dephosphorylation (Ciesla *et al*, 2007, Boissard *et al*, 2009, Moir *et al*, 2006). Maf1 activity is linked to various effects across model systems, in mice it has been observed that altering Maf1 activity through gene deletion or overexpression alters bone density and osteoblast formation (Phillips *et al*, 2022). Alongside shared regulation by Maf1, all transcripts of RNA pol III associate with the La protein, a ubiquitous protein required for RNA folding and processing (Wolin & Cedervall, 2002).

While RNA pol III transcripts contain shared transcription factors, the identification of a TATA box in the promoter of *SNR6*, a pol III transcribed gene, indicates the evolutionary conservation between the RNA polymerase complexes (Margottin *et al*, 1991). TATA boxes are a common feature of RNA pol II recruiting promoters. They are recognised by TATA binding protein (TBP) and recruit RNA pol II machinery. Later studies demonstrated that TBP is common at sites of RNA pol III transcription, where it rarely dissociates from promoter regions (Acker *et al*, 2013). This shared regulation between RNA

pol II and pol III is interesting as it shows that mRNA and rRNA/tRNA/snRNA synthesis may share common regulatory factors or a common evolutionary heritage. An implication of this could be that RNA pol II and III share a common ancestor and the use of TBP evolved as a regulator in RNA pol II transcribed genes but not in those transcribed by RNA pol III.

5S rRNA processing is a relatively simple process. The 5S rRNA is transcribed with an extended 3' end. From this end 7-10 nucleotides are removed by the action of the 3' exonuclease Rex1 to yield the mature 5S. 5S rRNA remains functional in the extended form (van Hoof *et al*, 2000). It should be observed that in *rex1Δ* cells an extended 5S is found but it remains partially processed compared to the initial transcript. Nascent 5S interacts with the La protein, Lhp1 in yeast, a non-ribosomal RNA chaperone. The 5S/Lhp1 interaction is transient and Lhp1 is quickly replaced with ribosomal protein L5 (Madru *et al*, 2015, Ciganda & Williams, 2011). Subsequently L11 is recruited to the complex to form a ribonucleoprotein (RNP). This RNP is incorporated into pre-ribosomes, however there is evidence that when the 5S RNP is not incorporated into ribosomes it interacts with the human Mdm2 protein associated with cell proliferation or apoptosis pathways (de Estrada *et al*, 2023). This indicates that under conditions in which ribosome assembly is interrupted, ribosomal components can be involved in regulating alternative cellular functions. Whether these mechanisms are universally conserved is unsure, in *E. coli* mutants lacking free 5S but instead expressing a 23S-5S conjugate remain viable and translationally active but accumulate non-functional 50S ribosomal subunits (Huang *et al*, 2020). The implication of this is that free 5S is required for functional ribosome assembly. *In vitro* analysis found that recombinant Rex1 is capable of processing the 3' end of the yeast 5S RNP (Daniels *et al*, 2022) (fig. 1.2), due to the rapid formation of the 5S RNP in yeast it is likely that the RNP is the Rex1 substrate *in vivo*. The regulation of Rex1 activity will be a major focus of this thesis.

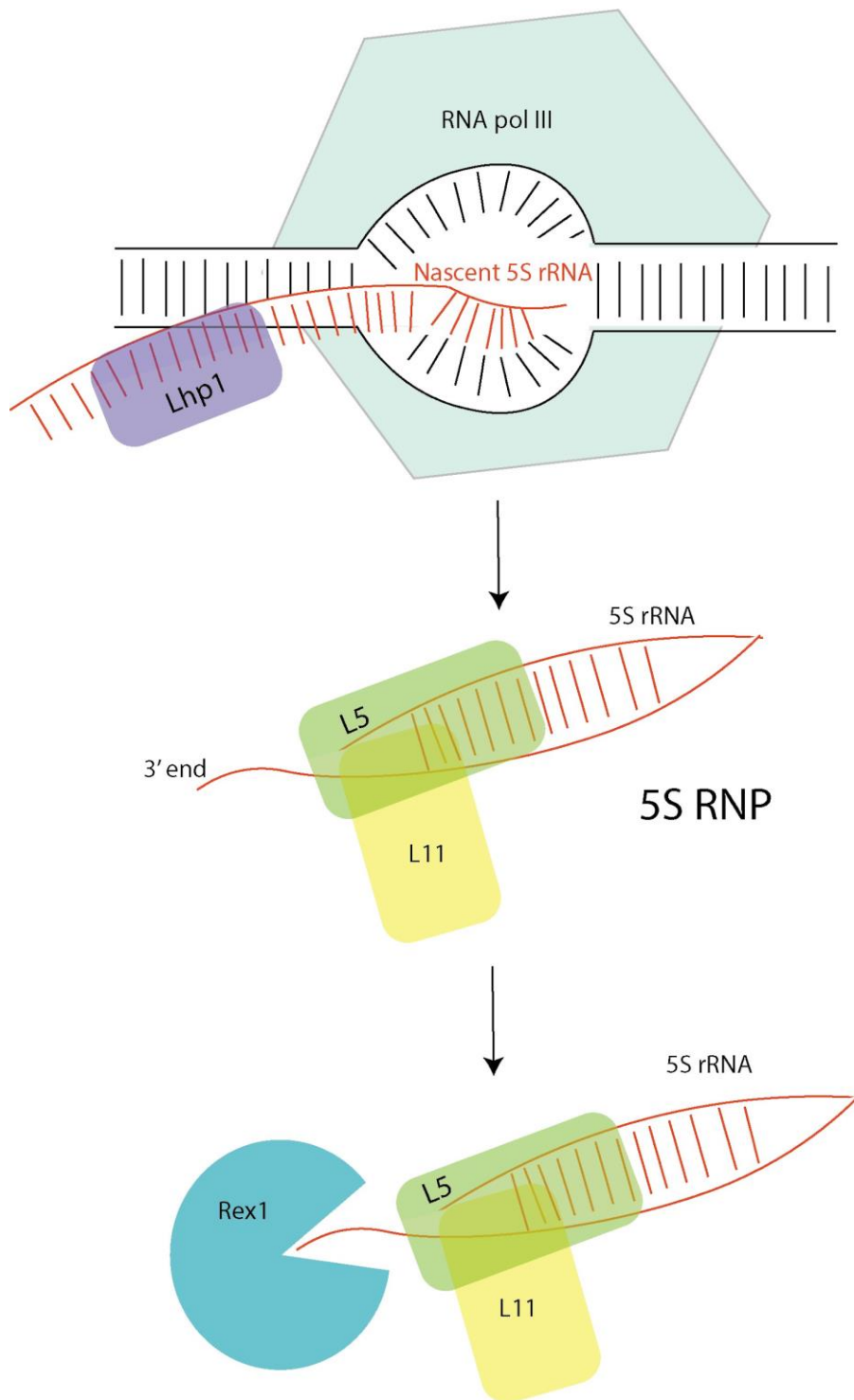


Figure 1.2. Nascent 5S RNA recruits Rpl5 and Rpl11 to form a Rex1-processed RNP. As 5S rRNA is transcribed, it experiences a transient interaction with Lhp1 prior to binding L5 and L11 to form an RNP with an exposed 3' end. These exposed nucleotides are trimmed by Rex1.

tRNA processing is more complex than 5S rRNA maturation. Yeast contain 274 tRNA genes composed of 42 varieties (Hani & Feldman, 1998), all transcribed by RNA pol III. The discrepancy between the 61

codons recognised by just 42 tRNAs is explained by the promiscuity of the wobble base. Meaning a single tRNA can recognise multiple codons. Post transcription, all tRNAs are processed and heavily modified to yield a mature product. There is lots of variation in tRNA processing across tRNA species (reviewed in Hopper, 2013). Some are transcribed directly and others are transcribed as dimers separated by a spacer. In these instances, the spacer must be cleaved prior to tRNA processing. tRNA act as signalling molecules and are found throughout the cell.

All tRNAs are transcribed with a poly-U tail of varying length. This tail is important for the interaction between tRNA and the La protein, (Maraia & Lamichhane, 2011). The La protein is a tRNA chaperone that protects the tRNA from exonuclease-associated degradation (Copela *et al*, 2006, Maraia *et al*, 2017). This process is thought to be mediated by Rpc11, a component of RNA pol III (Landrieux *et al*, 2006). A poly-U tail of a certain length is required for interaction between tRNA and La. tRNAs with an insufficient poly-U tail are processed through alternate pathways (Maraia & Lamichhane, 2011).

Approximately 20% of yeast tRNAs contain an intron, requiring splicing prior to maturation. While tRNA are transcribed in the nucleus, splicing takes place in the cytosol and all known tRNA splicing enzymes in yeast are known to have additional functions (Dhungel & Hopper, 2012). tRNA bases are heavily modified, to the extent that up to 15% of tRNA bases are thought to be an alternative to the canonical C, G, A or U. These modifications are important for translation fidelity and quality control.

Initial tRNA processing begins with 5' leader and 3' trailer cleavage (Chamberlain *et al*, 1998, Takaku *et al*, 2003). Subsequently a 3' terminal CCA is added, this is essential for amino acid attachment and for interaction with the ribosome (Tamura, 1994). 3' CCA addition is universal amongst tRNA, though separate tRNA species have their own specific modifications such as the addition of a 5' G to HIS tRNA (Gu *et al*, 2003).

Initial 5' leader cleavage is mediated by RNase P, a ubiquitous endonuclease (Nichols *et al*, 1988). 3' trailer cleavage is more complex, being performed both endonucleolytically by the yeast RNase Z, Trz1 and exonucleolytically by Rex1 (Skowronek *et al*, 2014). While Trz1 is typically thought to be dominant in tRNA 3' trailer cleavage, select tRNAs including LYS^{UUU}, LEU^{CUU}, ILE^{UAU}, TYR^{GUA} and MET^{AUG} are processed at the 3' trailer by Rex1 (Foretek *et al*, 2016, Skowronek *et al*, 2013, Ozanick *et al*, 2009).

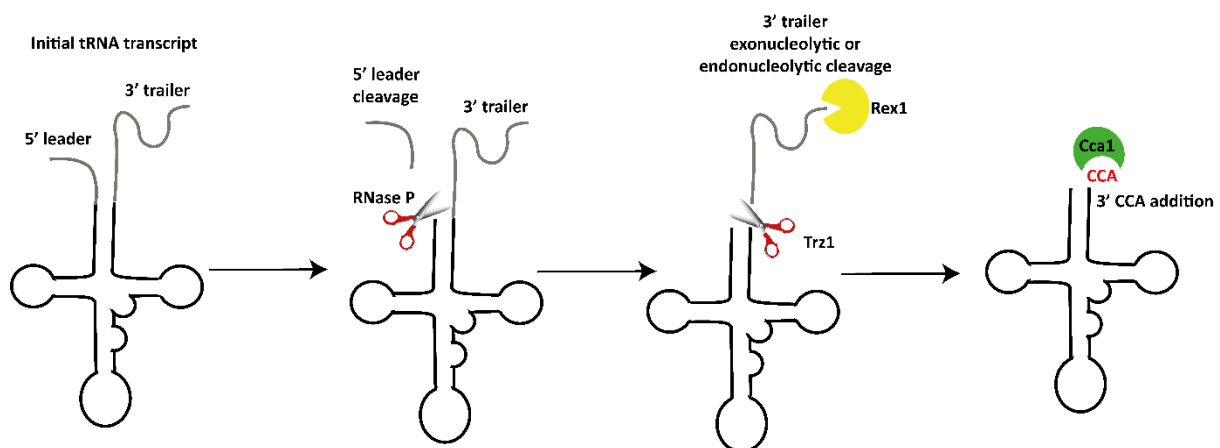


Figure 1.3. tRNA synthesis and processing. Shown is a schematic displaying the enzymatic steps in tRNA processing. Initially 5' leader cleavage is performed by RNase P. Subsequently the 3' trailer is removed exo- or endonucleolytically by Trz1 or Rex1. Finally, Cca1 adds the 3' terminal CCA, facilitating amino-acylation.

As products of RNA pol III transcription, tRNAs initially bind the La protein, Lhp1 in yeast. This binding is known to affect tRNA processing as select tRNAs bound to Lhp1 are known to be protected from Rex1 mediated 3' end processing. In these instances, tRNA:Lhp1 have been found to be endonucleolytically processed by Trz1 (Yoo & Woolin, 1997).

1.1.4 Stress and tRNA processing

The numerous steps between pre-tRNA transcripts and mature tRNA opens opportunities for regulated responses. tRNAs are implicated in many biological responses beyond translation including phospholipid modification (Ernst & Peschel, 2011), cell signalling (Murray *et al*, 1998) and non-ribosomal peptide bond formation (Fonvielle *et al*, 2009). These processes must be regulated to ensure efficient flux through metabolic pathways and to prevent runaway metabolism. tRNAs are extensively modified, these modifications are implicated in folding and stability. Additionally, yeast mutants lacking t⁶A tRNA modification showed severe growth defects and increased sensitivity to heat, salt and ethanol (Thiaville *et al*, 2016). This modification is adjacent to but not within the anticodon loop, though is thought to be associated with the decoding of numerous codons. A lack of this modification is associated with translation of unstable aggregated protein resulting in many cellular sensitivities. There are two known turnover pathways for degradation of incompletely modified tRNAs (reviewed in Hopper, 2013). In one pathway, hypomodified tRNA are 3' polyadenylated by Trf4 and subsequently degraded by the exosome from the 3' to 5' end (Kadaba *et al*, 2004, 2006). Trf4 is a non-canonical poly(A) polymerase which is recruited into the TRAMP complex. This heterotrimeric complex associates with the nuclear exosome where it enhances substrate specificity (Schmidt & Butler, 2013). Alternatively, hypomodified tRNAs can be degraded in a 5' to 3' direction through the rapid tRNA decay pathway (RTD). The 5' -> 3' exonucleases Rat1 and Xrn1 are implicated in this process (Chernyakov *et al*, 2008).

1.1.4.1 CCA addition and stress response

Numerous examples of alterations to tRNA regulation in response to stress have been observed. 3' CCA addition is essential for tRNA aminoacylation and subsequent translation (Tamura, 1994). HeLa cells exposed to arsenite, an oxidative stress inducer, responded with rapid removal of 3' CCA from tRNA (Czech *et al*, 2013). This represses mRNA translation and reduces growth, possibly to protect the cell from synthesizing proteins at a time when oxidation risks their integrity. Transferal to media lacking arsenite rapidly restored the 3' CCA allowing a rapid return to normal growth. This shows that 3' CCA addition can act to regulate tRNA activity with regard to mRNA translation, while being used to adjust growth in response to environmental stimuli. However, in mammalian cells extended exposure to oxidative stress conditions results in tRNA endonucleolytic cleavage at the anticodon loop (Fu *et al*, 2009), demonstrating the induction of distinct pathways mediating tRNA stress responses depending on the extent of the stress. 3' CCA addition has been linked to additional regulatory activity, with CCA nucleotidyltransferase enzymes showing polymerase activity when extending hypomodified tRNA. In these instances hypomodified tRNA have a 3' CCACCA added (fig. 1.4). The double CCA is recognised as a degradation tag and these transcripts are depleted (Wilusz *et al*, 2011). This example shows the modularity of enzymes in performing multiple functions and stresses the demand for quality control in tRNA synthesis. The mechanism behind this was elucidated in *Archaeoglobus fulgidus* where it was found that unstable tRNAs were able to interact with the CCA adding enzyme twice, inducing two

rounds of CCA addition, whereas stable tRNAs were unable to be recruited a second time (Betat & Mörl, 2015).

1.1.4.2 tRNA modifications and stress response

tRNA bases are heavily modified, in yeast 25 unique modifications have been found on 36 bases (reviewed in Phizicky & Hopper, 2010). Some of these modifications are simple methylations but others are multi-step processes. 10-20% of tRNA bases are commonly modified. The function of these modifications can be implied by their location on the tRNA but range from translation efficiency, codon fidelity and facilitating correct tRNA structure and folding (Edwards *et al*, 2020).

Under elevated temperatures, numerous tRNA modifications are adjusted (Han *et al*, 2015, Alings *et al*, 2015), including a decrease in pseudouridylation in the anti-codon loop (Han *et al*, 2015). This altered modification decreases the activity of certain tRNAs and is thought to be a growth regulator under stress conditions. It was identified that newly synthesized tRNA lacked thiolated bases at position 34 ($mcm^5s^2U_{34}$) at elevated temperatures due to altered expression of tRNA modifying enzymes (Alings *et al*, 2015). In yeast strain W303 and S288C it was shown that the cells progressively showed decreasing amounts of the $mcm^5s^2U_{34}$ modification when grown at temperatures increasing from 30°C to 39°C though this was not associated with a specific growth phenotype at any permissive temperature (Alings *et al*, 2015). These examples demonstrate a link between environmental conditions and tRNA condition within the cell.

Similarly, yeast exposed to H_2O_2 showed an increase in tRNA modifications m^5C and M^2G (Chan *et al*, 2010). This effect was not replicated through the addition of alternative oxidative stressors methylmethane sulfonate, arsenite or hypochlorite. This indicates that these altered modifications are specific to H_2O_2 . Knocking out the enzymes mediating these modifications resulted in hypersensitivity to H_2O_2 (Chan *et al*, 2010). Similarly, it was shown that in the bacteria *Pseudomonas aeruginosa* the enzyme TrmB, involved in modifying a subset of tRNAs rich in tRNAs aminoacylated with Phe and Asp is upregulated in response to H_2O_2 stress. This is interesting as catalase is rich in Phe and Asp, and it is thought that the upregulation of TrmB activity in response to H_2O_2 is an adaptation to increase synthesis of proteins protecting the cell from increased oxidative stress (Thongdee *et al*, 2019). These example demonstrates the importance of tRNA modification and shows the specific responses evolved to deal with varying environmental conditions.

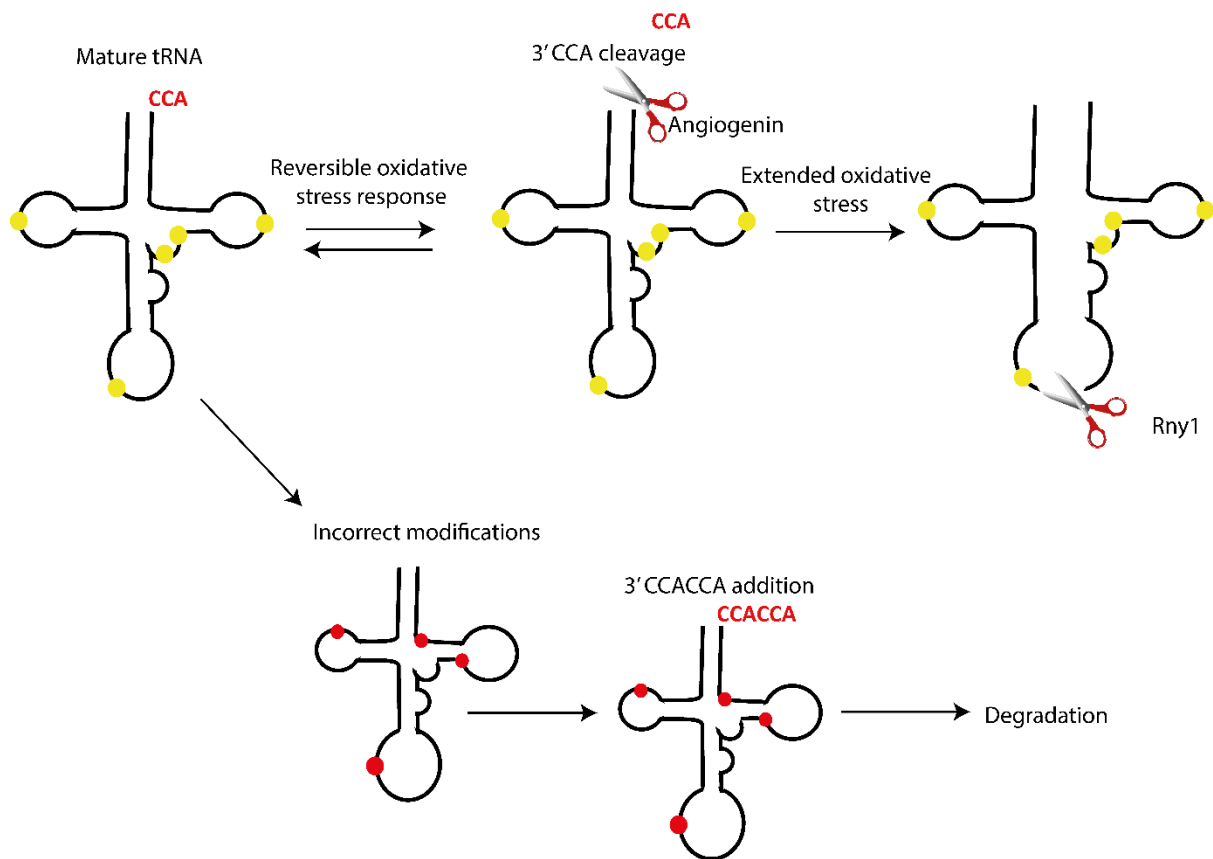


Figure. 1.4. tRNA phenotypes in response to stress. Schematic shows two regulatory tRNA mechanisms. Short-term exposure to oxidative stress tRNA activity is reduced through removal of the 3' CCA. Extended exposure results in tRNA endonucleolytic cleavage by Rny1. Incorrectly modified tRNA are identified and tagged for degradation through addition of a 3' CCACCA tag.

1.1.4.3 tRNA subcellular localisation and stress response

tRNAs are synthesized in the nucleus, the 5' leader and 3' trailer cleaved. Subsequently tRNAs are cytoplasmically exported, spliced, modified and reimported into the nucleus where they undergo additional quality control (Kramer & Hopper, 2013) prior to re-export to the cytoplasm (reviewed in Chatterjee *et al*, 2018). Under nutrient stress, tRNAs rapidly accumulate in the nucleus (Whitney *et al*, 2007). Analysis of tRNA forms accumulated in the nucleus indicates that tRNA cytosolic re-export is inhibited. This effect is pronounced upon glucose starvation but not under amino acid stress. Interestingly, under conditions inducing tRNA nuclear accumulation two nuclear proteins associated with tRNA export are found in the cytosol, Los1 and Msn5. The implication is that these proteins are involved with tRNA re-export (Ghavidel *et al*, 2007, Quan *et al*, 2007, Pierce *et al*, 2014) and that by translocating them to the cytosol they are unable to interact with tRNAs and translocate them from the nucleus to the cytosol. Rex1 is a nuclear protein involved in the 3' end processing of various tRNA. If Rex1 activity remains constant under stress conditions, we would expect nuclear tRNA accumulation to result in increased tRNA processing by Rex1.

1.1.5 Rex1 is a 3' exonuclease which catalyses the maturation of RNA pol III transcripts

Rex1 is a yeast 3' exonuclease involved in the maturation of RNA pol III transcripts, its regulation in response to heat stress is a major focus of this thesis. Rex1 is functionally homologous to RNase T in *E. coli*. Rex1 belongs to the DEDD family of exonucleases, named after the four acidic residues essential to their active site. These acidic residues recruit two Mg²⁺ ions essential for catalytic activity (Zuo & Deutscher, 2001). Proofreading subunits of DNA pol I, DNA pol III and DNA exonuclease I also show DEDD family activity (Moser *et al*, 1997). We showed that both the C- and N-terminus of Rex1 is required for correct folding and formation of the active site (Daniels *et al*, 2022). *rex1Δ* cells remain viable but *rex1* gene deletion is synthetic lethal in *rrp6/rrp47Δ* strains. Rrp6 and Rrp47 form a stable exosome associated heterodimer with 3' to 5' activity (Feigenbutz *et al*, 2013). This implies redundancy in an essential function between Rex1 and Rrp47/Rrp6.

Rex1 processes 5S rRNA and tRNA species LYS^{UUU}, LEU^{CUU}, ILE^{UAU}, and MET^{AUG} (Foretek *et al*, 2016, Skowronek *et al*, 2013, Ozanick *et al*, 2008). In yeast, this occurs in the nucleus and Rex1 shows nuclear localisation in logarithmically growing cells (Frank *et al*, 1999). We identified a bipartite nuclear localisation signal (NLS), essential for nuclear localisation, at Rex1 amino acid 17-52 (Daniels *et al*, 2022) through imaging increasingly fine GFP-*rex1* truncations. WT cells grown under stress conditions, through exposure either to the heat-stress inducing temperature, 39°C, or through a shift onto media containing a non-fermentable carbon source, glycerol, showed a tRNA phenotype reminiscent of *rex1Δ* cells (Foretek *et al*, 2016). This was shown through northern blots of RNA extracted from cells grown on glycerol or exposed to heat shock. Therefore, we conclude that Rex1 activity is downregulated in response to temperature stress or growth on non-fermentable carbon sources.

Mass spectrometric analysis has revealed that Rex1 contains numerous post-translation modifications (PTMs) within its NLS (Holt *et al*, 2009, Lanz *et al*, 2021, Swaney *et al*, 2013). Phosphorylated residues are found at S24, T26, S27 and T34. Downstream of these is a ubiquitinated lysine at K58 (fig. 1.5). This pattern of several phosphorylated residues followed by a ubiquitination site is reminiscent of a phosphodegron, a phosphorylation mediated protein degradation pathway. Many phosphodegrons are known due to their importance in the actions of CDK and progression through the cell cycle (Al-Zain *et al*, 2015, Wood & Endicott, 2018). An example of this is the phosphorylation of Cdc6 by Mck1 to induce Cdc6 degradation and allow progression through the cell cycle (Al-Zain *et al*, 2015). Numerous phosphodegron motifs exist but many remain uncharacterised, though use of deep learning is being used to predict them (Hou *et al*, 2022). They are often characterised by an S/T-P-X-X-S/T-P motif (Holt, 2012), which is not present on Rex1.

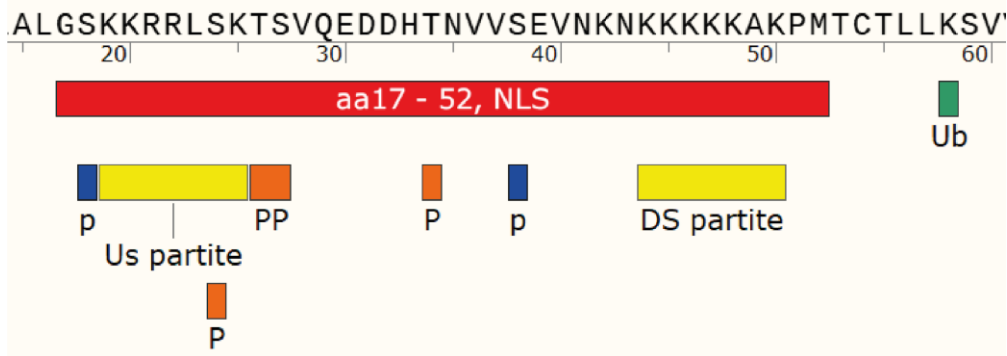


Figure 1.5. Schematic showing prevalent features of the Rex1 NLS. Rex1 shows a bipartite NLS with a cluster of positive residues between aa 19-25, and a second downstream of this at aa 44-50. The four identified phosphorylation PTMs are found within this region (orange 'P'). Additional serine residues found adjacent to these are denoted in blue 'p' as potential kinase targets.

Protein phosphorylation is linked to numerous responses including activation/deactivation of enzymes, cell cycle progression, phosphorylation mediated degradation and protein subcellular trafficking (Ardito *et al*, 2017, Bilbrough *et al*, 2021).

Instances of phosphorylation mediated nuclear trafficking have been identified. Numerous proteins are exported to the cytosol in response to phosphorylation, including Maf1, Pho4, and Swi6 (Boguta, 2013, Oshima, 1997, Sidorova *et al*, 1995). Simultaneously human proteins Erk5 and CK II are imported into the nucleus in response to phosphorylation (Nardozzi *et al*, 2010, Jans & Hubner, 1996). As Rex1 phosphorylation is limited to the region of the protein we identified as an NLS (Holt *et al*, 2009, Lanz *et al*, 2021) we will consider whether these PTMs are involved in Rex1 subcellular trafficking.

1.1.6 Protein degradation in response to stress

Protein degradation is an essential aspect of cell biology. In logarithmically growing cells, the regulated degradation of cyclins is essential for transition between stages of the cell cycle (Glotzer *et al*, 1991). One mechanism in which we see this is the increase in catalytic activity of cyclin-B/cyclin-dependent-kinase (CLB/CDK) through the proteasomal degradation of the CLB/CDK inhibitor, Sic1 (Deshaeis, 1997). Oscillations between activity and degradation of Sic1 and CLB/CDK are characteristic of the transition between G₁ and M/S phase.

In yeast, there are two protein degradation systems. Vacuolar protein degradation, where proteins are transported to the vacuole for degradation. Alternatively, proteins are degraded throughout the cell through the action of proteasome complexes. The vacuole is a site of recycling and molecular storage, it is an acidic organelle containing many endo- and exo-proteinases (Thumm & Wolf, 1998). Many of these are specific to the vacuole, including prA (Jones *et al*, 1982), this powerful aspartic acid proteinase is confined to the vacuole as its activity would be harmful elsewhere. This is indicated by the cytoplasmic presence of prA inhibitor I_{A3} (Saheki *et al*, 1974). As the primary degradation organelle in the cell, the vacuole also accumulates breakdown products and retains them as a storage site for later anabolism. There are well-established transport pathways to and from the vacuole.

Additionally, the cell expresses two variants of the multi-subunit proteasome complex for localised protein degradation (Achstetter *et al*, 1984, Hilt & Wolf, 1995). A smaller 20S proteasome shows general protease activity. A larger 26S variant sharing the same core subunits as the 20S is altered to target poly-ubiquitinated proteins (Voges *et al*, 1999, Thumm & Wolf, 1998, Luan *et al*, 2016). This provides a system where proteins can be specifically targeted for degradation via 26S proteasome degradation. 26S proteasome degradation occurs when proteins are ubiquitinated at an exposed lysine by ubiquitin ligase enzymes. This ubiquitin is further ubiquitinated, resulting in a poly-ubiquitin modification on the target protein. This is recognised by the proteasome, which denatures the protein and cleaves its peptide bonds (fig. 1.6). Initial ubiquitination occurs by the formation of a peptide bond between a C-terminal glycine of ubiquitin and the side chain of an exposed lysine on the target protein. Subsequently this ubiquitin is ubiquitinated at K48 with the C-terminal glycine of another ubiquitin molecule (reviewed in Pickart, 2001). This pattern of repeated ubiquitination acts as a degradation signal on the target protein. It is known that ubiquitination globally increases upon heat shock (Maxwell, *et al*, 2021). Accordingly, the small heat shock protein HSP27, which is upregulated in heat-shocked cells, has an affinity for poly-ubiquitinated proteins and mediates their interaction with proteasome complexes (Bozaykut *et al*, 2014).

Proteasome complexes can be inhibited through the action of MG132, a synthetic peptide aldehyde. This drug is permeable to *erg6Δ* yeast cell membranes (Liu *et al*, 2007). *ERG6* is involved in ergosterol biosynthesis and *erg6Δ* results in cells with membranes permeable to lipid-soluble drugs. Interestingly, proteasome inhibition through MG132 does not show any immediate change to maximum growth rate (Fleming *et al*, 2002). The 20S proteasome core contains three proteolytic subunits with chymotryptic, tryptic and caspase-like activity. Analysis demonstrated that MG132 inhibits the chymotrypsin activity of the 20S proteasome core without inhibiting the others. Mutations inhibiting the tryptic and caspase proteasome activity dramatically increased yeast sensitivity to MG132 and severely impeded yeast growth (Collins *et al*, 2010).

HeLa cells show increased proteasomal and ubiquitin ligase activity in response to heat stress (Lee & Goldberg, 2022). Misfolded proteins experience an increase in ubiquitination (Kuechler *et al*, 2021). Under heat stress conditions, we see an increase in protein misfolding and aggregation, perhaps explaining why a greater fraction of proteins are ubiquitinated and degraded. Interestingly in HeLa cells, it was observed that proteins susceptible to aggregation and misfolding are upregulated in response to elevated temperatures to account for aggregation-related loss of protein (Lee & Goldberg, 2021).

Chaperone proteins in yeast are simultaneously upregulated to protect newly synthesized proteins from aggregation (Muhlhofer *et al*, 2019). Alongside an increase in proteasomal activity, heat shock at various temperatures was found to increase transcription of vacuolar genes associated with catabolic activity (Muhlhofer *et al*, 2019). As we see a loss of Rex1 activity under heat stress conditions (Foretek *et al*, 2016), we have considered whether Rex1 is targeted for degradation in the heat shock response, as we will explore in this thesis.

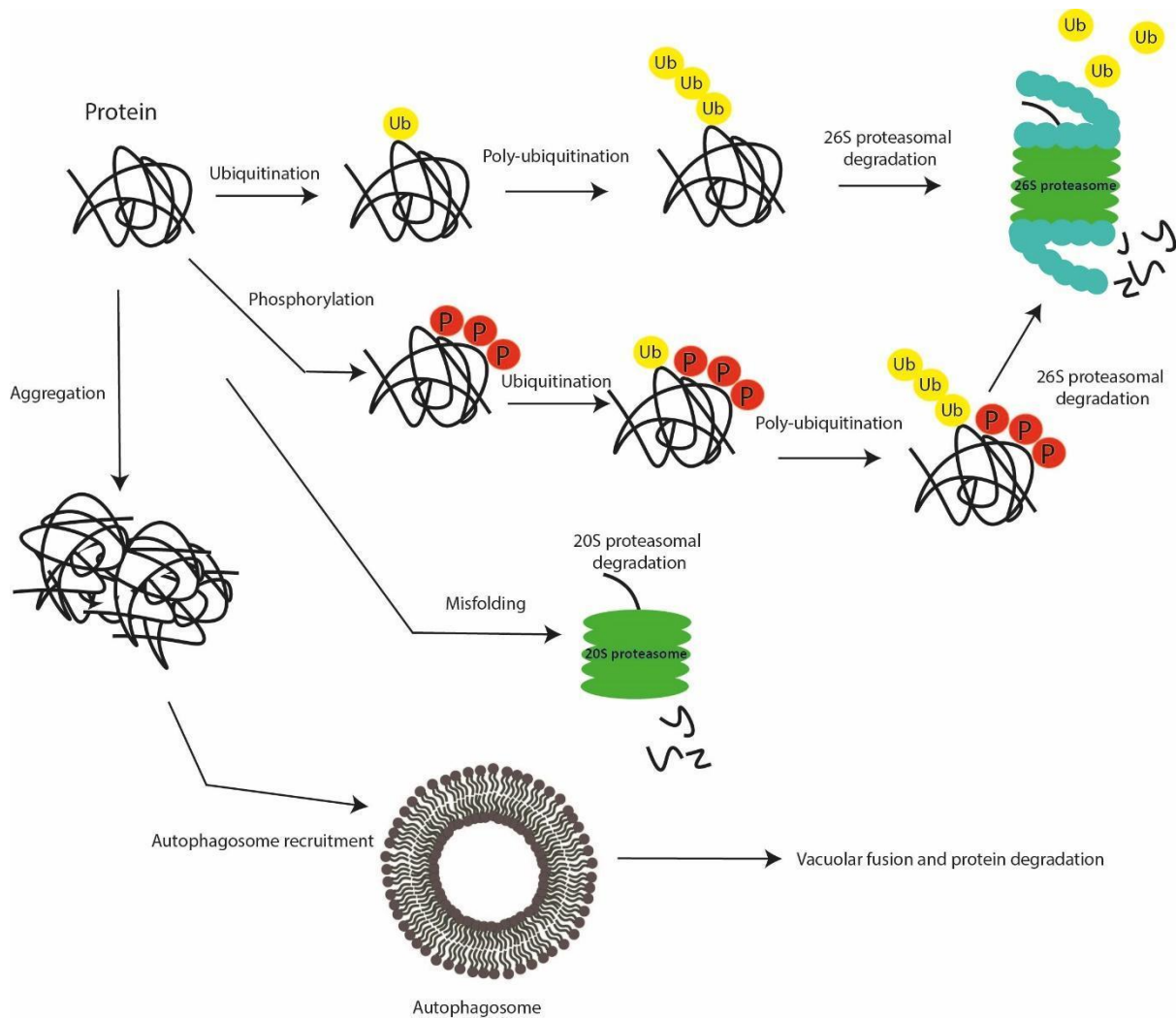


Figure 1.6. Mechanisms of protein degradation in yeast. Schematic details common to proteolytic pathways in yeast. Ubiquitin ligase targeted enzymes are recruited to 26S proteasome complexes for proteolysis. Some regulatory contexts use phosphorylation to induce this. 20S proteasome complexes perform quality control, breaking down misfolded protein. Aggregates can be recognised by autophagy machinery, which eventually fuses to the vacuole for degradation.

1.1.7.1 Nuclear localisation of proteins

Eukaryotic cells show metabolic compartmentalisation to facilitate the formation of concentrated metabolic regions. As proteins are synthesized in the cytoplasm, there is a need to import proteins into organelles for access to substrates. The nucleus is a double-membrane bound organelle; the membrane is perforated with nuclear pore complexes. This is a large and highly conserved complex consisting of ~30 different proteins arranged with many repeated symmetrical structures (Akey *et al*, 2022). In yeast, each nuclear pore complex contains ~550 proteins arranged to leave a pore in the nuclear membrane. It is thought that the nuclear pore acts as a firm barrier to molecules 30-60kDa or

greater in size (Ma *et al*, 2012, Mohr *et al*, 2009) though there is some evidence that much larger proteins can slowly diffuse through over a period of hours (Popken *et al*, 2015). The size limits for passive diffusion of molecules into the nuclear pore were deduced using fluorescent probes of varying molecular sizes and confocal microscopy to identify their diffusion into the nucleus (Mohr *et al*, 2009). Alongside the diffusion of molecules into the nuclear lumen, the nuclear pore provides an entry for regulated import and export using importin/exportin proteins and nuclear localisation signals on cargo molecules.

1.1.7.2 Nuclear localisation signals

Many organelles import proteins through transporters that recognise a particular amino acid motif on cargo proteins. This has been identified for ER, nuclear, mitochondrial and vacuolar import (Reid, 1991). Nuclear proteins contain an NLS, which commonly exists as either a cluster of positive residues, or two clusters separated by a short amino acid spacer available near the surface of the protein (Conti *et al*, 1998). The consensus sequence for monopartite and bipartite NLS is K(K/R)X(K/R) and KRX₁₀₋₁₂K(K/R)X(K/R) respectively (Bernardes *et al*, 2020). Nuclear export signals are also found in yeast, these signals are Crm1 dependent (Kosugi *et al*, 2008). There are numerous consensus sequences for yeast nuclear export signals which are broadly characterised by 6 conserved hydrophobic residues (Kosugi *et al*, 2008).

Nuclear import is mediated by the action of karyopherins, proteins that take cargo to the nuclear pore for stimulated import. Importin- α , Srp1 in yeast, is a highly conserved karyopherin. Srp1 contains two NLS binding sites, a major site and a minor site. Bipartite NLS containing cargo proteins bind both sites while monopartite containing proteins preferentially bind the major site (Bernardes *et al*, 2020) (fig 1.7). Srp1 has an auto-inhibitory domain that is bound by importin- β , Kap95 in yeast, in the cytosol. This blocks the Srp1 auto-inhibitory domain. The Srp1:Kap95 dimer is free to bind cargo in the cytosol and interact with the nuclear pore (Riddick & Macara, 2005). The Srp1/Kap95/cargo complex is then imported into the nucleus (fig. 1.8). The movement through the nuclear pore is mediated through interactions between Kap95 and the nuclear pore complex (Kutay *et al*, 1997). Once inside, Ran-GTP interacts with Kap95, removing it from the complex. This liberates the auto-inhibitory region of importin- α which outcompetes the cargo-binding domain, freeing the cargo from the complex. Finally Srp1 is exported through interactions with Cse1p (Chen & Madura, 2014, Hood & Silver, 1998). It should be noted that most importin- β proteins act independently as importins (Ullmann *et al*, 1997). In the case of Srp1, it is the action of Kap95 that mediates the interaction with the nuclear pore and induces import. Srp1 acts as an adapter protein and is used to regulate the import of Srp1 specific targets.

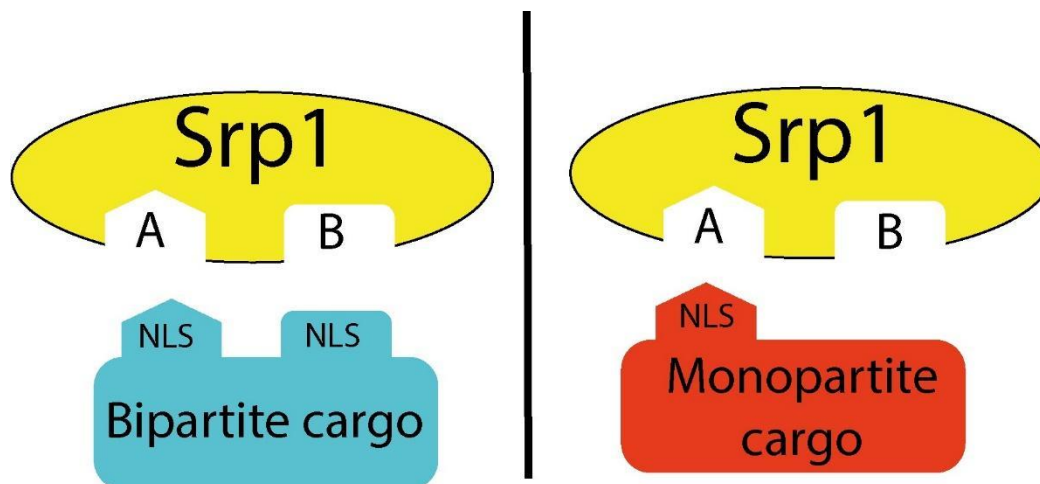


Figure 1.7. Schematic showing distinction between monopartite and bipartite NLS containing cargo binding to Srp1.

Srp1 is shown with its major (A) and minor (B) NLS binding sites. Bipartite NLS containing proteins have positive residues spaced with an affinity for both binding sites. Monopartite containing cargo proteins contain a single NLS with preferential affinity for the major binding site.

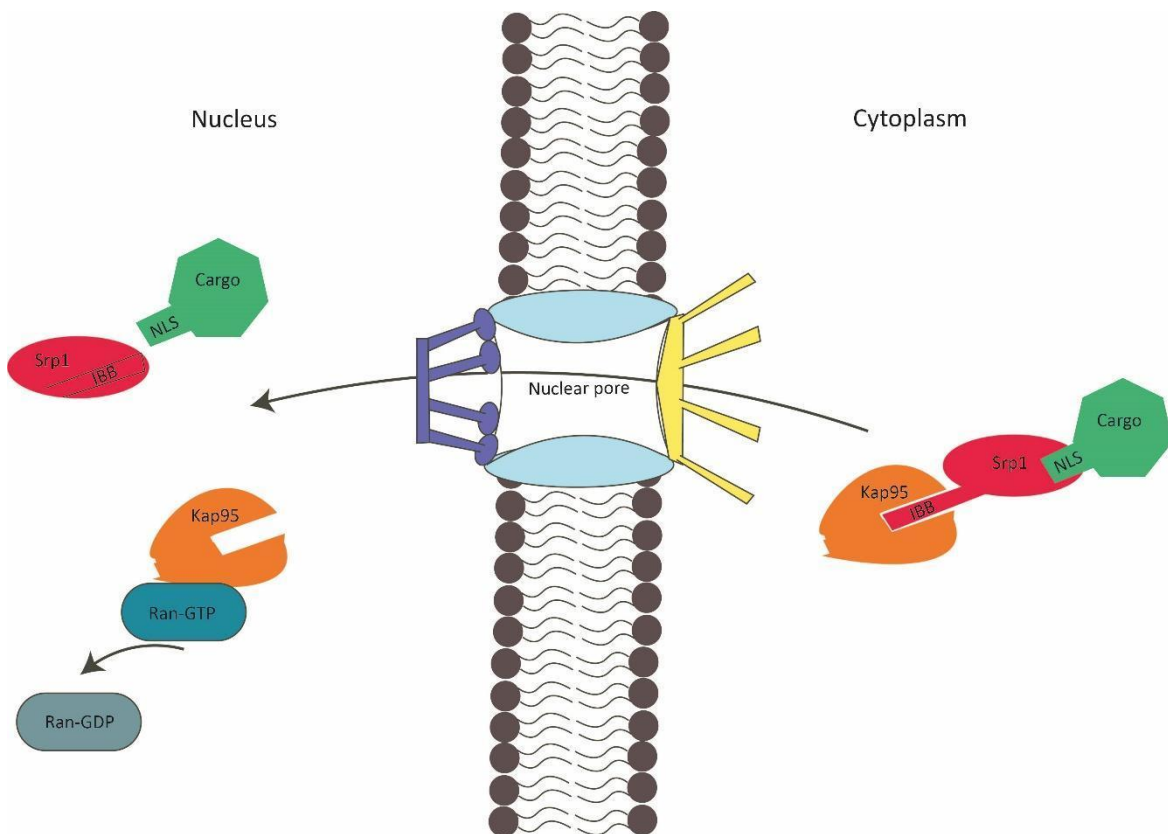


Figure 1.8. Shown is the import mechanism for the yeast importin- α , Srp1. In the cytosol, Srp1 binds to the yeast Kap95 via its importin- β binding domain (IBB). This heterodimer is capable of binding cargo proteins through an interaction of Srp1 with the NLS of cargo proteins. This complex is then imported into the nucleus. Inside the nucleus, Kap95 is removed from Srp1 through the action of Ran-GTP. The IBB domain then outcompetes the cargo proteins NLS binding site on Srp1, resulting in excision of the cargo from Srp1 and nuclear import.

It has been observed in mammalian cells that there is a reduction in importin- α mediated import when the cells are exposed to heat stress, oxidative stress, ethanol stress or starvation (Stochaj *et al*, 2000, Miyamoto *et al*, 2004, Kodiha *et al*, 2008, Furuta *et al*, 2004). It was also observed that importin- α accumulates in the nucleus of heat-shocked cells, implying a reduction of importin- α export from the nucleus. If yeast Srp1 shows reduced shuttling back to the cytoplasm under heat-shock conditions, it is possible that we see reduced overall nuclear import under these conditions. Rex1 17-52 contains a bipartite NLS, which may be recognised by Srp1. If heat stress reduces Srp1 mediated nuclear import, we would expect to see cytosolic accumulation of Rex1 in response to heat stress.

1.1.8 Ribosome biogenesis in response to stress

The TOR pathway is a signalling cascade regulated by two protein kinase complexes in yeast, TORC1 and TORC2 (Loewith *et al*, 2002). It is involved in the regulation of cell growth but not cell division (Schmelzle & Hall, 2000). TORC1 can be inhibited with the drug rapamycin, inducing metabolic signalling comparable to the effects of nutrient deprivation. Inhibition of TORC1 results in numerous catabolic process including autophagy, apoptosis, protein turnover, and RNA degradation. TOR activation is associated with an increase in cell growth, and ribosome biogenesis. TORC1 regulates the activity of all three major RNA polymerase complexes (Warner, 1999, Wei *et al*, 2009).

The TORC1 complex is composed of 4 subunits, Tor1/2, Lst8, Kog1 and Tco89. TORC1 is found in both the nucleus and cytoplasm. Upon exposure to starvation or rapamycin, the nuclear fraction of TORC1 is moved to the cytoplasm from the nucleus (fig. 1.9) as verified through fluorescence microscopy and sub-cellular fractionation (Li *et al*, 2006). ChiP-Seq in yeast has identified that the TORC1 complex interacts with chromatin at the site of the 5S and 35S rDNA (Li *et al*, 2006, Wei *et al*, 2009). This interaction was weakened through exposure to starvation or rapamycin. This effect was mitigated through expression of rapamycin resistant *tor1-RR*, implying that Tor1 ceases interacting with the 5S promoter region under nutrient stress conditions. Expression of a nuclear export deficient Tor1 (*tor1 NES Δ*) displayed a greater degree of interaction with the 5S promoter region when exposed to rapamycin or nutrient stress (Wei *et al*, 2009), implying that TORC1 subcellular localisation is used to control regulative ability. This evidence suggests that TORC1 is directly involved in regulating rRNA transcription rates.

The mammalian TORC1 homologue, mTOR, has been linked to rRNA processing (Ladevaia *et al*, 2012). mTOR inhibition by rapamycin leads to rRNA decay (Ladevaia *et al*, 2012). This was shown by *in vivo* labelling of rRNA with 4-thiouridine allowing biotinylation and pulldown of newly synthesized transcripts followed by reverse-transcription and qPCR with specific primers for rRNA identification. Cells treated with rapamycin were found to have decreasing levels of 5S and 18S rRNA over a 90 minute time course (Ladevaia *et al*, 2012). Further experiments demonstrated that rapamycin inhibited processing of 18S and 28S rRNA from the extended precursor, indicating that mTOR inhibition is interfering with rRNA processing. This indicates a link between nutrient stress and rRNA processing. TOR inhibition by rapamycin has also been observed to alter rRNA processing in yeast, with altered rRNA cleavage patterns resulting in non-functional rRNA and inhibition of ribosome biogenesis (Kos-Braun *et al*, 2017). This altered rRNA cleavage is consequent of a shift in cleavage of the 32S pre-rRNA at the A2 site to the A3 site 76 nucleotides away. This shift to A3 cleavage ceases downstream processing of the 32S pre-rRNA into 20S and 7S rRNA and inhibits production of novel ribosomes. This shift from A2 to A3 32S rRNA processing was observed in cells exposed to osmotic stress, heat shock or rapamycin (Kos-Braun *et al*, 2017). This indicates that as well as TORC1 having direct effects on rRNA transcription rates, it is also involved in its processing and maturation.

Excess tRNA has been found to inhibit TORC1 *in vitro* (Kamada, 2017, Otsubo *et al*, 2020). Additional ChIP-Seq experiments targeting tDNA-associated chromatin found that TORC1 did not associate with tDNA genetic loci. This is interesting as TORC1 interacts with other RNA pol III transcription sites. However, known interactions between tRNA, amino acid availability and TORC1 provide insights into indirect TORC1/tDNA interactions. tRNA availability affects the TORC1 activity depending on the availability of free amino acids, with TORC1 being activated by tRNA when amino acids are available (Otsubo *et al*, 2020). This mechanism is thought to depend on whether tRNA are bound to cognate amino acids. As amino acids become unavailable, free tRNAs increase and inactive TORC1. As tRNA has been found to inhibit TORC1 activity *in vitro* (Otsubo *et al*, 2020), this effect may occur directly when free tRNA concentrations reach a threshold in the cell.

There are links between Maf1 inhibition of RNA pol III, Maf1 nuclear localisation and TORC1. Maf1 is imported into the nucleus upon dephosphorylation, where it inhibits the action of RNA pol III (Moir *et al*, 2006). Maf1 contains an N-terminal and C-terminal NLS which are phosphorylated by PKA and Sch9 to regulate Maf1 nuclear import (Moir *et al*, 2006, Wei *et al*, 2009). However in yeast strains in which Maf1 nuclear export is non-functional, RNA pol III continues to be normally regulated by Maf1 (Towpik *et al*, 2008). A similar observation is that in the absence of Sch9, Maf1 continues to regulate RNA pol III activity (Wei *et al*, 2009), this indicates the presence of additional Maf1 regulation. As TORC1 inactivation stimulates Maf1 inhibition of RNA pol III (Michels *et al*, 2010), this demonstrates a link between TORC1 and Maf1 activity. Both TORC1 and Maf1 localise to the sites of 5S rDNA promoters. TORC1 has been shown to phosphorylate Maf1 *in vitro*, implying that TORC1 acts as a direct Maf1 kinase (Wei *et al*, 2009). As 5S rDNA are located in the nucleolus, it is thought that Maf1 phosphorylation by TORC1 acts to export Maf1 from the nucleolus. As tDNA genes are concentrated in the nucleolus, this would allow TORC1 to regulate tDNA and 5S rDNA transcription in the same compartment.

Rex1 activity is reduced under nutrient stress conditions, the same conditions in which Maf1 inhibits the RNA pol III transcription. It would be efficient for these activities to share common regulation as Rex1 processes RNA pol III transcripts. Such a mechanism may come in the form of Sfp1, a zinc-finger transcription factor known to affect Rex1 transcription (Cipollina *et al*, 2008). Sfp1 is involved in regulation of ribosome biogenesis and is regulated by TORC1 (Fingerman *et al*, 2003).

Additional links between TORC1 and ribosome biogenesis have been observed. It has been noted that mRNA encoding ribosomal proteins contain a 5' pyrimidine rich sequence referred to as a 5'TOP. A ribosomal protein, S6, is phosphorylated by TOR to interact with the 5'TOP. Upon addition of rapamycin, S6 is dephosphorylated and fails to interact with the 5'TOP, ending the interaction between the ribosome and ribosomal mRNAs and ending the translation of ribosomal mRNAs (Jefferies *et al*, 1996). Such mechanisms allow mTOR inactivation by rapamycin to reduce the synthesis of ribosomal proteins.

The Tor pathway is a major regulator controlling cell growth. Given the links between growth, nutrient sensing and ribosome biogenesis regulation, it is plausible that the Tor pathway interacts with the regulation of Rex1. We will consider the following possibilities of interactions between TORC1 activity and Rex1 regulation. TOR inhibition prevents the maturation of 5S rRNA from pre-rRNAs. As 5S is a Rex1 substrate, there could be an energetic incentive to alter Rex1 activity when 5S rRNA is not being synthesized. Excess tRNA inhibits TORC1, Rex1 is involved in processing mature tRNA. This could create a feedback loop where sufficient levels of mature tRNA are made by Rex1. These mature tRNA inhibit TORC1 that subsequently reduces 5S rRNA transcription and rRNA processing, mitigating the need for Rex1. Once tRNA levels reduce, TORC1 activity is again activated and rRNA transcription and processing levels increase. Nutrient stress in the form of cells growing on glycerol as a carbon source

has been shown to have reduced Rex1 activity through identification of 3' extended tRNA. If glycerol media provides sufficient nutrient stress to induce Maf1 import and block 5S upregulation by TORC1, this could link conditions that block Rex1 activity and produce Rex1 substrates. Additionally, Heat shock diverts the processing of 32S pre-rRNA from the A2 to A3 pathway, blocking the synthesis of 5S rRNA. Evidence shows that Rex1 activity is reduced in heat-shocked cells. These effects are metabolically linked and could be regulated together.

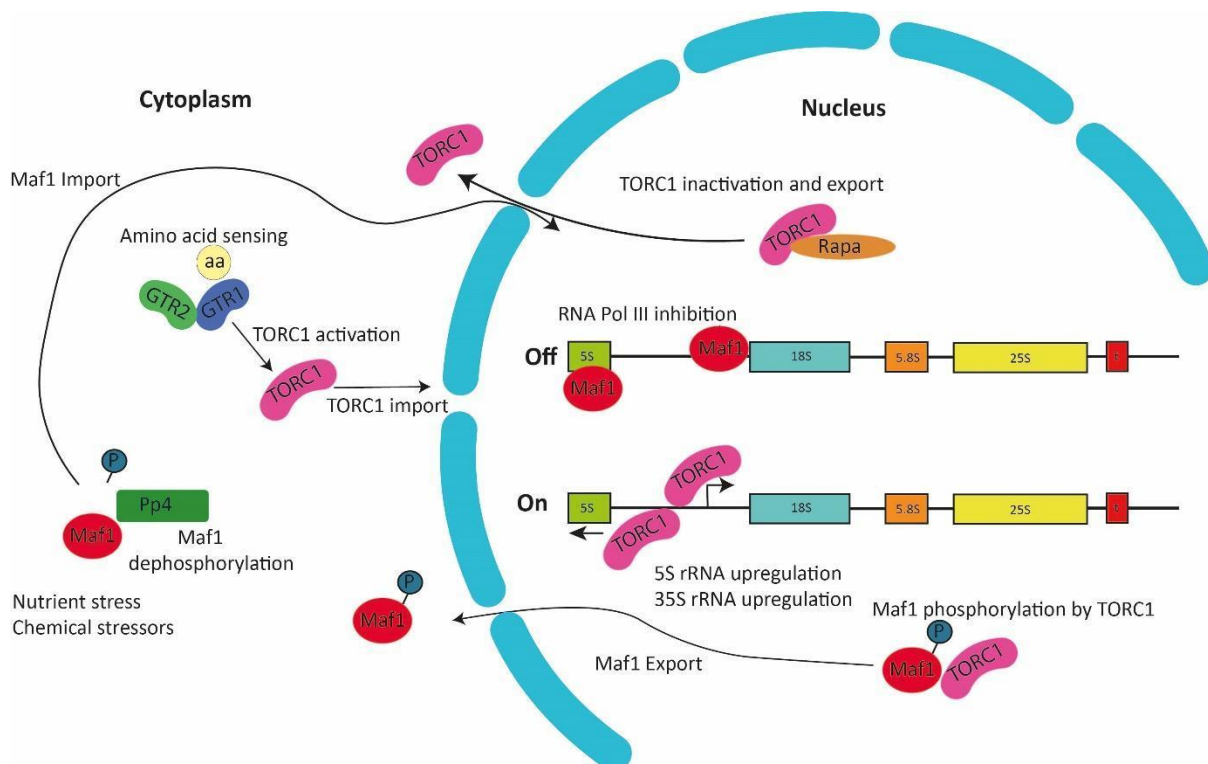


Figure 1.9. TORC1 nuclear import upregulates rRNA transcription and is inhibited through the action of Maf1. Shown are links between TORC1, amino acid sensing and Maf1 inhibition of RNA pol III. High amino acid availability induces activation of TORC1 through the GTR1:GTR2 complex. This induces TORC1 nuclear import where it associates with rDNA loci, enhancing transcription. tDNA genes are indirectly upregulated under these conditions. Once in the nucleus TORC1 phosphorylates Maf1, stimulating its nuclear export. Nutrient/chemical stress causes Maf1 dephosphorylation and nuclear import. RNA pol III is inhibited by the action of Maf1. Nutrient stress/rapamycin exposure induces TORC1 inactivation and nuclear export.

1.8 Biotechnology

1.8.1 Biotechnological chemical manufacture

As the capacity to engineer microbes to produce high titres of molecules improves, we have seen an increased prevalence of chemicals being produced biotechnologically by cultivating organisms in large bioreactors for later extraction of target molecules (Niosi, 2001, Sturmer, 2010). This approach offers numerous advantages over conventional chemical manufacture. Bioreactors allow modular chemical production. By re-inoculating the reactor with a different strain you can alter the molecule being produced. This is in contrast to conventional chemical plants that are hard to retrofit and are typically optimized for the production of a single compound. Through alterations of a biosynthetic pathway, it is possible to produce a range of molecules *in vivo*, this gives the ability to produce complex biological molecules that can be difficult to synthesize. The variety of molecules derivable through biotechnology is immense, including therapeutic drugs, antibodies, biofuels, agrochemicals and high value chemicals with industrial uses (Jongedijk *et al*, 2016, Malik *et al*, 2016, Gaid *et al*, 2018, Yamamoto *et al*, 2012). Furthermore, it is possible to grow cells on a variety of carbon sources, including from industrial or agricultural waste streams (Garlapati *et al*, 2016, Panesar *et al*, 2016), allowing use of inexpensive feedstocks while contributing to a circular economy. These practices reduce human dependence on oil reserves while giving access to novel chemicals. Part of this thesis will focus on products of fungal metabolism with emphasis on glycolipids with surfactant activity.

Biotechnological production of all microbially produced compounds is far from feasible. Many microbes cannot be cultured, or fail to produce target compounds under laboratory conditions. While bioinformatics tools are facilitating the discovery of gene clusters, the regulatory context in which they are expressed is often unknown. Simultaneously, the development of toolkits of molecular parts to adjust gene expression in novel organisms is very labour intensive. There is an incentive to develop model organisms as a chassis for biotechnological production. Expressing novel genes in a well-established host yields numerous advantages regarding optimising gene expression and culture conditions.

1.9 Biosurfactants

Surfactants are a class of molecules that lower the surface tension between the interfaces of two fluids. They are amphipathic molecules containing a hydrophobic and a hydrophilic region. These molecules have many industrial uses from increasing crude oil recovery, a wide array of functions in the cosmetics industry to use in foods and beverages and traits beneficial to the pharmaceutical industry (Santos *et al*, 2016, Campos *et al*, 2013). Surfactants derived from organisms (biosurfactants) have numerous advantages over petroleum derived equivalents in that they are frequently non-toxic and biodegradable, allowing for use in the remediation of oil spills without further contamination of the environment (Silva *et al*, 2014). Petroleum derived surfactants have numerous disadvantages. They are the most prevalent organic contaminant in wastewater (Li *et al*, 2018). This is a problem as they are often toxic, have long half-lives, and tend to accumulate in sediments (Lewis, 1991). Biosurfactants naturally exist in a near infinite array of forms, leaving a lot of potential for discovering molecules optimally suited to a purpose. Glycolipids are commonly used biosurfactants, consisting of a saccharide bonded to a fatty acid to produce an amphipathic compound. However, a number of other molecules including lipopeptides, phospholipids, fatty acids and polymeric biosurfactants have gained interest as effective biosurfactants (Geetha *et al*, 2018).

I will focus on glycolipid biosurfactants. They already have many industrial uses and research into their biosynthetic pathways has been carried out. It has been found that *Ustilago maydis* (*U. maydis*), a basidiomycetous fungi secretes large volumes of glycolipids (Spoeckner *et al*, 1999, Lemieux *et al*, 1951). *U. maydis* secretes a mixture of mannosylerythritol lipids (MELs) (table 1.2) and ustilagic acid.

The natural function of these are unknown but they are suspected to enhance nutrient uptake and adhesion to non-polar substrates (Teichmann *et al*, 2007). Genes associated with the biosynthesis of MELs have been found to exist in clusters (Hewald *et al*, 2006). This is convenient for identification of genes associated with the pathway, as they can be found by searching open reading frames upstream and downstream of the cluster for enzymes that act on glycolipids. This allows straightforward compilation of the biosynthetic pathway. Large-scale cultivation of *U. maydis* is possible, but it is a plant pathogen targeting corn. Due to the importance of corn as an agricultural crop, it could be unwise to cultivate large volumes of an organism pathogenic to it. The transformation of the gene cluster into a more suitable biotechnological host would allow for exploitation of these secretory pathways for the recovery of biosurfactants while tailoring production to a single molecule. This thesis describes research investigating the possibilities of transforming yeasts to create strains suited to biotechnological production of glycolipids.

1.10 Host organisms

Typically, well-studied model organisms such as the bacteria *Escherichia coli* (*E. coli*), or the yeast *S. cerevisiae*, are used for biotechnological production of chemicals (Lazarus *et al*, 2014, Liu *et al*, 2012). Using eukaryotes has advantages over prokaryotes due to the cell's compartmentalisation. This can be used to isolate essential processes in the cell from the accumulation of target molecules that may be harmful to its metabolism. This is particularly relevant for the production of biosurfactants that can have a soap-like activity (Md, 2012). MELs are secreted by fungi into the extracellular environment. This works as there is a membrane transporter protein within the gene cluster (Hewald *et al*, 2006). In eukaryotes, plasma membrane proteins are synthesized by ribosomes and then inserted into the endoplasmic reticulum (ER) for modification and quality control. These are subsequently sorted into secretory pathways for insertion into the plasma membrane. This process is stringent and bacterial plasma membrane transporters rarely get further than the ER in eukaryotes. Rhamnolipids are bacterial glycolipids with industrial value in the food and cosmetic industries. They are composed of one or two rhamnose moieties, bound to fatty acids. Some studies were conducted attempting to express the bacterial rhamnolipid pathway in yeasts but the results were poor and no rhamnolipids were certified as being produced (Bahia *et al*, 2018). For these reasons, we are interested in transforming yeasts with the MEL biosynthetic pathway as the fungal secretory transporters are more likely to work.

The obvious yeast for this is *S. cerevisiae*. It has been extensively studied and a large number of molecular tools exist for its modification including promoters, terminators, autonomous replicating sequences, centromeres, selectable markers, plasmids and a variety of tools for recombinant modification of DNA (Besada-Lombana *et al*, 2018). Its natural tendency to repair double strand breaks using homologous recombination simplifies the process of integrating foreign DNA into its genome. Despite this, it has disadvantages as a biotechnological host for lipid production. *S. cerevisiae* is biased towards sugar metabolism, with particular emphasis on ethanol production for energy storage, meaning lipids would have to be directly supplied for MEL biosynthesis, whereas *U. maydis* accumulates lipids in large volumes in nitrogen-limiting conditions (Aguilar *et al*, 2017). Nonetheless, *S. cerevisiae* is a strong candidate as a proof of concept.

1.11 Biosurfactant gene clusters

Numerous biosynthetic pathways for the production of glycolipids, and secondary metabolites in general, have been identified to exist in gene clusters in fungi (Hewald *et al*, 2006, Brakhage & Shroeckh, 2011, Teichmann *et al*, 2011, Roelants *et al*, 2014). Examples of gene cluster encoded secondary metabolites include penicillin, cyclosporin and lovastatin (Rokas *et al*, 2020). This is advantageous for rapid identification of the genes associated with that pathway, allowing for the

creation of a catalogue of enzymes, each modifying the product in a specific manner. This approach allows for the tailored selection of necessary enzymes for producing a target compound. With enough enzymes from related gene clusters it should be possible to create a library of strains, each producing a single, pure biosurfactant. Subsequently, the correct strain could be grown for the production of a specific molecule that is best suited to an industrial purpose.

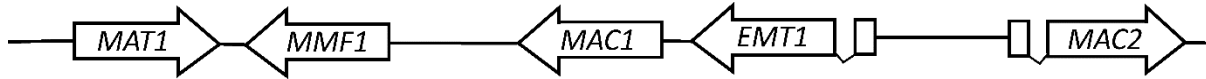


Figure 1.10. Organisation of genes in the MEL biosynthetic gene cluster. Displayed is the MEL biosynthetic gene cluster from *U. maydis*. The genes are located on chromosome 7. Note the intron present in *EMT1* and *MAC2*.

MELs secreted in large volume by *U. maydis* have a number of uses in cosmetics, food and agriculture industries (Mnif & Ghribi, 2016), with particular value as an additive to high value face and hair creams (Morita *et al*, 2013). The cluster is composed of five genes (fig. 1.10) (table 4). Four of the five genes in the cluster are essential for MEL synthesis and secretion, only if *MAT1* is knocked out are MELs still secreted although completely lacking acetylation. This is a starting point for producing custom biosurfactants. Should the pathway remain functional in yeasts, a strain lacking *MAT1* could be developed for the production of unacetylated MELs which show reduced hydrophilicity. Alongside MELs, *U. maydis* also produces ustilagic acid, another glycolipid based on the glucose disaccharide cellobiose (Bolker *et al*, 2008, Teichmann *et al*, 2007). Ustilagic acid is in less demand from industry and there is an incentive to produce pure MELs. Additionally, there is demand from industry for the production of pure compounds with a specific activity such as mono-acylated MELs that are better suited to the formation of oil-in-water emulsions (Saika *et al*, 2018). By transforming yeasts, which do not produce glycolipids, with a gene cluster we can prioritize production of a single biosurfactant, resulting in a more desirable product.

Understanding the role of different genes in the biosynthetic pathway facilitates customising it, when the function of an enzyme is known it becomes possible to search for similar enzymes with subtle differences in activity. The MEL biosynthetic pathway has already been characterized (Hewald *et al*, 2006), (fig. 1.11) and using this information we can theorise methods for rebuilding the pathway in a new organism for a specific product.

Table 1.1. MEL biosynthetic genes and their function. Table below details the five *U. maydis* genes required for MEL biosynthesis and secretion.

Gene	Function
<i>EMT1</i>	Glycosyltransferase, associated with formation of mannosylerythritol disaccharide.
<i>MAC1</i>	Essential acyltransferase for production of MELs, required for acylation of fatty acid chains on C1 or C2 on mannosyl moiety.
<i>MAC2</i>	Essential acyltransferase for production of MELs, required for acylation of fatty acid chains on C1 or C2 on mannosyl moiety.
<i>MAT1</i>	Catalyses the acetylation of MELs at 2 carbons on the mannosyl moiety.
<i>MMF1</i>	Major facilitator, transporter protein which exports MELs extracellularly.

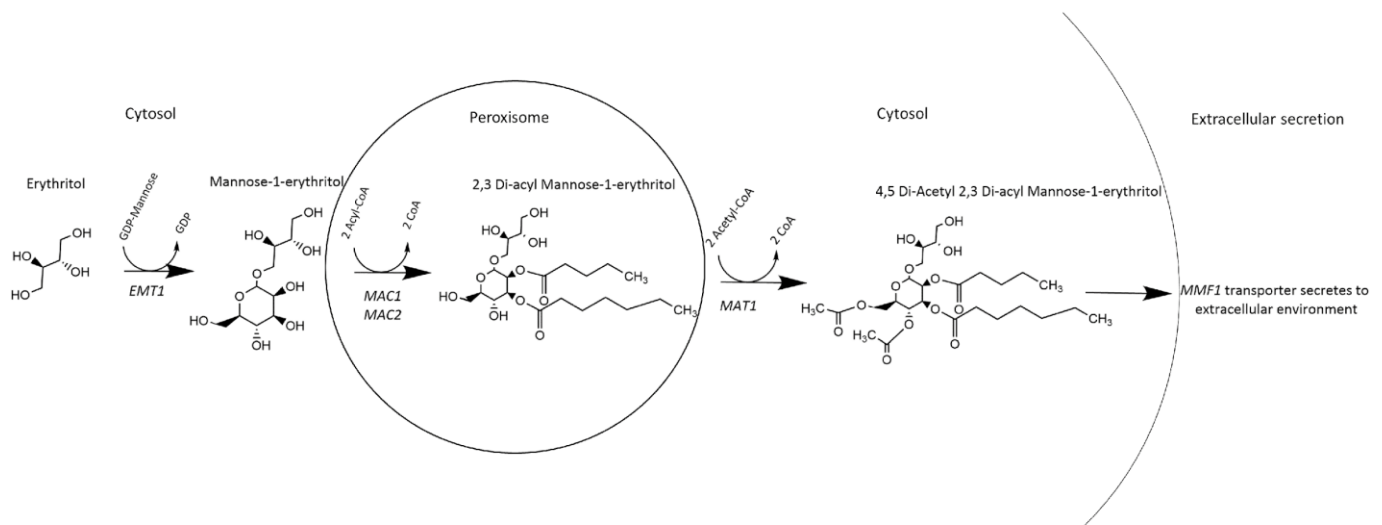


Figure 1.11. Schematic representation of the biosynthetic pathway for mannosylerythritol lipids in *Ustilago maydis*. Shown is the biosynthetic pathway for the synthesis of MELs in *U. maydis* as well as the enzymes sub-cellular localisation. Initially erythritol is bound to mannose in the cytosol by Emt1. The produced mannosylerythritol is imported into the peroxisome where it is acylated at C1 and C2 by Mac1 and Mac2, this di-acylated MEL is returned to the cytosol through unknown means. Mat1 adds an acetyl group to C4 and C5 on the di-acylated MEL, yielding the finished product, which is exported from the cell by the plasma membrane transporter Mmf1.

1.12 MEL biosynthetic pathway

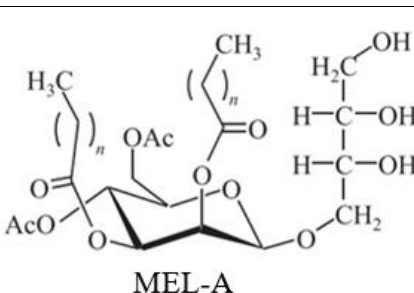
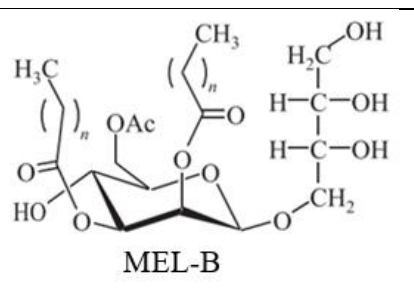
The process begins with the formation of a disaccharide between erythritol and mannose by Emt1 (fig. 1.11). Subsequently, Mac1 and Mac2 acylate the mannosylerythritol with fatty acid chains at the C1 and C2 position. It is thought that each of these enzymes acylates a different position on the sugar, in cells lacking either one of these enzymes there is no secretion. This indicates that both acylations are necessary for MEL secretion (Hewald *et al*, 2006). This process occurs in the peroxisome, and acylation takes place using short and medium chain fatty acids. It is possible to control the length of fatty acid chains found in the peroxisome through modification of acyl-CoA oxidase enzymes, which break down fatty acid chains to a specific length. An example of this is the deletion of the *POX1* gene in *S. cerevisiae* which blocks decay of medium chain fatty acids (Chen *et al*, 2014), resulting in a strain capable of accumulating medium chain fatty acids (Chen *et al*, 2014). Fatty acid chain length can be further adjusted using specific carnityl transferases, these replace the CoA group on a fatty acid with a carnityl group, stimulating secretion of the fatty acid from the peroxisome. By using carnityl transferases targeting fatty acids of a specific length we can remove fatty acid chains of a specific length from the peroxisome (Hetteema & Tabak, 2000), potentially blocking their incorporation into complete MELs. It is also possible to provide growth media enriched with fatty acids of a specific length to encourage

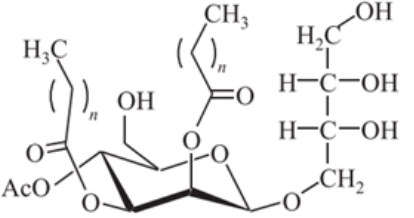
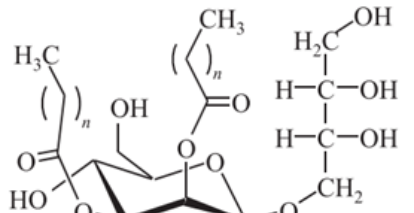
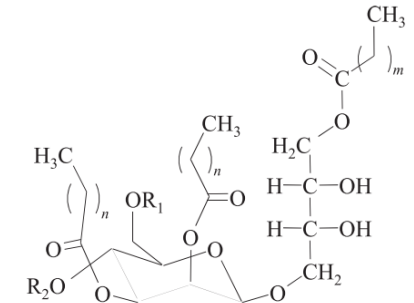
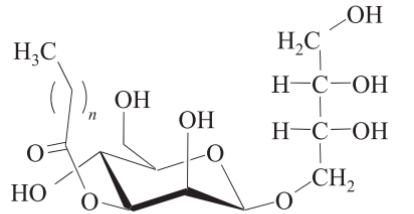
their incorporation into MELs. A combination of these approaches could allow for production of MELs containing fatty acids of a target length. *Moesziomyces antarcticus* (*M. antarcticus*), a yeast species closely related to *U. maydis*, has been found to produce mono-acylated MELs (Fukuoka *et al*, 2007). These were extracted from the culture broth. The implication is that the yeast secretes mono-acylated MELs, this is of interest as the native transporter in *U. maydis* can only export MELs containing two fatty acid chains. Should an alternate transporter exist in *M. antarcticus* we could transform it into a heterologous host for secretion of mono-acylated MELs. These show increased hydrophilicity, which is a desirable trait in some industrial applications (Fukuoka *et al*, 2007).

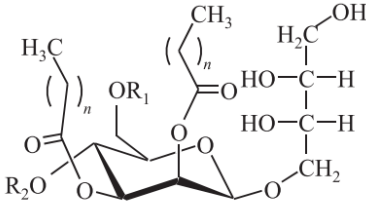
The presence of transporters for secretion of MELs strongly enhances the potential of this pathway for the creation of biotechnological hosts. Secreted compounds are easier to recover as there is no need to lyse cells, a process which greatly increases the complexity of the mixture to purify. MELs are denser than water, a feature that can facilitate product recovery when grown on water-soluble substrates such as glycerol or sugars.

Here we have focussed on the MEL biosynthetic gene cluster from *U. maydis*, however other biosurfactant pathways have been identified as clusters. Ustilagic acid, the cellobiose glycolipid also produced by *U. maydis* are synthesized by genes that form a cluster (Teichmann *et al*, 2007). Numerous species of the genus *Ustilago*, *Moesziomyces* and *Pseudozyma* have been identified as producing MELs from genes suspected to exist in clusters (Morita *et al*, 2015) (table 1.2). In more distantly related species, we also see biosurfactant gene clusters including the sophorolipid gene cluster in the yeast *Starmerella bombicola* (Van Bogaert *et al*, 2013). However, this yeast already produces such high titres of these chemicals that attempting to produce a more optimal host in a different species is redundant. Searching for additional enzymes in order to further modify this pathway has potential as sophorolipids are in demand from industry and being able to produce them in a multitude of forms could be advantageous.

Table 1.2. Structure and variations of MEL glycolipids. The table shows the variability in known MELs and lists the organisms which secrete them.

MEL structure	Features	Organism
 <p>MEL-A</p>	<p>MEL-A, the most commonly secreted MEL. It is di-acylated with two fatty acid chains and has 2 acetyl groups on the mannosyl sugar moiety at position C4 and C5.</p>	<p><i>U. maydis</i> <i>P. churashimaensis</i> <i>P. parantarctica</i> <i>P. rugulosa</i> <i>P. aphidis</i> <i>P. antartica</i></p>
 <p>MEL-B</p>	<p>MEL-B, these are similar in structure to MEL-As but have just one acetyl group on C5 of the mannosyl moiety of the disaccharide.</p>	<p><i>Ustilago scitaminea</i></p>

 <p style="text-align: center;">MEL-C</p>	<p>MEL-C, similar to MEL-B in that these are mono-acetylated but the acetyl group is found on C4 of the mannosyl moiety as opposed to C5 in MEL-Bs.</p>	<p><i>P. hubeiensis</i> <i>P. graminicola</i> <i>P. shanxiensis</i> <i>P. siamensis</i> <i>U. cynodontis</i></p>
 <p style="text-align: center;">MEL-D</p>	<p>MEL-D, these are similar in structure to MEL-As but completely lack acetylation. Instead hydroxyl groups are present at positions C4 and C5 of the mannosyl moiety of the disaccharide. These can be produced by knocking out the Mat1 gene in <i>U. maydis</i>.</p>	<p><i>mat1Δ U. maydis</i></p>
 <p style="text-align: center;">Tri-acylated MEL</p>	<p>Tri-acylated MELs contain 3 fatty acid chains, resulting in a molecule with decreased hydrophilicity. The R groups present at C4 and C5 of the mannosyl moiety are typically hydroxyl groups but can be modified through the use of enzymes.</p> <p>Note that these have been found as a small fraction of <i>P. churashimaensis</i> secretions but due to their interesting properties they merit study.</p>	<p><i>P. churashimaensis</i></p>
 <p style="text-align: center;">Mono-acylated MEL</p>	<p>Mono-acylated MELs contain just one fatty acid chain. They show increased hydrophilicity which can be beneficial for aqueous industrial reactions. The hydroxyl groups on the mannosyl sugar moiety can be altered into side chains with a suitable enzyme.</p> <p>Note that these have been found as a small fraction of MEL secretions but due to desirable properties they merit attention.</p>	<p><i>P. churashimaensis</i> <i>M. antarcticus</i> <i>P. parantarctica</i></p>

 <p>Diastereomer type of MEL</p>	<p>Diastereomer forms of MELs with the erythritol orientated in reverse have been found in two species. With a diastereomer of MEL-A found from <i>P. crassa</i> and a diastereomer form of MEL-B isolated from <i>P. tsukubaensis</i>. These are suspected to form due to an altered Emt1 protein which creates the new form of the disaccharide.</p>	<p><i>P. tsukubaensis</i> <i>P. crassa</i></p>
-------------------------------------------------------------------------------------------------------------------	--------------------------------------------------------------------------------------------------------------------------------------------------------------------------------------------------------------------------------------------------------------------------------------------------------------------------------------------------------	----------------------------------------------------

1.13 Heterologous gene expression

A major bottleneck to engineering biotechnological hosts for chemical manufacture is the optimization of gene expression levels when expressing heterologous pathways (Siddiqui *et al*, 2012). Overexpression of heterologous proteins often causes complications in the cell and can fail to increase titre of target molecules (Ro *et al*, 2008).

Many regulatory networks *in vivo* control gene expression levels in the cell. These include promoter strength, which affects RNA polymerase recruitment and subsequent translated protein levels (Chen *et al*, 2017). Terminator sequences affect protein levels by governing mRNA persistence times (Curran *et al*, 2015). Other systems for fine tuning protein levels are known to exist including the influence of introns and enhancer RNAs, integration into multiple loci using transposon recognised sequences, and codon optimization (Rose, 2019, Arnold *et al*, 2020). However, manipulating these mechanisms is challenging without offering large advancements in gene expression control. Optimising single gene expression levels is challenging and the difficulty is compounded when compiling multi-gene pathways.

Numerous approaches have been implemented to create multi-gene expression cassettes for heterologous hosts. Li & Elledge used *in vitro* homologous recombination with refined bacterial Rec-A to assemble up to 10 genetic fragments into a plasmid simultaneously (Li & Elledge, 2006). This approach reduces cloning steps when combining ORFs of interest with promoters/terminators. The use of large multi-gene plasmids is limiting, as large plasmids are susceptible to degradation when extracted from *E. coli* (Yang & Yang, 2012). Much larger yeast artificial chromosomes ranging between 10-120kb have been assembled through *in vivo* homologous recombination in yeast (Ebersole *et al*, 2005). These were constructed from tandem repeats and clones were inconsistent in size. Nonetheless, it demonstrates the ability of yeast to assemble multi-fragment DNA. The study was limited to the use of a select yeast strain and spheroplast transformation, which mitigates many of the biotechnological advantages earned from the use of alternative strains. Gibson *et al* used *in vitro* Gibson assembly to compile four 144kb fragments that were recombined in yeast to yield the entire *Mycoplasma genitalium* (*M. genitalium*) genome (Gibson *et al*, 2008). However, this required extensive preparatory work and *M. genitalium* genome extraction from the yeast genome was particularly adapted to such large fragments. Nonetheless, these approaches demonstrate impressive capacity to use *S. cerevisiae* to assemble large regions of DNA.

A more typical approach to heterologous gene expression in *S. cerevisiae* is to amplify an ORF of interest and place it between a promoter/terminator pair for expression. This is limited to characterised yeast promoters and complicates the expression of numerous genes as having

numerous repeated sequences increases the probability of recombination within expression cassettes. Recent advances using synthetic short yeast promoters reduced the use of native promoter sequences (Redden & Alper, 2015). While a synthetic promoter 116bp in length was developed promoting gene expression comparatively to *pTDH3*, many synthetic sequences failed due to weak or inconsistent expression, limiting this approach for the expression of multiple genes.

Once a pair of promoters/terminators have been allocated to ORFs within a gene cluster, the assembly and expression must be contemplated. As biotechnological applications frequently depend on gene overexpression, gene copy number must be considered. Plasmid expression is a common tool when expressing genes in *S. cerevisiae*. Limits to plasmid expression are the need to select for their succession and recovery of large plasmids can be difficult. In yeast, YCp (yeast chromosomal plasmid) and YEp (yeast episomal plasmid) plasmids are commonly used as a means to control gene copy number. YCp vectors, containing a CEN/ARS sequence are stable and prevalent at 1-2 copies per cell (Clarke & Carbon, 1980). For higher gene copy number YEp vectors are used, based on the native yeast 2 μ vector. Various YEp plasmids are used, while copy numbers vary, they are generally thought to be 10 – 40 copies per cell (Romanos *et al*, 1992). While this appears advantageous over YCp vectors, high 2 μ expression of certain genes leading to accumulation of biotechnological products can result in negative growth phenotypes or poor plasmid stability (Moore *et al*, 1990, Ro *et al*, 2008, Verwaal *et al*, 2007). In some instances expression from YCp vectors results in greater biotechnological yields than when using YEp vectors (Wittrup *et al*, 1994). This has been attributed to the bottleneck of posttranslational processing and folding which mitigates advantages from having higher levels of mRNA. Very high copy numbers of 2 μ were reported by adding a *leu2-d* selectable marker to the plasmid and growing on leu- growth media. These contain a deficient *LEU2* gene functioning at <5% of native activity. Cells containing these vectors maintained 40-100 copies of the plasmid and plasmid stability was enhanced (Erhart & Hollenburg, 1983). However, this is considered advantageous for overexpression, due to toxicity associated with high heterologous gene expression these plasmids are rarely used for constructing biotechnological hosts.

Integration into chromosomal loci is preferable as it is genetically stable; this is particularly advantageous when expressing multiple genes as the long-term maintenance of several plasmids can be challenging (Futcher & Carbon, 1986). Due to chromatin structure and epigenetic modifications, some regions of chromosomal DNA are not open and transcription rates are low. This means that integration loci must be verified prior to integration of a gene cassette. Numerous sites in yeast have been identified as good locations for high gene expression (Flagfeldt *et al*, 2009, Mikkelsen *et al*, 2012, Fang *et al*, 2011). As heterologous genes are frequently equipped with native promoters/terminators, integration loci flanked by essential genes are chosen to select against removal of heterologous genes by recombination between integrated and native promoters/terminators. Alternative approaches involve integrating into LTR of TY transposons that are present on every yeast chromosome and consist of repeat sequences. This means that integration cassettes target numerous loci and encourages multiple simultaneous integrations. The use of *KL URA3*-degradation signal, a gene encoding an unstable Ura3 protein as a selectable marker, stimulated multiple integrations of a cassette (Maury *et al*, 2016).

S. cerevisiae has highly effective homologous recombination machinery, allowing for integration of PCR fragments into the genome with short flanks 25-50bp in length. This approach has been extensively used to introduce gene deletions, insertions, generating fusion alleles and promoter insertions (Lorenz *et al*, 1995, Manivasakam *et al*, 1995, Goldstein *et al*, 1999). The efficiency of recombination and the short flanks required permits integration of multiple fragments simultaneously, which is particularly applicable for *in vivo* construction of heterologous expression

cassettes requiring native promoters/ORFs/terminators. As a limited number of selectable markers exist for a specific yeast strain, they can become a limiting factor when performing numerous integrations into chromosomal loci, particularly if later genetic alterations wish to be made to optimise production. Several approaches have been developed to allow marker recycling. Cells expressing *URA3* can be selected against by growing cells on 5-fluoroorotic acid that is metabolised into toxic 5-fluorouracil by *Ura3*. Integrating genes using *URA3* as a selectable marker flanked by 400-500bp of sequence identical to a downstream region can stimulate excision of the *URA3* gene as the identical sequences recombine with each other during mitosis (fig. 1.12). This can be selected for using 5-FOA. Such an approach can be used to recycle the *URA3* marker for multiple chromosomal integrations. However, as 5-FOA is mutagenic, repeated use of this technique can result in off-target phenotypes.

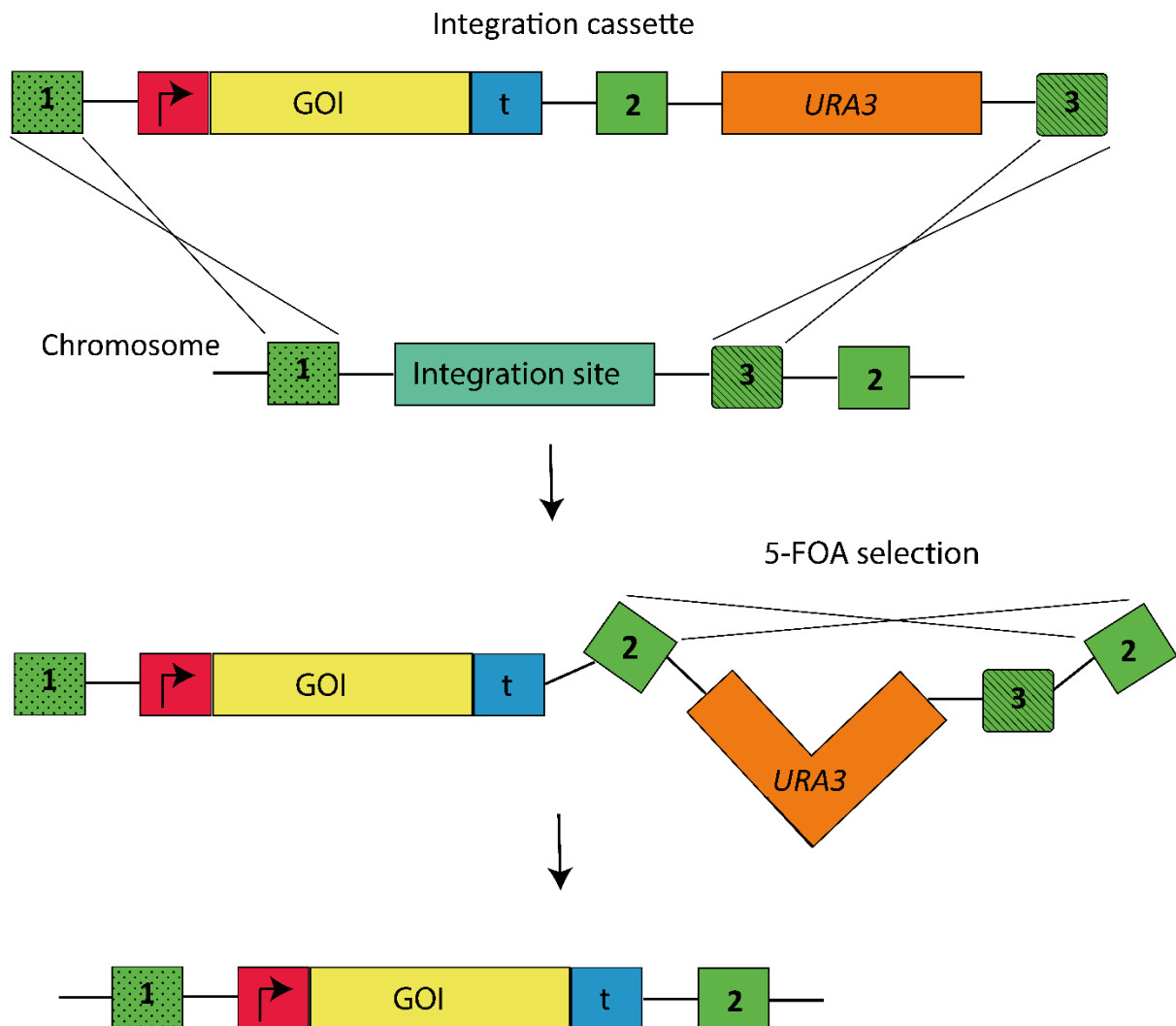


Figure 1.12. Stimulation of marker excision by selection for two round of homologous recombination. Shown is the insert cassette design for marker recycling using *URA3*. Placing 400-500bp identical to a region downstream (labelled 2) of the integration site between the gene of interest and the *URA3* marker, you can select for recombination stimulated marker excision by placing cells on 5-FOA.

Alternative approaches involve integration of selectable markers flanked with 34bp *loxP* sites (fig 1.13). Induced expression of the *CRE* recombinase gene from P1 bacteriophage brings together the

loxP sites and excises them from the chromosome, leaving one *loxP* site (Guldener *et al*, 1996). This allows for repeated use of selectable markers though *loxP* sequences accumulate on the genome at each integration site. There is a risk of recombination at these loci, particularly if repeatedly inducing *CRE* expression; however, this risk is mitigated by selecting distant integration sites.

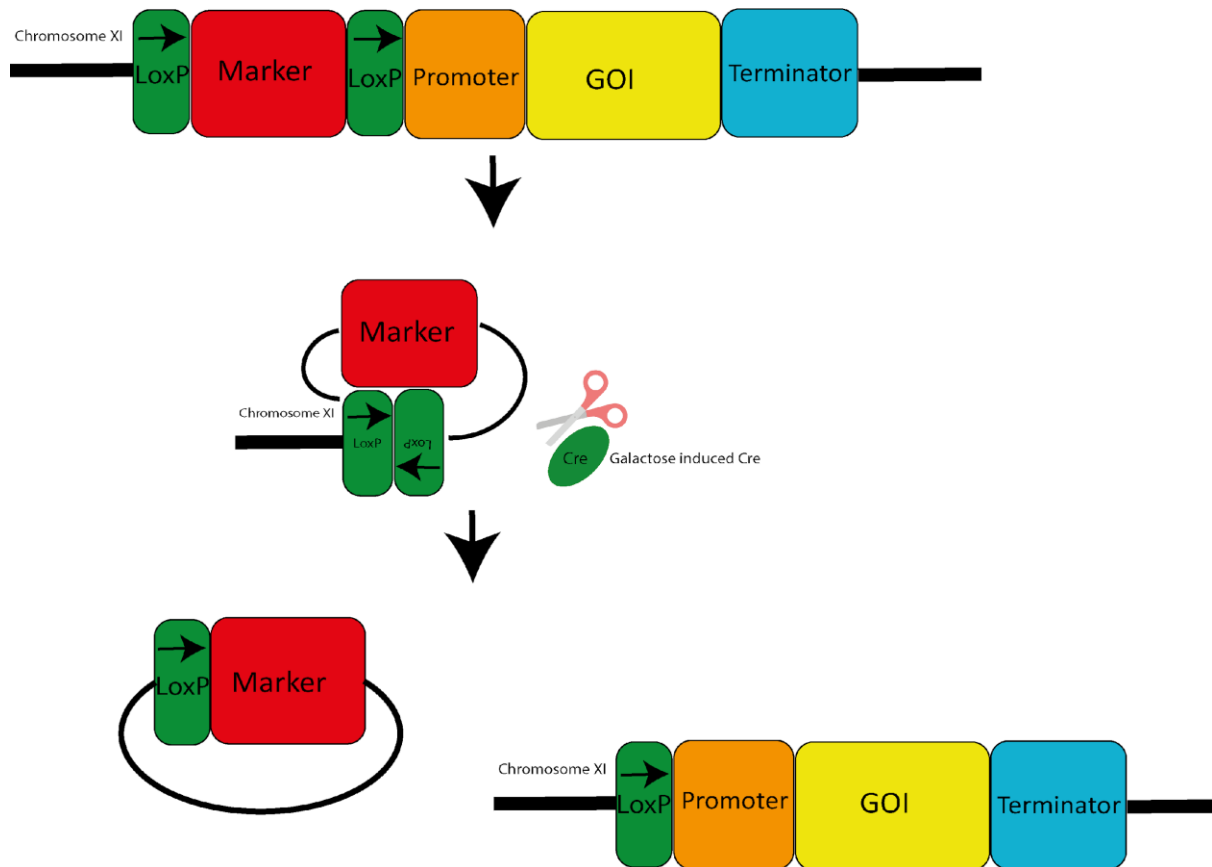


Figure 1.13. Genetic organisation of Cre recombinase mediated marker excision. The schematic details integration organisation for marker excision and recycling expressing Cre recombinase. Upon induction of Cre recombinase expression the LoxP sites are brought together and cleaved by the recombinase. As these flank the selectable marker it is removed from the genome and can be re-used. One LoxP scar remains in place.

1.14 The use of promoters/terminators in optimising gene expression

While gene copy number and gene location can be used to alter gene expression levels, the most common way to adjust expression levels is through promoter/terminator selection. Promoters are found immediately upstream of ATG start codons and recruit RNA pol II to initiate transcription. Promoters dependent on glucose are frequently used as ‘constitutive promoters’ due to the standard practice of using glucose as a carbon source. The most common constitutive promoters are from the glycolytic pathway including *pPGK1* (Ogden *et al*, 1986), *pTPI1* (Alber & Kawasaki, 1982), and *pTDH3* (Holland & Holland, 1980), the promoter *pTEF1* from translation elongation factor is also frequently used. Glycolytic promoters tend to express genes at high levels, which is not always desirable. Mutant variants of *pTEF1* were made displaying a range of activity (Alper *et al*, 2005). Numerous other native

promoters have been identified with a range of strengths, which have been used to study genes with toxic effects.

Alternative approach to regulate gene expression is the use of inducible promoters. These promoters can be induced/repressed through addition of chemicals within the medium. While expression can be varied by altering the concentration of inducing agents, these promoters often show a degree of 'leaky' transcription. The most tightly regulated inducible promoter in yeast are the *GAL* promoters. These regulate the transcription of galactose metabolism genes and are strongly repressed by glucose (Adams, 1972). Numerous genes show galactose induction, in some cases up to a 1000x increase in gene transcription levels when exposed to galactose. A modified *GAL1* promoter was developed which showed variation in induction dependent on the percentage of galactose present in the medium (Hawkins & Smolke, 2008). Such a tool is not as subject to the 'switch' like control of natural *GAL1* induced genes. Inducible promoters controlling heterologous gene expression are advantageous for biotechnological processes demanding a large logarithmically growing seed-culture prior to initiating synthesis.

Terminators are positioned immediately downstream of ORFs at the 3' end, they are generally <300bp long in yeast. These encode 3' UTRs which govern mRNA cleavage and polyadenylation (Richard & Manley, 2009). Additionally, polyadenylation is involved in mRNA stability, localisation and translation efficiency (Yamanishi *et al*, 2012). Common terminator sequences used include the *PGK1* and *TEF1* terminator. A large study used robotics to clone ~5300 yeast terminators onto a *pTDH3-GFP*-terminator construct. Measurement of fluorescence in strains expressing these constructs revealed an 81-fold variation in fluorescence dependent on the terminator used (Yamanishi *et al*, 2012). This indicates that terminators and the 3' UTRs they encode can play a large role in gene expression levels. This has yielded a database of terminator strength that is of value for adjusting heterologous gene expression levels.

1.15 Downstream processes

When developing a biotechnological manufacturing process, it is crucial to consider downstream processes for efficient recovery of the target molecule. High titre producers of biosurfactants may release a visible oily phase into the culture broth. This phase forms as beads and is enriched in MELs but also contains residual triglycerides, fatty acids and water (Rau *et al*, 2005, Fan *et al*, 2014, Goossens *et al*, 2016). These crude MELs do not satisfy the high purity demands of the cosmetics and pharmaceutical industry (Shen *et al*, 2019). The MEL enriched beads are thought to appear when the concentration of MELs is >45g/L. Enrichment of the beads from culture broth can be performed by mechanical separation through a 1mm sieve (Goossens *et al*, 2016). Pure MELs can be refined from these beads through dissolving in ethyl acetate, drying with sodium sulphate and washing with hexane, methanol and water. Most research into MEL production depends on ethyl acetate/hexane as a solvent for extraction (Hewald *et al*, 2005, Saika *et al*, 2016, Morita *et al*, 2015, Mnif *et al*, 2016). Solvent-free methods for MEL enrichment have been developed using ultrafiltration and heat treatment (Andrade *et al*, 2017, Rau *et al*, 2005). These have limited industrial use; ultrafiltration is susceptible to fouling (de Andrade *et al*, 2017). Heating MEL containing culture media to 121°C for 20 minutes separates the MELs from the aqueous phase though the recovered product is not very pure (Rau *et al*, 2005). As MELs are heavier than water they can be recovered through centrifugation and pouring off the supernatant, this is effective but the resulting MEL is too impure for many applications. Demands for high purity MELs mean that most MEL refinement is performed using solvent extraction.

1.16 Aims and objectives

S. cerevisiae is a brilliant model organism. The first eukaryote to have its whole genome sequenced (Goffeau *et al*, 1996), and much understanding of fundamental molecular mechanisms comes from using this model. In this thesis, we shall demonstrate the range of scientific objectives achievable using *S. cerevisiae*, using it to elucidate mechanisms regulating protein activity and as chassis for biotechnological chemical manufacture. This means our aims are dichotomous, exploring fundamental molecular biology as well as demonstrating biotechnological possibilities with *S. cerevisiae*.

Rex1 catalytic activity and substrate specificity has been explored in numerous studies (van Hoof *et al*, 2000, Foretek *et al*, 2016, Skowronek *et al*, 2013, Daniels *et al*, 2022). While Rex1 substrates have been identified, less research has gone into studying its regulation concerning its subcellular localisation or activity in response to environmental conditions. Chapter 3 aims to identify novel Rex1 regulatory effects in stress conditions. Using epifluorescence microscopy, western blot analysis and *in vivo* phospholabelling we explore Rex1 localisation, depletion and post-translational modification in response to heat stress. We also identify an N-terminal NLS domain on Rex1 and demonstrate that Rex1 nuclear import is mediated by the yeast importin- α , Srp1. In chapter 4, we demonstrate numerous genetic techniques for the assembly of multi-gene biosynthetic pathways in *S. cerevisiae*. We verify functional upregulation of this pathway using proteomics and shed light on the limitations of heterologous gene expression for effective biotechnological production of glycolipid biosurfactants in *S. cerevisiae*.

Chapter 2 - Materials and methods

2.1 Chemicals and enzymes

Chemicals used have been sourced from Sigma Aldrich. Media components were purchased from Formedium. Enzymes were sourced from New England Biolabs (NEB) and used in buffers advised by NEB. Enzymes sourced from NEB are supplied at a concentration of 20U/ μ l. Plasmid extraction miniprep kits used are from Qiagen, and gel-purification/PCR cleanup kits were purchased from Omega-Biotek.

2.2 Growth media

2.2.1 Generic growth media

Numerous liquid and agar mediums were used, the composition of which is detailed in table 2.1. All media components were dissolved in MilliQ water and autoclaved at 121°C for 20 minutes. Stock solutions were made of 20% glucose and 30% glycerol, as well as 100x stocks of adenine, leucine, methionine, lysine, uracil, histidine and tryptophan, these were mixed up and autoclaved. Yeast minimal media was made and aliquoted into 90ml bottles prior to sterilization, when needed 10ml of 20% glucose was added to each bottle along with 1ml of amino acid stock solutions leaving out auxotrophic markers. Media was allowed to cool to to ~50°C prior to the addition of sterile amino acid stocks or antibiotics when necessary.

Table 2.1 Composition of media for growth of select organism.

Media	Composition	Organism
Minimal medium 1 (Ym1)	5g Ammonium sulphate 1.9g Yeast nitrogen base 900ml H ₂ O 400 μ l 10M NaOH	<i>S. cerevisiae</i>
Minimal medium 2 (Ym2)	5g Ammonium sulphate 1.9g Yeast nitrogen base 10g Casamino acids 900ml H ₂ O 400 μ l 10M NaOH	<i>S. cerevisiae</i>
Rich yeast medium (YPD)	20g Peptone 10g Yeast Extract 20g Glucose Up to 1l H ₂ O	<i>S. cerevisiae</i>

YPgalactose	20g Peptone 10g Yeast extract 20 Galactose Up to 1l H ₂ O	<i>S. cerevisiae</i>
YPglycerol	20g Peptone 10g Yeast extract 20ml Glycerol Up to 1l H ₂ O	<i>S. cerevisiae</i>
2TY	16g Tryptone 10g Yeast extract 5g NaCl Up to 1l H ₂ O	<i>E. coli</i>
Potato dextrose medium (PDM)	4g Potato extract 20g Glucose Up to 1L H ₂ O	<i>U. maydis</i> <i>M. antarcticus</i>
N-limiting media	1.7g yeast nitrogen base 50ml 0.1M potassium phosphate buffer pH 6 Up to 1L H ₂ O	<i>U. maydis</i> <i>M. antarcticus</i>
YpO 0.12%	1.2ml Oleic acid 20g Glucose 20g Peptone 10g Yeast extract 2ml Tween 20 50ml 0.1M Potassium phosphate buffer pH 6 Up to 1L H ₂ O pH adjusted to 6.5	<i>S. cerevisiae</i>
YpO 0.3%	3ml Oleic acid 20g Glucose 20g Peptone	<i>S. cerevisiae</i>

	<p>10g Yeast extract</p> <p>2ml Tween 20</p> <p>50ml 0.1M Potassium phosphate buffer pH 6</p> <p>Up to 1L H₂O</p> <p>pH adjusted to 6.5</p>	
YpO 0.8%	<p>8ml Oleic acid</p> <p>20g Glucose</p> <p>20g Peptone</p> <p>10g Yeast extract</p> <p>2ml Tween 20</p> <p>50ml 0.1M Potassium phosphate buffer pH 6</p> <p>Up to 1L H₂O</p> <p>pH adjusted to 6.5</p>	<i>S. cerevisiae</i>
YpGn 1%	<p>10ml Groundnut oil</p> <p>20g Glucose</p> <p>20g Peptone</p> <p>10g Yeast extract</p> <p>2ml Tween 20</p> <p>50ml 0.1M Potassium phosphate buffer pH 6</p> <p>Up to 1L H₂O</p> <p>pH adjusted to 6.5</p>	<i>S. cerevisiae</i>
YpGn 4%	<p>40ml Groundnut oil</p> <p>20g Glucose</p> <p>20g Peptone</p> <p>10g Yeast extract</p> <p>2ml Tween 20</p> <p>50ml 0.1M Potassium phosphate buffer pH 6</p> <p>Up to 1L H₂O</p>	<i>S. cerevisiae</i>

	pH adjusted to 6.5	
YpGn 8%	80ml Groundnut oil 20g Glucose 20g Peptone 10g Yeast extract 2ml Tween 20 50ml 0.1M Potassium phosphate buffer pH 6 Up to 1L H ₂ O pH adjusted to 6.5	<i>S. cerevisiae</i>
YpME 5% Gn	50ml Groundnut oil 20g Glucose 20g Peptone 10g Yeast extract 2ml Tween 20 50ml 0.1M Potassium phosphate buffer pH 6 Up to 1L H ₂ O pH adjusted to 6.5	<i>S. cerevisiae</i>
Solid media	2% (w/v) agar was added to media described above prior to autoclaving. Once sterile agar was allowed to cool until ~50°C and poured into sterile petri dishes. These were left to dry under sterile laminar flow before being stored at 4°C.	<i>S. cerevisiae</i> <i>U. maydis</i> <i>M. antarcticus</i>

2.2.2 Phosphate depleted YPD

10g yeast extract, 20g peptone and 2.46g MgSO₄ was dissolved in 950ml dH₂O. 4ml NH₄OH was added and the media left stirring while a white precipitate formed. This was filtered through Whatman GF/B paper and brought to pH 7.0 with HCL. 20g glucose was added, dH₂O was added to 1L and the media autoclaved.

2.3 Strains and plasmids

2.3.1 Strains

Table 2.2. Yeast strains used in this study. Gene deletions/insertions were performed as described in (Longtine <i>et al</i> , 1998). 5-FOA counterselection was performed as described in (Boeke <i>et al</i> , 1987).		
<i>S. cerevisiae</i> strain	Genotype	Source
BY4741 WT	MATA <i>his3Δ leu2Δ met15Δ ura3Δ</i>	Euroscarf
BY4742 WT	MATα <i>his3Δ leu2Δ met15Δ ura3Δ</i>	Euroscarf
REX1-HTP	MATA <i>his3Δ leu2Δ met15Δ ura3Δ REX1-HTP::KLURA3</i>	Mitchell lab
REX1-mNG	MATA <i>his3Δ leu2Δ met15Δ ura3Δ REX1-mNG::URA3</i>	Mitchell lab
<i>srp1-31</i>	MATα <i>ade2-1 his3-11 trp1Δ63 ura3-1 leu2-3, 112 can1-100 srp1-31</i>	Tabb <i>et al</i> , 2000
<i>srp1-49</i>	MATα <i>ade2-1 his3-11 trp1Δ63 ura3-1 leu2-3, 112 can1-100 srp1-49</i>	Tabb <i>et al</i> , 2000
<i>rex1-mNG S/A</i>	MATA <i>his3Δ leu2Δ met15Δ ura3Δ rex1-mNG S/A</i>	This study
<i>rex1-mNG S/E</i>	MATA <i>his3Δ leu2Δ met15Δ ura3Δ rex1-mNG S/E</i>	This study
<i>rex1-HTP S/A</i>	MATA <i>his3Δ leu2Δ met15Δ ura3Δ rex1 S/A-HTP::KLURA3</i>	This study
<i>rex1-HTP S/E</i>	MATA <i>his3Δ leu2Δ met15Δ ura3Δ rex1 S/E-HTP::KLURA3</i>	This study
MAC2	MATA <i>his3Δ leu2Δ met15Δ ura3Δ MAC2::KL LEU2</i>	This study
EMT1	MATα <i>his3Δ leu2Δ met15Δ ura3Δ EMT1::HIS3MX6</i>	This study
MAC2, EMT1	MATAα MATA <i>his3Δ leu2Δ met15Δ ura3Δ MAC2 EMT1</i>	This study

MAC2, EMT1, MMF1	MATA α MATA <i>his3Δ leu2Δ</i> <i>met15Δ ura3Δ MAC2 EMT1</i> <i>MMF1::HIS3MX6</i>	This study
------------------	------------------------------------------------------------------------------------------------------------------------------------------------------------------------	------------

2.3.2 *E. coli*

Table 2.3. Strains of *Escherichia coli* used in this study.

<i>E. coli</i> strain	Genotype	Purpose	Source
DH5 α	<i>supE44 ΔlacU169</i> (Φ 80 <i>lacZ ΔM15</i>) <i>hsdR17 recA1</i> <i>endA1gyrA96 thi-1</i> <i>relA1</i>	Plasmid recovery and amplification.	Hanahan, 1983

2.3.3 Plasmids

The plasmids used in this study were generated using select vectors detailed in table 2.4. From these, plasmids were made through restriction digestion of vector followed by insert ligation and transformation to *E. coli*. Alternatively, they were constructed *in vivo* through homologous recombination in *S. cerevisiae*. These are detailed in table 2.5.

Table 2.4. Plasmid vectors used for plasmid construction in this study.

Plasmid	Description	Source
Ycplac33	<i>URA3/Amp</i> marker, CEN4, single copy vector	Gietz and Sugino, 1988
Ycplac111	<i>LEU2/Amp</i> marker, CEN4, single copy vector	Gietz and Sugino, 1988
pRS313	<i>HIS3/Amp</i> marker, CEN6, single copy vector	Sikorski & Hieter, 1989
pRS416	<i>URA3/Amp</i> marker, CEN6, single copy vector	Sikorski & Hieter, 1989
pTL26	<i>HIS3/Amp</i> , CEN6, single copy vector	Lafontaine & Tollervey, 1996

pUG72	<i>loxP</i> flanked <i>KLURA3</i> integration cassette vector	Gueldener <i>et al</i> , 2002
pUG27	<i>loxP</i> flanked <i>SPHIS3</i> integration cassette vector	Gueldener <i>et al</i> , 2002
pSH62	Gal inducible <i>CRE</i> recombinase, <i>HIS3</i> marker	Gueldener <i>et al</i> , 2002

Table 2.5. Plasmids used in this study. Descriptions, parental vectors, original vectors and plasmid source are shown.

Plasmid	Made from	Vector	Source
Rex1 truncation analysis			
GFP- <i>REX1</i>	zz- <i>REX1</i>	pTL26	Mitchell lab
GFP- <i>REX1</i> 428-476 Δ	zz- <i>REX1</i>	pTL26	Mitchell lab
GFP- <i>REX1</i> W509X	zz- <i>REX1</i>	pTL26	Mitchell lab
GFP- <i>REX1</i> 1-202 Δ	zz- <i>REX1</i>	pTL26	Mitchell lab
GFP- <i>REX1</i> 1-82 Δ	zz- <i>REX1</i>	pTL26	Mitchell lab
GFP- <i>REX1</i> 12-52 Δ	zz- <i>REX1</i>	pTL26	Mitchell lab
GFP- <i>REX1</i> 42-52 Δ	zz- <i>REX1</i>	pTL26	Mitchell lab
GFP- <i>REX1</i> 17-52	zz- <i>REX1</i>	pTL26	Mitchell lab
GFP- <i>REX1</i> 17-52 Δ + SV40NLS	zz- <i>REX1</i>	pTL26	Mitchell lab
Phosphomimetic and non-phosphorylatable <i>REX1</i> alleles			
GFP- <i>rex1</i> S24,T26,S27,T34/A	GFP- <i>REX1</i>	pTL26	This study
GFP- <i>rex1</i> S24,T26,S27,T34/E	GFP- <i>REX1</i>	pTL26	This study
GFP- <i>rex1</i> S18, S24,T26,S27,T34,S38/A	GFP- <i>REX1</i>	pTL26	This study
GFP- <i>rex1</i> S18, S24,T26,S27,T34,S38/E	GFP- <i>REX1</i>	pTL26	This study
p<i>REX1</i> promoter synthesis			
p <i>REX1</i> -GFP- <i>REX1</i>	GFP- <i>REX1</i>	pTL26	This study

<i>pREX1-GFP-rex1-S/A</i>	<i>pREX1-GFP-REX1</i>	pTL26	This study
<i>pREX1-GFP-rex1-S/E</i>	<i>pREX1-GFP-REX1</i>	pTL26	This study
<i>1kbpREX1-GFP-REX1</i>	<i>GFP-REX1</i>	pTL26	This study
<i>1kbpREX1-GFP-rex1-S/A</i>	<i>1kbpREX1-GFP-REX1</i>	pTL26	This study
<i>1kbpREX1-GFP-rex1-S/E</i>	<i>1kbpREX1-GFP-REX1</i>	pTL26	This study
GFP fusion proteins of <i>U. maydis</i> MEL biosynthetic enzymes			
<i>MMF1-GFP</i>	<i>pTPI-tPGK1-GFP</i>	Ycplac33	This study
<i>MAT1-GFP</i>	<i>pTPI-tPGK1-GFP</i>	Ycplac33	This study
<i>GFP-MAC1</i>	<i>GFP-pTPI-tPGK1</i>	Ycplac33	This study
<i>EMT-GFP</i>	<i>pTPI-tPGK1-GFP</i>	Ycplac111	This study
<i>GFP-MAC2</i>	<i>GFP-pTPI-tPGK1</i>	Ycplac33	This study
MEL pathway expression constructs			
<i>pHIS3-MMF1-tSPO7</i>	<i>MAT1-GFP</i>	Ycplac33	This study
<i>pTDH3-EMT1-tPRS1</i>	<i>MAT1-GFP</i>	Ycplac33	This study
<i>pTPI-MAT1-tAI2</i>	<i>MAT1-GFP</i>	Ycplac33	This study
<i>pTEF1-MAC1-pPGK1</i>	<i>MAT1-GFP</i>	Ycplac33	This study
<i>pADH1-MAC2-VPS71</i>	<i>MAT1-GFP</i>	Ycplac33	This study
<i>pHIS3-MMF1-tSPO7</i> spacers removed	<i>pHIS3-MMF1-tSPO7</i>	Ycplac33	This study
<i>pTDH3-EMT1-tPRS1</i> spacers removed	<i>pTDH3-EMT1-tPRS1</i>	Ycplac33	This study
<i>pTPI-MAT1-tAI2</i> spacers removed	<i>pTPI-MAT1-tAI2</i>	Ycplac33	This study
<i>pTEF1-MAC1-pPGK1</i> spacers removed	<i>pTEF1-MAC1-pPGK1</i>	Ycplac33	This study
<i>pADH1-MAC2-VPS71</i> spacers removed	<i>pADH1-MAC2-VPS71</i>	Ycplac33	This study
<i>pTPI-MAT1-tAI2</i> + <i>pTEF1-MAC1-pPGK1</i>	<i>MAT1-GFP</i>	Ycplac33	This study
MEL biosynthetic enzyme integration cassettes			
<i>pTDH3-EMT1-tPRS1, SPHIS5</i>	<i>pTDH3-EMT1-tPRS1</i>	Ycplac33	This study

pADH1-MAC2-VPS71, KLLEU2	pADH1-MAC2-VPS71	Ycplac33	This study
pHIS3-MMF1-tSPO7, SPHIS5	pHIS3-MMF1-tSPO7	Ycplac33	This study

2.4 Long term storage of organisms

For long-term storage, liquid cultures of all organisms were grown shaking at a suitable temperature until a visibly dense culture was obtained. Typically, this was overnight but in the case of *M. antarcticus* and *U. maydis* 48 hours was needed. 0.7ml of this dense suspension was added to 1ml of 30% glycerol in a cryo-tube. This was inverted several times and left on the bench for 5 minutes prior to storage at -80°C. For novel organisms, a loop was used to streak some of this glycerol stock onto agar to ensure viability.

2.5 *S. cerevisiae* molecular biology protocols

2.5.1 Growth and maintenance of *S. cerevisiae* strains

S. cerevisiae lab strain BY4741 was used for all experiments, grown on either yeast rich media (YPD, see table 2.1) or on yeast minimal media (YM1, YM2).

Glycerol stocks were taken from the -80°C freezer and streaked onto YPD plates, these were grown at 30°C until visible colonies formed. Subsequently the plate was stored on the bench and colonies were taken as needed. Plates were re-streaked every 2 weeks onto fresh agar. Liquid cultures were prepared by inoculating 5ml of a suitable media with a single colony from a plate and left shaking at 200RPM at 30°C overnight.

2.5.2 One-step transformation

Yeast were transformed with plasmids through the one-step transformation protocol (Chen *et al*, 1992). 5ml of appropriate media was inoculated with the strain to be transformed and allowed to grow overnight at 30°C, shaking at 200 RPM. The following day 200µl of this culture was centrifuged at 12000 *g* and the supernatant removed. To the pellet was added 50µg of single stranded DNA (ssDNA) from salmon sperm, and 50µl of one-step buffer (0.2M LiAc pH 5.0, 40% (w/v) PEG 4000 (polyethylene glycol), 0.1M DTT). The tube was vortexed for 30s and left to stand at room temperature for 3-5 hours. The tube was heat shocked at 42°C for 30 minutes prior to being spread on selective solid media. Plates were incubated at 30°C for 2 days until visible colonies appeared.

2.5.3 High efficiency yeast transformation

High efficiency yeast transformations were performed for genetic integrations and to construct plasmids. High efficiency transformations were conducted using the lithium acetate method as described in (Gietz & Woods, 2002). Overnight cultures of *S. cerevisiae* are grown on YPD, shaking at 200RPM at 30°C. The following day this culture is used to inoculate 5ml of fresh YPD at OD₆₀₀ = 0.1 and left shaking at 200RPM at 30°C until the cells reach log phase, measured as OD₆₀₀ = ~0.5. This culture is centrifuged at 1118 *g* for 5 minutes and the supernatant discarded. The cells are washed with 1ml sterile water and transferred to a 1.5ml eppendorf tube. This is centrifuged at 2041*g* for 1 minute, the

supernatant discarded and the cells resuspended in 1ml TE/Li-Ac buffer (100mM LiAc pH 7.5, 10mM Tris-Cl pH 7.5, and 0.1 mM EDTA). This mixture is centrifuged at 2041g for 2 minutes and the supernatant is discarded. The pellet is then resuspended in 50µL of TE/Li-Ac and 100ng of cut vector is added alongside 100-200ng of the PCR product insert depending on concentration. To this we add 300µL sterile 40% PEG3350 and 50ng single stranded salmon sperm DNA (Sigma Aldrich). This tube is inverted numerous times and left standing at room temperature for 30 minutes. The mixture is then transferred to 30°C for 30 minutes before being heat shocked at 42°C for 15 minutes. Subsequently, the cells are centrifuged for 30 seconds at 13800g, the pellet is resuspended in 75µL of 1x TE and plated out on selective agar. Cells are incubated at 30°C until colonies are visible approximately 2 days later.

2.5.4 Isolation of yeast genomic DNA

Cells are scraped from a plate or inoculated into liquid media and grown overnight, shaking at 200RPM at 30°C. The culture is centrifuged for 1 minute at 11758 g in 2ml screw-capped tubes. The supernatant is removed and the pellet washed in 1ml of sterile water. This mixture is centrifuged at 11758g for 1 minute and the supernatant removed. 200µl of TENTS solution (20mM Tris-Cl pH 8.0, 1mM EDTA, 100mM NaCl, 2% Triton X100, 1% SDS), 200µl of glass beads (0.5mm in diameter) and 200µl of phenol/chloroform (25:24:1 phenol/chloroform/isoamyl alcohol) is added and the tube is shaken in a bead beater for 45s. The tubes are then spun at 11758g for 30s. Another 200µl of TENTS is added and the tubes are vortexed and centrifuged at 11758g for 5 minutes. 350µl of the supernatant is removed and added to a fresh 1.5ml microfuge tube. To this a further 200µl of phenol/chloroform is added, the mixture is vortexed and centrifuged at 11758g for 5 minutes. 300µl of the supernatant is transferred to a fresh 1.5ml microfuge tube. Nucleic acids are precipitated using 30µl 3M NaAc (pH 5.2) and 750µl 100% ethanol. The mixture is vortexed and stored at -20°C for 1 hour. Subsequently, the sample is centrifuged at 11758g for 10 minutes, the supernatant is removed and the pellet washed with 500µl of 70% ethanol prior to being centrifuged at 11758g for a further 10 minutes. The supernatant is removed and the pellet resuspended in 200µl 1xTE pH 8.0. 2µl RNase (10mg/ml) is added and the mixture left at room temperature for 10 minutes. 30µl 3M NaAc (pH 5.2) and 500µl 100% ethanol is added and the sample left to precipitate at -20°C for 1 hour. The sample is centrifuged at 11758g for 15 minutes, the supernatant removed and the pellet washed with 500µl of 70% ethanol prior to being re-centrifuged at 11758g for 5 minutes. The supernatant is removed and the pellet dried at 54°C for 15 minutes. The pellet is resuspended in 100µl 1xTE and stored at -20°C.

This protocol was repeated for genomic DNA isolation from *U. maydis* except a liquid culture was grown for 48 hours prior to extraction.

2.5.5 *in vivo* ³²P phospholabelling and protein extraction

50ml of culture is grown to OD₆₀₀=0.6 in phosphate depleted YPD, this culture is centrifuged at 4653 g for 5 minutes. The pellet is resuspended in 3ml of fresh phosphate depleted YPD. ³²P orthophosphate is added to the culture and it is left shaking at 30°C for 1 hour. Subsequently cells are pelleted in a 2ml screwcap tube for protein extraction.

Pellets are resuspended in 250µl TBST, 1µ PMSF, 1µl protease inhibitor cocktail and 2.5µ okadaic acid are added alongside 200µl of glassbeads (0.5mm in diameter). The samples are vortexed for 30s and placed on ice for 30s. This is repeated 10x. Samples are centrifuged at 11758 g for 5 minutes at 4°C

and the supernatant is moved to a fresh tube. 750µl of TBST is added to the cell debris, vortexed for 30s and centrifuged at 11758 *g* for 5 minutes at 4°C. AS much of this supernatant as possible is removed and pooled with the previous lysate. The total lysate is clarified by centrifuging at 11758 *g* for 30 minutes at 4°C.

Per sample 50µl IgG affinity sepharose beads are pooled. These are washed with 1ml TBST, centrifuged at 760 *g* and the supernatant removed. This is repeated 3x and the beads are placed in 50µl aliquots for each sample tube.

The clarified lysate is added to the beads and left rotating at 4°C for 2 hours. Subsequently the samples are washed by centrifuging at 760 *g* for 2 minutes, removing the supernatant, adding 1ml TBST and rotating for 5 minutes at 4°C. The samples are washed 3x with TBST, 3x with TBST + 2M MgCl₂ and 3x with TBST. After the final wash, the samples are centrifuged at 760 *g* for 2 minutes and as much supernatant as possible removed. Protein is eluted from the beads through addition of 50µl 0.5M acetic acid, manual mixing for 5 minutes and centrifugation at 760 *g* for 2 minutes. The eluate is moved to a fresh tube and elutions are repeated 2x. 10µg of glycogen and 1ml butanol is added to the elution and it is left at -80°C overnight. The following day the sample is thawed and centrifuged at 11758 *g* for 30 minutes at 4°C. The supernatant is removed and the pellet is washed with 40µl -20°C ethanol. The sample is centrifuged at 11758 *g* for 10 minutes at 4°C. The supernatant is removed and the pellet is dried at 65°C for 10 minutes. The pellet is resuspended in 20µl 50% urea and 5µl 5x PLB, this can be analysed through SDS-PAGE.

2.5.6 SDS-PAGE

Sodium dodecyl sulphate polyacrylamide gel electrophoresis (SDS-PAGE) was performed as described in (Sambrook & Russel, 2006). 10-12% gels were cast from mixtures described in table 2.6. Protein-loading dye was added to protein extracts at 1x final concentration prior to gel loading. A constant voltage (75-130V) was applied to gels until the dye front ran off the bottom of the gel.

Composition of buffers used in gel running are as follows;

Protein running buffer (10x): 30.28g Tris base, 144.13g glycine, 1% (w/v) sodium dodecyl sulphate, dH₂O up to 1L.

Protein loading dye (4x): 250mM Tris pH 6.8, 9.2% (w/v) sodium dodecyl sulphate, 40% glycerol, 0.2% (w/v) bromophenol brilliant blue, 100mM DTT.

Table 2.6. Composition of SDS acrylamide gels used in this study.			
Reagent	10% Resolving gel	12% Resolving gel	4% Stacking gel
Protogel (Acrylamide, Bis-acrylamide mix) 30% stock	3.3ml	4ml	0.65ml
Resolving buffer 4X stock	2.6ml	2.6ml	N/A
Stacking buffer 4X stock	N/A	N/A	1.25ml
APS 10% (w/v) stock	100µl	100µl	50µl
TEMED 1000X stock	10µl	10µl	5µl
dH ₂ O	4.1ml	3.4ml	3.05ml

Total volume	10ml	10ml	5ml
--------------	------	------	-----

2.5.7 Alkaline protein lysis

Protein extracts for analysis through SDS-PAGE/western blot were prepared as described in Motley *et al*, 2012.

10OD₆₀₀ of logarithmically growing yeast cells were harvested by centrifugation at 4653 *g*. The pellet is resuspended in 500µl ice-cold 0.2M NaOH/0.2% β-mercaptoethanol and incubated on ice for 10 minutes. 100µl of 30% trichloroacetic acid is added and the mixture incubated on ice for a further 5 minutes.

Centrifuge mixture at 13000 *g* for 5 minutes at 4°C. Remove the supernatant and resuspend in 75µl 50% urea. Add 25µl of 4x protein loading buffer. Heat for 10 minutes at 95°C and spin at 13000 *g* for 5 minutes prior to loading on gel. 10µl can be used to resolve 1OD of protein by SDS-PAGE.

2.5.8 Protein analysis by western blot.

Protein samples were resolved by SDS-PAGE. Transfers to nitrocellulose membrane were performed using a Biorad Mini Trans-Blot Electrophoretic transfer cell. A 2-hour transfer was conducted applying a 200mA current for 2 hours in transfer buffer (25mM Tris pH 8.3, 150mM Glycine, 40% (v/v) methanol). Protein transfer was verified using Ponceau S solution (0.1% (w/v) Ponceau S in 5% (v/v) acetic acid). Blots were blocked in 1 hour using a blocking buffer (2% (w/v) skim milk powder in TBS–Tween 20 (50 mM Tris-HCl, pH 7.5, 150 mM NaCl, and 0.1% (v/v) Tween 20)). Membranes were incubated with primary antibodies for 2 hours at room temperature in TBS-Tween 20. Membranes were incubated with secondary antibodies for 1 hour in TBS-Tween 20. Membranes were washed 3x for five minutes with TBS-Tween 20 between antibody treatments. Primary A

antibodies were used at the given dilutions: anti-GFP (1:3000), anti-PGK1 (1:7000), peroxidase anti-peroxidase (1:10000). Secondary antibody was HRP-linked anti-mouse polyclonal (1:10000). Blots were developed using Enhanced Chemi-Luminescence (ECL) substrates and tagged proteins were detected and imaged using a Syngene GBox imaging system and Genesys software

2.5.9 Protein extraction for analysis by mass-spectrometry

200 ODs of logarithmically growing cells were harvested through centrifugation to a 2ml screw capped tube. The cell pellet was washed with 1ml 0.9% NaCl, centrifuged at 13000 *g* and the supernatant removed. The cell pellet is resuspended in 400µl lysis buffer (5% SDS, 50mM TEAB pH 9.5). 1µl protease inhibitor cocktail, 1µl PMSF, 2.5µl okadaic acid and 1µl phosphatase inhibitor cocktail is added to the sample. ~2-4x cell pellet volume of glass beads (0.5mm in diameter) is added to the tube. The sample is shaken in a beadbeater for 40s and placed on ice for 30s to cool. This is repeated 10x. The sample is centrifuged at 13000 *g* at 5°C for 30 minutes. The supernatant is moved to a fresh 1.5ml microfuge tube and is centrifuged at 13000 *g* at 4°C again. This lysate is transferred to a fresh 1.5ml microfuge tube. The lysate is ready for analysis by SDS-PAGE and MS.

2.5.10 Fluorescence microscopy

Cells were analysed by microscope (Axiovert 200M; Carl Zeiss, Inc.) equipped with Exfo X-cite 120 excitation light source (Carl Zeiss, Inc. and Chroma), a Plan-Apochromat 63x 1.4 NA objective lens (Carl Zeiss, Inc.) and a digital camera (Orca ER; Hamamatsu Photonics). Image acquisition was performed

taking 0.5µm z-stacks in Volocity software (PerkinElmer). z-stacks were merged into one plane using imageJ/FIJI and further processed using Photoshop (Adobe). Single focal planes are shown where necessary. Brightfield images were processed to show the circumference of cells in blue. For relative fluorescence intensity throughout the cell an equivalent area was measured in areas of interest and intensity measured using ImageJ/FIJI.

2.5.10 Heat shock assays

For analysis of tagged protein levels over a shift to heat-stress conditions the following assay was developed. *S. cerevisiae* expressing tagged proteins were grown overnight in 3ml suitable media at 30°C, shaking at 200RPM. The following day this culture was diluted 1/10000x in 50ml fresh media and allowed to grow overnight shaking at 200RPM at 30°C. When the culture reached mid/late log phase ($OD_{600} = 0.6-0.9$), 5 ODs were harvested and stored at -80°C. The flask was heat shocked at 39°C shaking for 10 minutes and moved to a 39°C incubator. 5 OD cell pellets were harvested every 10 minutes and stored at -80°C for later protein extraction by alkaline lysis.

2.5.11 *S. cerevisiae* mating

Cells of opposite mating types were grown on liquid YPD at 30°C until log phase ($OD_{600} = 0.5$). 5µl of each liquid culture was pipetted directly onto each other on solid YPD and allowed to grow overnight at 30°C. The following day cells were streaked onto YM1 lys- met- media to select for mated diploids.

2.6 *Escherichia coli* protocols

2.6.1 Growth and maintenance of *E. coli*

E. coli strain DH5αTM (Invitrogen, Life Technologies Corporation, Paisley, UK) were obtained and used for making chemically and electrocompetent cells. Stocks were kept at -80°C in 15% glycerol and streaked onto 2TY solid media when required. Liquid cultures were grown overnight at 37°C, shaking at 200RPM. When selecting for transformants 75µg/ml ampicillin or 50µg/ml kanamycin was added.

2.6.2 Transformation of chemically competent *E. coli*

50µl chemically competent DH5α were removed from -80°C storage and thawed on ice. ~200ng plasmid DNA or 10µl ligation mixture was added to the cells and incubated on ice for 20 minutes. The cells were heat shocked at 42°C for 2 minutes and transferred back onto ice for 5 minutes. 900µl 2TY was added to each sample and the tube incubated at 37°C for 45 minutes. The tube was centrifuged at 5225 *g* and 850µl of the supernatant removed. The cell pellet was carefully resuspended in the remaining supernatant and spread onto selective solid 2TY. Plates were incubated at 37°C overnight until colonies were visible. Subsequently plates were stored at 4°C.

2.6.3 Transformation of electrocompetent *E. coli*

40µl of electrocompetent *E. coli* were removed from storage at -80°C and thawed on ice. 10µl of diluted gDNA was added to the cells. The mixture was loaded into a 2mm electroporation cuvette (Geneflow) and loaded into a Biorad MicroPulser and the cells electroporated at 2.5kV for a single pulse. 600µl of 2TY was immediately added to the cells and they were transformed to a 1.5ml microfuge tube. The mixture was incubated at 37°C for 45 minutes. The mixture was centrifuged at

3000 *g* or 1 minute, the supernatant removed and the cells plated onto selective solid 2TY. The plate was incubated at 37°C overnight until colonies appeared. Plates were subsequently stored at 4°C.

2.6.4 Production of chemically competent *E. coli*

E. coli were rendered competent as described in Hanahan, 1983.

E. coli DH5 α were thawed from -80°C and grown overnight at 37°C on solid 2TY agar. The following day 4ml of liquid 2TY was inoculated with a single *E. coli* colony and allowed to grow overnight at 37°C shaking at 200RPM. The following morning this culture was used to inoculate 200ml liquid 2TY in a 1L flask at OD₆₀₀ = 0.1. This culture was left in an orbital shaker at 37°C at 200RPM until the cells reached exponential phase (OD₆₀₀ = 0.5). The culture was cooled on ice for 10 minutes. Subsequently, the culture was split into 4 50ml falcon tubes and centrifuged at 1610 *g* at 4°C. The supernatant was discarded and the pellets resuspended in 35ml ice-cold RF1 (table 2.7). 2 tubes were pooled, leaving 2 70ml tubes, these were incubated on ice for 20 minutes and centrifuged as before. The supernatant was discarded and each pellet resuspended in 8ml ice cold RF2, the pellets were pooled yielding 16ml. 200 μ l aliquots were prepared into pre-cooled 1.5ml microfuge tubes. These were snap frozen in liquid N₂ and stored at -80°C.

Table 2.7. Composition of buffers for producing chemically competent *E. coli* DH5 α .

RF1 (pH 5.8)	RF2 (pH 6.8)
100mM RbCl	10mM MOPS
50mM MnCl ₂	10mM RbCl
30mM Potassium acetate	75mM CaCl ₂
10mM CaCl ₂	15% (v/v) Glycerol
15% (v/v) Glycerol	

2.6.5 Production of electrocompetent *E. coli*

E. coli DH5 α were thawed from -80°C, streaked on solid 2TY again and left at 37°C to grow overnight. The following day a single colony was picked to inoculate 4ml liquid 2TY and grown overnight at 37°C shaking at 200RPM. The following morning this culture was used to inoculate 1L liquid 2TY at OD₆₀₀ = 0.1. This culture was grown until the cells reached exponential phase (OD₆₀₀ = 0.5). The culture was split into 2, 500ml cultures in a sterile centrifuge bucket and centrifuged at 1610*g* for 15 minutes at 4°C. The supernatant was discarded and each pellet resuspended in 250ml ice-cold 10% (v/v) glycerol. The cells were centrifuged twice more as before with the pellets being resuspended first in 125ml ice cold 10% (v/v) glycerol and then in 50ml ice cold 10% (v/v) glycerol, subsequently, both cultures were transferred to 50ml falcon tubes. The falcon tubes were centrifuged at 1610*g*, the supernatant discarded and both pellets resuspended in 0.35ml of ice-cold 10% (v/v) glycerol. The suspensions were pooled and 40 μ l aliquots of cells were placed into pre-cooled 1.5ml microfuge tubes. The aliquots were flash-frozen in liquid N₂ and stored at -80°C.

2.7 DNA procedures

2.7.1 Polymerase chain reaction

PCR was used to amplify regions of DNA or whole plasmids for SDM. Where proofreading activity was required VELOCITY™ DNA polymerase (Bioline) was used. MYTAQ™ DNA polymerase (Bioline) was used for colony PCR. 25µl reactions were set up as outlined in table 2.8. PCR reactions were performed with 30 cycles and temperature conditions conditions are detailed in table 2.9.

Table 2.8 Composition of PCR reaction tubes. Reaction tube set up for PCR amplification of DNA fragments using Velocity and MyTaq DNA polymerase is shown below. PCRs were set up in 25µl reactions.

VELOCITY™ DNA polymerase	MYTAQ™ DNA polymerase
10.25µl MilliQ H ₂ O	14.75µl MilliQ H ₂ O
5µl Hifi buffer	5µl MyTaq reaction buffer
2.5µl 5mM Forward Primer	2.5µl 5mM Forward primer
2.5µl 5mM Reverse primer	2.5µl 5mM Reverse primer
2.5µl 2.5mM dNTPs	1µl Template DNA (1-5ng/µl)
1µl Template DNA (1-5ng/µl)	0.25µl MyTaq DNA polymerase
0.25µl Velocity DNA polymerase	

Table 2.9. PCR reaction conditions. Detailed below are the cycling conditions used for Velocity and MyTaq DNA polymerase used in this study.

	VELOCITY™	MYTAQ™
1 – Initial DNA denaturation	2 min at 98°C	2 min at 95°C
2 - DNA denaturing	30s at 98°C	30s at 95°C
3 – Annealing of primers	30s at 50-65°C	45s at 50-65°C
4 – DNA elongation	72°C 30s/kb	72°C 1min/kb

5 – Final extension	5 min at 72°C	10 min at 72°C
----------------------------	---------------	----------------

2.7.2 Primer Design

Primers were sourced from Merck (formerly Sigma-Aldrich), coding sequences for sequences of interest were sourced from Uniprot or the NCBI website. Primers were designed to have a melting temperature >60°C based on the formula;

$$T_m = 4(G+C) + 2(A+T)$$

Primers were designed to have a GC content between 45% and 55% and be between 20 - 25 bp long. The 3' end of primers was capped with one, or 2 G's or C's. Primers arrived as powders, these were made into 100mM stocks in 1xTE following. Stocks were diluted 20x with dH₂O yielding 5mM working stocks. All primers were stored at -20°C following suspension.

All primers used are available in table 2.10

Table 2.10. Table list all primers used in this study and details their function.

Primer number	Description	Sequence 5' -> 3'
49	M13 in ycplac F	GTTTTCCCAGTCACGACG
4231	pHIS3 F	AACGACGGCCAGTGAATTATATGGAATGGACGAATTCCTAGTACACTCTATATTTT TTTATGC
4232	pHIS3 R	AAGCTTTCATATTAGGTACCTTTGCCTTCGTTTATCTTGCCTG
4233	MMF1 ORF F	GGTACCTAATATGAAAGCTTAAAATGGCCGACGAGAAGAGGAC
4234	MMF1 ORF R	TTGATCTATCGATAAGCTCCCGGTATACTATTAGGATCCCTAACTAGTGGGCAAGGT ACTCG
4239	tSPO7 F	GGATCCTAATAGTATACCCGGGAAGAGTTGGAGGGCTTCTCC
4240	tSPO7 R	ATCTATCGATAAGCTCCCGTTATACTTACATCTAGATTAGAAGGCTGGCGATTCA TC
4292	pTDH3 F	TTGTAAAACGACGGCCAGTGAATTATATGGAATGGACGAGCTCTCAGTTCGAGTT TATCATTA TCAATAC
4293	pTDH3 R	AAGCTTTCATATTAGGTACCTTTGTTTGTATGTGTGTTTATTTCG
4207	EMT ORF 1 F	AAGGAGAAAAAATATAGAGCTCAAAATGAAGGTTGCCCTCCTTGC

4208	<i>EMT</i> ORF 1 R	GGAGAGTGCATCAACAGCAATCATGTCAGGTTTCGATCTCG
4209	<i>EMT1</i> ORF 2 F	TTGCTGTTGATGCACTCTCC
4210	<i>EMT1</i> ORF 2 R	ATTGCACCCGCCCTGCTCCCTGCAGTCAATCGCTCCCAACAGTGG
4275	<i>tPRS1</i> F	GGATCCTAATAGTATAACCCGGGACAGAAGAGAGTGTGCGCAA
4276	<i>tPRS1</i> R	ATCTATCGATAAGCTCCCAGTTATACTTCACATCTAGAGGCAAAGAAGCAAAGTCC AG
4245	<i>pTPI</i> F	AACGACGGCCAGTGAATTATATGGAATGGACGAATCCATCAGGTTGGTGGAAG ATTACC
4246	<i>pTPI</i> R	AAGCTTTCATATTAGGTACCGTTTATGTATGTGTTTTTTGTAGTTATAG
4247	<i>MAT1</i> ORF F	GGTACCTAATATGAAAGCTTAAAATGAAGAGCAACGTGGATACTG
4248	<i>MAT1</i> ORF R	TTGATCTATCGATAAGCTCCCGGTATACTATTAGGATCCTTATTCGACAAAGATG TACCTTCC
4249	<i>tAI2</i> F	GGATCCTAATAGTATAACCCGGGTATTAATATGCGTTAAATGGAGAG
4250	<i>tAI2</i> R	GATCTATCGATAAGCTCCCGTTATACTTCACATCTAGAAGCACCTCTAACAAATGC TTCA
4251	<i>pTEF1</i> F	AACGACGGCCAGTGAATTATATGGAATGGACGAATCCATAGCTTCAAATGTTT CTACTCC
4252	<i>pTEF1</i> R	AAGCTTTCATATTAGGTACCCTTAGATTAGATTGCTATGCTTTC
4253	<i>MAC1</i> ORF F	GGTACCTAATATGAAAGCTTAAAATGATCAACAACGCTCTCCGAAC
4254	<i>MAC1</i> ORF 2	TTGATCTATCGATAAGCTCCCGGTATACTATTAGGATCCCTAGAGACGAGCAAAA CACAGG
4255	<i>pADH1</i> F	CGTTGTAAAACGACGGCCAGTGAATTATATGGAATGGACGAATTCATCCTTTTGT GTTTCCGG
4256	<i>pADH1</i> R	TTTAAGCTTTCATATTAGGTACCAGTTGATTGTATGCTTGG
4211	<i>MAC2</i> ORF 1 F	GCATGGATGAACTATACAAAGGAGCAGGTGCGGGATCCATGCAGGCAGATAAAC ATGCTTGG
4212	<i>MAC2</i> ORF 1 R	ATGGCAGCCGACAGTTGGAAATTGCCGTTTTGATAATATTCTGCG
4213	<i>MAC2</i> ORF 2 F	TTCCAAGTGTGCGGTGCC

4214	MAC2 ORF 2 R	AAAAAAATTGATCTATCGATAAGCTTGTGCGCAGAGTGACTAGAGC
4404	tVPS71 F	GGATCCTAATAGTATAGTCGACTAATGATCAGTATGTATTCGTAAGC
4405	tVPS71 R	AAATTGATCTATCGATAAGCTAGTTATACTTCACATCTAGATGTCGATCGTCATTTCTTCGGTC
4507	MMF1 no spacers F	AGGCAAGATAAACGAAGGCAAAAAAATGGCCGACGAGAAGAGGAC
4508	MMF1 no spacers R	AAGGAAGAAGCCCTCCAACCTCTTCTAACTAGTGGGCAAGGTACTCG
4504	EMT1 no spacers F	AATAAACACACATAAACAAACAAAAAATGAAGGTTGCCCTCCTTG
4506	EMT1 no spacers R	AAAATATTGCGCACACTCTTTCTGTCCCTCAATCGCTCCCAACAGTGG
4525	MAT1 no spacers F	AAAAAACACATACATAAACAAAATGAAGAGCAACGTGGATACTG
4526	MAT1 no spacers R	ATTTAACGCATATTTAATACCCTTATTCGACAAAGATGTACCTTCC
4522	MAC1 no spacers F	AAAGCATAGCAATCTAATCTAAGAAAATGATCAACAACGCTCTCCGAAC
4523	MAC1 no spacers R	TTTAAAATAAAAATATACCTGGCCCCCTAGAGACGAGCAAACACAGG
4502	MAC2 no spacers F	AAGCATAGCAATCTAATCTAAGAAAATGCAGGCAGATAAACATGC
4503	MAC2 no spacers R	AGAAAAAAATTGATCTATCGATAAGCTGTGCGCAGAGTGACTAGAGC
4604	MAT1 WG into plasmid F	AGTCACGACGTTGTAAAACGACGGCCAGTGAATTCATCAGGTTGGTGAAGATTA CC
4605	MAT1 WG into plasmid R	AGCACCTTAACAAATGCTTCATATTTAGG
4606	MAC1 WG into plasmid F	CCTAAATATGAAGCATTTGTTAGAGGTGCTCCTCGAGGCATAGCTTCAAATGTTT CTACTCC
4607	MAC1 WG into plasmid R	AAAGAAAAAAATTGATCTATCGATATCTAGAGACAAGTTTTCTCCGCGAACATAC

4528	<i>HIS3MX6</i> into <i>EMT</i> WG F	ATATATGGACTTCCACACCAAACGCTGCAGGTCGACAACC
4529	<i>HIS3MX6</i> into <i>EMT</i> WG R	ATAATGATAAACTCGAACTGAGCACTAGTGGATCTGATATCACC
4550	<i>KLURA3</i> into <i>MAC2</i> WG F	ATATATGGACTTCCACACCAACGACAACCCTTAATATAACTTCG
4551	<i>KLURA3</i> into <i>MAC2</i> WG R	TAGAAACATTTTGAAGCTATGGCTAGTGGATCTGATATCACC
4571	<i>HIS3MX6</i> into <i>MMF1</i> WG F	AGGAGAAAATACCGCATCAGGACGCTGCAGGTCGACAACC
4572	<i>HIS3MX6</i> into <i>MMF1</i> WG R	AAAAAATATAGAGTGTACTAGGACTAGTGGATCTGATATCACC
4801	<i>rex1-nls-</i> <i>S/A 1</i>	AACCTTCTTTTCTTTGCTCC
4802	<i>rex1-nls-</i> <i>S/A 2</i>	CAAAGAAAAGAAGGTTAGCCAAGGCTGCAGTACAAG
4688	<i>rex1-nls-</i> <i>S/A 3</i>	CACATTTGCATGATCATCCTCTTGTACTGCAGCCTTGGCT
4803	<i>rex1-nls-</i> <i>S/A 4</i>	AGGATGATCATGCAAATGTGGTAGCGGAAGTGAATAAGAA
4804	<i>rex1-nls-</i> <i>S/A 5</i>	TTGCCTTTTTTTCTTCTTATTCTTATTCACTTCCGCTAC
4681	<i>rex1-nls-</i> <i>S/A 6</i>	TAAGAAGAAAAAAAAGGCAAAGCCTATGTAACCCGGGGTG
4819	<i>rex1-nls-</i> <i>S/E 1</i>	AGCCTTCTTTTCTTTCTCCTG
4818	<i>rex1-nls-</i> <i>S/E 2</i>	GGAGAAAAGAAAAGAAGGCTCGAGAAGGAGGAAGTACAAG
4707	<i>rex1-nls-</i> <i>S/E 3</i>	CACATTTTCATGATCATCCTCTTGTACTTCTCCTTCTCG
4817	<i>rex1-nls-</i> <i>S/E 4</i>	AGGATGATCATGAAAATGTGGTAGAGGAAGTGAATAAGAA

4820	<i>rex1-nls-S/E 5</i>	CATAGGCTTTGCCTTTTTTTCTTCTTATTCTTATTCACTTCCTCTAC
4938	<i>pREX1</i> assembly 1	TGGCGGCCGCTCTAGAACTAGTACATATTTTTGTATATTTTATTGTTGTAG
4951	<i>pREX1</i> assembly 2	TTCCTATTATTTTATTGTTAGTATTTTATAAGTGGCGCGAGGACACAATAGAAAT GGAGGGAAGATTTTTGCTCGATGG
4952	<i>pREX1</i> assembly 3	CAATACCAAGGATGACTGAGGAAGAAAACAATAATAGACTATACTCAGGCAAAC ATGGCAGGCCTTGCGCAACACGATGAA
4953	<i>pREX1</i> assembly 4	TTTTCTTCTCAGTCATCCTTGGTATTGCCATCGAGCAAAAATCTTCCCTCCATTCT ATTGTGTCCTCGCGCCACTTAT
4954	<i>pREX1</i> assembly 5	AAAATACTAACAATAAAAATAATAGTGAAC TACAACAATAAAAATATACAAAAATAT GTACTAGTTCTAGAGCGGCCCA
4947	<i>pREX1</i> assembly 6	TTCATCGTGTTGCGCAAGGCCTGCCATGTTTGCCTGAGTATAGTCTATTATTG
5051	<i>rex1</i> into <i>pREX1 F</i>	TAGACTATACTCAGGCAAACATGGCAGATATCAGTAAAGGAGAAGAAC
5052	<i>rex1</i> into <i>pREX1 R</i>	TAAAGGATGCTACACCACCCGGATCCTTATTTTACAGTAAAGGATGCTACACC
5048	<i>pREX1 1kb F</i>	AAAAGCTGGAGCTCCACCGCGGTGGCGGCCGCTCTAGACTCATTCCAGTTGGATT CTGC
5049	<i>pREX1 1kb R</i>	AAAGTTCTTCTCCTTTACTGATATCTGCCATGTTTGCCTGAGTATAGTCTATTATTG
o664	<i>KANMX</i> into <i>ERG6 F</i>	GATCAGCAAAATTTAGGG
o665	<i>KANMX</i> into <i>ERG6 R</i>	TTGAAAAGCACATGCCG

2.7.3 Gel electrophoresis

DNA samples were analysed by agarose gel electrophoresis. 0.7% (w/v) agarose gels were prepared by dissolving high grade agarose powder in 1x TAE buffer solution (40mM Tris pH 8.3, 20mM acetic acid, 1mM EDTA) and ethidium bromide (final concentration 0.5µg/ml). 6x loading buffer (0.25% bromophenol blue, 0.25% xylene cyanol FF, 30% (v/v) glycerol) was added to DNA samples to a final 1x concentration. Samples were run alongside Bioline Hyperladder I to determine fragment size. Agarose gels were run at 90V for 40 minutes in 1xTAE buffer. Gels were analysed by viewing through a ultraviolet (UV) transilluminator imaging system (GeneSys).

2.7.4 DNA gel extraction

DNA was separated on agarose gel as described in section 2.6.3. The gel was visualised on a blue-light transilluminator and relevant bands were excised from the gel using a sterile scalpel. DNA was extracted using a QIAquick gel extraction kit (Qiagen) according to the manufacturers instructions.

2.7.5 Plasmid extraction from *E. coli*

4ml cultures of *E. coli* transformants were grown overnight in selective media at 37°C. Plasmids were extracted from these cultures using a Qiagen miniprep kit in line with the manufacturers instructions. Plasmid DNA was eluted into 1.5ml microfuge tubes and the concentration measured using a Nanodrop.

2.7.6 Restriction digestion

DNA was cut through restriction digestion. All restriction enzymes were sourced from New England Biolabs (NEB). 20µl reactions were set up containing 0.2-2µg of DNA, 2µl of 10x cutsmart buffer and 0.5µl of each restriction enzyme required. The remaining volume was made up with dH₂O. Reactions were set up on ice and incubated at 37°C for a minimum of 2 hours, but typically overnight.

2.7.7 DNA sequencing

DNA sequencing was performed by SourceBio through Sanger sequencing. Samples were prepared to their specifications. Sequencing data was visualised in SnapGene and analysed using online multiple sequences alignment tool ClustalW.

2.7.8 DNA Ligation

DNA ligations were set up in 20µl reactions containing a 3:1 ratio of gel-purified insert:vector with approximately 500ng of vector. 2µl 10x ligation buffer was added alongside 1µl T4 DNA Ligase (NEB). Reaction volume was made up to 20µl with dH₂O. Reactions were ran overnight at 16°C prior to transformation to chemically competent *E. coli*.

2.7.9 Assembly of DNA fragments from oligos

Assembly of DNA sequences containing numerous point mutations was accomplished by ligating tiled oligos (fig. 2.1). Oligos containing desired sequence were purchased from Merck (formerly Sigma-Aldrich). Oligos were designed so that when assembled they had sticky ends complementary to a cut vector. Each oligo was individually phosphorylated by polynucleotide kinase (PNK). 20µl PNK reactions were set up containing; 12µl dH₂O, 5µl oligo (5µM), 2µl ligase buffer (NEB) and 1µl t4 PNK (NEB). PNK reactions were incubated at 37°C for 1 hour and then heat inactivated at 65°C for 20 minutes. 50µl annealing reactions were set up as follows; 5µl each PNK treated oligo, 10µl annealing buffer (1.5M NaCl, 50mM Tris-HCL pH 7.5, 10mM EDTA, pH 8.0) and dH₂O up to 50µl. Annealing reactions were heated to 70°C in a dry heat block, the heat block switched off and the tubes left to cool within. 2µl of the annealed oligos were added to a DNA ligation mix as an insert as in section 2.6.8.

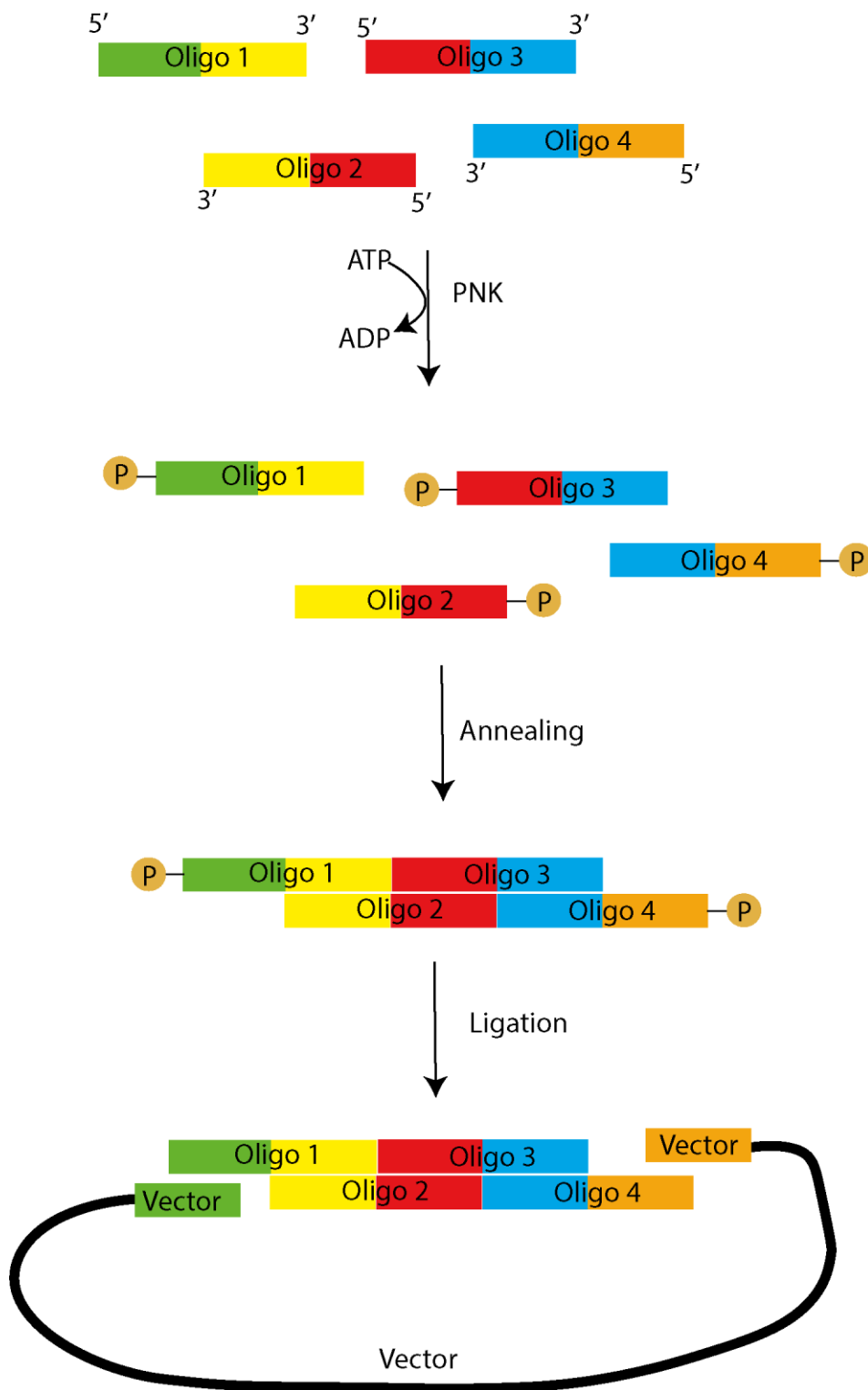


Figure 2.1. Schematic detailing the assembly of DNA fragments from single stranded oligos.

Complementary oligos were designed, the annealing of which resulted in a target fragment. Oligos were treated with T4 PNK to phosphorylate 5' ends, annealed and ligated into a cut vector.

2.7.10 Homologous recombination based cloning

Target sequences were cloned into plasmids via *in vivo* homologous recombination in *S. cerevisiae*. Target sequences were amplified by PCR. Primers were designed to ensure that amplified fragments were flanked by 18-20 nucleotides identical to the insertion site in a cut vector. The vector plasmid was linearized using restriction enzymes at the insertion site. The PCR fragment and linearized vector were transformed into *S. cerevisiae* using the high efficiency transformation (section 2.5.3). *in vivo* homologous recombination induces gap repair and circularises the vector, incorporating the PCR product. Yeast cells containing the recombinant plasmid are identified by growth on selective media. Genomic DNA isolated from these colonies (section 2.5.4) can be electroporated into *E. coli* (section 2.6.3) for plasmid recovery.

2.7.11 5-FOA counterselection mediated gene integration

KL URA3 was PCR amplified with flanks identical to the 5' and 3' end of the *REX1* ORF (fig. 2.2) and transformed into yeast for disruption of the *REX1* ORF with *KL URA3*. Subsequent PCR amplification of *rex1* alleles with flanks identical to the 5' and 3' end of *REX1* were prepared for integration into the *KL URA3* site. Successful integrants were selected when plated on 5-FOA which selects against cells expressing *URA3* genes.

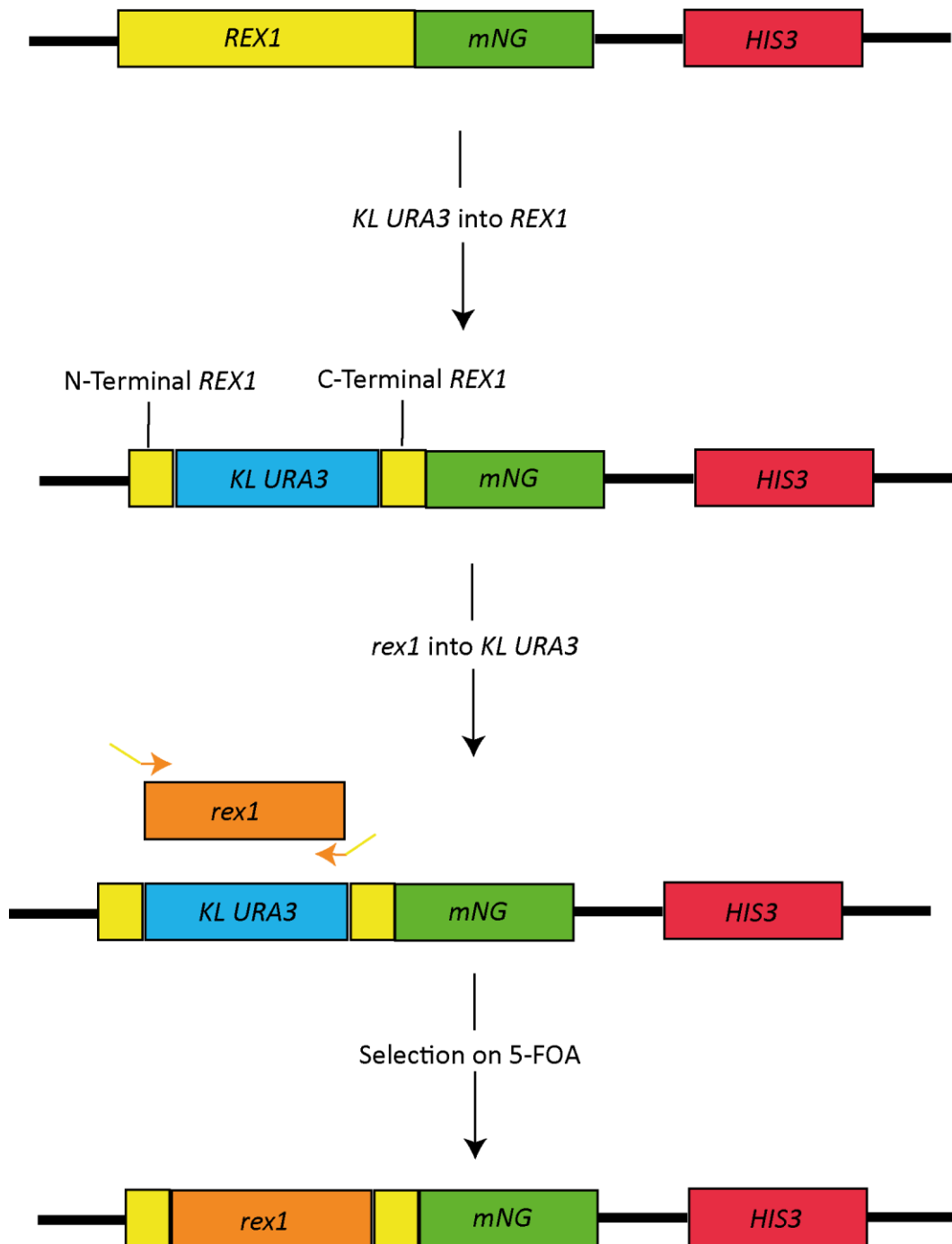


Figure 2.2. Use of 5-FOA to select for correct integrants. Schematic details the strategy for integrating mutant alleles into native loci. Initially the gene is disrupted through the integration of *KL URA3*, selected for on *ura⁻* media. This insertion left a 5' and 3' remnant of the original gene as a recombination target for integration of mutants. Subsequently a PCR amplified fragment containing the mutant allele is targeted to recombine with the 5' and 3' end of the original gene. Selection for loss of the *KL URA3* gene is performed by plating transformants on 5-FOA media.

2.8 MEL analysis

2.8.1 MEL extraction

MELs were extracted from culture supernatants and cell pellets. 50ml production cultures were grown for 48 hours, shaking at 200 RPM at 30°C. Cultures were centrifuged at 4600 *g* for 10 minutes and culture broths were separated from cell pellets.

50ml ethyl acetate was added to supernatant samples and left mixing on a magnetic stir plate for 15 minutes. Stirring was stopped and phases allowed to separate. The ethyl acetate phase was poured from the top into a fresh beaker. This was allowed to evaporate in a fume hood overnight. The resulting extract was washed twice with 2ml hexane. The hexane was poured off and remaining extract resuspended in 2ml ethyl acetate and transferred to a 2ml microfuge tube. This was dried under a stream of N₂ and stored at -20°C for later analysis by NMR.

Cell pellets were resuspended in 500µl ethyl acetate and transferred to a 2ml screw capped microfuge tube. 200µl glass beads (0.5mm) were added to the tube and it was shaken in a bead beater for 3 minutes in 45s increments. In between bead beating the sample was cooled on ice for 1 minute. The tube was centrifuged at 11568 *g* for 5 minutes and the supernatant transferred to a fresh 2ml microfuge tube. 1.5ml ethyl acetate was added to the cell debris and the tube was vortexed for 30s. The tube was centrifuged at 11568 *g* for 5 minutes and as much of the supernatant as possible removed and pooled with the previous supernatant. The ethyl acetate was dried under a stream of N₂ and the super stored at -20°C for later analysis by NMR.

2.8.2 MEL analysis by nuclear magnetic resonance

MEL extracts were resuspended in 600µl chloroform-d (ThermoScientific) and transferred to NMR tubes. NMR spectra were acquired on a 600 MHz Bruker DRX-600 spectrometer at 25°C. Spectra were analyzed using Felix (Felix NMR Inc., San Diego, CA).

Chapter 3 - Rex1 contains an N-terminal NLS and is phosphorylated and delocalised in response to heat stress.

3.1 Introduction

Rex1 is found in the nucleus of the cell (Frank *et al*, 1999). *rex1Δ* cells remain viable but show a 3' extended form of numerous RNAs. Most notable of these is the 5S rRNA but also several species of tRNA, all are transcribed by RNA pol III (Harismendy *et al*, 2003). The 5S rRNA is unusually transcribed in yeast as its rDNA genes are found adjacently to 35S rDNA genes but on the opposite strand while in higher eukaryotes such as the oocytes of *Xenopus laevis*, the 5S is transcribed in the nucleus prior to a convoluted import into the nucleolus via the cytosol (Steitz *et al*, 1988, Rudt & Pieler, 1996). In human cells, some of the cytosolic pool of 5S is not imported into the nucleus but instead diverted into the mitochondria in complex with mitochondrial import proteins (Smirnov *et al*, 2008).

Alongside 5S rRNA, Rex1 is implicated in the 3' end processing of numerous tRNAs including species of lysine, isoleucine, leucine, methionine and tyrosine tRNA, as these species of tRNA extracted from *rex1Δ* cells show an extended 3' end (Foretek *et al*, 2016, Skowronek *et al*, 2014). 3' extended tRNA are incapable of becoming aminoacylated and are not available for protein translation. It is conceivable that downregulation of tRNA processing would be advantageous in conditions in which ribosome biosynthesis is also reduced. This would prevent the accumulation of tRNAs in a cell with reduced ribosomal capacity. 3' extended tRNA are detectable by northern blot (Skowronek *et al*, 2014, Foretek *et al*, 2016) and so are thought to remain stable though their subcellular localisation is unknown.

It has been observed that cells exposed to stressors including heat stress or a shift to media containing glycerol as a carbon source show a tRNA phenotype similar to *rex1Δ* cells with a 3' end which is extended by 3-8 nucleotides (Foretek *et al*, 2016). The implications of this are that Rex1 activity is downregulated upon exposure to stress conditions. In Chapter 3, we will observe changes in Rex1 subcellular localisation and protein level in response to stress conditions. We will also investigate the role of post-translational modifications on Rex1.

3.2 The NLS of Rex1 is found within amino acid 17-52

Previously made plasmids expressing full-length GFP-*REX1* as well as truncations were expressed in *rex1Δ* cells (Daniels *et al*, 2022). Epifluorescence microscopy was used to identify full-length Rex1 as a nuclear protein (fig. 3.2). C-terminal Rex1 truncation *rex1 428-476Δ* showed a nuclear signal indicating the presence of an NLS in this truncation. N-terminal truncation *rex1 1-202Δ* was found to show a cytosolic signal. Increasingly fine truncations, *rex1 1-82Δ* and *rex1 17-52Δ* showed a cytosolic signal, confirming that Rex1 amino acid 17-52 is required for nuclear import. An RFP-Nic96 marker was coexpressed to label the nuclear pore complex. This marker was used to verify the subcellular localisation of GFP-*rex1*. GFP-Rex1 amino acid 17-52 was imported into the nucleus, demonstrating that this sequence is necessary and sufficient for nuclear import. In addition an SV40 NLS, sequence PKKKRKV (Lanford & Butel, 1984), fused to Rex1 17-52Δ restored nuclear import (fig. 3.2). This confirmed that Rex1 17-52 has activity similar to a known NLS. An AlphaFold model of Rex1 predicted that Rex1 17-52 would protrude outwards from the protein, away from the catalytic domain (fig 3.1). From this predicted structure, it is conceivable that this region would be recognised by import machinery to control Rex1 localisation.

Rex1 truncations showed vastly reduced stability. Western blots verified intact proteins for GFP-Rex1, GFP-*rex1 17-52Δ* and GFP-Rex1 17-52 (fig. 3.3). This verified that these truncations were of the

expected size. Western blot signals could not be obtained for the remaining *rex1* truncations due to low expression levels and poor affinity of the α -GFP antibody.

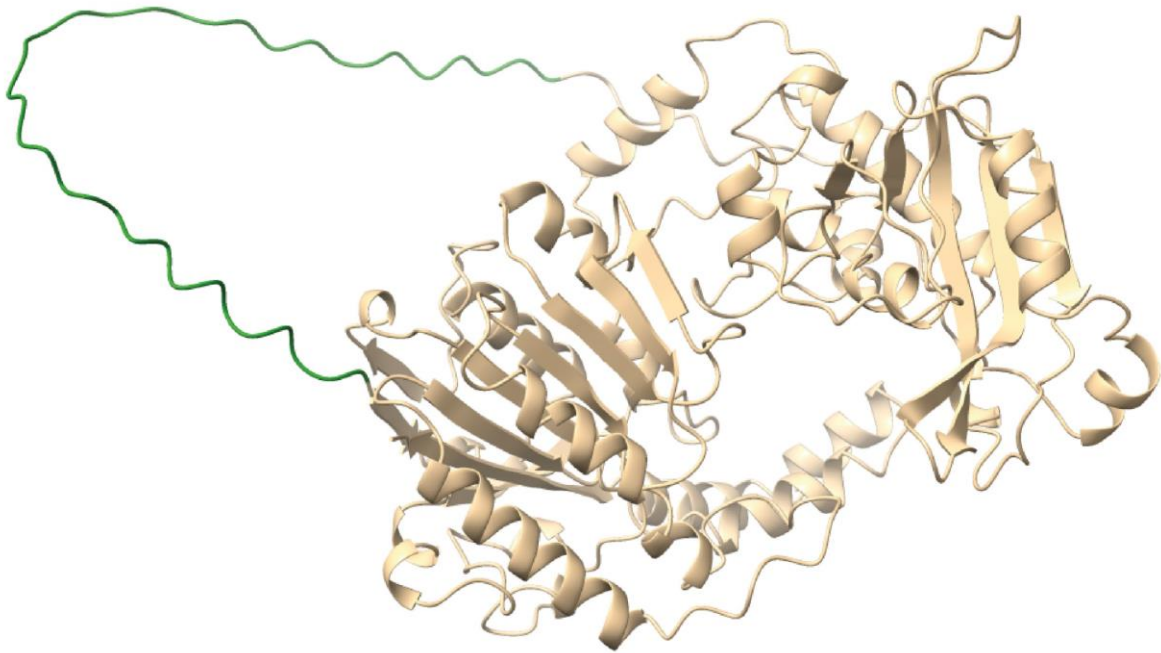


Figure 3.1. AlphaFold model depicting location of Rex1 amino acid 17-52.

Show is an AlphaFold model predicting the structure of Rex1. Amino acid 17-52, experimentally shown to contain an NLS is indicated in green. The catalytic domain of the protein formed by the N- and C-terminal is shown in beige. The AlphaFold model predicts the NLS as protruding from the protein, this would explain its NLS activity as this region is not near the catalytic domain.

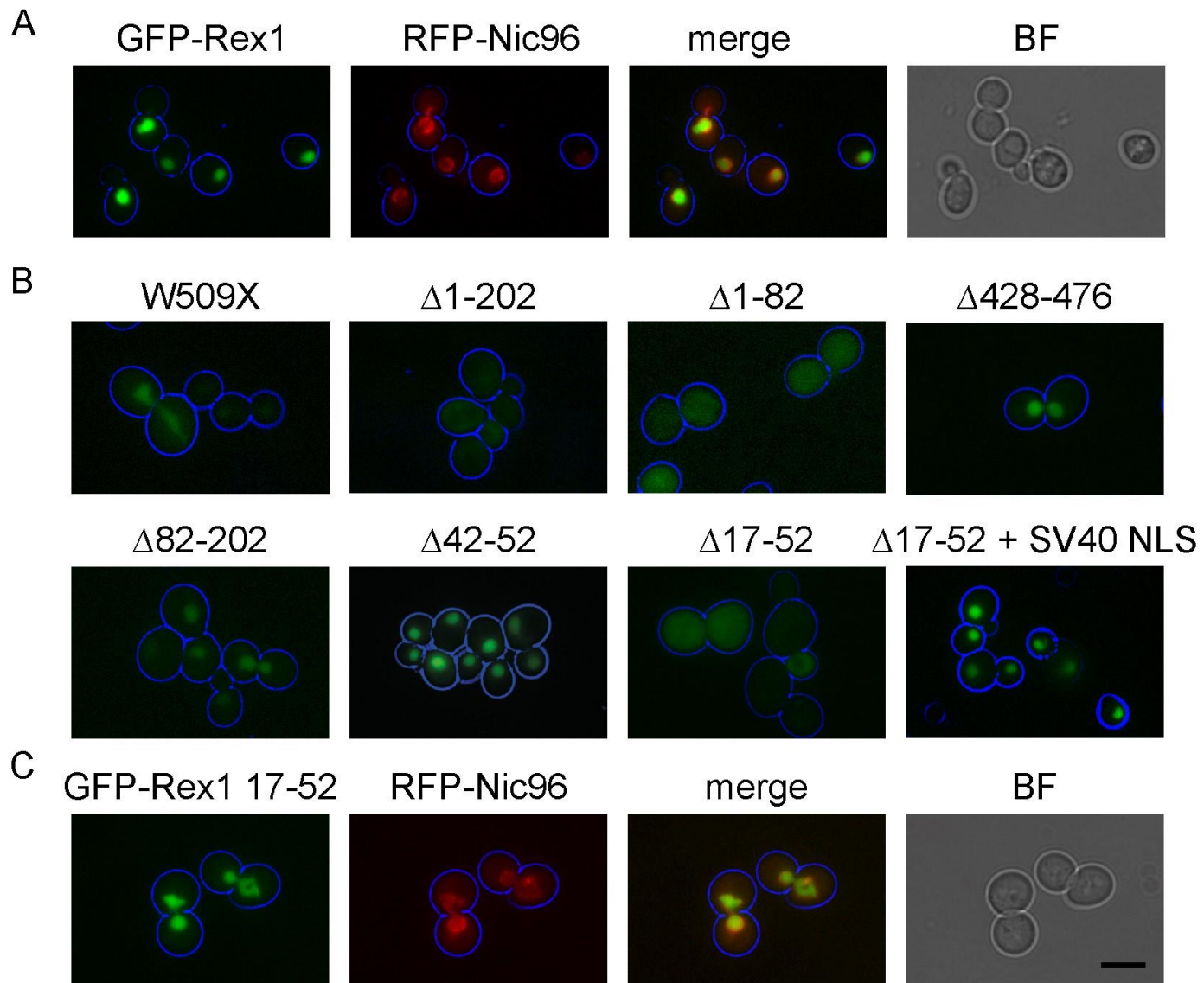


Figure 3.2. Rex1 17-52 contains a functional NLS sequence. Fluorescence microscopy images of GFP-*rex1* truncations are shown. Green channels show GFP-*rex1* truncations. Red channels indicate an RFP-Nic96 nuclear pore marker. Scale bar indicates 5 μ m. A, GFP-Rex1 shows a nuclear signal. B, Localisation of GFP-*rex1* truncations are shown. Large truncations resulted in protein instability and a reduced GFP signal. GFP-*rex1* 1-202 Δ shows a cytosolic signal, GFP-*rex1* 1-82 Δ shows a cytosolic signal, GFP-*rex1* 428-476 Δ shows a nuclear signal, GFP-*rex1* 82-202 Δ shows a nuclear signal, GFP-*rex1* 42-52 Δ shows a nuclear signal, GFP-*rex1* 17-52 Δ shows a cytosolic signal, fusion of an SV40 NLS to this mutant restores nuclear localisation. C, GFP-Rex1 17-52 is imported into the nucleus.

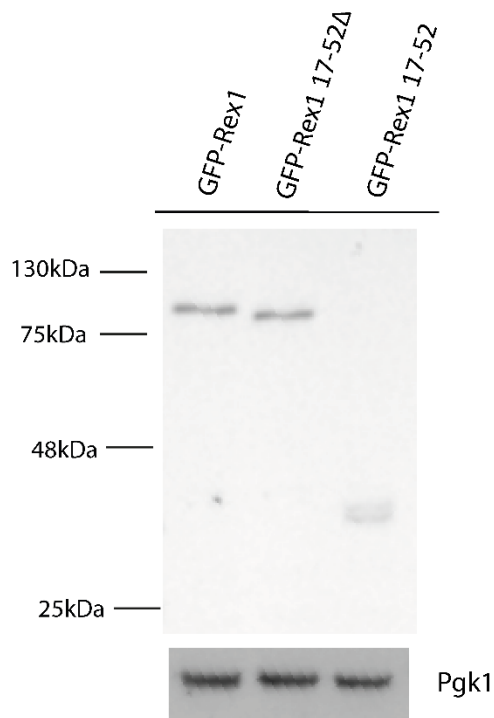


Figure 3.3. α -GFP western blot on GFP-r α 1 truncations demonstrates intact fusion proteins.

Western blot signal for GFP-Rex1, GFP-r α 1 17-52 Δ and GFP-Rex1 17-52 indicate correct full length fusions. An α -GFP antibody was used for GFP-fusion protein detection. Rex1 and truncations proteins levels were normalised against Pgk1 levels.

3.3 Rex1 is imported into the nucleus through the action of the yeast importin- α , Srp1

Importin- α is a conserved karyopherin involved in translocation of cargo proteins and proteasome complexes to the nucleus. Numerous TS mutants exist for the yeast importin- α , Srp1. Srp1-31 fails to translocate cargo proteins to the nucleus at temperatures above 37°C (Tabb *et al*, 2000), whereas Srp1-49 cannot translocate proteasome complexes to the nucleus at temperatures above 37°C (Chen & Madura, 2014) (fig 3.4). These strains were generously donated from the Nomura lab (University of California, Irvine, CA). Srp1-31 and Srp-49 strains were transformed with GFP-*REX1* plasmids. Imaging these cells at permissive and heat stress temperatures demonstrated that the sub-cellular localisation of GFP-Rex1 matches the phenotype of import deficiencies in *srp1-31* and *srp1-49* mutants (fig. 3.5). This indicates that Srp1 acts as the importin responsible for Rex1 nuclear import.

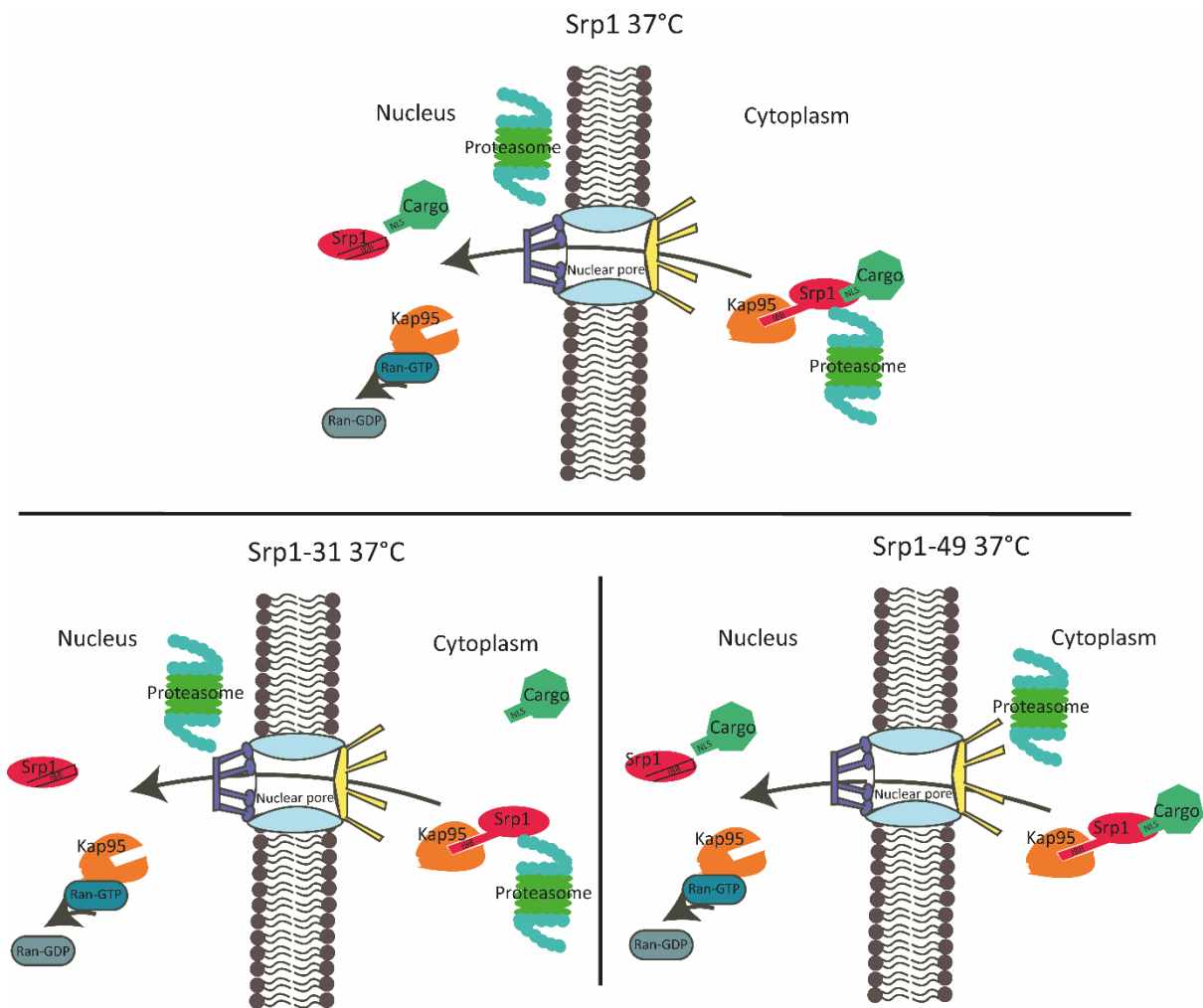


Figure 3.4. Schematic demonstrating phenotypes of Srp1 TS mutants

Shown is a schematic detailing the phenotypes of the TS *SRP1* mutants used in this study. Kap95 binds to the auto-inhibitory domain of Srp1 (IBB) in the cytosol. This allows it to bind to either cargo proteins or proteasome complexes. It takes these to the nuclear pore for stimulated import. Within the cytosol Kap95 is removed from Srp1 through interaction with Ran-GTP, liberating the IBB of Srp1. The IBB domain then outcompetes the cargo, leaving it in the nucleus and Srp1 is exported to the cytosol for recycling. This mechanism remains functional at 37°C with WT Srp1 whereas at 37°C Srp1-31 is capable of binding to proteasome complexes to the nucleus but not cargo proteins and Srp1-49 is capable of binding to cargo proteins but not proteasome complexes.

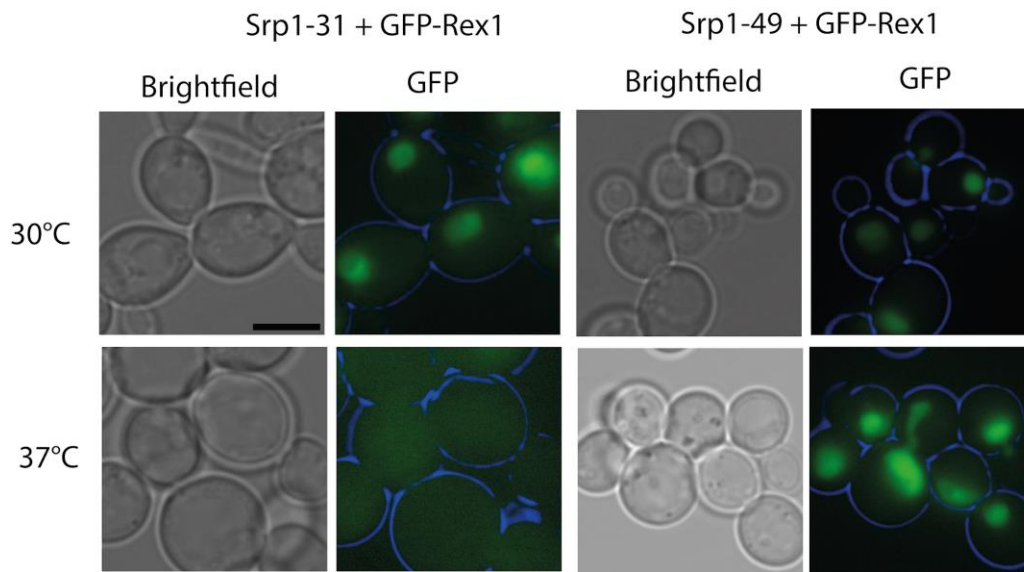


Figure 3.5. TS Srp1 mutant fails to import Rex1 at 37°C.

Images show two TS Srp1 strains expressing GFP-Rex1 grown at 30°C and 37°C. Srp1-31 accumulates a cytosolic GFP-*REX1* signal after 5 hours at 37°C. GFP-*REX1* shows a nuclear signal in Srp1-49 expressing strains after 5 hours at 37°C.

3.4 Rex1 is depleted in response to heat stress

Alongside a change in sub-cellular localisation we observed a large decrease in total fluorescent signal when exposing *REX1*-mNG expressing cells to 39°C. To quantify rates of protein depletion, a culture of logarithmically growing cells expressing an integrated *REX1*-HTP (His-TEV-protein A) allele was heat shocked for 10 minutes in a waterbath at 39°C prior to being moved to a 39°C incubator. Cell pellets were harvested every 10 minutes and protein extracts were prepared for analysis by western blot (fig. 3.6). The data shows a rapid breakdown of the protein that plateaus after about 40 minutes exposure to 39°C with ~10% of the original protein remaining. Control cultures grown at 30°C did not show protein depletion.

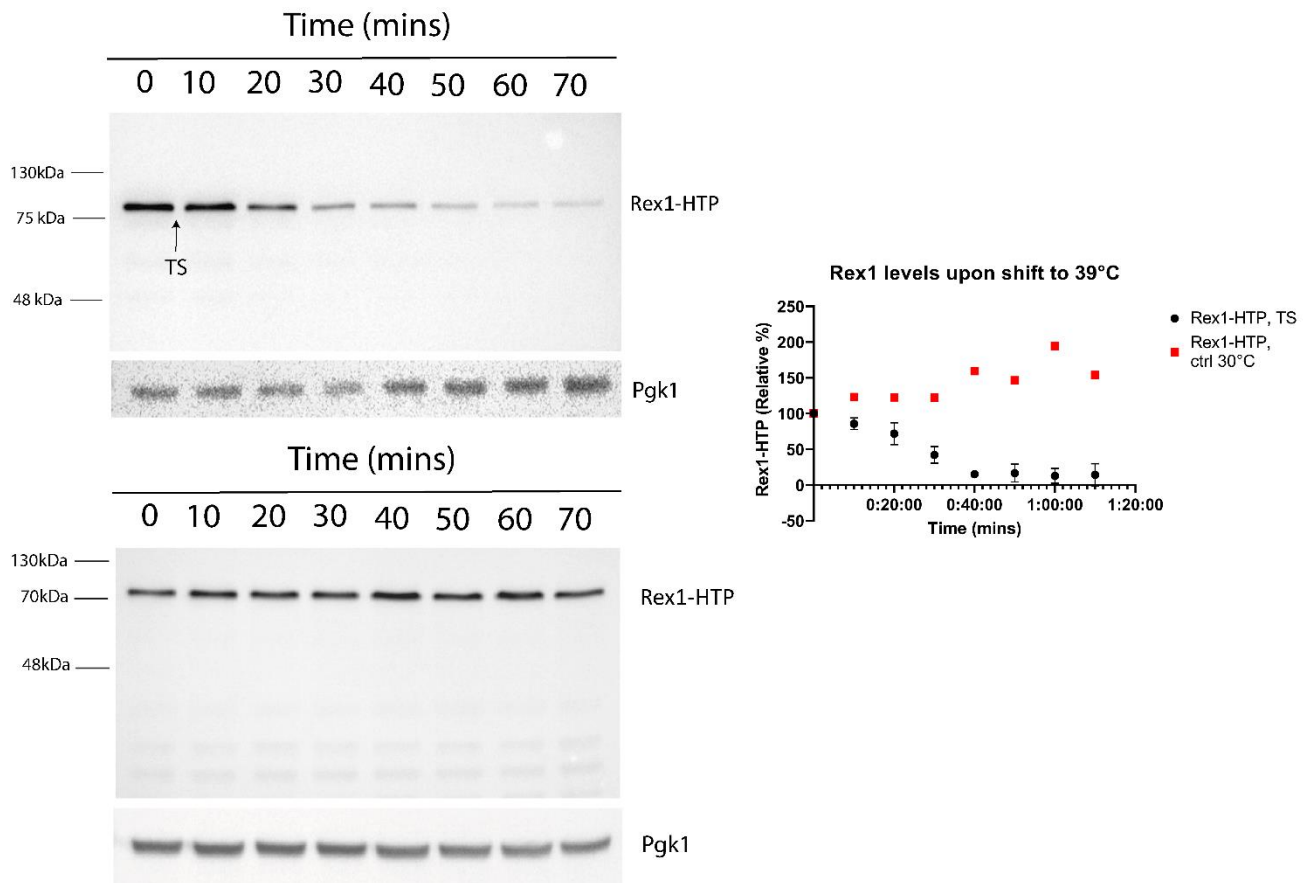


Figure 3.6. Rex1-HTP is depleted in cells moved to 39°C. Above, shown is a western blot of cell pellets expressing the integrated *REX1-HTP* allele over the course of a temperature shift to 39°C. The temperature shift is marked 'TS'. The protein is of the correct size for the fusion and we see a rapid drop in protein levels over the course of exposure to the elevated temperature. The protein level plateaus at ~10% of WT levels after 40 minutes. Error bars for the 40 minute mark are too small to show. This experiment was repeated in triplicate. Standard deviations are shown in error bars. Below, a control western blot from cells continually grown at 30°C shows that Rex1-HTP remains stable. An α -PAP antibody was used for detection of HTP tags. α -Pgk1 antibody was used as a loading control.

This experiment was repeated with the addition of cycloheximide (CHX) to investigate the effects of heat shock on Rex1 stability (fig. 3.7). Cycloheximide inhibits translation and thus any observations apply to the pre-existing pool of protein present in the cell.

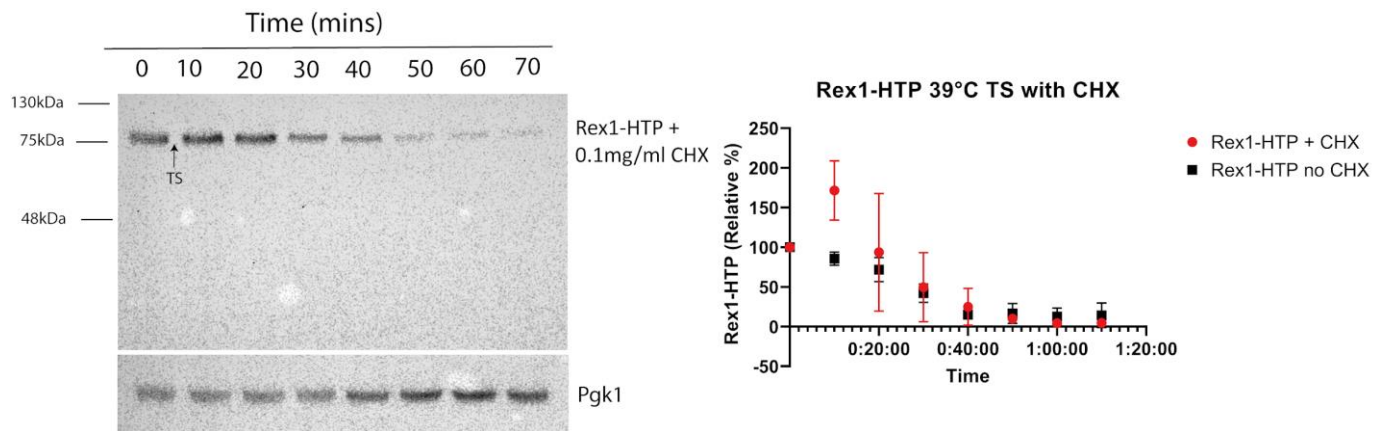


Figure 3.7. Rex1-HTP protein is unstable at 39°C. Shown is a western blot of protein from cells expressing a *REX1-HTP* integrated allele harvested over the course of a shift to 39°C in the presence of cycloheximide. The initial shift to 39°C is indicated by the arrow marked TS. An α -Pgk1 antibody was used on the blot as an internal loading control. The graph shows plotted values for two replicates of this experiment with the standard deviations. Results from equivalent experiments lacking CHX are plotted alongside for comparison. The temperature shift is marker TS. An α -PAP antibody was used for detection of HTP tags. Protein levels were normalised to levels of Pgk1.

Rex1 depletion was observed in samples treated with CHX, indicating instability of the Rex1 protein at 39°C. The rate of depletion closely resembles samples without CHX with ~10% of Rex1 remaining after 40 minutes. This demonstrates the instability of the Rex1 protein upon exposure to heat stress. The use of CHX removes changes caused by transcription/translation. As Rex1 depletion in CHX treated cells shifted to 39°C resembles untreated cells it could indicate that Rex1 translation is inhibited in cells moved to 39°C.

Plasmids are often used for analysis of mutants, previously a *pRRP4::zz-REX1* plasmid had been made in the lab. Given the ease with which plasmids are manipulated and the speed with which they can be used to ask research questions, these experiments were repeated in *rex1Δ* cells expressing the *pRRP4::zz-REX1* plasmid to determine whether the same trend in breakdown was observed (fig. 3.8).

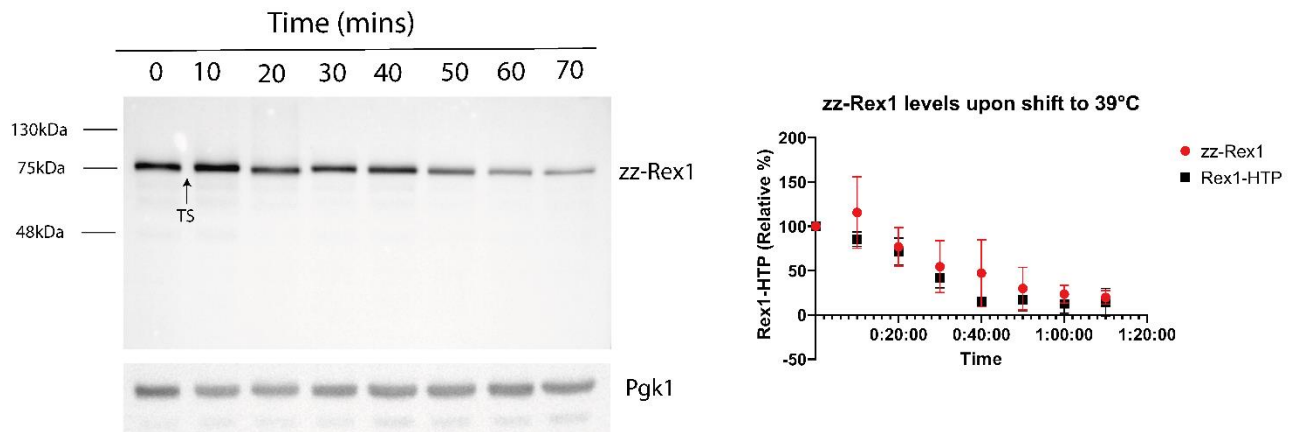


Figure 3.8. Plasmid expressed *pRRP4::zz-REX1* is depleted in cells moved to 39°C. Shown are western blot results of cell pellets harvested from a *rex1Δ* culture expressing *zz-Rex1* on a plasmid moved from 30°C to 39°C (red). *zz-Rex1* dropped ~80% after 50 minutes of exposure to 39°C. This experiment was repeated in triplicate, standard deviations are shown in error bars. The temperature shift is marked TS. An α -PAP antibody was used for detection of *zz*-tags. *Rex1* protein levels are normalised against *Pgk1*. The decay rate for the integrated *REX1-HTP* allele is shown in black for comparison. A t-test was performed and no significant differences were found between integrated *Rex1-HTP* and plasmid expressed *zz-Rex1*, $P=0.4646$.

The *pRRP4::zz-REX1* decay curve appears similar to that of the integrated allele. This evidence indicated that the plasmid system could be used to study *Rex1* depletion. The experiment was repeated with the addition of CHX (fig. 3.9) to determine stability of the *zz-Rex1* pre-existing pool.

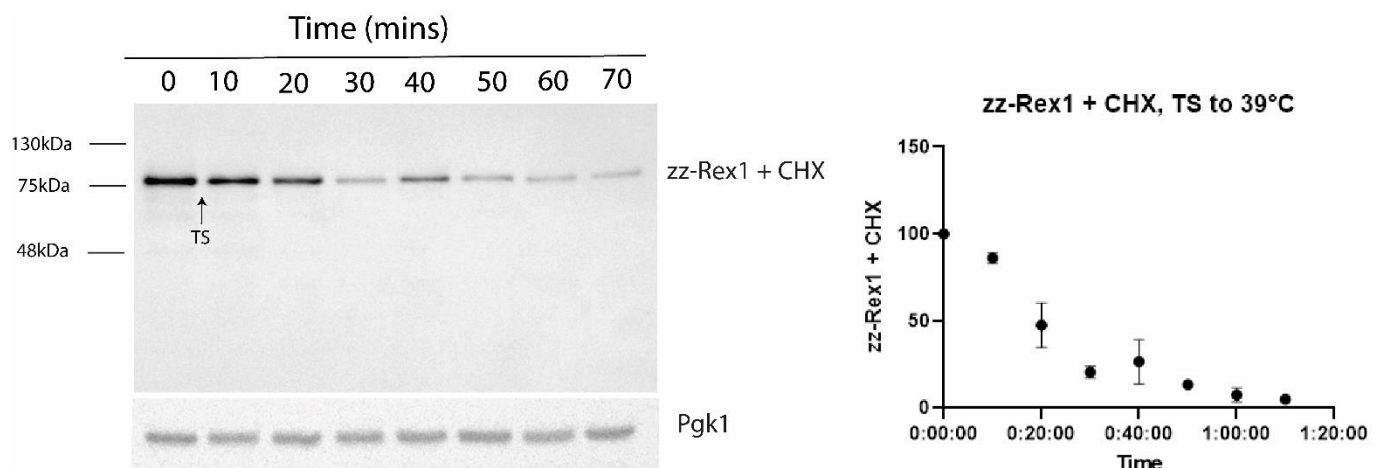


Figure 3.9. Western blot showing decay of *zz-Rex1* in CHX treated cells shifted to 39°C. Shown is a western blot of CHX treated *rex1Δ* cells expressing *zz-REX1* from a plasmid. *zz-Rex1* levels are rapidly depleted. The temperature shift is marked TS. This experiment was duplicated, standard deviations are shown in error bars. An α -PAP antibody was used for detection of *zz*-tags. Protein levels were normalised against *Pgk1*.

Several TS experiments showed an initial spike in Rex1 levels. It is hard to explain this jump in protein level. An increase in temperature could accelerate reaction rate in the cell, increasing the speed of Rex1 mRNA translation into mature proteins though this is unlikely as it is not seen in every sample. Experiments showing the initial jump in Rex1 levels tend to be westerns with a poorer signal and it is possible the jump is caused by unusually high background pixel values.

As the plasmid expressed allele is under control of the *RRP4* promoter, expressing at higher levels than native Rex1 we expect that the protein is relatively overexpressed it is interesting to observe that its breakdown occurs at a proportionally similar rate.

3.5 Rex1 is not depleted in cells shifted onto glycerol media

Yeast cells moved to glycerol media accumulate a pre-tRNA intermediate akin to those found in *rex1Δ* cells, implying that Rex1 processes these tRNAs (Foretek *et al*, 2016). To assess whether this increase in pre-tRNA is attributable to Rex1 depletion, logarithmically growing cells expressing *REX1-HTP* were shifted from YPD to YPGly and cell pellets were collected (fig. 3.10). Over the course of this experiment Rex1 levels remained constant or increased. Previously collected images of cells expressing GFP-Rex1 on YPGly media have shown that the cells grow large vacuoles on glycerol, rendering Rex1 localisation undiscernible in these conditions. The increase in Rex1 levels after 40 minutes on glycerol media is difficult to explain but may be an experimental artefact as the experiment was conducted only once. We conclude that the loss of tRNA processing by Rex1 in cells grown on glycerol media is not related to Rex1 protein levels.

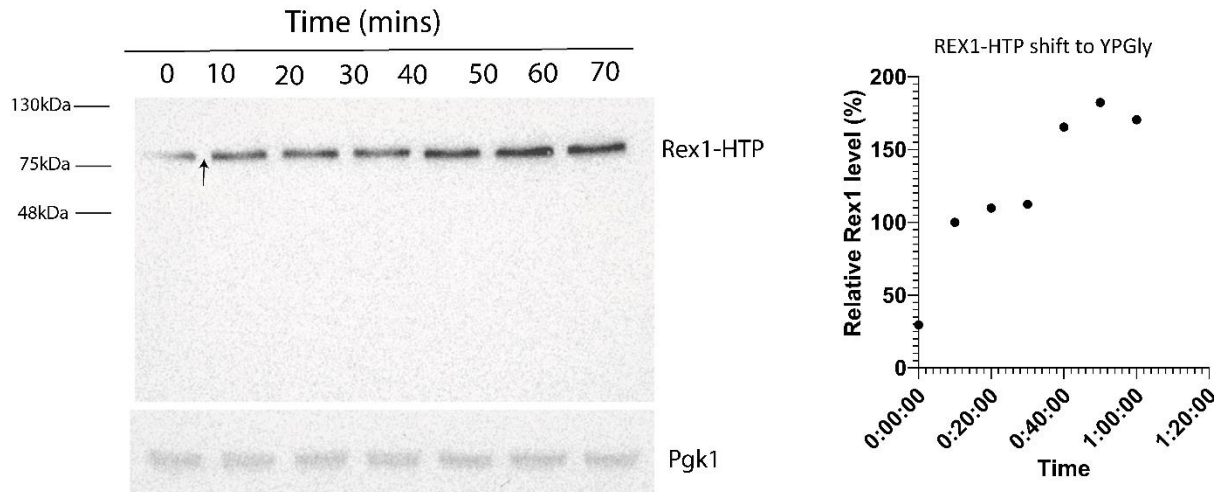


Figure 3.10. Rex1-HTP levels remain constant in cells shifted to glycerol medium. Shown is a western blot of cell pellets harvested every ten minutes over a shift from YPD media to YPGly media. The arrow indicates the shift of growth media. Rex1-HTP levels remained constant or increased over a shift to a non-fermentable carbon source. An α -PAP antibody was used for detection of HTP tags. α -Pgk1 antibody was used as a loading control.

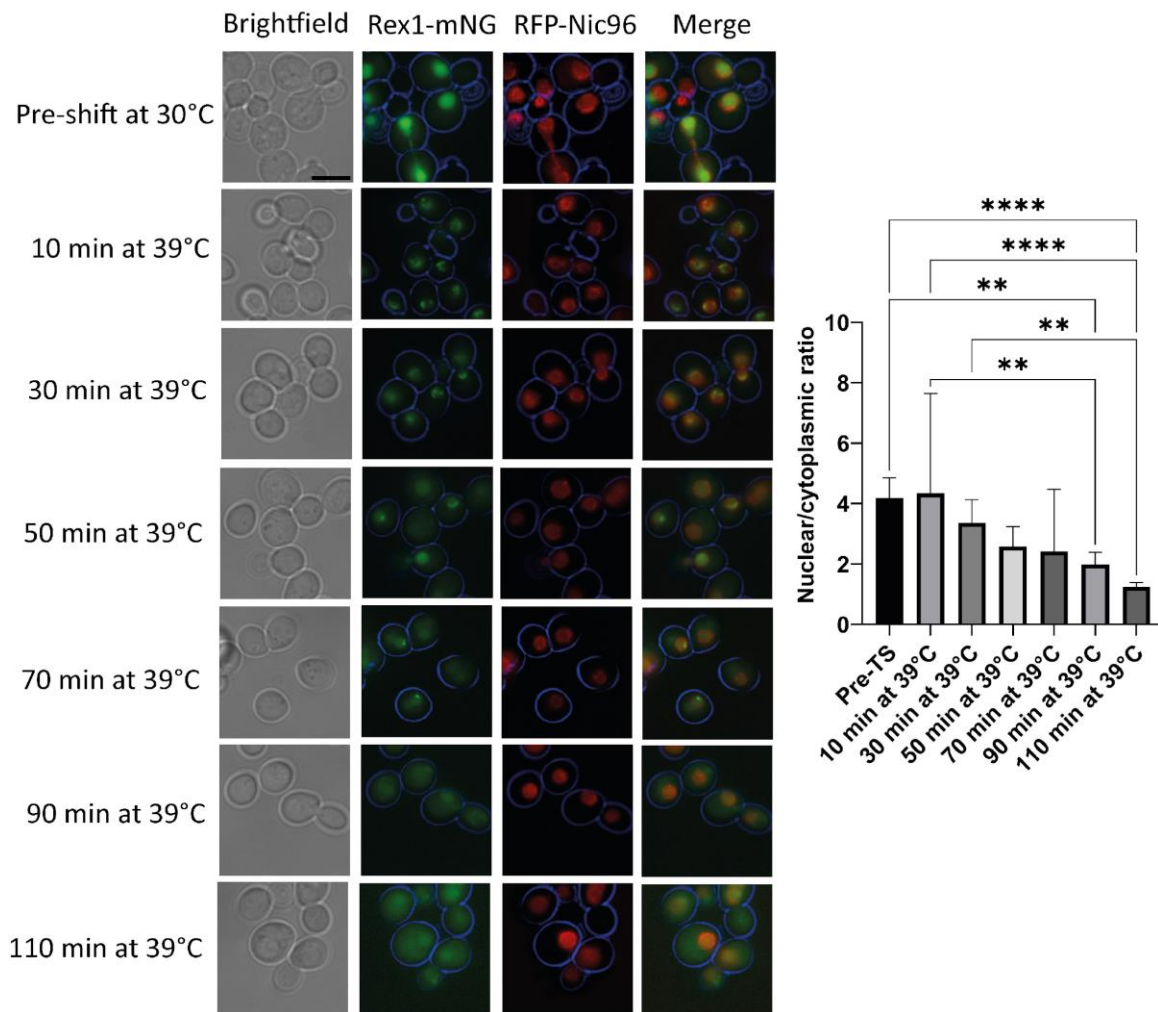
3.6 Rex1 is delocalised from the nucleus in response to heat stress under native regulation

Published data has identified four phosphorylation sites in Rex1 17-52 (S24, T26, S27, T34) (Holt *et al*, 2009, Lanz *et al*, 2021, Zhou *et al*, 2021). These phosphosites are adjacent to our experimentally defined NLS. Numerous cases of phosphorylation dependent import are known, leading to our hypothesis that Rex1 phosphorylation governs nuclear import such as the phosphorylation dependent nuclear import of STAT1 (Nardozzi *et al*, 2010). It has been observed that WT cells display tRNA phenotypes reminiscent of *rex1Δ* at 39°C with 3-8nt extensions at the 3' end. This phenotype is observable at 37°C though with a fraction of the population showing mature 3' end processing. We hypothesized that tRNA 3' extension at 39°C is due to Rex1 delocalisation at heat-shock temperatures.

We conducted epifluorescence microscopy on yeast cultures expressing an integrated *REX1*-mNG allele. Imaging logarithmically growing cultures of these cells over a shift from 30°C to 39°C identified a reduction of fluorescent Rex1 signal. Cytosolic accumulation was observed in cells expressing *REX1*-mNG at 39°C (fig. 3.11). This effect was less visually assessable in cells expressing *pprP4::GFP-REX1* from a plasmid (fig. 3.12). However, quantification of fluorescent signal in plasmid-expressed *GFP-REX1* identified a decrease in nuclear/cytoplasmic signal when cells were moved to heat-shock conditions. This indicates that Rex1 nuclear accumulation is reduced by heat stress. As signal loss occurred rapidly upon a shift to 39°C, three stacks from a z-stack were merged to yield sufficient data to accurately assess sub-cellular localisation. In both instances ANOVAs were run identifying significant differences between the nuclear/cytoplasmic fluorescent ratios over the course of the TS ($P < 0.0.1$).

It was observed that after 10 minutes at 39°C, both plasmid expressed and integrated Rex1 displayed a granular fluorescent signal with distinct foci in the nucleus. It is unknown whether these are present at permissive temperatures and are only visible upon signal depletion or whether they form as concentrated pockets of protein depletion.

REX1-mNG sub-cellular localisation over temperature shift



3.11 Rex1-mNG is depleted and delocalised from the nucleus at 39°C.

Shown are cells expressing Rex1-mNG over a shift from 30°C to 39°C. The nuclear signal decreased in strength while the cytosolic signal increased. Measurements of fluorescent signal showed that nuclear/cytoplasmic ratio decreased over the course of the shift. An ANOVA was performed to determine significant differences between time points. Asterisk indicate P values < 0.01, n=25. The scale bar indicates 5µM.

GFP-REX1 sub-cellular localisation over temperature shift

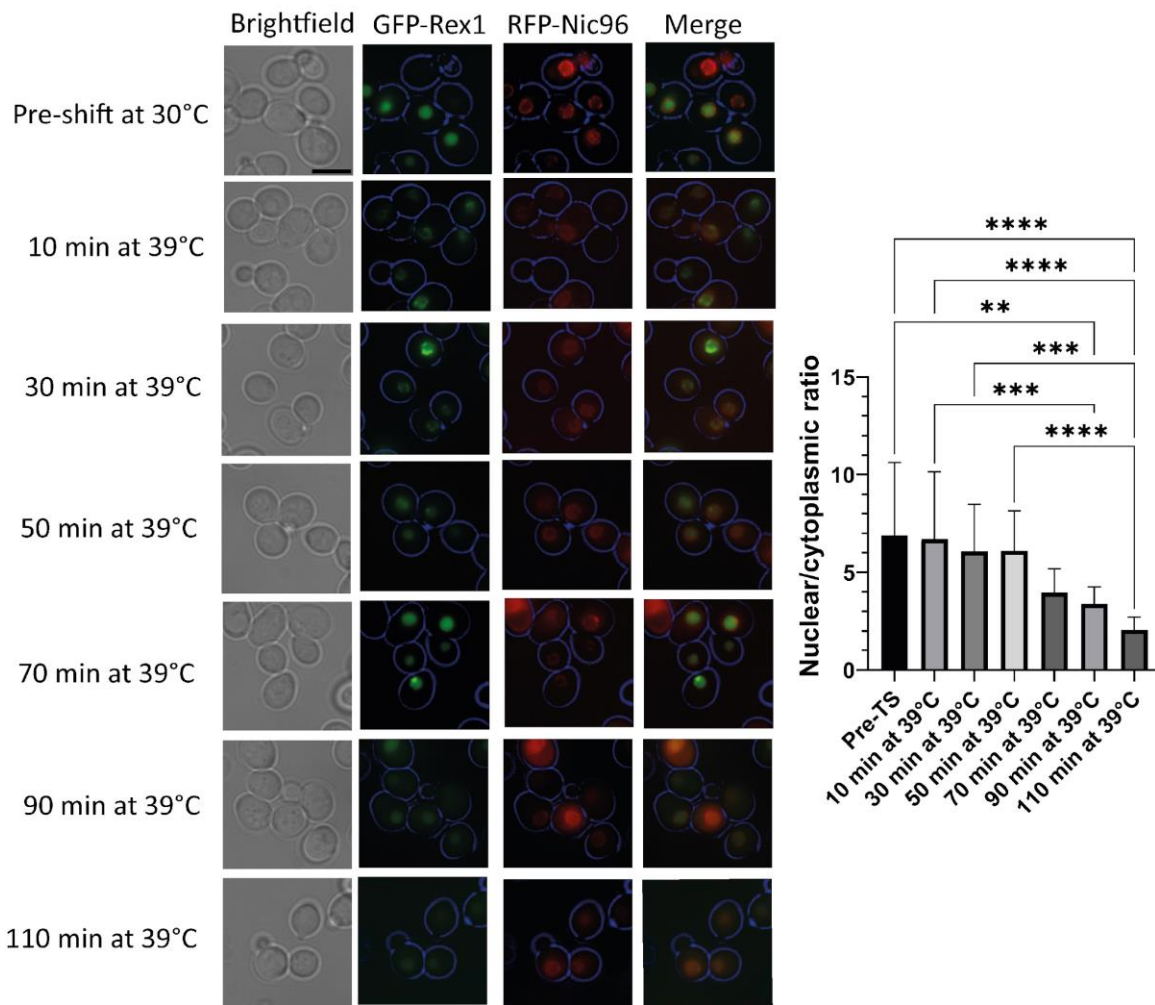


Figure 3.12. Plasmid expressed GFP-Rex1 is depleted at 39°C and moves from the nucleus to the cytoplasm. Cells expressing *pRRP4::GFP-REX1* from a plasmid and shifted to 39°C show a reduction in signal over the temperature shift. Fluorescence measurements show a decrease in nuclear/cytoplasmic ratio over the timescale of the experiment. Some samples show a cytosolic signal in the red channel, auto fluorescent molecules are common at this wavelength or we could be observing a build-up of RFP-Nic96 unincorporated into the nuclear membrane. An ANOVA was performed to define significant differences denoted with asterisks. $P < 0.01$, $n=25$. The scale bar indicates 5 μ M.

3.7 Plasmid vs chromosomal Rex1 expression

Western blot data from logarithmically growing samples at 30°C demonstrates that plasmid-expressed zz-Rex1 is expressed at ~5x greater levels than integrated Rex1-HTP (fig. 3.13). As the HTP tag has a greater atomic mass than the zz tag we see that it migrates slower through the gel. Importin- α

recycling is reduced under heat stress in mammalian cells (Furuta *et al*, 2004, Miyamoto *et al*, 2004). If yeast share this mechanism, we would expect cytoplasmic accumulation of Rex1 in all samples grown in heat stress. While cytoplasmic accumulation of plasmid-expressed GFP-Rex1 was not visually apparent over a shift from 30°C to 39°C, measurement of fluorescent signal indicated a reduction of nuclear accumulation in these samples (fig. 3.12).

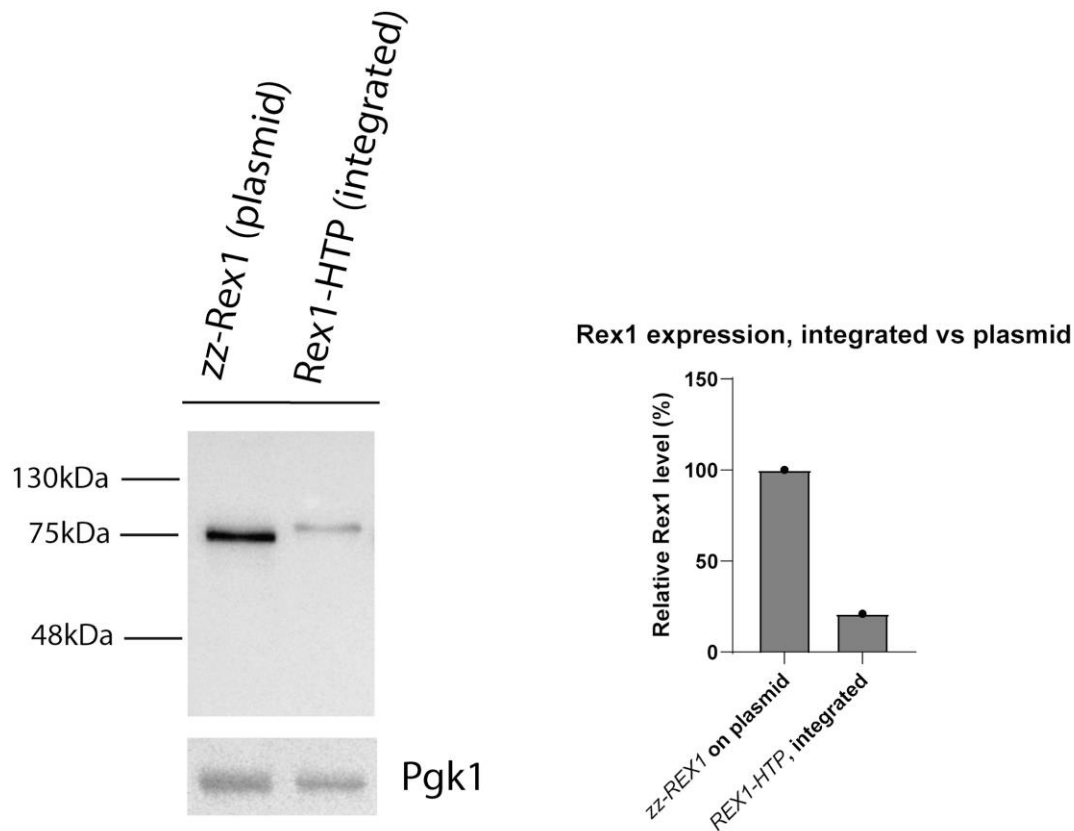


Figure 3.13. Plasmid expressed pRRP4-zz-REX1 is ~5x overexpressed compared to integrated REX1-HTP. Shown is a western blot for plasmid expressed zz-Rex1 vs chromosomally expressed Rex1-HTP from cultures growing logarithmically at 30°C. α -PAP antibody was used for detection of zz/HTP tags. Pgk1 is used as an internal loading control to account for discrepancies in protein loading volume. We see that the plasmid expressed Rex1 is overexpressed relative to the integrated allele. This experiment was repeated only once.

GFP-*REX1* was placed under the control of the *REX1* promoter on a plasmid to develop a plasmid-based assay for stress-related Rex1 regulation. These constructs were GFP tagged as GFP is suitable for microscopy and protein quantification via western blot. Two *REX1* promoter regions were selected; the upstream intergenic region of *REX1*, amounting to 187bp from the start codon of Rex1 to the stop codon of the next upstream gene, we dubbed this promoter p*REX1*. A second promoter was cloned, a 1kbp region upstream of the Rex1 start codon which may contain regulatory sequences with a role in native expression, this promoter was named p1k*REX1* (fig. 3.14).

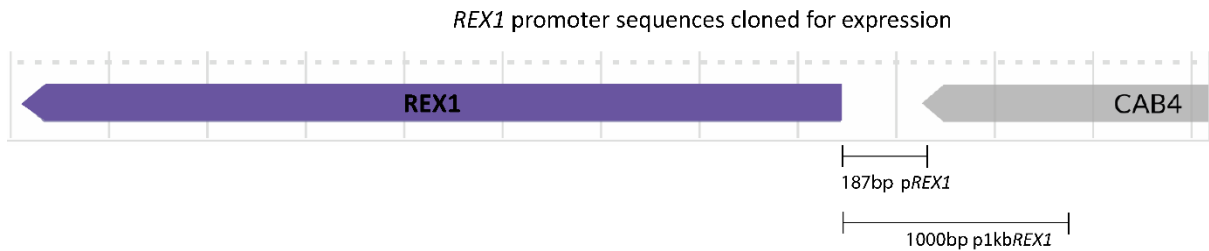


Figure 3.14. Schematic showing *REX1* promoter sequences cloned into plasmids. Shown are the sequences amplified and cloned into plasmids to mimic *REX1* promoters when exploring the effects of Rex1 alleles. The shorter 187bp sequence, dubbed p*REX1*, is the entire intergenic region from the start codon of *REX1* to the stop codon of the next upstream gene, *CAB4*. The larger 1kbp region was later selected as it may contain additional transcription factor binding sites this was named p1kb*REX1*.

Visualisation of the p*REX1*::GFP-*REX1* plasmids was difficult, as GFP is not as bright as mNeongreen, the reduced signal makes it difficult to discern the sub-cellular localisation of Rex1 (3.15). However, the protein is correctly imported at 30°C and is depleted in a shift to 39°C. Attempts to perform western blots on samples expressing the p*REX1*::GFP-*REX1* plasmid failed due to a combination of low expression levels and poor affinity of the α-GFP antibody. We were unable to discern rates of GFP-Rex1 depletion in these samples.

To mimic native expression, the larger 1kb*REX1* promoter was expressed. Cells containing this plasmid failed to express detectable GFP-Rex1 either through microscopy (fig. 3.16), or western blotting (fig. 3.19). This result shows that part of the *CAB4* ORF acted as a transcriptional inhibitor at permissive temperatures.

pREX1::GFP-Rex1, shift to 39°C

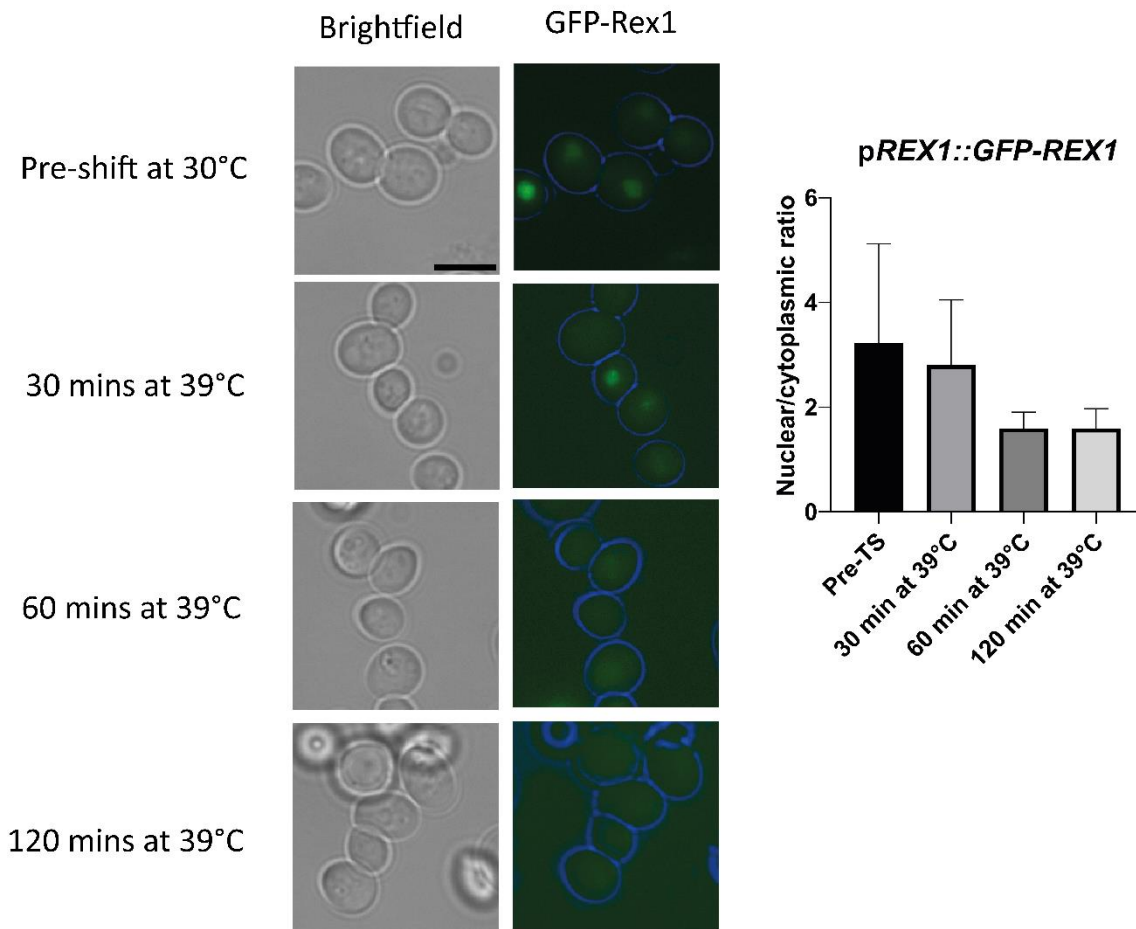


Fig 3.15. Plasmid expressed *pREX1::GFP-Rex1* delocalised from the nucleus upon a shift to 39°C. Shown are images of Rex1 localisation from plasmid expressed GFP-Rex1 under control of the *REX1* promoter. The expression levels are much lower than on the RRP4 promoted alleles and the level drops over the shift. Measurements of cytosolic vs nuclear fluorescence shows a decrease in the nuclear/cytoplasmic fluorescent signal. The scale bar indicates 5µm.

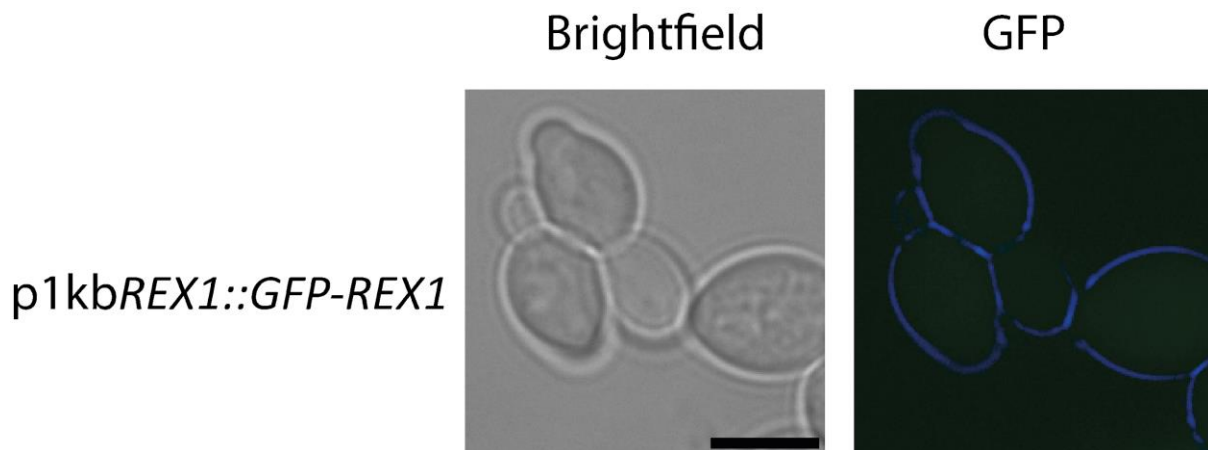


Figure 3.16. Cells expressing p1kbREX1::GFP-REX1 fail to show protein expression. Logarithmically growing cultures of *rex1Δ* transformed with plasmids expressing *REX1* under control of the larger *1kbREX1* promoter are shown. No fluorescent signal was observable in these samples. The scale bar indicates 5μm.

3.8 Rex1 shows numerous stability associated phosphorylation sites within its NLS

Mass spectrometric analysis has shown that four serines/threonines on Rex1 are phosphorylated (S24, T26, S27, T34) (Holt *et al*, 2009, Lanz *et al*, 2021), all of which are located near the NLS (fig. 1.5). If Rex1 nuclear import is regulated, it is plausible that phosphorylation is the mechanism driving it. Examples of phosphorylation driven nuclear import are known, with nuclear import being driven by both phosphorylation and dephosphorylation. Downstream of these phosphosites lie a ubiquitinated lysine at K58. This configuration of phosphorylated residues followed by ubiquitinylation site is reminiscent of a phosphodegron motif. Rex1 PTMs may also function as a phosphodegron, with phosphorylation driving Rex1 degradation. We hypothesized that Rex1 localisation or stability is regulated through phosphorylation. To investigate the role of Rex1 phosphorylation, mutant GFP-*rex1* 17-52 constructs were made with known phosphosites and adjacent serines mutated to either glutamate as a phosphomimetic mutant or alanine to create a non-phosphorylatable mutant. As the phosphate modifications occur either on a serine (S), or a threonine (T), we will be referring to the phosphomimetic mutants as S/E and the non-phosphorylatable mutants as S/A from here on. Glutamate can mimic phosphorylated residues as both glutamate and phosphate modifications are negatively charged. Therefore S/E mutants may act as if constitutively phosphorylated. As phosphate modifications have a 2- charge and glutamate only a 1-, phosphomimetics are not always effective. S/A mutants are non-phosphorylatable and the non-polar, uncharged alanine mimics constitutively non-phosphorylated residues.

Initially, GFP-S/A or S/E *nls* mutants were made with all four known phosphosites mutated. These mutant *nls* constructs were assembled from oligos and ligated into an N-terminal GFP tagging vector. Restriction digestion was performed to verify correct insert size. Subsequently, Sanger sequencing with a primer annealing to *GFP* gene verified the correct point mutations. These constructs showed nuclear import (fig. 3.17). As kinases/phosphatases are known to have promiscuous activity, we suspected that adjacent serines may become kinase targets. This could result in sufficient phosphorylation to stimulate nuclear import. Subsequently we made additional mutations at two additional serines found within the NLS. Imaging of these constructs also yielded a nuclear localisation

(fig. 3.17). The GFP-*nls* mutants are largely truncated compared to a full-length Rex1 protein; this may affect protein activity so the *nls* mutants were placed into full-length Rex1 context.

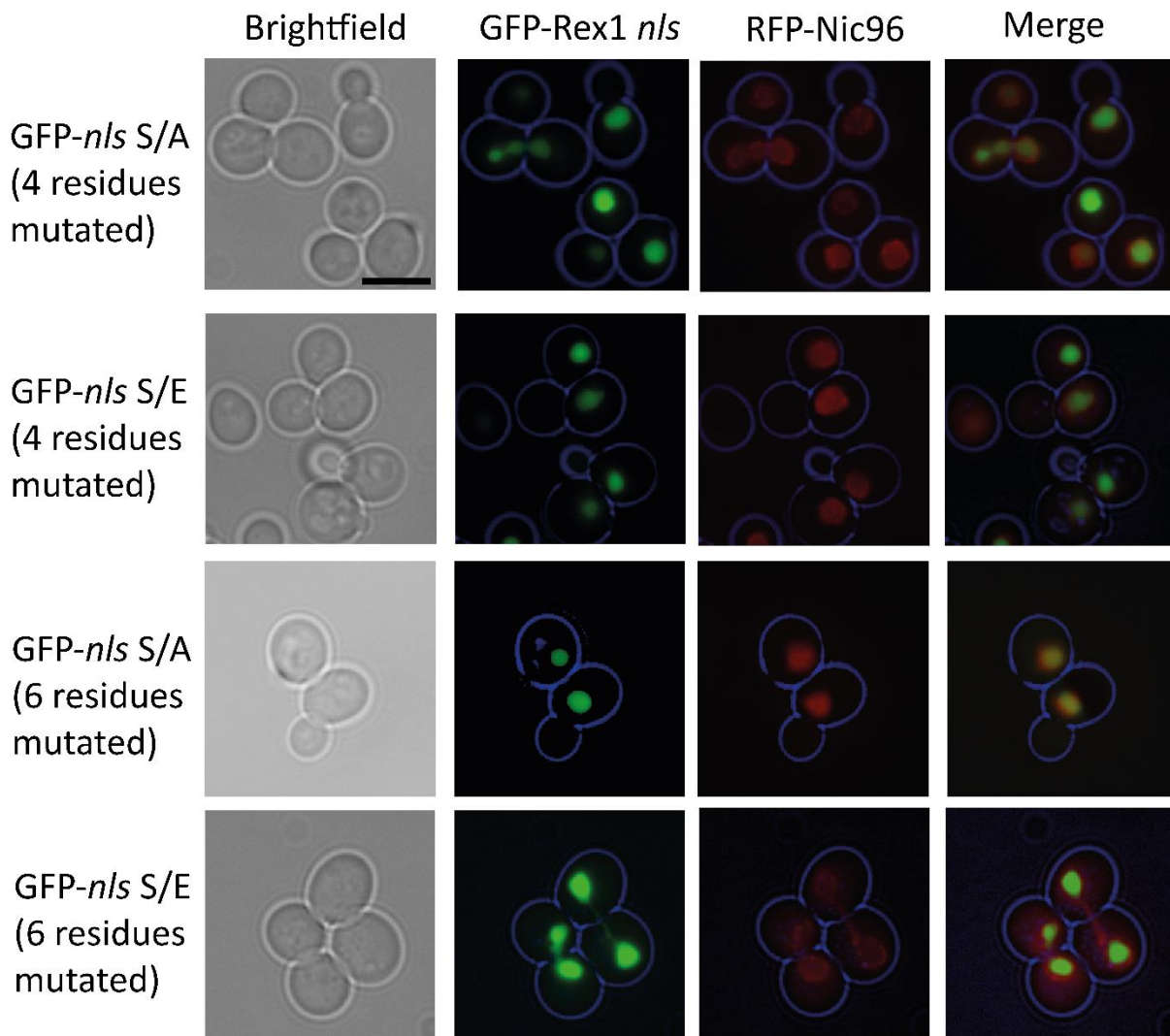


Figure 3.17. Phosphomimetic and non-phosphorylatable Rex1 *nls* constructs are imported into the nucleus. Shown are images of *rex1Δ* cells expressing a plasmid encoding a GFP-*rex1 nls* construct in both a phosphomimetic and non-phosphorylatable form. The images above are from cells harvested growing logarithmically at 30°C and expressing four GFP-*nls* alleles. Phosphomimetic (S/E) and non-phosphorylatable (S/A) mutants in which the four native phosphosites have been mutated are shown, as are S/E and S/A alleles with an additional two serines mutated. The scale bar indicates 5μm.

Full-length phosphomimetic and non-phosphorylatable mutants under control of both the *REX1* and *RRP4* promoter were made. These were made through restriction digestion at a unique *StuI* site in a GFP-*rex1 NLSΔ* plasmid and inserting a mutant NLS through homologous recombination. Correct alleles were validated through restriction digestion and by sequencing the entire ORF. Imaging of cells expressing these plasmids at 30°C demonstrated that both alleles showed nuclear accumulation at

30°C (fig. 3.18). Western blot data showed that Rex1-S/A showed greater stability when compared to WT Rex1 or Rex1-S/E when expressed from a plasmid at 30°C (fig. 3.19). It is possible that the inability for this allele to be phosphorylated causes it to resist turnover.

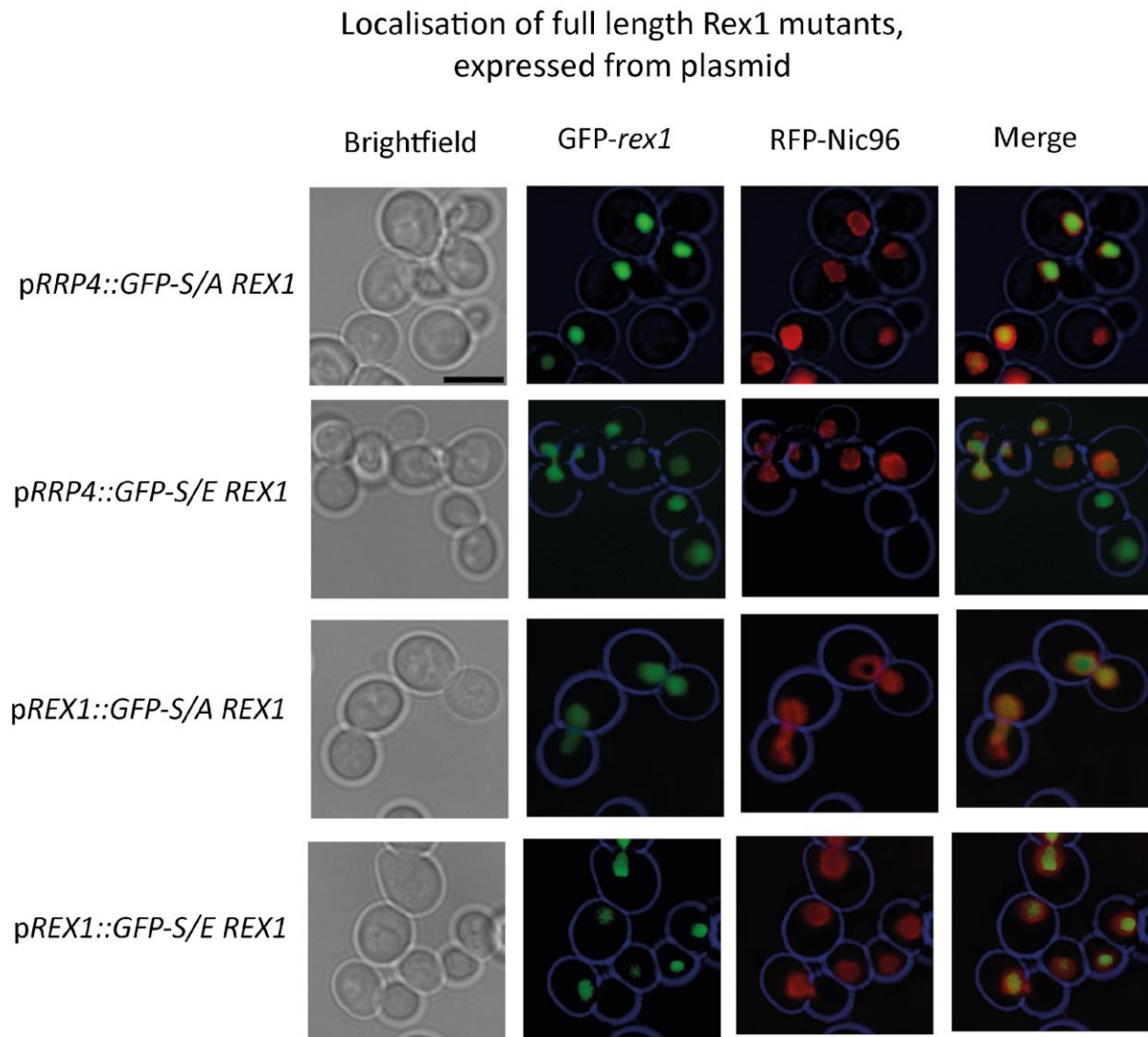


Figure 3.18. Phosphomimetic and non-phosphorylatable Rex1 is imported into the nucleus regardless of allele or promoter context. Shown is microscopy data for cells expressing full-length GFP- phosphomimetic (S/E) and non-phosphorylatable (S/A) *rex1* alleles under the control of the *RRP4* and *REX1* promoter at 30°C. The cells are co-expressing an RFP-Nic96 marker labelling the periphery of the nucleus. The alleles under control of the *REX1* promoter were notably dimmer and images were taken with a longer exposure time. The signal was artificially enhanced to discern the sub-cellular localisation. In all cases, the *rex1* alleles were efficiently imported into the nucleus. The scale bar indicates 5µm.

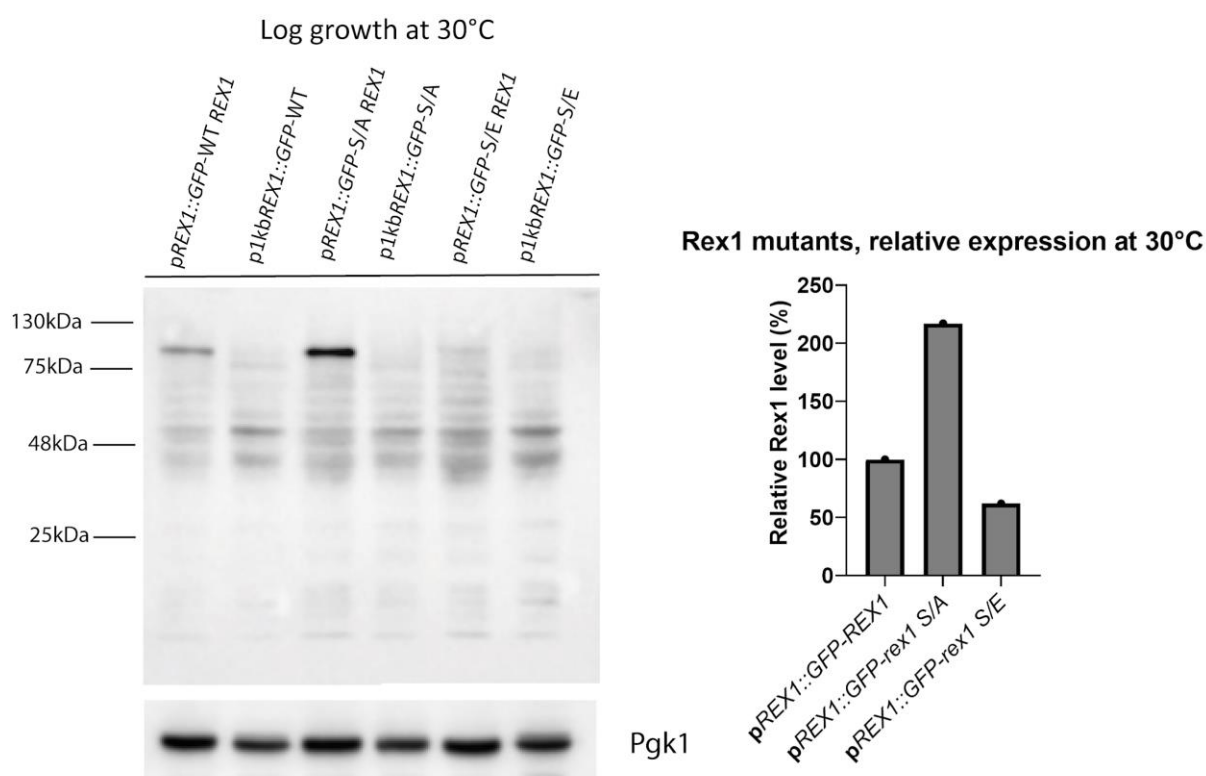


Figure 3.19. S/A Rex1 shows increased stability at 30°C. Shown is a western blot from cells growing logarithmically at 30°C expressing WT, S/A and S/E *rex1* alleles from a plasmid under control of *REX1* promoter and *1kbREX1* promoter. GFP-Rex1 alleles are shown at ~82kDa. Genes promoted by *p1kbREX1* were not expressed. S/A *rex1* under control of *pREX1* was expressed ~2x higher than *REX1* or *rex1* S/E. α -GFP was used to detect GFP-*rex1*, protein levels were normalised against Pgk1. The 25kDa band represents the expected location of free GFP. Non-specific bands are commonly found when using the α -GFP band and are not thought to be degradation products.

3.9 Non-phosphorylatable Rex1 resists degradation in response to heat stress

Localisation phenotypes of phosphomimetic and non-phosphorylatable mutants was difficult to determine in plasmid expressed GFP tagged genes. Problems with our α -GFP antibody made discerning GFP-*rex1* depletion rates difficult. To bypass these obstacles we opted to integrate our phosphomimetic and non-phosphorylatable alleles into the genome with C-terminal -mNG or -HTP tags. This was done by knocking out *REX1* with *KL URA3* in *REX1-HTP* and *REX1-mNG* strains. PCR fragments of *rex1* S/A and *rex1* S/E were integrated into the native locus and loss of the *KL URA3* gene was selected for on 5-FOA. Mutant ORFs were PCR amplified from selected colonies and sequenced through Sanger sequence to verify the correct *rex1* allele.

Cultures expressing *rex1-S/A-HTP* and *rex1-S/E-HTP* were shifted from 30°C to 39°C and pellets collected. These were lysed and analysed by western to determine effects on protein level in response to heat stress (fig. 3.20). S/A Rex1 showed increased resistance to degradation compared with S/E or

WT alleles, an ANOVA was performed on decay rates and no significant differences were found between alleles ($P = 0.2629$).

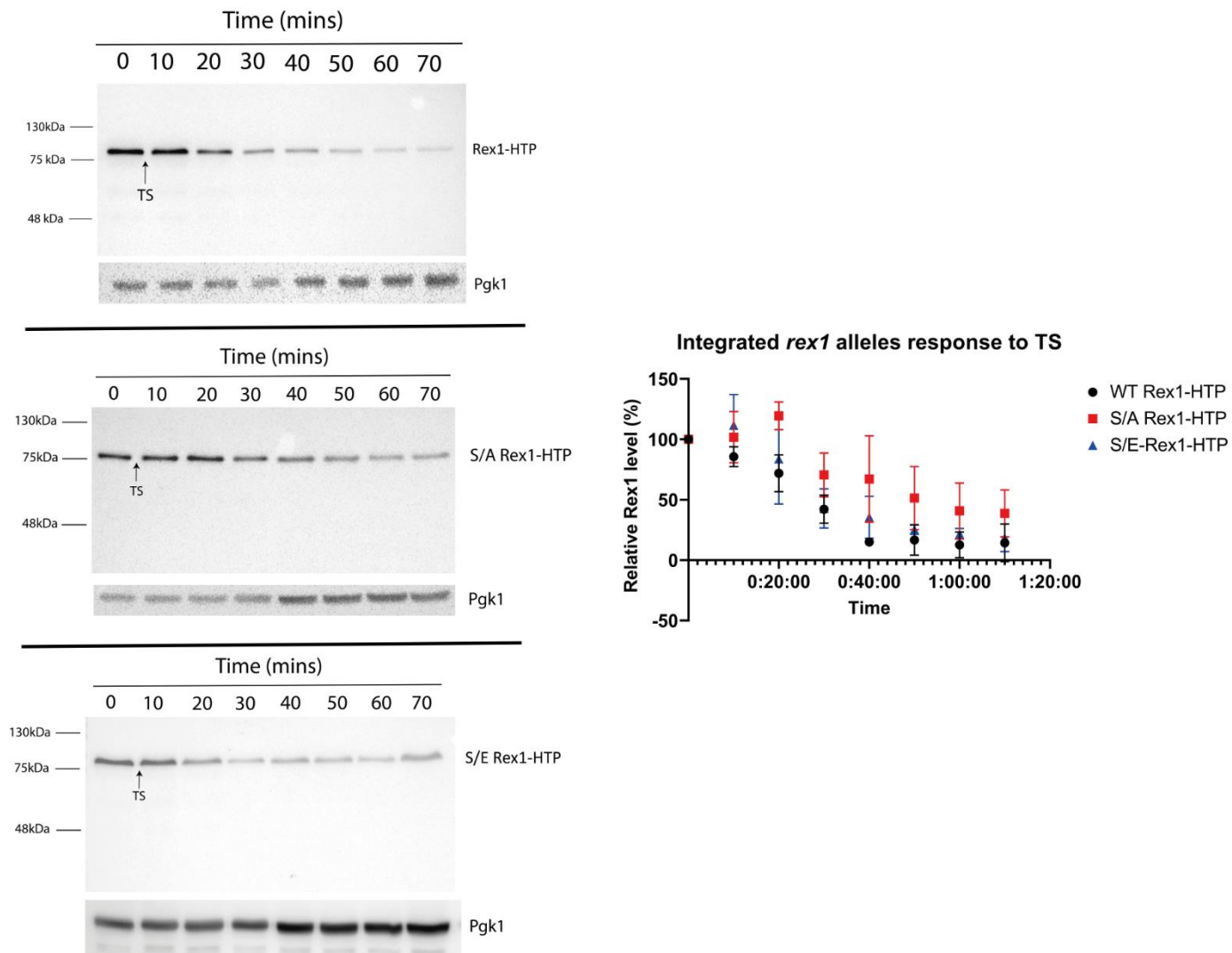


Figure 3.20. *rex1*-S/A shows resistance to depletion compared to WT or *rex1*-S/E. Westerns showing levels of phosphomimetic and non-phosphorylatable Rex1 in cells over a shift from 30°C to 39°C are displayed. The S/A allele resists depletion when compared to the S/E or WT protein. At the end of the experiment, approximately ~30% of the S/A allele remains compared with 10-15% for the S/E and WT. All experiments were completed in triplicate and standard deviations are shown in the error bars. An ANOVA was performed and differences between Rex1 alleles were not significant ($P = 0.2629$). α -PAP was used to detect *rex1*-HTP and protein levels were normalised to Pgk1.

Westerns performed on steady state samples of these three mutants at 30°C validated that *rex1* S/A is more stable than *rex1* S/E (fig. 3.21), though the effect was diminished compared to when expressed from the *REX1* promoter on a plasmid. As we had seen differences in Rex1 behaviour when comparing integrated and plasmid-expressed alleles this experiment was performed to validate differences in stability between phosphomimetic and non-phosphorylatable alleles in integrated strains. We conclude that our phosphomimetic allele is less stable and more prone to depletion.

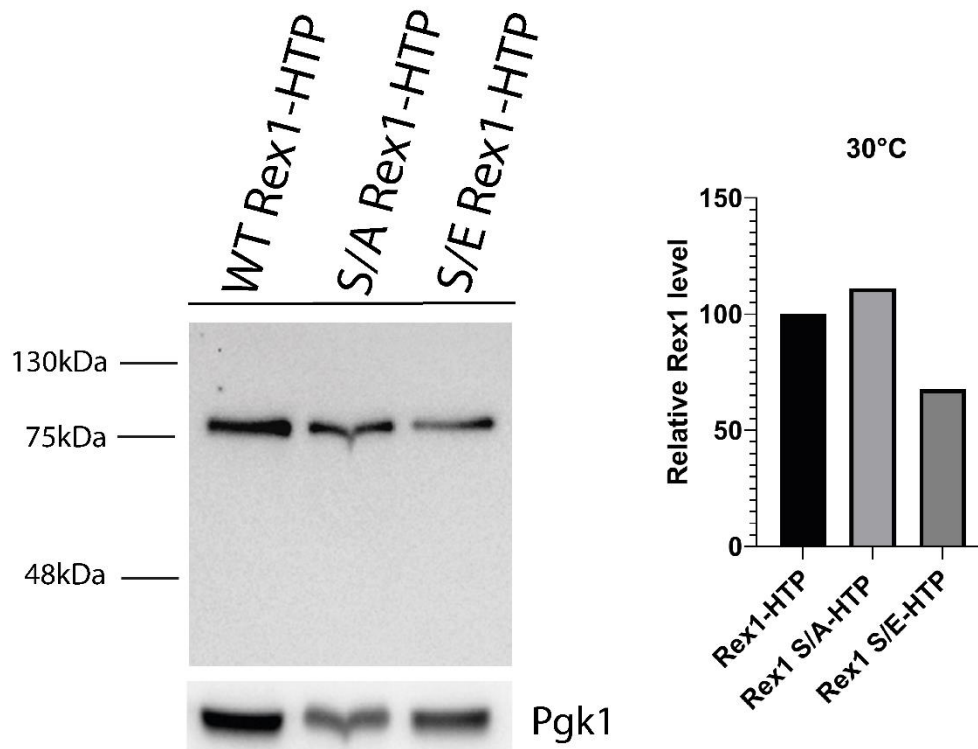


Figure 3.21. Rex1 and non-phosphorylatable Rex1 are expressed at higher levels at 30°C than phosphomimetic Rex1. Protein extracts from cultures expressing Rex1, *rex1* S/A and *rex1* S/E at 30°C are shown. WT Rex1 was normalised to 100%, non-phosphorylatable *rex1* (S/A) is expressed at comparable levels to WT. Phosphomimetic Rex1 (S/E) is expressed at 66% of the WT. α -PAP was used to detect *rex1*-HTP and protein levels were normalised against Pgk1.

3.10 Heat stress associated Rex1 degradation is proteasome mediated.

Phosphorylation mediated protein degradation is known to occur in phosphodegron systems where phosphorylation triggers ubiquitylation and subsequent recruitment to the proteasome (Holt, 2012). An *erg6* Δ was introduced into the *REX1-HTP* strain. MG132 can be added to cultures as a proteasome inhibitor however, the drug will not penetrate the cell in the absence of an *ERG6* deletion. Logarithmic cultures of *erg6* Δ , *REX1-HTP* were grown and treated with MG132 immediately prior to initiating a heat shock to 39°C. Western blot analysis of protein lysates harvested throughout the shift to 39°C showed an increase in Rex1 stability when compared to control cultures (fig. 3.22). This leads us to conclude that the degradation of Rex1 observed in the absence of MG132 is proteasome mediated.

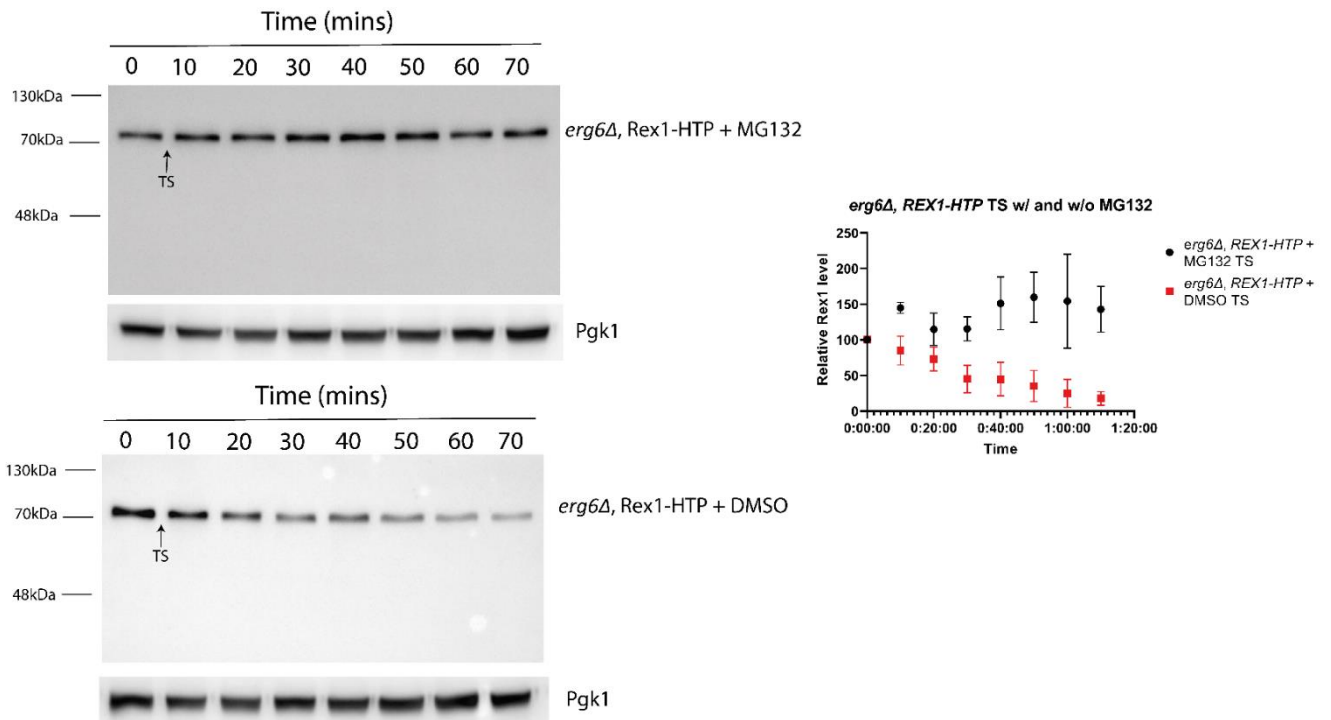


Figure 3.22. Proteasome inhibition stabilises Rex1 in heat-shocked cells. Shown are western blots for *erg6Δ*, *REX1-HTP* cultures harvested every ten minutes over a shift from 30°C to 39°C. Cultures were treated with either MG132 or DMSO prior to collection of the zero time point. The cultures treated with MG132 show resistance to degradation, with Rex1 remaining stable or increasing over the course of the temperature shift. Cells treated with the DMSO control see a breakdown pattern similar to seen in WT cells. All experiments were performed in triplicate, standard deviations are shown in error bars. α -PAP was used to detect rex1-HTP and all protein levels are normalised to Pgk1.

3.11 Rex1 is phosphorylated in response to heat shock

Western blot data had shown slight differences in stability between phosphomimetic and non-phosphorylatable Rex1 alleles. To measure this we performed *in vivo* ^{32}P phospholabelling and Rex1-HTP pulldown to measure Rex1 phosphorylation state in response to heat shock. Three cultures of *erg6Δ*, *REX1-HTP* cells were grown in phosphate depleted YPD at 30°C until mid-log phase. We harvested 30 OD₆₀₀ units of these cells and labelled them with ^{32}P -orthophosphate. A control sample was harvested from 30°C. The remaining cultures were treated with either 50 μM MG132 or an equivalent volume of DMSO and heat shocked at 39°C for 30 minutes. These cultures were pelleted and Rex1-HTP was purified on IgG sepharose under stringent conditions. These samples were ran on SDS-PAGE and transferred to nitrocellulose. The ^{32}P signal was measured and Rex1-HTP detected using α -PAP (fig. 3.23). Due to the prevalence of low molecular weight bands in which we were not confident were correlated to Rex1 in both the western and radioactive signal only the upper fraction of the blot was measured. Heat shocked samples yielded less protein but gave a greater radioactive signal, indicating that Rex1 is phosphorylated upon exposure to heat stress. The radioactivity/western blot ratio was ~5-10x greater in heat-shocked samples treated with DMSO or MG132 when compared to cells harvested at 30°C. An ANOVA was performed and the radioactivity/protein ratio was found to be significantly different between cells grown at permissive temperatures and under heat shock (P =

0.0006). A caveat of this experiment is that we did not test for non-specific binding to IgG sepharose. This was due to the stringent washing conditions with 2M MgCl₂ that was performed to strip non-specific protein from the beads. This experiment is due to be performed in the future. From these data, we conclude that Rex1 is phosphorylated in response to heat shock at 39°C.

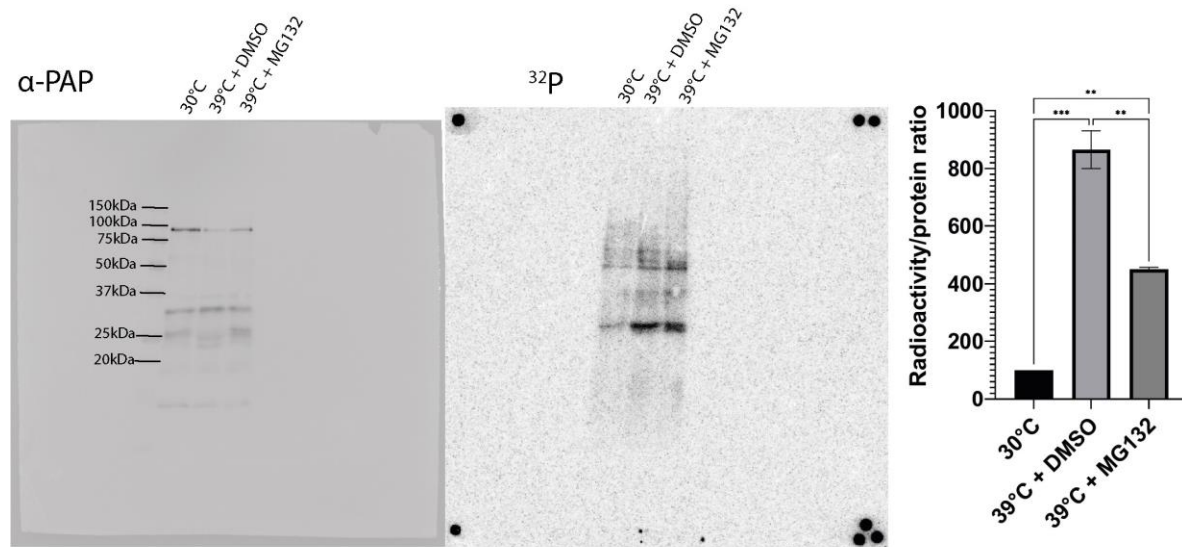


Figure 3.23. Rex1 is phosphorylated in response to heat shock. *erg6Δ*, *REX1-HTP* cells were grown on phosphate-depleted YPD and incubated with ³²P-orthophosphate. Control samples were collected from logarithmic cultures growing at 30°C. Cultures were treated with either DMSO or MG132 and heat-shocked at 39°C for 30 minutes. Rex1-HTP was pulled down from all cultures, resolved by SDS-PAGE and transferred to nitrocellulose. ³²P signal was measured and α-PAP antibody was used to detect protein. ¹⁴C dots were placed on the corners of the blot to facilitate alignment of the radioactive signal with the western blot for determination of radioactive band size. An ANOVA was performed and heat shocked samples were found to be significantly different from control cells grown at 30°C (P = 0.0006), significant differences are denoted with asterisks.

3.12 Phosphorylation-associated degradation of Rex1 may be primed by TOR inhibition

The TOR pathway is a known signalling cascade associated with stress response, particularly nutrient sensing, and it is associated with ribosome biogenesis (Powers & Walter, 1999, Lippmann & Broach, 2009). The pathway works through phosphorylation of a master regulator that initiates a large phosphorylation mediated signalling cascade, resulting in the activation of many kinases/phosphatases. Inhibition of TOR activity through the addition of rapamycin causes a wide range of effects including growth arrest in G₀, reduction of ribosome biogenesis and a starvation mimicking response. As Rex1 is involved in ribosome biogenesis and is phosphorylated and degraded upon heat stress conditions, we thought this could be regulated by the TOR pathway. A preliminary experiment was conducted to determine whether inhibiting TOR resulted in a lack of Rex1 phosphorylation and Rex1 protection in response to heat stress. *REX1-HTP* cells were treated with

rapamycin (200nM) and incubated for 1 hour prior to initiation of a heat shock. Cell pellets were then collected every ten minutes and Rex1 levels analysed by western blot (fig. 3.24).

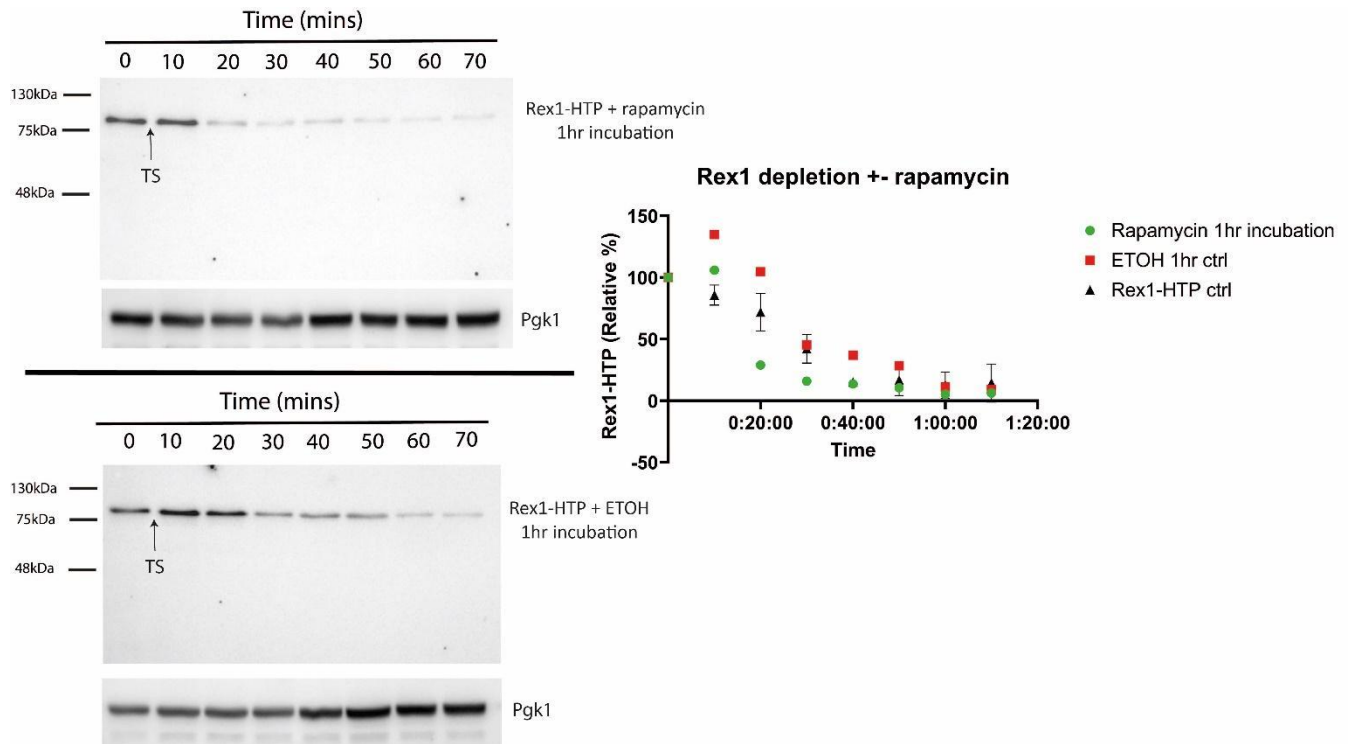


Figure 3.24. Cultures incubated with rapamycin for 1hr show an increased rate of Rex1 depletion in response to heat shock. Shown are western blots for *REX1*-HTP cultures undergoing a shift from 30°C to 39°C treated with 200nM of rapamycin. Cultures were incubated with rapamycin for 1hr prior to initiation of the heat shock. A control sample was heat-shocked after 1hr incubation with ethanol. The temperature shift is marked with the arrow labelled TS. Protein levels were detected using the α -PAP antibody and protein levels were normalised against Pgk1. Results from untreated *Rex1*-HTP heat shocks are plotted adjacently for comparison. This experiment was repeated just once.

Rapamycin treated samples depleted more rapidly when shifted to 39°C than control samples or initial experiments on untreated *REX1*-HTP. Rex1 levels were easily detectable after a 1hr incubation with rapamycin, indicating that TOR inhibition did not induce Rex1 degradation in a manner equivalent to heat shock. The increased rate of Rex1 depletion in TOR treated samples could demonstrate priming effect of TOR inhibition. We were not confident in the quality of our rapamycin so we performed growth curves of cultures treated with varying concentrations of rapamycin to determine optimal conditions for rapamycin inhibition (fig. 3.25). These curves led us to repeat the experiment with cultures treated incubated with 200nM rapamycin for four hours.

Rapamycin vs ethanol concentration, growth rate

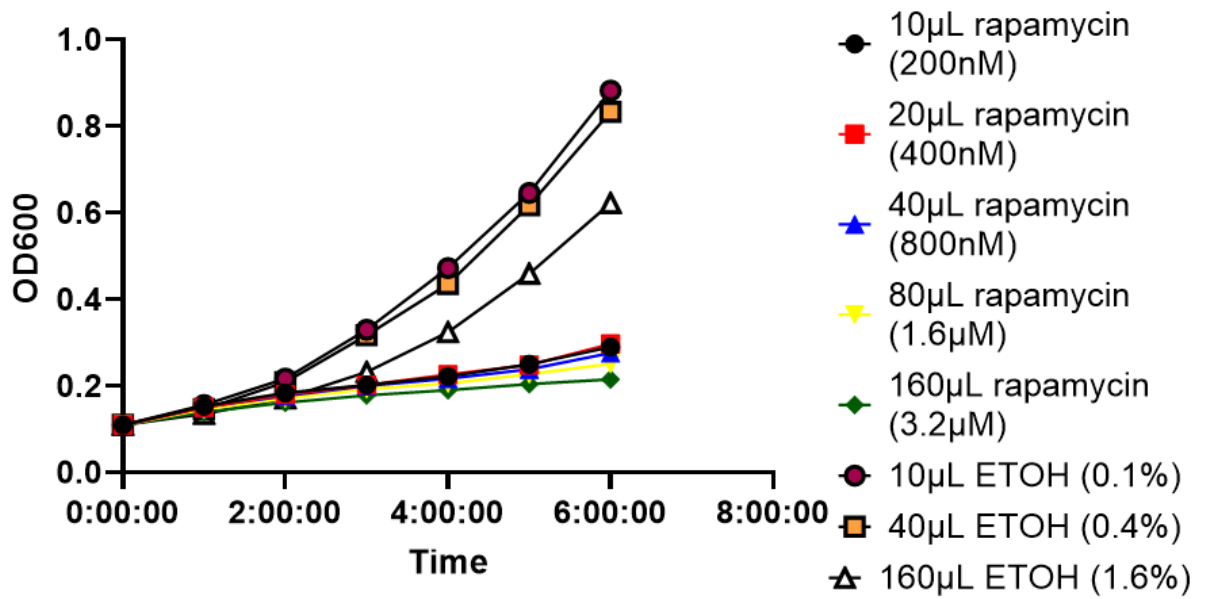


Figure 3.25. Rapamycin concentrations above 200nM inhibit growth. Shown are growth curves from WT yeast cultures treated with varying concentrations of rapamycin. Control cultures treated with ethanol were also measured. The volume of liquid added to cultures is indicated alongside concentration to facilitate comparison between treatments and controls. All cultures treated with rapamycin showed inhibited growth. Samples containing 1.6% ethanol showed notably reduced growth compared with cultures containing less ethanol.

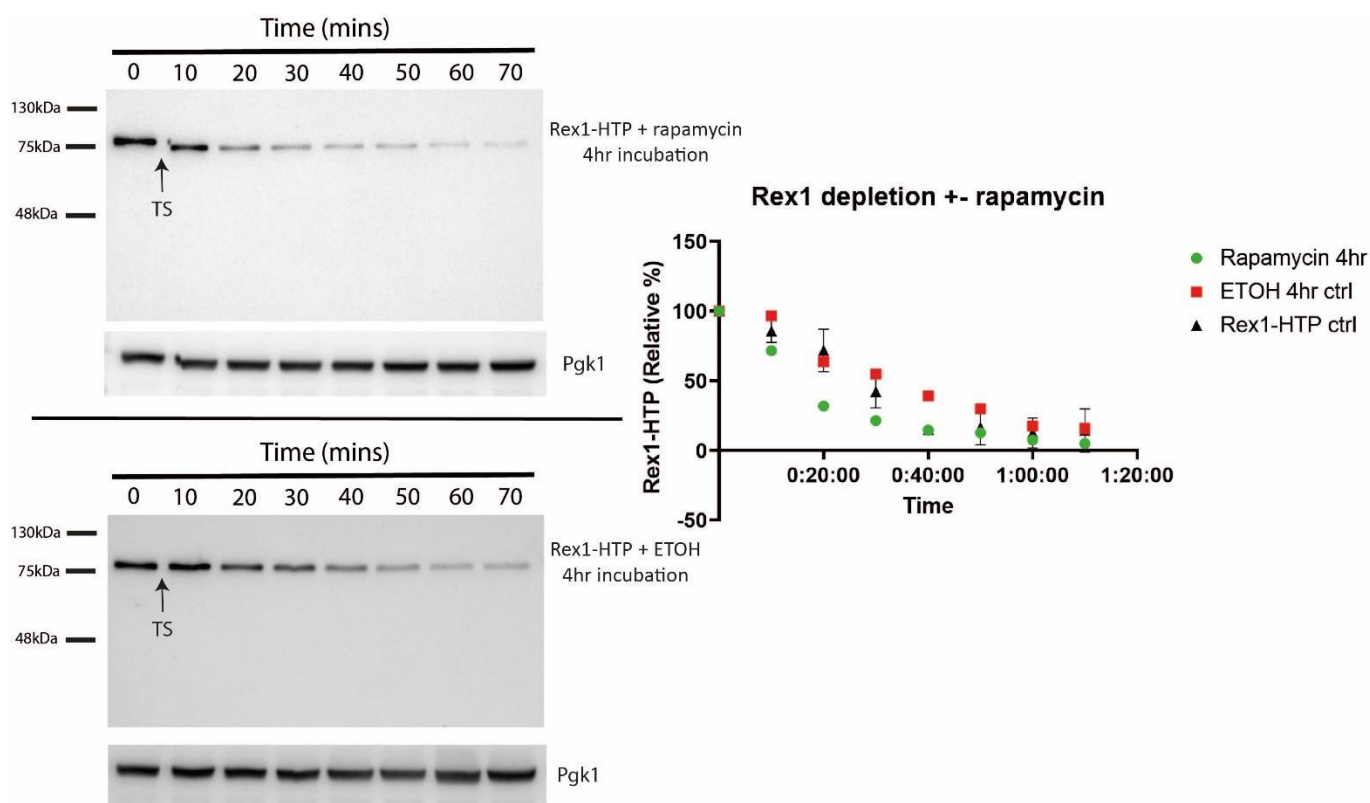


Figure 3.26. Cultures incubated with rapamycin for 4hrs show increased rate of Rex1 depletion in response to heat shock. Shown is a western blot depicting a temperature shift of *REX1*-HTP expressing cells from 30°C to 39°C after a four-hour incubation on rapamycin. A control culture incubated with an equivalent volume of ethanol was also ran. Heat-stress induced depletion was faster in rapamycin treated samples. Shift to 39°C is indicated with the arrow marked 'TS'. Protein levels were detected using the α -PAP antibody and normalised against Pgk1. This experiment was repeated just once.

The temperature shift was repeated after a four-hour incubation on 200nM rapamycin (fig. 3.25). In both experiments treating cells with rapamycin we see faster Rex1 depletion in cultures treated with rapamycin versus controls.

It could be that the starvation mimicking effect of rapamycin stresses the cell initiates pathways preparing for rapid stress response. This may result in rapid heat-shock induced changes. Rex1 depletion rate in cells treated with ethanol is reduced compared with untreated or rapamycin treated samples. This is an interesting observation, the concentration of ethanol in these cultures is just 0.1% and we are unsure of the extent to which this would alter yeast metabolism.

3.13 Bioinformatic tools do not identify a phosphodegron motif in Rex1 protein sequence

To explore whether phosphorylation-mediated Rex1 degradation is related to known phosphodegrons, we ran the Rex1 protein sequence through three online degron predicting tools. Degronpedia predicted six possible degrons in the Rex1 sequence. An N-degron and a C-degron at the terminal ends of the protein was predicted. Additional degrons were predicted at amino acid 91-98, 208-216, 241-248 and 365-372. All of these degrons were predicted from animal models and none are located in the NLS or at PTM sites of Rex1.

Genomenet MOTIF search identified solely an RNase T like domain between amino acid 227-372 of Rex1, associated with Rex1 catalytic activity. Degronpedia did not identify any degron motifs in the Rex1 amino acid sequence.

3.14 Discussion

In this chapter, we have assessed Rex1 regulation in response to heat stress. We have found that Rex1 is delocalised and depleted in response to heat stress (fig. 3.11, 3.6). Furthermore, we have identified that Rex1 degradation is proteasome mediated (3.22) and that Rex1 phosphorylation increases under heat stress (fig. 3.23). GFP-*rex1* fusion truncations identified an NLS between amino acid 17-52 (fig. 3.2) and the expression of GFP-*REX1* in temperature-sensitive *srp1* mutants indicated that Rex1 import is Srp1 mediated (fig. 3.5).

In section 3.6 we have observed that Rex1 is delocalized from the nucleus and degraded when shifted from permissive to heat stress temperatures (fig. 3.11). This implied a multi-faceted stress response. By initiating the degradation of Rex1, the cell inhibits Rex1 activity, while delocalizing it separates it from its substrate, additionally reducing activity. There are other examples of changing protein localization in response to stress in yeast.

Rat8, an mRNA export protein, is sequestered in the nucleus, away from the nuclear pore, in response to ethanol stress (Takemura *et al*, 2004). This effect was accompanied by reduced mRNA export. While this response was observed in response to 10% ethanol, it was not seen in cells exposed to 42°C. This indicates that multiple stress response pathways exist. However, the observation that Rat8 localization changes and that its function as an mRNA exporter is impaired demonstrates the use of compartmentalization as a regulatory metabolic tool. A further observation that not all mRNA export is hindered under heat stress but that heat-shock protein (HSP) mRNAs continue to be exported (Izawa *et al*, 2008) shows additional complexity in stress responses. In this instance, the difference between imported and exported transcripts appeared to be related to fluctuations in the degree of polyadenylation in response to ethanol or heat shock stress.

We did not study Rex1 transcription in response to heat shock so we do not know the availability of Rex1 mRNA in heat shocked cells, nor did we study Rex1 levels over a return to permissive from heat-shock conditions. Observing Rex1 transcription and protein levels over a shift from permissive to heat-shock and back to permissive temperatures would be insightful for determining the magnitude of the cells response.

Microscopy data showed the accumulation of 'granule-like' foci early on in heat-shocked cells (fig. 3.11). These granules resemble mRNA stress-granules known to accumulate in response to numerous stressors (Hoyle *et al*, 2007, Brengues & Parker, 2007). mRNA stress granules accumulate in the cytoplasm while the granular structures we see are confined to the nucleus, though due to the

crescent-like structure often observed it could be nucleolar localization. Co-expression alongside nucleolar markers could elucidate whether this is the case. However, it is not apparent whether these foci form in response to heat stress or are always present yet only resolvable upon signal depletion. It could be that these foci represent sites of degradation, with an increased concentration of proteasome complexes. Such proteasome granules have been observed in the nucleus as well as in the cytosol in response to oxidative, nutrient and heat stress (Enekel *et al*, 2022).

The use of *in vivo* ³²P phospholabelling showed us that Rex1 is phosphorylated in response to heat stress (fig. 3.23). Heat-stress induced Rex1 phosphorylation coincides with the Rex1 protein depletion. Phosphodegrons are known motifs in which phosphorylation induces recruitment of a ubiquitin ligase, resulting in protein degradation in the proteasome. The observation that MG132 stabilizes Rex1 in response to heat-stress demonstrates that Rex1 depletion is proteasome mediated. There is a known ubiquitinated lysine downstream of Rex1 phosphosites. The culmination of these observations indicate that Rex1 may contain a phosphodegron motif. The use of three available online degron predicting tools (degronpedia, Degpred, genomnet MOTIF search) did not identify any degron motif in the NLS of Rex1. This indicates that a phosphodegron motif in Rex1 may be novel or unlike previously characterized examples. While phosphodegrons are best known for their significance in moving cells through the cells cycle such as in the case of Cdc6 (Al-Zain *et al*, 2015). It is possible that this mechanism has been evolutionarily adapted to stress response as well.

In 3.10 we have used MG132 in an *erg6Δ*, *REX1-HTP* strain to deduce that stress-induced Rex1 depletion is proteasome mediated (fig. 3.22). It is known that Srp1 also acts to translocate proteasome complexes across the nuclear membrane (Chen & Madura, 2014). Importin- α re-export to the cytosol is known to be inhibited during heat shock in mammalian cells (Furuta *et al*, 2005, Miyamoto *et al*, 2004). If this were conserved in yeast, it would mean a global Srp1 mediated reduction in nuclear import in response to heat shock. By having the degradation machinery imported simultaneously as the cargo it ensures the cells is equipped to respond to heat shock which would inhibit its ability to move proteasomes to the nucleus.

Cse1 is a yeast protein found in the nuclear lumen. Numerous studies using mutant *cse1* identified that Cse1 interacts with Srp1 in the presence of Ran-GTP (Hood & Silver, 1998, Solsbacher *et al*, 1998, Kunsler & Hurt, 1998). The use of cold-sensitive *cse1* was used to observe that functional Cse1 is required for Srp1 cytoplasmic accumulation (Hood & Silver, 1998). These observations indicate that Cse1 is required for Srp1 re-export from the nucleus. Observations in the Cse1 human homologue CAS have identified nuclear accumulation of importin- α in response to numerous stressors including UV irradiation, oxidative stress and heat shock (Miyamoto *et al*, 2004). If these mechanisms are conserved between yeast and human it is possible that we get Srp1 nuclear accumulation under heat shock conditions and a lack of Rex1 import as opposed to Rex1 export from the nucleus. As we see a cytosolic accumulation of Rex1 in the cytosol of heat-shocked cells it could be that Rex1 degradation occurs more rapidly in the nuclear lumen than in the cytosol, altering the nuclear/cytoplasmic Rex1 ratio.

We have found that Rex1 is phosphorylated and degraded in a heat-shock response. We are unaware of any kinases which mediate this reaction though if they were identified, exploration of their sub-cellular localization would be insightful as to whether induced Rex1 degradation is present throughout the cell or solely in the nucleus. It is known that MAPK kinases are activated under osmotic stress but also under heat shock (Winkler *et al*, 2002). It is possible that these kinases are involved in the observed Rex1 phosphorylation. A model for how heat-shock affects Rex1 phosphorylation status and nuclear accumulation based on our data is shown in figure 3.27.

This chapter characterizes Rex1 nuclear localization and regulation in response to stress. We have also explored the role of PTM's on the Rex1 NLS and used *in vivo* phospholabelling to determine that Rex1 is phosphorylated as a stress response degradation signal. We will expand upon these topic in chapter 5.

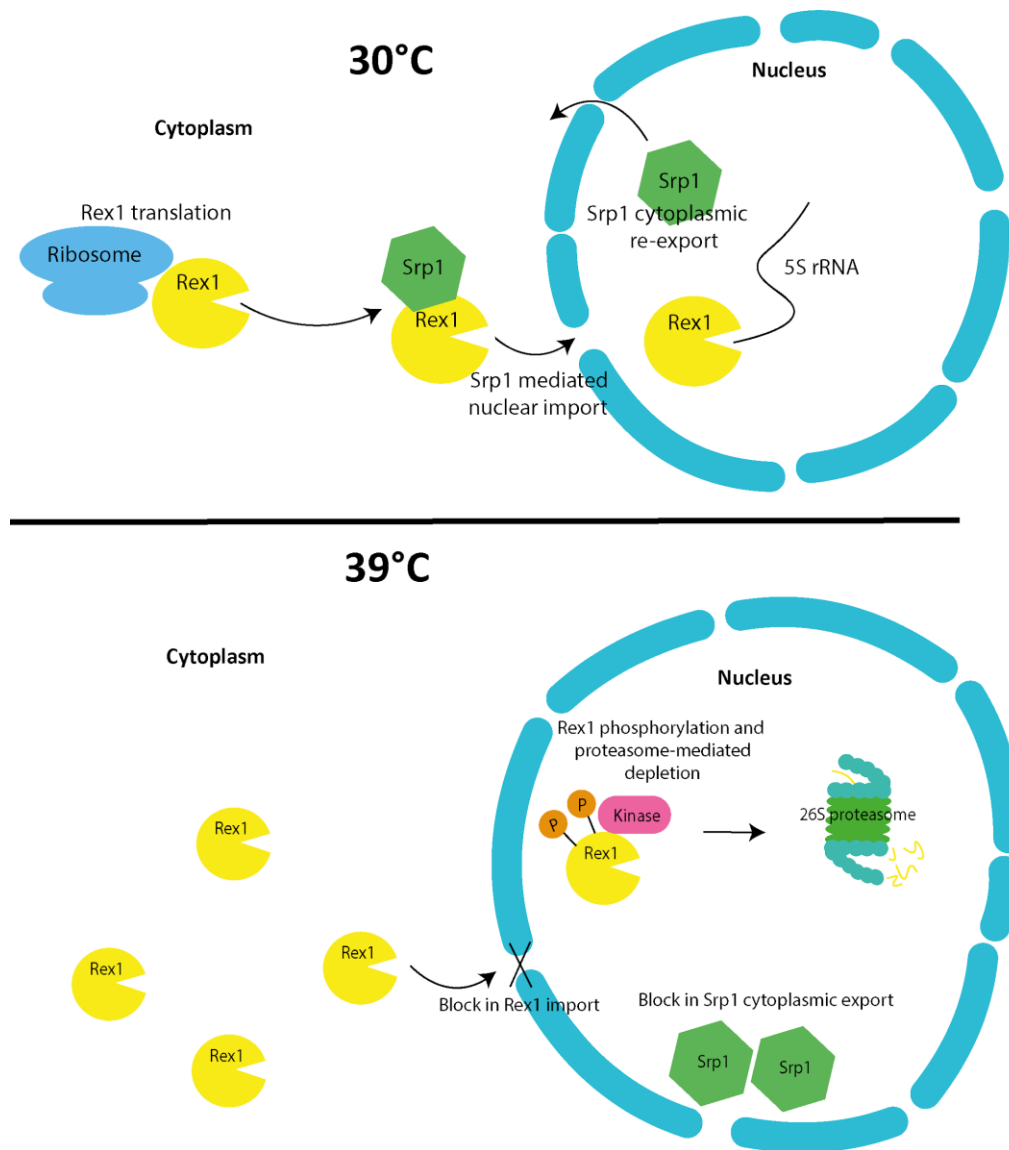


Figure 3.27. Model for Rex1 regulation in response to heat stress based on data collected in this study. At 30°C, Rex1 translated in the cytoplasm is imported into the nucleus through the action of Srp1. Rex1 shows limited post-translational modifications and is stable. At 39°C, Rex1 is phosphorylated by an unknown kinase, leading to its proteasome-mediated degradation. Srp1 accumulates in the cytoplasm through a block in Srp1 cytoplasmic export shuttling. The lack of cytoplasmic Srp1 results in an increased cytoplasmic pool of Rex1.

Chapter 4 Heterologous expression of the MEL biosynthetic pathway in *S. cerevisiae*

4.1 Introduction

Mannosylerythritol lipids (MELs), are glycolipids with promising emulsifier activity. They are produced by numerous fungi including the phytopathogenic fungi *Ustilago maydis* (*U. maydis*). As this organism is a maize pathogen (Christensen, 1963), there is an aversion to growing it in large cultures for MEL production. *U. maydis* produces a second glycolipid biosurfactant, ustilagic acid, which has fewer high value applications than MELs (Morita *et al*, 2015, Ullmann *et al*, 2022). This incentivises developing means to produce pure MELs. The MEL biosynthetic pathway was characterised in 2006 (Hewald *et al*, 2006), and found to be transcribed from a five gene cluster. The five genes encode Emt1, a glycosyltransferase catalysing formation of mannosylerythritol, a disaccharide of erythritol and mannose. Mac1 and Mac2 subsequently add a fatty acid chain to C1 and C2 of the mannose moiety of mannosylerythritol in the peroxisome. The mechanism of mannosylerythritol import into the peroxisome is unknown. There is evidence that molecules below 700Da diffuse through the peroxisomal membrane without a specific transporter in *S. cerevisiae* (DeLoache *et al*, 2016), mannosylerythritol has an atomic mass of 284Da and we presume it can diffuse into the peroxisome. Mechanisms of mannosylerythritol peroxisomal import in *U. maydis* are unknown. The di-acyl-mannosylethritol is returned to the cytosol; again, the movement of the di-acylated MEL from the peroxisome to the cytosol is uncharacterised. While the length of the fatty acid chains varies, the di-acylation frequently adds 19-22 carbons to the mannosylerythritol yielding a molecule with an atomic mass between 550-700Da (Beck *et al*, 2021), and we expect it to diffuse through the peroxisomal membrane in *S. cerevisiae*. Post-peroxisomal export, it is acetylated on C4 and C5 by Mat1 in the cytosol, yielding the complete glycolipid. The molecule is then exported to the extracellular environment by Mmf1 (Hewald *et al* 2006) (fig. 1.11).

This export system is biotechnologically advantageous as it removes the need for cell lysis to recover the finished product. Allowing the culture supernatant to be recovered and the finished MEL extracted from it. Recovery from the supernatant increases the potential for continuous manufacturing which is industrially preferable. Similar pathways have been found in organisms *Moesziomyces antarcticus* (*M. antarcticus*) and various fungi in the genera *Pseudozyma* (Morita *et al*, 2015, Konishi *et al*, 2013). While MEL synthesis in these organisms is reported, it comes with nutritional requirements, particularly a shift from rich to nitrogen limiting (N-limiting) media (Akkermans *et al*, 2020, Lorenz *et al*, 2014). Reconstituting the pathway in a model organism allows the pathway to be placed under constitutive regulation, simplifying manufacture by using a single growth media. Additionally the use of a *S. cerevisiae* opens opportunities for targeted metabolic alterations, for example changing the length of available fatty acids to produce a glycolipid with specific activity. Therefore, we aim to express the MEL biosynthetic pathway in *S. cerevisiae* to create a model system for optimising MEL production.

Making an *S. cerevisiae* strain expressing five heterologous proteins comes with several challenges. Each protein needs to be encoded by its open reading frame and expression must be controlled by a promoter and terminator, resulting in a lot of time consuming cloning. Each promoter/terminator pair

must be of adequate strength to support high enough expression of the protein to allow flux of metabolites through the pathway. The use of native regulatory sequences opens the possibility of homologous recombination between promoters/terminators used in the MEL pathway expression constructs and native loci in the *S. cerevisiae* genome. Additionally, the pathway must be functional in its novel host with a suitable capacity for correct protein folding. Additionally, there must be suitable availability of precursors as well as transport of precursors and intermediates between cell compartments and availability of any required cofactors for the enzymes to function correctly. Furthermore, should heterologous expression of the MEL genes function in *S. cerevisiae*, there is likely to be optimization required with regard to culture media, gene expression levels, growth conditions and extraction protocol to increase efficiency of the manufacturing process.

In chapter 4 we will detail the cloning strategy resulting in a strain of *S. cerevisiae* containing the MEL biosynthetic gene cluster as well as attempts to synthesize MELs in the completed strain.

4.2 Heterologous expression of *U. maydis* proteins shows correct sub-cellular localisation in *S. cerevisiae*

4.2.1 Cloning of MEL biosynthesis genes and expressing them as GFP fusion proteins

Four of the five MEL biosynthetic gene cluster genes, *EMT1*, *MAC1*, *MAC2*, and *MAT1* had to be PCR amplified from the genome of *U. maydis* for expression in *S. cerevisiae*. The final gene, *MMF1*, had been previously synthesized in the lab for expression in a different biotechnological host, the oleaginous yeast *Debaryomyces hansenii* (*D. hansenii*). A plasmid containing the *MMF1* open reading frame could be used as a PCR template. Genes *EMT1* and *MAC2* were bioinformatically identified as containing an intron, while *S. cerevisiae* has splicing machinery, only a small proportion of its genes contain introns. Therefore, we produced a continuous ORF to reduce our dependence on the splicing machinery. This was done by PCR amplifying the ORF in two exons, with exon 1 containing 20bp at the 3' end identical to the 5' end of exon 2 over the splice donor/acceptor site. In the case of *MAC2* we PCR amplified a 114bp and a 1542bp exon. We digested a vector with BamHI and HindIII to yield a 6512bp linearized fragment which would leave in an in frame N-terminal GFP ORF when the *MAC2* exons were assembled within (fig. 4.1). These fragments were then transformed into *S. cerevisiae* for plasmid assembly through homologous recombination. The same procedure was performed for *EMT1*.

The remaining genes lack introns and the complete ORFs could be obtained by a single PCR amplification step. These amplicons were then cloned into vectors containing an in frame GFP ORF for the construction of fusion proteins. A DNA sequence encoding a linker of three glycine-alanine repeats was placed between the ORF and the GFP tag. This acts to distance the two domains of the fusion protein with the purpose of reducing the chance of steric hindrance and therefore any negative effects on folding, stability or activity through addition of a tag to the protein. Proteins containing a native peroxisomal targeting signal 1 (PTS1, C-terminal SKL) were GFP tagged at the N-terminus, while proteins lacking a PTS1 were GFP tagged at the C-terminus. This allowed verification that the peroxisomal proteins Mac1 and Mac2 are imported into peroxisomes in *S. cerevisiae*. All ORFs were cloned into vectors upregulated by the *TPI* promoter and the *PGK1* terminator except *MMF1*, which was placed under control of the *HIS3* promoter. *Tpi* is a highly expressed glycolytic enzyme, frequently used in plasmids to achieve high levels of gene expression. This was done as previous work in the lab expressing *MMF1* under the *TPI* promoter had led to quality control failure in the ER and a build-up of protein that failed to be incorporated into the plasma membrane (data not shown).

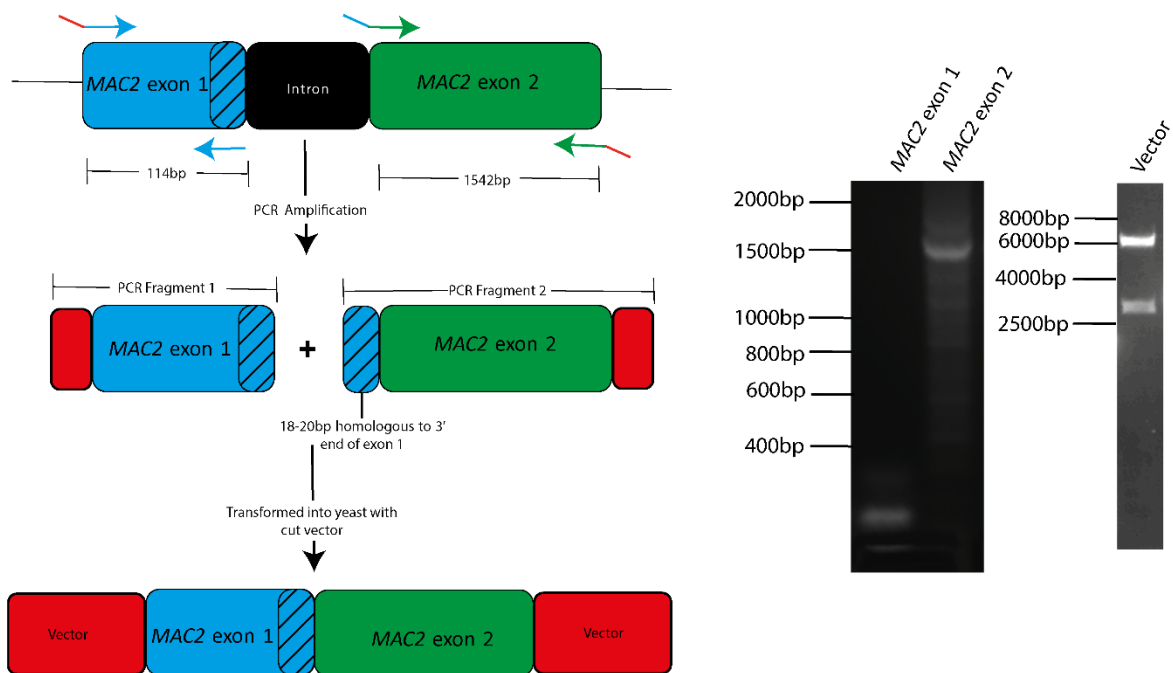


Figure 4.1. Schematic *MAC2* cloning without introns. Shown is the primer design strategy for amplifying exons from intron containing genes. Primers designed for *MAC2* exons contain flanking regions containing identical sequence to either the vector or the following exon. The outer flank of both exon-amplifying primers contains 18-20bp identical to the integration site in our vector. While inner primers used for intron excision leave each exon fragment with 18-20bp of identical sequence. This allows the final plasmid to be constructed *in vivo* by homologous recombination DNA repair. The agarose gels show successful amplification of exon fragments at 114bp and 1542bp. The vector restriction digest shows correct linearization and excision of a ~2700bp band. Both exons and the linearized vector were assembled through *in vivo* homologous recombination in yeast.

4.2.2 *U. maydis* MEL biosynthetic proteins localise correctly within *S. cerevisiae*

The MEL biosynthetic genes were expressed as N-terminal or C-terminal GFP fusion proteins in *S. cerevisiae*. (fig. 4.2). Microscopy data demonstrated equivalent subcellular localisation in *S. cerevisiae* as in *U. maydis*. Cytosolic proteins Emt1-GFP, and Mat1-GFP displayed cytosolic GFP signals. GFP-Mac1 and GFP-Mac2 showed punctate signals reminiscent of peroxisomes. Co-expression of GFP-Mac1 and GFP-Mac2 alongside a HcRed-PTS1 peroxisomal marker validated peroxisomal accumulation (fig. 4.3). The plasma membrane transporter, Mmf1-GFP, exhibited enriched signal around the periphery of the cell, implying membrane incorporation.

The expected atomic mass for each MEL-GFP fusion enzyme is as follows; Mmf1-GFP – 92kDa, Mat1-GFP – 84kDa, GFP-Mac1 – 91kDa, Emt1-GFP – 93kDa and GFP-Mac2 – 85kDa. Western blots of these fusion proteins identified with an α -GFP antibody showed bands of the correct size (fig. 4.4). Mac1 and Mac2 displayed two bands, suggesting PTMs are present but there is no mention of this in the literature. Protein levels under the *TPI* promoter was comparable, while Mmf1 showed lower expression from the *HIS3* promoter. Checking for a 27kDa free GFP band was crucial to avoid

misinterpretation due to potential GFP cleavage from the fusion protein, yielding a cytosolic signal. In no instances was this identified. This indicated that our heterologous genes were expressed as full-length fusions and validated our interpretation of Emt1 and Mat1 as cytosolic.

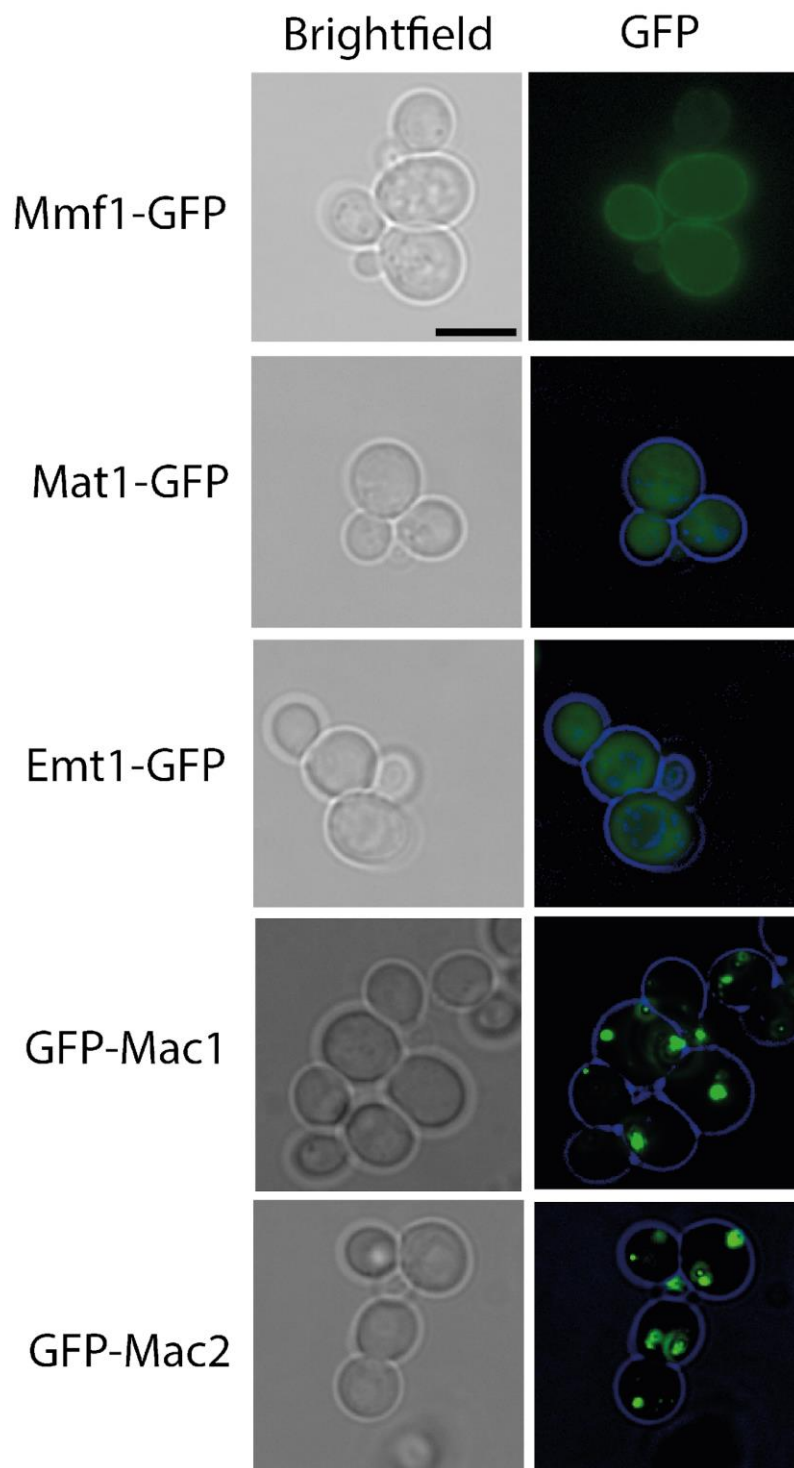


Figure 4.2. *U. maydis* proteins show correct sub-cellular localisation in *S. cerevisiae* when expressed as GFP fusion proteins. Shown is fluorescence microscopy data for the five MEL biosynthetic proteins in *S. cerevisiae*. Mmf1, the plasma membrane transporter shows an enriched peripheral signal. Mat1 and Emt1 show a cytosolic signal. Mac1 and Mac2 show a punctate pattern reminiscent of peroxisomes. Brightfield images are labelled as such while GFP excitation is labelled GFP. The scale bar indicates 5 μ m.

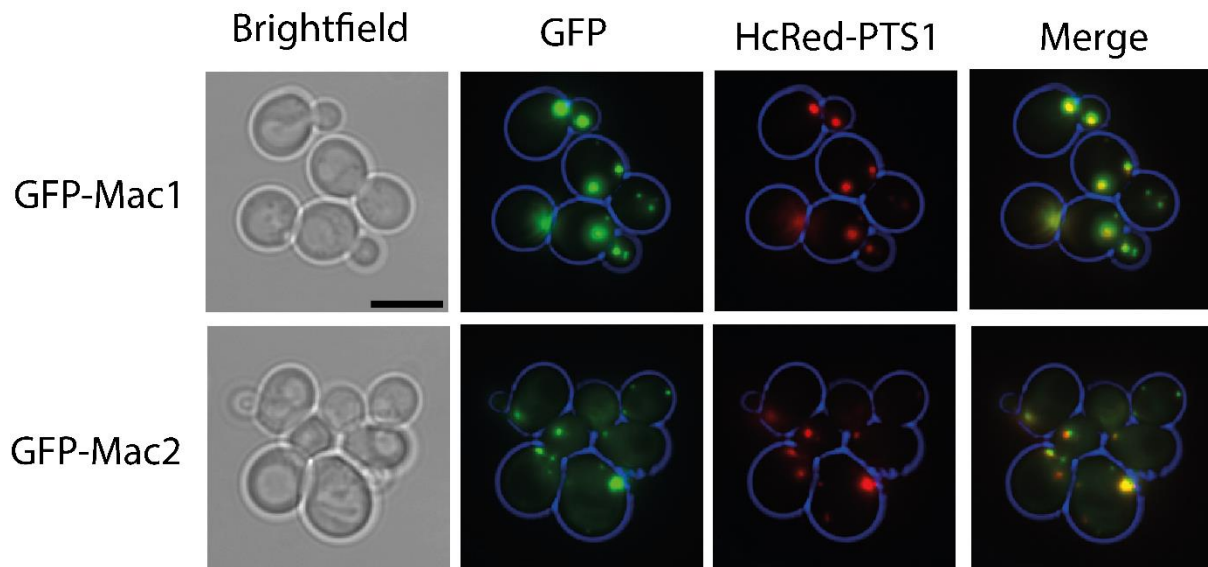


Figure 4.3. Colocalisation of GFP-Mac1/2 with HcRed-PTS1 indicates peroxisomal localisation of Mac1 and Mac2. Cells expressing the fusion proteins GFP-Mac1 and GFP-Mac2 alongside a HcRed-PTS1 red peroxisomal marker are shown. The green and red signals co-localise, indicating that GFP-Mac1 and Mac2 accumulate in the peroxisome. GFP excited images are labelled GFP. The scale bar indicates 5 μ m.

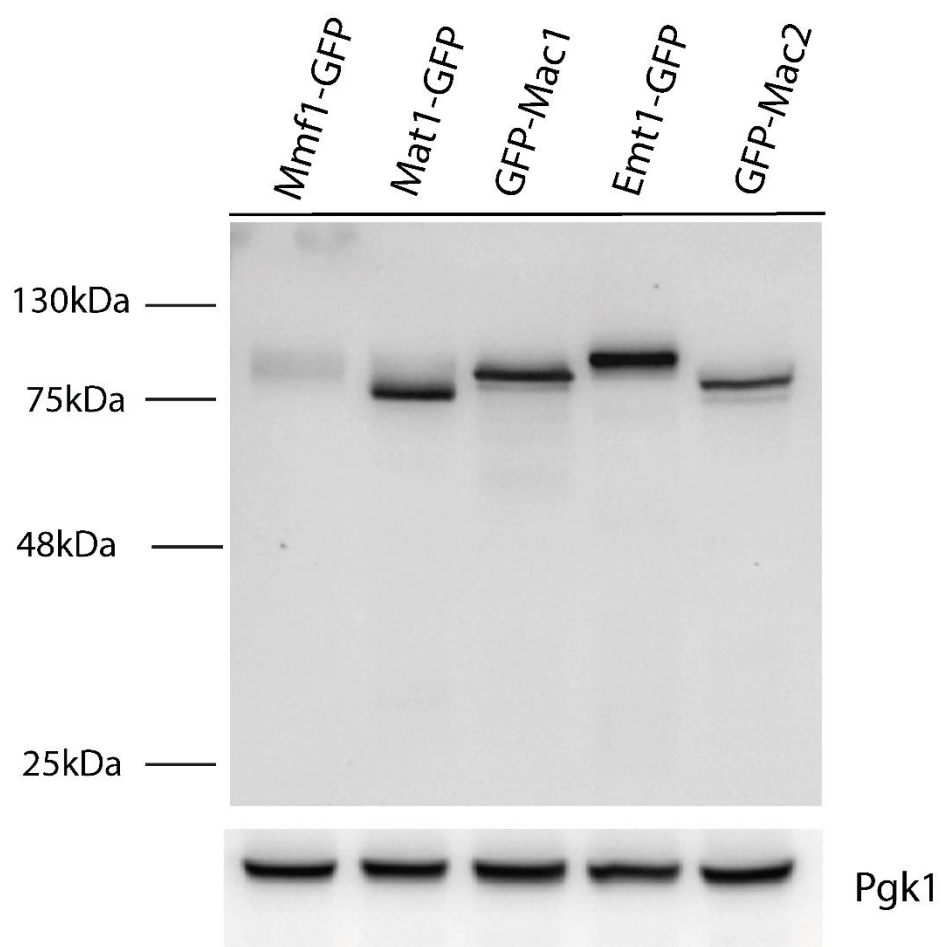


Figure 4.4. Western blots indicate that MEL biosynthetic genes are intact in *S. cerevisiae*. Western signal indicates that each MEL biosynthetic fusion-protein is intact when expressed in *S. cerevisiae*, accounting for the 27kDa GFP tag. The sizes for each fusion protein are; Mmf1-GFP – 92kDa, Mat1-GFP – 84kDa, GFP-Mac1 – 91kDa, Emt1-GFP – 93kDa and GFP-Mac2 – 85kDa. Proteins were detected using an α -GFP antibody and an α -PGK1 antibody was used as an internal loading control.

4.3 Expression of 5 genes simultaneously in *S. cerevisiae*

4.3.1 Development of a modular gene expression system

To enhance flux of metabolites through a pathway it is important to optimize gene expression level (Peng *et al*, 2015, Redden *et al*, 2015, Da Silva & Shrikrishnan, 2012). Overexpression can lead to protein misfolding and aggregation while weak promoters may result in insufficient protein levels to process high titres of substrates. To tackle the challenge of optimizing gene expression we devised a system in which ORFs would be assembled on a 'construction' plasmid regulated by a promoter/terminator pair chosen for desired protein levels. A 'spacer' placed between promoters/ORFs/terminators yields a consistent sequence for cloning through ligation, homologous recombination or Gibson assembly. Finished construction vectors are cloned into a separate 'expression vector' containing two of the biosynthetic genes. This approach permits construction of a primer library for amplification of interchangeable regulatory sequences. Amplifying ORFs with the spacers incorporated as primer flanks allows rapid retrofitting of the system for studying alternative metabolic pathways.

Spacer insertion between the promoter and ATG start codon showed minimal impact on gene expression based on previous studies (Dvir *et al*, 2019). Variation mostly arose from changing the 3bp immediately upstream the ATG start codon. This was countered by placing 3 A's at spacer 2's 3' end, placing 3 A's immediately prior to the ATG start codon as this is known to enhance expression (fig. 4.5).

Each gene in the pathway was cloned into the modular gene expression system with a unique promoter/terminator pair, this reduced the amount of homologous sequences in the system, reducing the chance of offtarget genetic rearrangements. As tagging proteins can inhibit their functionality, the decision was made to express each gene in its native form to reduce the chance of creating experimental artefacts and inhibiting the pathway.

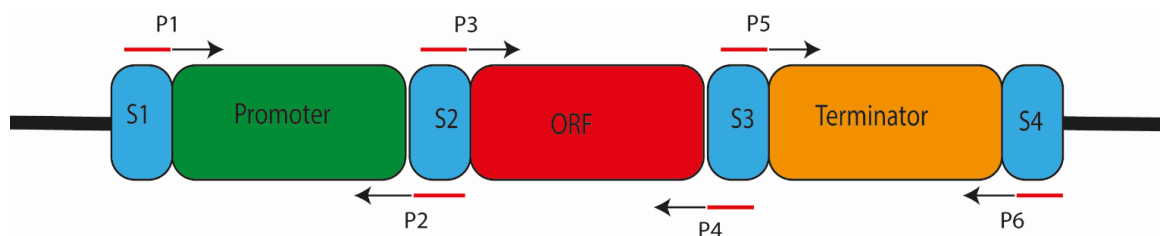


Figure 4.5. Schematic showing 'construction' vector design. Shown is a 'construction' cassette for heterologous gene expression. 18bp spacers, labelled S1-S4 (blue) are inserted between promoters/ORFs/terminators with unique restriction sites flanking each end. ORFs are amplified with primers flanked with DNA sequence identical to S2 and S3. This allows for interchangeability between promoters/ORFs/terminators. Primers priming onto S1 and S6 can be used to PCR the complete gene for cloning into an expression vector.

Table 4.1. Promoters and terminators used for expression of MEL biosynthetic pathway. Shown are the regulatory regions used for each gene in the MEL biosynthetic pathway. Promoters were chosen for equivalent strength to the *TPI* promoter. Terminators were chosen for a strength equivalent to the *PGK1* terminator.

Promoter	ORF	Terminator
HIS3	MMF1	SPO7
TDH3	EMT1	PRS1
TPI	MAT1	AI2
TEF1	MAC1	PGK1
ADH1	MAC2	VPS71

GFP fusion protein microscopy confirmed functional gene expression at suitable levels using the *TPI* promoter and *PGK1* terminator. To prevent recombination errors from repeatedly using the same sequences, we assigned different promoter/terminator pairs for each ORF, targeting p*TPI*/*PGK1* terminator-like expression levels. Promoters were chosen based on literature and lab derived data (Liu *et al*, 2012). For terminators, we consulted a database (Yamanishi *et al*, 2013), and picked five terminators with activity akin to *tPGK1*.

To assess spacer impact on gene expression, GFP-*MAC1* was placed between S2 and S3. Most cells expressing this construct exhibited notably reduced or undetectable protein levels. Counting 100 cells showed that 49% showed a significantly reduced expression, 37% showed no expression at all and just 14% showed normal protein levels compared with the absence of spacers (fig. 4.6). This represented a failure of the modular gene expression system, leading to development of a new approach for expression of the MEL pathway in yeast.

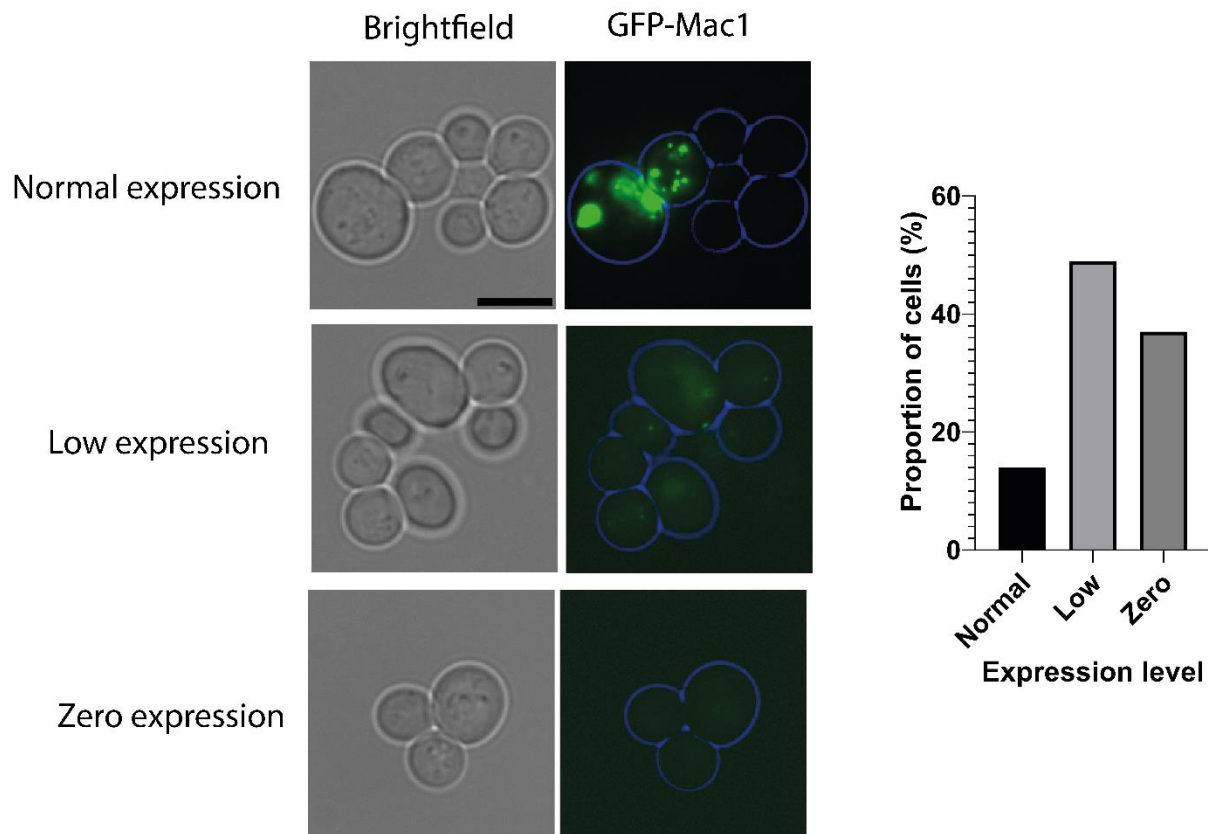


Figure 4.6. Gene expression from construction vectors is greatly impaired. Shown are cells expression GFP-Mac1 within the modular gene expression system. The cells observed were binned into three categories; normal expression, low expression and no expression. Amongst the normally expressing cells, we see individuals showing no gene expression. Cells were counted and categorised to assess gene expression within the population. 49% of cells showed low expression, 37% showed no expression and 14% showed normal expression. The scale bar indicates 5 μ m.

4.3.2 A novel approach to the production strain.

A new approach to cloning the five MEL genes in *S. cerevisiae* was devised (fig. 4.7). Due to cloning challenges with large plasmids we opted to integrate several of the genes. *EMT1* and *MAC2* were integrated into chromosome XI in haploid strains of opposite mating types. Integration loci were selected based on studies by Jensen *et al*, 2013. loxP-flanked integration markers were excised by galactose induced Cre recombinase (fig. 4.8) to allow for marker recycling. DNA was extracted from cells pre and post Cre-lox, and PCR conducted to verify the integration of the genes (fig. 4.8) as well as excision of the marker. *EMT1* was integrated into chromosome XI of a mata strain. *S. pombe HIS5* was used as a selectable marker allowing for colony selection through ability to grow on his- media. DNA extracted from these colonies was used as a PCR template to verify integration. Primers VIP 4612 and VIP 4293 were used to amplify a ~2400bp fragment between the *EMT1* ORF and upstream of the integration cassette. Primers VIP 4504 and VIP 4613 were used to amplify a ~2900bp fragment from the *EMT1* ORF to a region downstream of the integration cassette. This confirms integration at the correct chromosomal locus. The culture was transformed with a galactose-inducible Cre recombinase plasmid and grown for 8 hours on YPGal to induce Cre recombinase expression. Subsequent DNA extraction and amplification of the upstream fragment with primers VIP 4612 and VIP 4293 resulted

in a ~1000bp amplicon, confirming excision of the *S. pombe HIS5* marker. This was phenotypically verified through an inability to grow on his- media. The same procedure was employed for insertion of *MAC2* into a *mat α* strain using *K. lactis LEU2* as a selectable marker. Upstream integrations were confirmed through PCR using primers VIP 4614 and VIP 4212 yielding a ~3600bp fragment. PCR attempts to amplify a downstream fragment failed. DNA extracted from cultures post Cre-lox induction was used as a template in the same PCR reaction, resulting in a ~1250bp amplicon, indicating excision of the *K. lactis LEU2* gene. Marker excision was further validated through an inability to grow in leu- media (fig. 4.8).

The *MAC2* and *EMT1* integrants were mated to form a diploid 2-gene strain. Subsequently, *MMF1* was integrated into chromosome XII using the recycled *S. pombe HIS5* marker, yielding a 3-gene strain. *MMF1* integrations were validated through PCR (fig. 4.9). An upstream fragment was amplified using primers VIP 4616 and VIP 4232, yielding a fragment ~2300bp in length. Downstream integration was confirmed using primers VIP 4609 and VIP 4617, yielding an amplicon ~2400bp in length. A plasmid with *MAC1* and *MAT1* was transformed into both the 2-gene and 3-gene diploids, resulting in a strain containing the 5-gene pathway and one lacking the plasma membrane transporter *MMF1*. These were tested for MEL production to assess secretion or accumulation of MELs.

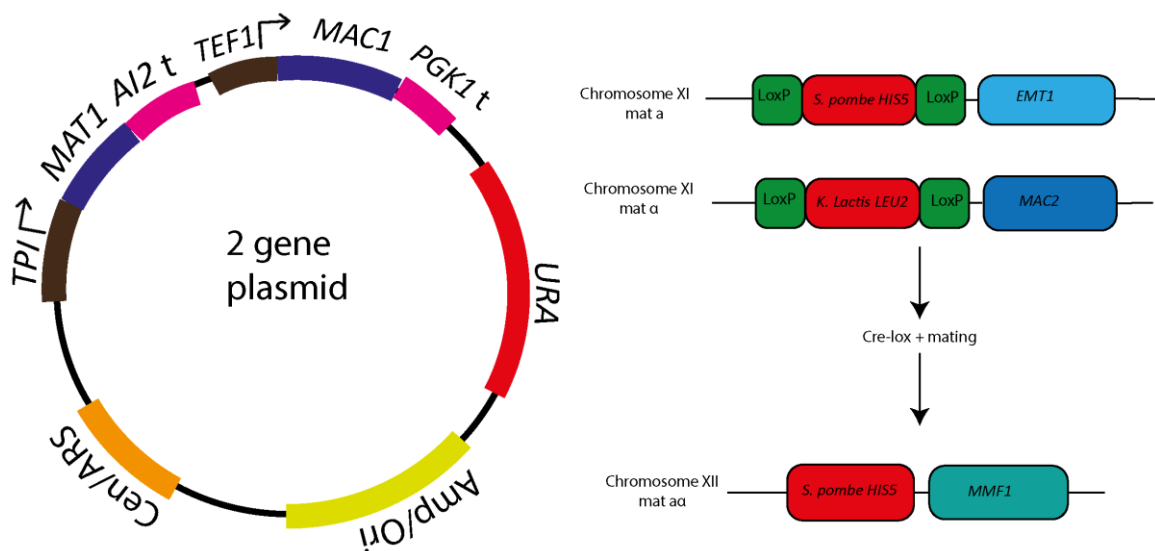


Figure 4.7. Schematic for expression of MEL biosynthetic pathway in *S. cerevisiae*. The novel approach for expressing the 5 MEL biosynthetic genes is shown. *EMT1* and *MAC2* are integrated into haploid strains of opposite mating types. Both integrations flank selectable markers with *loxP* sites, allowing excision of the marker through expression of Cre recombinase. Subsequently these integrants are mated and *MMF1* integrated to yield a 3-gene diploid. This is transformed with a 2-gene plasmid encoding *MAT1* and *MAC1*, resulting in a strain expressing the MEL biosynthetic pathway.

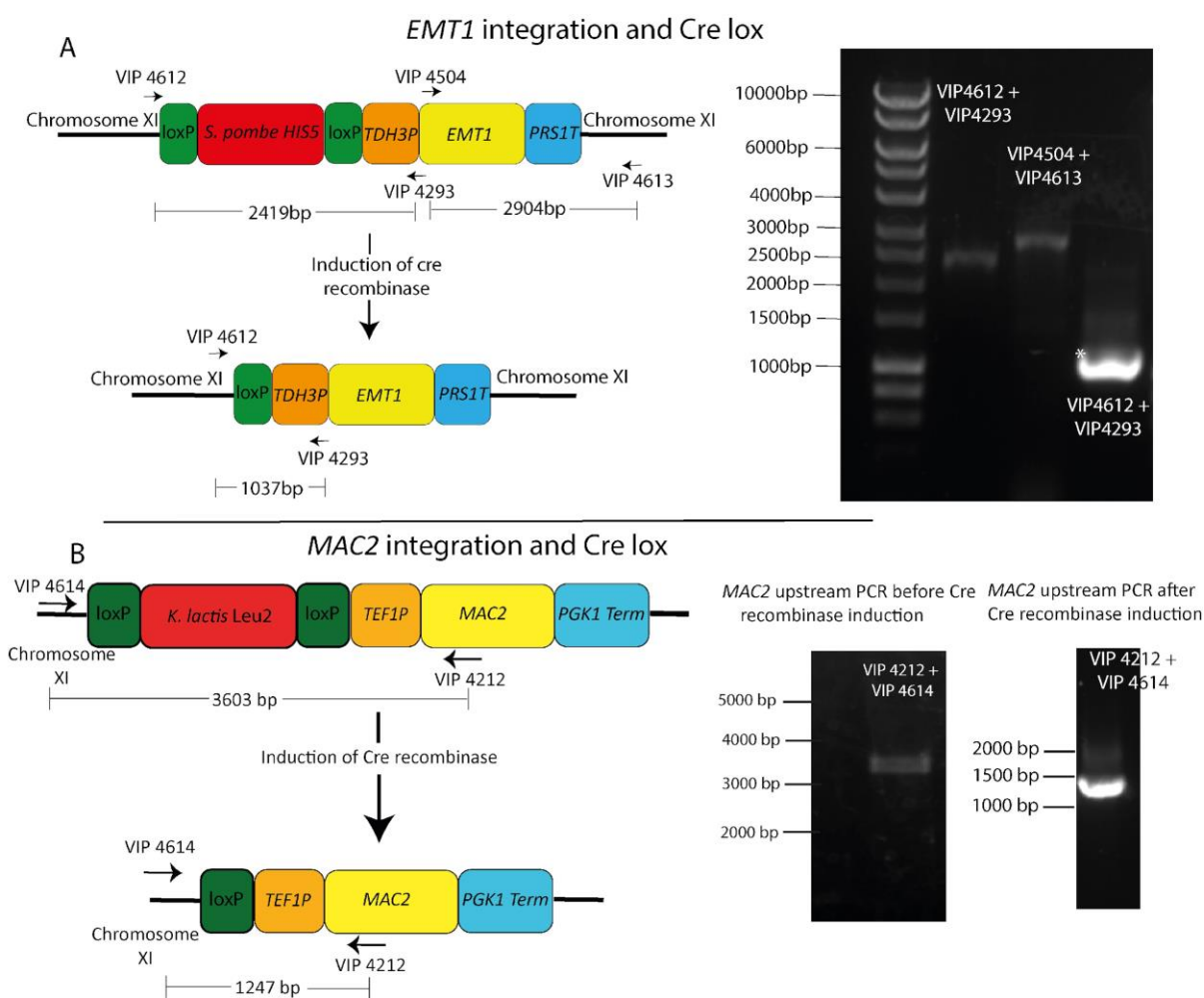


Figure 4.8. PCR verified success of gene integration and Cre lox induced marker excision.

A, Schematic shows *EMT1* integration cassette and the sizes of genetic components. PCR performed with primers VIP 4293 and VIP 4612 are used to verify upstream cassette integration pre and post- Cre lox. Agarose electrophoresis of PCR product shows that this band shifts from ~2400bp to ~1000bp when post Cre lox DNA is used as a template.

B, Schematic shows the *MAC2* integration cassette. PCR conducted using primers VIP 4212 and VIP 4614 shows a fragment ~3600bp prior to Cre lox induced marker excision. Repeating the PCR using DNA from cells that had induced Cre loc resulted in a fragment ~1200bp in length, corresponding to the expected fragment size post marker excision.

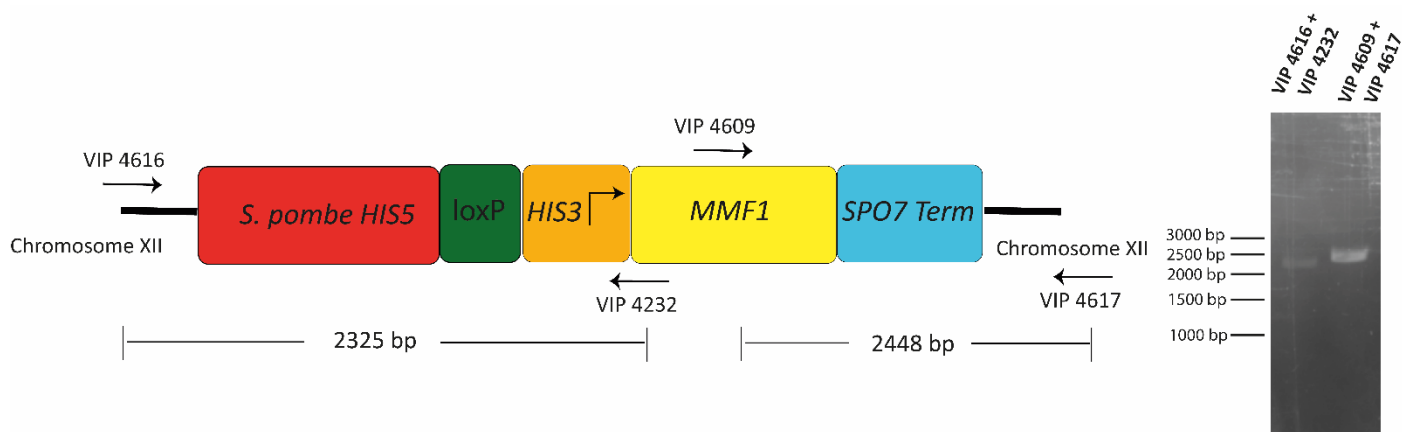


Figure 4.9. PCR validation of *MMF1* integration. Schematic shows the PCR primers used to validate *MMF1* insertion into chromosome XII of the 2-gene diploid cells. PCR conducted with primers VIP 4616 and VIP 4232 yielded an amplicon ~2300bp in length representative of the upstream fragment. Downstream integration was confirmed through PCR with primers VIP 4609 and VIP 4617, resulting in a fragment ~2400bp in size, matching the expected fragment size.

4.4 Cell culture for the production of MELs

4.4.1 Cells expressing the gene cluster reach higher optical density on lipid-enriched media

Numerous media were tested to induce MEL production in the final strain. Media in the literature are focused on native producers, often requiring N-limiting conditions to induce MEL production (Zavala-Moreno *et al*, 2014, Hewald *et al*, 2005, Niu *et al*, 2019). Using constitutive promoters, we mitigated the need for inducing conditions and developed our own media for production in *S. cerevisiae*. Rich media were used despite a requirement for plasmid selection as previous experiments repeatedly inoculating cultures containing Ycplac plasmids on rich media demonstrated that several weeks of reinoculation was required for plasmid loss in the population. Media included glucose as a sugar, and either oleate or groundnut oil as a lipid substrate. Both oleate and groundnut oil contain fatty acids of a similar length though groundnut oil is significantly cheaper than oleate. Mannose, a yeast cell wall component (Northcote & Horn, 1951), is freely available as GDP-mannose when glucose is used as a substrate (Beck *et al*, 2019). Metabolic erythritol is a product of reduction of erythrose-4-phosphate, synthesized from glycolytic intermediates in the pentose phosphate pathway (Horecker, 2002). However, the cellular concentration of erythritol in the cell is presumed to be low. Additional media was made containing mannose, erythritol and groundnut oil, in an attempt to supply the cell with direct MEL precursors.

Production runs began by inoculating 50ml of media at $OD_{600}=0.1$ with saturated precultures of the 4-gene and 5-gene strains. Production cultures were grown for 48 hours, shaking at 200RPM at 30°C. Cell pellets and supernatants were separated to assess Mmf1 functionality. Control diploids expressing an empty vector, Ycplac33, were inoculated for comparison. Strains expressing the MEL pathway achieved a higher OD than those without (fig. 4.10). 4-gene cells grown on 0.3% YPO media reached $OD = 22.9$, compared with 27.4 for the 5-gene strain and 9.1 in controls expressing an empty vector, Ycplac33. On 8% YPGn media 4-gene strains reached $OD = 30.7$ after 48 hours compared with 28.35 for 5-gene strains and 19.55 for controls expressing Ycplac33. Supernatant extractions from MEL

pathway-expressing samples revealed an emulsion-like 'gel' atop the extraction tube, lacking from control samples. This gel was found solely in supernatant extractions and was harvested separately for analysis by nuclear magnetic resonance (NMR).

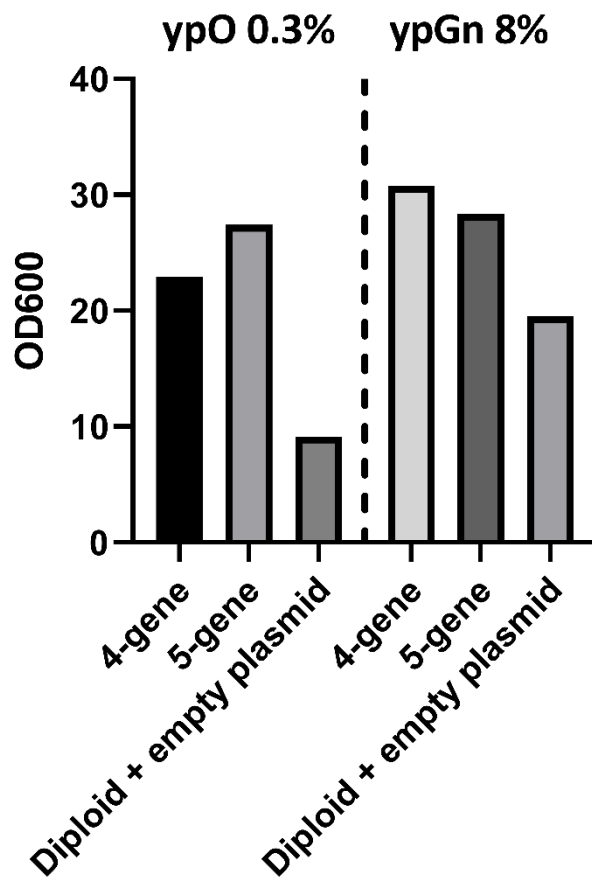


Figure 4.10. Cells expressing MEL biosynthetic genes reach higher OD in 48 hour cultures. OD measurements from production cultures after 48 hours of growth are shown. Cultures were grown on rich media containing both glucose and a lipid substrate, either oleate (ypO) or groundnut oil (ypGn). All flasks were started at $OD_{600} = 0.1$. Cells expressing all MEL biosynthetic enzymes reached a higher OD compared to controls expressing an empty vector.

4.4.2 NMR analysis of cell supernatant and pellet extracts.

Ethyl acetate extracts from cell pellets, culture supernatants, and gel-like emulsions were washed with hexane and suspended in d-chloroform for NMR analysis. Samples included 4-gene, 5-gene and control strains. Additionally, *M. antarcticus* grown on rich media and shifted to N-limiting media was tested, as was *U. maydis* and *M. antarcticus* grown on rich media. Control samples of pure MEL-A

dried from an ethyl acetate solution were included as a standard. Control cell pellet and supernatant samples (empty vector) were spiked with 5mg of 95% MEL prior to extraction to assess extraction and detection efficiency. NMR results for all samples are summarized in table 4.3.

NMR analysis began with a MEL standard, establishing a reference for comparison. This was compared with supernatant extractions from *M. antarcticus* shifted from rich to N-limiting media. Although the *M. antarcticus* extract was impure, a detectable MEL trace identifying proton coupling on the erythritol moiety was observed (fig. 4.11). While these peaks were identified, numerous other MEL specific peaks were obscured by impurities. Subsequent 2D NMR analysis identified a greater number of MEL specific protons in the sample (fig. 4.12). MELs were not detected in *M. antarcticus* grown directly on rich media and only in samples shifted to N-limiting conditions. This experiment validated our MEL identification capability. An additional control of *U. maydis* cell pellet and supernatant grown on rich media failed to produce detectable MELs.

No MELs were detected in any 4-gene or 5-gene samples (fig. 4.13), not all spectra are displayed as they all look very similar. Extractions from control strains spiked with pure MEL affirmed our ability to extract and detect low levels of MEL. Initially 17 samples were tested from glucose and groundnut oil media, all yielding negative results. Additional media was developed, YpME, containing mannose, erythritol and groundnut oil as carbon sources. The direct precursors to the pathway available in this media aimed to encourage production success. 4-gene and 5-gene strains cultured on YpME failed to accumulate or secrete MELs.

As none of the enzymes was tagged in the 4-gene or 5-gene strain, we had no way to monitor expression of the pathway. We therefore opted to perform bulk protein extractions and send them for proteomic analysis for identification of peptides from the MEL biosynthetic enzymes.

Table 4.2. Results of NMR analysis for MEL production runs. Shown are the samples analysed through NMR for the production of MELs. Production was only observed in *M. antarcticus* when shifted from rich media to N-limiting conditions. MELs were detected in extractions spiked with a pure MEL standard but not in any of our producing strains.

Sample	Strain	Media	MELs detected?
Solution	MEL-A (>95%)	N/A	Yes
Supernatant	$\alpha\alpha$, empty plasmid	4% YpGn + MEL-A	Yes
Cell pellet	$\alpha\alpha$, empty plasmid	4% YpGn + MEL-A	Yes
Supernatant	<i>M. antarcticus</i>	8% YpGn -> N-limiting	Yes
Cell pellet	<i>M. antarcticus</i>	8% YpGn -> N-limiting	Yes
Cell pellet	<i>M. antarcticus</i>	8% YpGn	No
Supernatant	<i>U. maydis</i>	8% YpGn	No
Cell pellet	<i>U. maydis</i>	8% YpGn	No

Gel	5-gene	8% YpGn	No
Gel	5-gene	0.3% YpO	No
Gel	4-gene	0.8% YpO	No
Cell pellet	4-gene	YpME	No
Supernatant	4-gene	YpME	No
Cell pellet	5-gene	YpME	No
Supernatant	5-gene	YpME	No
Supernatant	4-gene	0.8% YpO	No
Cell pellet	4-gene	0.8% YpO	No
Supernatant	5-gene	0.3% YpO	No
Cell pellet	5-gene	0.3% YpO	No
Supernatant	4-gene	1% YpGn	No
Cell pellet	4-gene	1% YpGn	No
Supernatant	4-gene	0.3% YpO	No
Cell pellet	5-gene	0.3% YpO	No
Supernatant	4-gene	0.8% YpO	No
Supernatant	5-gene	0.8% YpO	No
Cell pellet	4-gene	8% YpGn	No
Supernatant	4-gene	4% YpGn	No
Supernatant	5-gene	4% YpGn	No
Cell pellet	5-gene	8% YpGn	No
Supernatant	$\alpha\alpha$, empty plasmid	1% YpGn	No
Supernatant	$\alpha\alpha$, empty plasmid	0.8% YpO	No
Supernatant	$\alpha\alpha$, empty plasmid	0.3% YpO	No

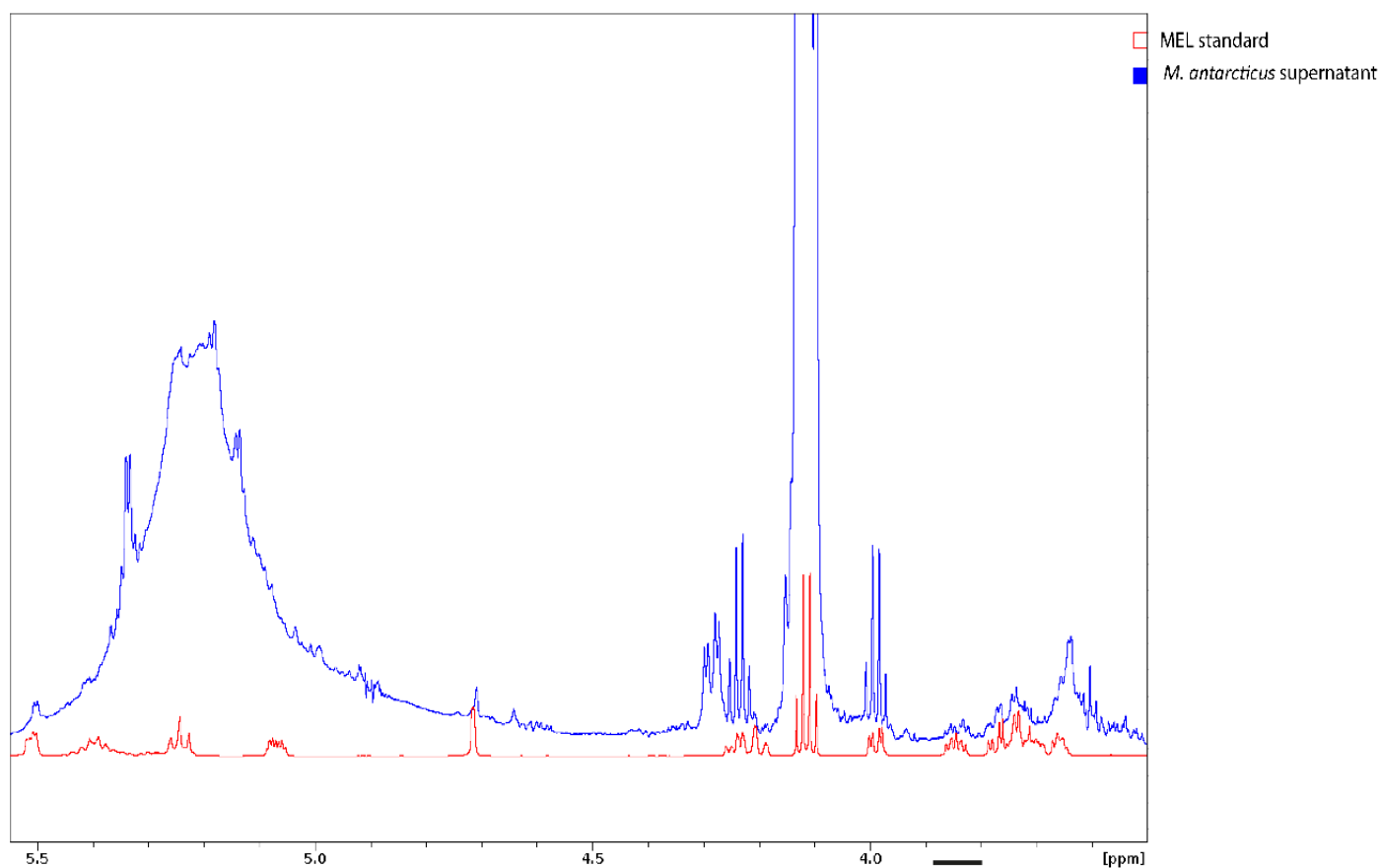


Figure 4.11. MELs detected in *M. antarcticus* sample NMR spectra for *M. antarcticus* supernatant extraction (blue) vs a known MEL standard (red). The *M. antarcticus* extraction shows additional peaks from compounds co-extracted alongside the MEL. Distinctive peaks are visible between 3.8 – 3.9 ppm associated with the erythritol moiety of the MEL disaccharide (indicated with a black line). Additional MEL specific peaks are obscured by impurities.

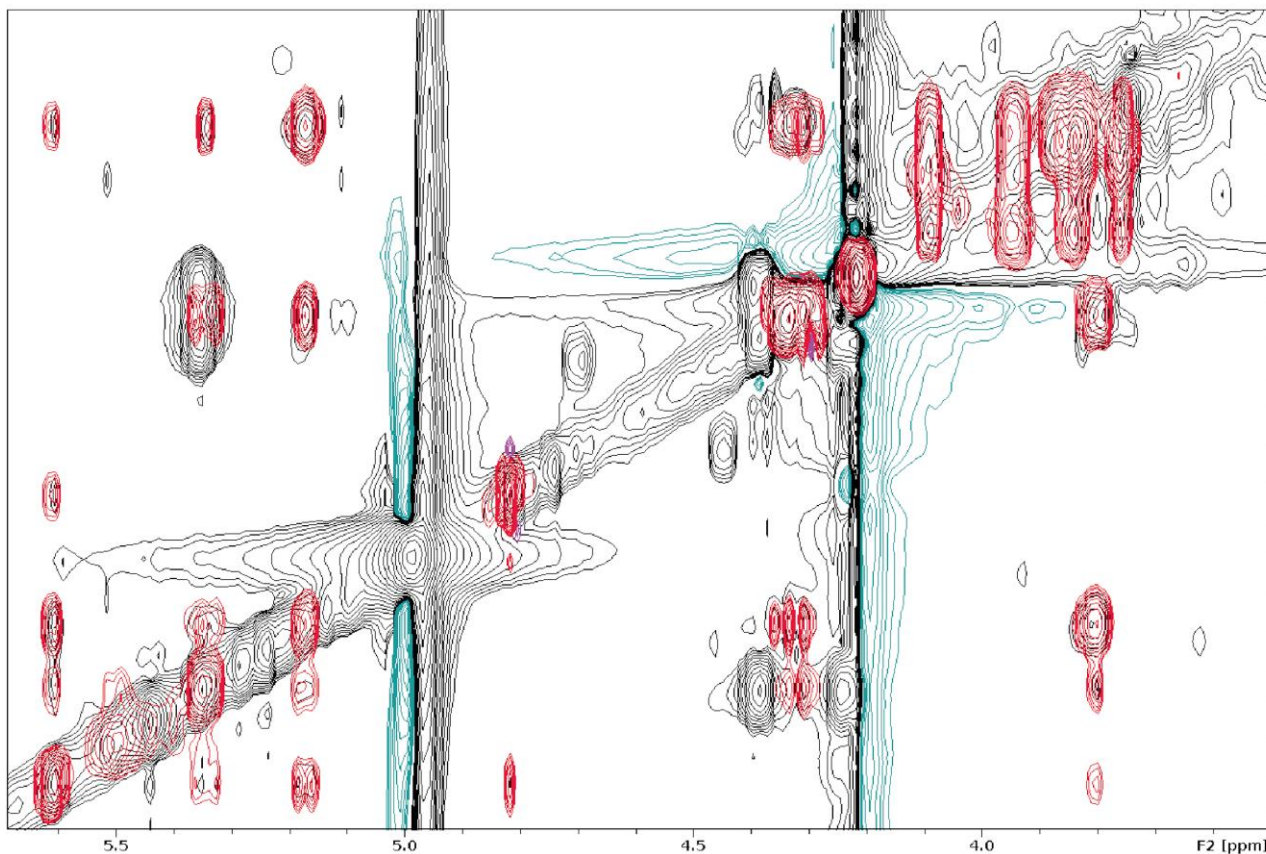


Figure 4.12. 2D NMR spectra confirms MEL presence in *M. antarcticus* sample. 2D NMR MEL standard peaks (red) and *M. antarcticus* supernatant extract (black/teal) are shown. The red peaks represent protons on the MEL standard, overlapping regions indicate equivalent protons found in both samples.

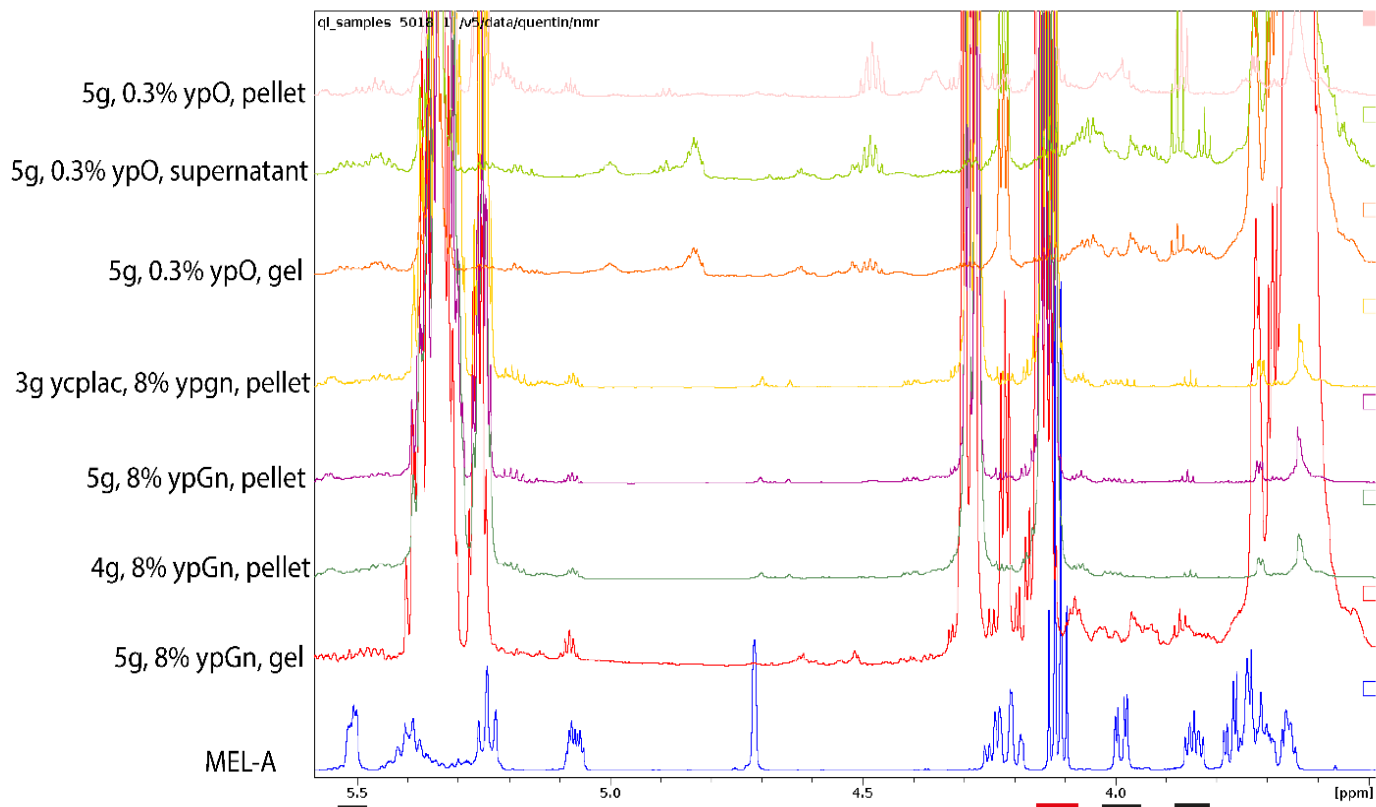


Figure 4.13 NMR spectra for 4-gene and 5-gene strains fail to show MEL trace. 1D NMR spectra for a MEL standard compared against numerous samples are shown. Black lines indicate pronounced MEL-A peaks lacking in production samples. The red line shows residual ethyl acetate. Samples labelled '5g' indicate 5-gene strain, '4g' indicates the 4-gene strain, '3g ycplac' indicates control samples. MELs were not detected in any production samples. Not all spectra are shown though details of all NMR runs are listed in table 4.3.

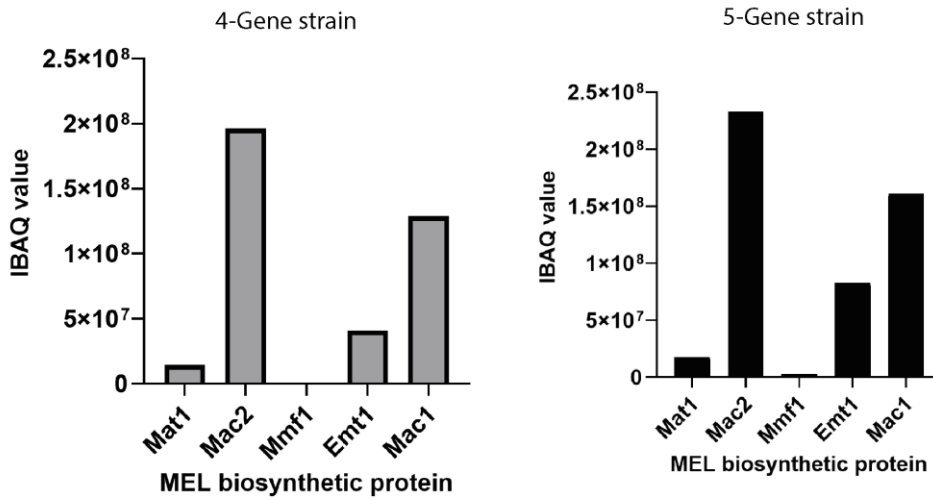
4.5 Proteomics to validate protein expression in production strains

To assess whether the 4-gene and 5-gene strains were expressing the MEL biosynthetic gene pathway 200 OD's of cells were harvested. Native protein extractions were performed on these cells pellets for analysis by mass spectrometry. As all genes were placed under control of strong promoters, it was estimated that the MEL gene cluster enzymes should account for a substantial proportion of the total protein in the cell with the exception of Mmf1. Proteomic analysis was ran on cultures of both the 4-gene and 5-gene strain grown on YPD. Unique peptides were found for the all proteins in the pathway.

Mass spec analysis yielded IBAQ and LFQ values for peptide abundance within our samples. IBAQ values take into account the proportion of peptides within the sample attributed to a specific protein, allowing for analysis of the abundance of a protein within the sample. LFQ values are determined by an algorithm that measures the abundance of precursor ions in a sample, these can only be resolved in high power mass spectrometers. LFQ quantification is such that comparisons can be made across samples analysed in the same way. Using these data, we observed that the four MEL enzymatic genes were expressed to similar levels between our 4-gene and 5-gene strains (fig. 4.14). However, the expression levels between genes was variable. This could be attributable to the different promoters

we used or the integration loci in the genome. It was observed that Mac1 and Mac2 are found at the highest levels, this is interesting as these are peroxisomal proteins. It is possible that enzyme sequestration into the peroxisome results in a protective effect, allowing the accumulation of a greater number of molecules.

IBAQ values



LFQ values

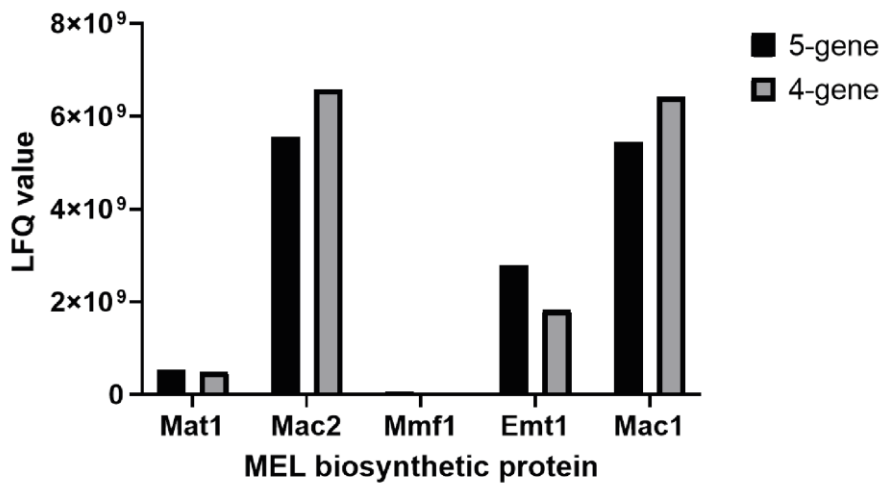


Figure 4.14. Relative MEL pathway protein levels resolved through mass spectrometry. Above, shown are IBAQ values for MEL biosynthetic enzymes. These can be compared within the 4-gene and 5-gene strains. LFQ values give relative protein abundance and can be compared across samples. LFQ values show comparable gene expression levels between the 4-gene and 5-gene strains. Protein levels varied between the four enzymatic MEL biosynthetic proteins but was highest in peroxisomal enzymes. Mmf1 is expressed at notably lower levels than other MEL genes and was only detected in the 5-gene strain.

Mmf1 was expressed at notably lower levels; this was likely due to its upregulation by the weak *HIS3* promoter. Comparing Mmf1 levels between strains we see that it was only expressed in the 5-gene strain (fig. 4.15). While the levels are low, this was intentional and indicated that the strain engineering had been correctly performed. This means that the failure to detect MELs is unlikely to have a genetic basis and is likely attributable to unforeseen metabolic problems. There are numerous possibilities for this as will be discussed.

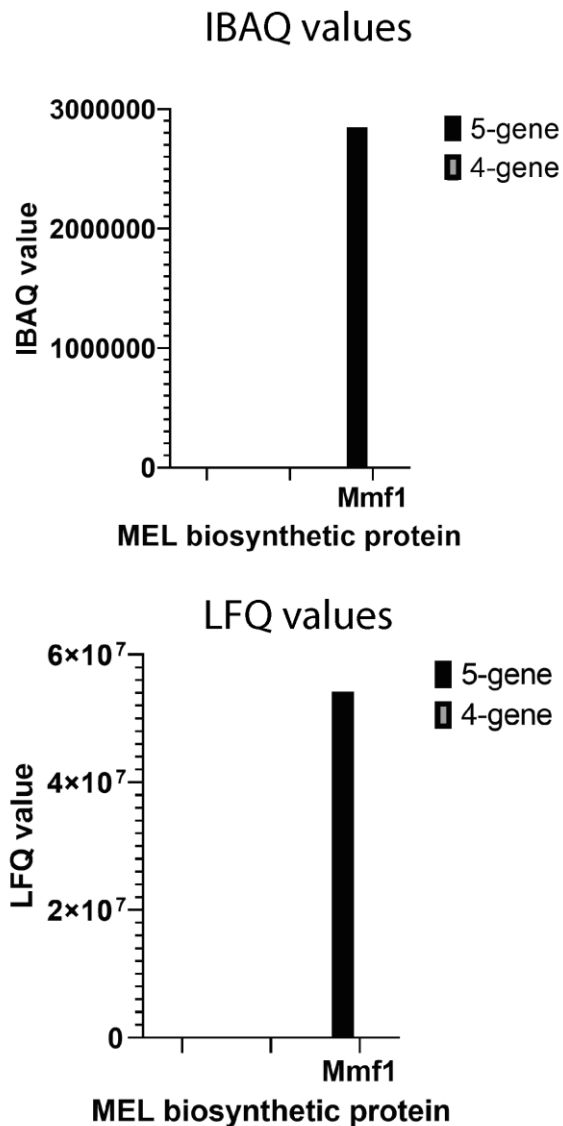


Figure 4.15. Mmf1 is expressed solely in the 5-gene strain. Graphs showing the IBAQ and LFQ values for Mmf1 detected through proteomics. It is clear that Mmf1 peptides are missing from the 4-gene strain, indicating successful expression of the 5 biosynthetic MEL genes.

4.7 Discussion

The data described in this chapter demonstrate the feasibility of heterologous gene cluster cloning alongside the difficulties encountered when trying to reconstitute metabolic pathways in non-native organisms. The proteomics data identifying the presence of peptides unique to our heterologous proteins indicate that even when overcoming the genetic difficulties associated with expressing five heterologous genes simultaneously, the presence of unknowns are still capable of preventing functionality.

We demonstrate that for biotechnological applications, the sub-cellular localisation of enzymes is not indicative of successful catalysis. In the case of the MEL biosynthetic pathway characterised by Hewald *et al*, 2006, we find that mechanisms for the movement of precursors within the cell are unknown. It could be that peroxisomal membrane proteins found outside of the MEL biosynthetic gene cluster are responsible for the movement of disaccharide mannosyl-erythritol into the peroxisome. Alternatively, a peroxisomal transporter may be required for export of di-acyl mannosylerythritol from the peroxisome to the cytoplasm. In the absence of knowledge about the flux of these metabolites, we cannot be certain that the proteins expressed are proximal to their required substrates.

It was observed that we saw a 'gel' like emulsion in samples extracted from cultures expressing the MEL biosynthetic pathway. Images of this were unfortunately lost however it was found numerous times solely in samples expressing the MEL pathway. This was an initial source of optimism as we expected to produce molecules with emulsifier activity. However, NMR analysis of this gel was indistinguishable from cell pellet or culture supernatant extracts (fig. 4.13). As we were able to detect very small amounts of MEL-A spiked in culture reactions we were confident that these gels did not contain any MEL-A though the use of more sensitive analytical techniques like GC-MS could have been used to further validate this.

Numerous alternative approaches could have increased the speed of assembly of this pathway. The use of the 2A autocleavage peptide between ORFs of MEL biosynthetic genes would have allowed the production of 'operon-like' expression, placing two ORFs under control of a single promoter/terminator pair (Souza-Morreira *et al*, 2018, Liu *et al*, 2017). This peptide works by creating a 'slipping' effect in the ribosome, effectively causing it to move from one ORF to the next. This would have increased the speed of cloning, as fewer combinations of promoter/ORF/terminator would have been required. Several times PCR amplification of a promoter or terminator failed, meaning time was spent re-designing a MEL enzyme expression construct. Saving time in cloning by using the 2A peptide would have created more time to troubleshoot failures in MEL production. Simultaneously we could have placed numerous ORFs in front of the *TPI* promoter. As *TPI* promoted enzymes were microscopically screened for successful sub-cellular localisation, we were more confident of the functionality of enzymes in this regulatory context. Epifluorescence microscopy was not conducted on MEL enzymes under control of the promoters used in the 4-gene and 5-gene strains. If the regulation of the protein affected their folding/sub-cellular localisation, we would not have detected this microscopically yet the peptides would still be detected through mass spectrometry.

While previously it was thought that the entire ustilagic acid gene cluster had been identified as a large 12 open reading frame gene cluster (Teichmann *et al*, 2010), a recent paper performing whole genome sequencing on 17 members of the family *Ustilagenaceae* identified novel genes involved in the ustilagic acid biosynthetic gene cluster (Ullmann *et al*, 2022). Such analysis could allow for identification of additional genes that associate with the MEL biosynthetic genes that were missed characterisation of the pathway.

Numerous approaches could have been better optimised for expression of this pathway, offering improved opportunities for analysis of function in a complete strain. These will be discussed more thoroughly in chapter 5.

Chapter 5 – Discussion

5.1 Introduction

Initially, the aims of this thesis were to characterise mechanisms of Rex1 import and identify whether Srp1 functions as an importin for Rex1. However, experiments imaging GFP-Rex1 at 37°C showed that Rex1 is exported from the nucleus and depleted under heat-stress conditions, inspiring us to explore its regulation.

5.2.1 Rex1 is part of nuclear delocalisation heat shock effect

It is known that importin- α accumulates in the nucleus under stress conditions (Miyamoto *et al*, 2004, Furuta *et al*, 2004, Kodiha *et al*, 2008). This prevents nuclear import of importin- α substrates. It is suspected that importin- α has alternative roles in the nucleus as identified by its binding to transcription factors. The inhibition of importin- α cytoplasmic export is an example of alterations in protein localisation in response to stress. In yeast, it was observed that many nuclear proteins aggregate around the periphery of the nucleolus in response to heat stress (Wallace *et al*, 2015). In some instances, these proteins later de-aggregated and returned functionally to their previous sub-cellular localisation. It is thought that this movement of enzymes is to inhibit their activity when the cell is under duress. This example demonstrates that cells have adaptations to inhibit the activity of enzymes without inducing their degradation.

It is possible that Rex1 activity is particularly detrimental under heat stress conditions and that cells cannot risk having errant Rex1 in the cell. Alternatively, it is possible that Rex1 activity is non-essential upon a return to permissive temperatures and the cell benefits from depleting it in the short term.

We heat-shocked our cells at 39°C as it was demonstrated that cells growing at this temperature showed a pre-tRNA phenotype akin to *rex1 Δ* cells (Foretek *et al*, 2016). A lessened pre-tRNA processing phenotype was also observed at 37°C. It is known that nucleocytoplasmic trafficking responses vary across a heat gradient in HeLa cells (Ogawa & Imamoto, 2018), with regulation of different importins changing at different heat stress temperatures. In this instance, it was observed that nucleocytoplasmic shuttling of importin- α proteins was impeded at a lower temperature than importin- β mediated proteins (Ogawa & Imamoto, 2018). This is interesting as both pathways are thought to be dependent on Ran-GTP cycling which is affected by heat stress, though it appears importin-beta is more resilient to disruptions in this mechanism. Furthermore, nuclear import of HSP70 occurs at a lower temperature than importin- α / β disruption and is an independent mechanism, requiring use of hikiishi, an unrelated, highly conserved import protein (Kose *et al*, 2012). This is to say that over the course of an increase in temperature we are observing numerous metabolic responses. In cells grown at 37°C, tRNA ILE^{UAU} showed an increased proportion of extended forms compared with at 30°C but still notably reduced when compared with cells grown at 39°C. It could be that between 37-39°C we initiate a novel heat stress mechanism which heightens the Rex1 depletion response. By measuring Rex1 levels and localisation at a broader range of heat shock temperatures it is possible we would observe a smaller degree of metabolic alterations, facilitating elucidation of the mechanism regulating Rex1 depletion.

5.2.2 Stress induced protein degradation

The reversible movement and ‘storage’ of proteins with harmful effects under stress conditions is indicative of the functionality these proteins have or the costs associated with recycling them. It is

known that when adapting to new conditions, proteolysis increases. In the extreme case of diploid yeast sporulation or the formation of pseudohyphal structures (Gimeno *et al*, 1992), we see dramatic changes in cell structure, mediated by proteome alterations.

In cells shifted to N-limiting media there is an 86% increase in protease activity (Teichert *et al*, 1989). The majority of this is attributed to vacuolar protease function. Deletion of vacuolar protease Pep4 leads to an inability of cells to survive a shift to N-limited media (Teichert *et al*, 1989). Using MG132 we have shown that Rex1 degradation is proteasome mediated (fig. 3.22). Rex1 is a nuclear protein, export links from the nucleus to the vacuole may be more complex than from the cytosol. This may explain why the cell has evolved a proteasome mediated stress-induced Rex1 degradation system as moving target proteins from the nucleus to the vacuole is likely to be more difficult than localised proteasome mediated degradation.

Heat stress induces upregulation of the UBI4 gene in yeast (Finley *et al*, 1987, Gemayel *et al*, 2017), this protein makes a polyubiquitin precursor consisting of 5 ubiquitin molecules. This in itself implies that yeast prepare for an increase in proteasome mediated degradation in response to heat stress. It was also observed that numerous E3 ubiquitin ligases function in heat shock. These signs describe an increase in targeted proteolysis. As we know Rex1 is degraded via the proteasome, it seems likely that the phosphorylation acts as an additional selective barrier to targeted depletion. Requiring the recruitment of both kinases and ubiquitin ligases gives the cell an additional layer of control over targeted Rex1 depletion. Additionally to E3 ubiquitin ligases, it is also known that numerous serine/threonine kinases are upregulated in response to heat shock (Wang *et al*, 2022, Zarzov *et al*, 1996). It is plausible that these enzymes are involved in targeting the breakdown of Rex1. It is also known that MAPK kinases are induced by heat stress, mediating numerous phosphorylation events and controlling proteasome abundance (Kamada *et al*, 1995). These pathways could be involved in regulating Rex1 depletion.

5.2.3 Alternative stressors

It is known that yeast cells moved to media containing glycerol as a carbon source showed a tRNA ILE^{UAU} phenotype akin to *rex1Δ* cells (Foretek *et al*, 2016). When we shifted cultures onto glycerol media, we did not observe any Rex1 depletion (fig. 3.10), indicating that the lack of tRNA processing is alternatively controlled. Rex1 protein levels were seen to increase over a 70-minute shift to YPgly. The easy interpretation of this data is that tRNA ILE^{UAU} is protected from Rex1 in cells grown on glycerol. We know that cells elicit different responses to different stressors (Takemura *et al*, 2004, Miyamoto *et al*, 2004). It is possible that additional Rex1 regulatory mechanisms exist in response to glycerol stress.

Importin- α is known to be retained in the nucleus in response to heat stress, oxidative stress, starvation and ethanol stress (Stochaj *et al*, 2000, Miyamoto *et al*, 2004, Kодиha *et al*, 2008). Rex1 sub-cellular localisation is difficult to discern in cells cultured on glycerol as the vacuole is enlarged, making elucidation of other organelles challenging. If nucleo-cytoplasmic shuttling of Srp1 is impaired in cells grown on glycerol media this could separate Rex1 from its tRNA substrates. However, if Rex1 delocalisation is a consequence of downregulated Srp1 shuttling, as opposed to active export, then the nuclear pool of protein should remain in the nucleus for some time in the absence of targeted degradation. If this were the case, we would expect Rex1 substrates present in either the nucleus or the cytoplasm to be processed. It is known that tRNA localisation is transient, with tRNAs found between the nucleus, cytosol and nucleolus (Maraia *et al*, 2001). If tRNA ILE^{UAU} is moved to the nucleolus upon a shift to glycerol media, it could be protected from Rex1 processing.

Studies using microarrays have shown that oxidative stress through the addition of 2.0mM H₂O₂ induced transcriptional upregulation of numerous rRNA processing enzymes (Shenton *et al*, 2006). These include the rRNA synthesis and maturation genes *RRP12*, *RRP5*, *RRP1*, *SOF1*, *NOP9* and *FAL1*, amongst others. Alterations in *REX1* transcription were not observed. Though it should be noted that oxidative stress alters translational rates (Shenton *et al*, 2006), and that the increased mRNA production may be to balance out protein levels in the face of slower translation. Quantitative mass spectrometry found that Rex1 is not thought to be very abundant in the cell (Kulak *et al*, 2013). If the aim of a stress response is to reduce its activity, it could be that the reduced translational rates observed in cells experiencing oxidative stress are sufficient for impeding activity without altering transcriptional levels.

5.2.4 Alternative Rex1 degradation pathways/alternative phosphorylation

Our *in vivo* phospholabelling experiments show that Rex1 is phosphorylated in response to heat stress (fig. 3.23). Simultaneously, we know that Rex1 is degraded under these conditions. It is easy to hypothesize a link between these traits with Rex1 phosphorylation inducing ubiquitin-ligase recruitment and subsequent degradation. However, western blot analysis of our phosphomutants shows that they are still rapidly depleted through a shift to 39°C (fig. 3.20). This could be due to several reasons. If Rex1 phosphorylation acts as a phosphodegron and is required for induced degradation, the Rex1 kinase may phosphorylate alternative exposed residues on the protein that may be sufficient for ubiquitin-ligase recruitment. Alternatively, there could be an alternate degradation pathway used by the cell to degrade Rex1 under stress conditions.

We did not perform mRNA analysis on Rex1 transcript levels. It has been observed that 62% of yeast mRNA species are altered upon heat stress (Castells-Roca *et al*, 2011). Reduction in Rex1 mRNA stability could be a contributing factor to the observed Rex1 depletion. Though the cytoplasmic accumulation of Rex1 in response to reduced importin- α shuttling could indicate that newly translated Rex1 is retained in the cytoplasm, resulting in an increased cytoplasmic pool. If this is the mechanism behind cytoplasmic accumulation of Rex1 under stress conditions, we expect that some Rex1 mRNA is sufficiently stable in the cytoplasm for protein synthesis.

It is thought that proteins between ~30-60 kDa rapidly diffuse through the nuclear pore (Ma *et al*, 2012, Mohr *et al*, 2009). Rex1 has an atomic weight of 63 kDa so is not far out with the expected range of proteins capable of passively diffusing into the nucleus. It is possible that Rex1 fusion proteins would be too large to diffuse through the nuclear pore. However, Rrp47 is a nuclear exosome associated exonuclease associated with RNA surveillance, *rrp47 Δ* , *rex1 Δ* double deletions show synthetic lethality. GFP-Rex1 17-52 Δ is a fusion protein of 85kDa lacking an NLS, at 85kDa we expect it to be too large to enter the nucleus passively. Expression of GFP-Rex1 17-52 Δ in *rrp47 Δ* , *rex1 Δ* cells rescued cell growth (Daniels *et al*, 2022). This indicates that in the absence of Srp1 mediated import, Rex1 continues to enter the nucleus to a sufficient degree to enable growth. In heat-shocked cells in which Srp1 shuttling is inhibited, passive entry of Rex1 into the nucleus may be problematic in the case that the cell is trying to inhibit Rex1 activity. This could be selective in the evolution of active Rex1 degradation.

5.2.5 The role of ubiquitination in Rex1 stability

We made mutants at the four identified Rex1 phosphosites, however downstream from these is a known ubiquitinated lysine (K58). We did not make mutants at this residue to see if disrupting this site would stabilise Rex1 in response to heat stress through an inability to recruit ubiquitin ligases. If disruption of this residue led to inhibition of ubiquitin-ligase recruitment, we would expect this mutant

to show increased stability vs the wild-type. However, ubiquitin ligase recruitment is often thought to be protein specific as opposed to lysine specific (Mattirolli & Sixma, 2014) and it is possible Rex1 would be targeted at an alternative site.

5.2.6 Plasmid vs chromosomally expressed Rex1 stability

While we observed that Rex1 S/A had a reduced rate of decay upon a shift to 39°C, this effect was not very large and the protein was still depleted (fig. 3.20). However, the large protective effect by the addition of MG132 indicates that most Rex1 depletion is proteasome mediated. The implication of this is that the point mutations we made do not inhibit the recruitment of Rex1 to proteasome complexes.

While the rates of Rex1 depletion were comparable amongst our three alleles, we saw greater steady state levels of Rex1 at 30°C in the Rex1 S/A allele (fig. 3.21). This effect was particularly pronounced in plasmid-expressed protein but was determinable in the integrated alleles (fig. 3.19, fig. 3.21). However, as we saw equivalent rates of decay between zz-Rex1 and REX1-HTP (where zz-Rex1 is expressed 5x higher) it seems that the rate of depletion is not indicative of the overall quantity of protein present. It would be more informative to run western heat shock assays of multiple strains on one blot to allow comparison of absolute protein levels within the different alleles. This would be helpful as the Rex1 S/E allele appeared to be expressed at lower levels at permissive temperatures meaning that during a heat shock response it may reach lower absolute levels, indicating its reduced stability compared to WT or non-phosphorylatable alleles.

5.2.7 Rex1 phosphorylation status in response to heat shock

When performing *in vivo* phospholabelling we used an *erg6Δ*, *REX1-HTP* strain. The *erg6Δ* allows MG132 to penetrate the cell and inhibit proteasome activity. By treating labelled cells with MG132 and exposing them to heat stress, we expected increased protein recovery in samples treated with MG132 vs DMSO controls. We did see larger Rex1 pulldown yields in samples treated with MG132, but the yield was still visibly lower than in control samples at 30°C (fig. 3.23). This is in contrast to our expectations based on the large Rex1 protective effect seen in temperature shift assays of cultures treated with MG132. MG132 was added 10 minutes before the initiation of heat shock, which is brief but was sufficient for an observed protective effect in initial experiments (fig. 3.22). However, we do recognise that pull-down experiments are variable and comparing yields across samples is difficult. Even if protein quantity varied, we expected to see an equivalent radioactivity/protein ratio in all samples heat stressed at 39°C for 30 minutes. This was not the case and cells treated with DMSO had a greater radioactivity/protein ratio compared with MG132 treated cells (fig. 3.23). In this case DMSO and MG132 treated heat shocked cells at 39°C had a radioactivity/protein ratio 9x and 4x greater than controls at 30°C respectively. It is possible that MG132 has some effect that limits the phosphorylation of Rex1, perhaps by inhibiting the degradation of an inhibitor of the Rex1 kinase.

5.3 Biosynthetic MEL production

5.3.1 Alternate enzymes in the cluster required for its function

The MEL biosynthetic cluster is present in numerous organisms related to *U. maydis* though variation in the specific activity of their enzymes has been identified. Shared regulation between MEL biosynthetic genes and alternative associated enzymes has been observed. It was observed that MEL biosynthesis was required for the upregulation of two secretory lipase enzymes in *M. antarcticus* (Ramdas & Rampersad, 2022). These enzymes are secreted and allow increased substrate uptake.

Additionally in *M. antarcticus* it was observed that when deleting *MaEMT1* that there was a significant drop in the expression of PaE, an enzyme capable of breaking down biodegradable plastic (Saika *et al*, 2019). Growing the *Maemt1Δ* strain on media supplemented with MELs restored identifiable levels of PaE enzyme. This link between products of the MEL biosynthetic gene cluster and upregulation of genes at other genetic loci is indicative of more complex genetic regulation that would be absent in a heterologous host. While we have removed the MEL pathway from its native regulation by placing it under the control of constitutive promoters, it is possible that MEL pathway induction stimulates the upregulation of different genes involved in the pathway, perhaps some transporters for moving intermediates in and out of the peroxisome.

Synteny analysis of 12 MEL producing species found that the gene number in the MEL biosynthetic gene cluster varies between producing organisms (Solano-Gonzalez & Solano-Campos, 2022). *Ustilago cynodontis* and *Sporisorium reilianum* contained just four of the genes, lacking *MAC2* and producing mono-acylated MELs. An alternative strain of *M. antarcticus* was found to have a small sixth ORF between *MAC2* and *EMT1*. This gene has not been characterised but its placement within the gene cluster implies that it may be upregulated under MEL producing conditions due to its location in a transcriptionally active zone. If this ORF encodes a protein that is present at a different genetic locus in other strains it could be lacking in our heterologous host and explain our lack of production.

Studies on *mmf1Δ*, *mat1Δ* *U. maydis* mutants identified that MELs lacking acetylation can be secreted in the absence of Mmf1 (Becker *et al*, 2022). It was observed that these intermediates could be secreted and taken up by co-cultured *U. maydis* of a different strain independently of Mmf1 activity. Furthermore, it was observed that these molecules could be taken up by a co-cultured *mmf1Δ* strain expressing *MAT1*, acetylated, and secreted again to the extracellular environment without a transporter. Co-culture of different mutants observed ready exchange of MEL intermediates between strains. This data shows that *U. maydis* is well adapted at dealing with MELs. We did not grow our production strains on media enriched with MELs and did not measure whether *S. cerevisiae* is capable of moving MELs or MEL intermediates through its membranes. It is possible that *U. maydis* membranes show adaptations for the movement of MELs through the cell. If this were the case for peroxisomal membranes, *S. cerevisiae* could be maladapted at dealing with MELs. Should these exist and be lacking in our production strain it could be responsible for the lack of MEL synthesis observed. While in this example we would expect to find evidence of the mannosylerythritol disaccharide, we were unable to observe this molecule through NMR due an obscurity of expected peaks by other cellular metabolites. There are methods of GC-MS that could be used to identify whether we achieved successful formation of mannosylerythritol.

5.3.2 Microscopy data was not representative of genetic context in production strains

Initial microscopy data collected by imaging GFP-fusion proteins of the MEL biosynthetic enzymes were all performed in the same genetic context. All genes were expressed on plasmids controlled by the *TPI* promoter and *PGK1* terminator. We know from previous data collected in the lab that expression levels matter regarding protein folding, stability and sub-cellular localisation. Overexpressed heterologous proteins can become non-functional outside of native contexts. When making the biotechnologically producing strain we placed the ORFs under the control of new regulatory regions under which we had not performed fluorescence microscopy. It is possible that these new expression cassettes overexpress the genes and that nascent proteins do not recruit sufficient chaperones to stabilise the molecule. In this case, we would have an accumulation of non-functional protein in the biotechnological cultures that would still be detected through mass

spectrometry due to the proteins fragmentation. Time permitting, it could be worthwhile to GFP-tag our constructs in the producing strains, allowing microscopic analysis of the proteins in their final context. Alternatively, *S. cerevisiae* strains overexpressing ER chaperone proteins have been developed which are more resilient against heterologous protein folding response (Tang *et al*, 2015). It is possible that alternative strain backgrounds provide biotechnological advantages for MEL biosynthesis.

5.3.3 Variations in MEL pathway protein expression level

Proteomics experiments verified that our pathway was being expressed. When choosing promoters/terminators/integration loci we had planned for all the genes to be expressed at equivalent levels except *MMF1*. The proteomics analysis showed a ~5x variation in MEL biosynthetic gene expression (4.14). Mac1 and Mac2 were the most abundant of the expressed MEL biosynthetic enzymes. It is possible that as these are peroxisomally located, they are protected from targeted degradation or from vacuolar recruitment by being in the peroxisome, leading to their accumulation. While we failed to identify MEL production it offers an insight into the use of the peroxisome as a space for heterologous protein sequestration for later extraction. Alternatively, if native *S. cerevisiae* substrates found in the peroxisome can be altered to a valuable molecule the addition of PTS1 to relevant biotechnological enzymes may be an efficient strategy for its synthesis.

A note on gene expression levels is that despite choosing promoters estimated to be of equivalent strength, we see a large difference in expression level when comparing Mac1 to Mat1. As these were both expressed from a plasmid, it is unlikely that the variation is due to chromatin structure at their genetic loci. While there is likely some variation in promoter/terminator strength, the markedly higher levels of Mac1 may be attributable to a protective effect of peroxisomal localisation. Protection of peroxisomal proteins in biotechnological hosts have been observed in *S. cerevisiae* (Choi *et al*, 2022) and in *Pichia pastoris* (*P. pastoris*) (Abad *et al*, 2010).

5.3.4 Extraction efficiency

As we had a limited supply of MEL-A, we used only 5mg when spiking cell pellet and supernatant samples prior to extraction. MEL in these samples was easily detected through NMR. This was partially due to ethyl acetate extraction stringency and due to the lack of molecules with peaks adjacent to MEL peaks on the NMR spectra. Cell pellet extractions were performed on ~1000 OD units of yeast cells, simultaneously supernatant extracts were performed on 50ml of culture broth. As 5mg of MEL-A from such a culture extraction represents a poor yield, it is unlikely that some production was present at sub-detectable limits. The detection of these small MEL-A additions is impressive and gives hope for future work in identifying successful modifications to the producing strains.

5.4 Future work

The work described in this thesis has eluded to a number of future experiments to determine additional effects involved in the Rex1 response to stress. Analysis on the stability of a Rex1 K58A mutant could be used to validate that the ubiquitinated residue at K58 is involved in poly-ubiquitination and proteasome recruitment. Furthermore, we could perform screen with ubiquitin ligase/kinase overexpression and knockout libraries to determine which ubiquitin ligases/kinases are required for Rex1 modification. Should additional information be available about these enzymes and the pathways they are involved in this could be used to determine additional mechanisms occurring simultaneously to Rex1 degradation and delocalisation during heat shock. While we have observed

these effects happening to the Rex1 protein it would be worthwhile to perform qPCR on reverse transcribed mRNA from cells taken in and out of heat shock to determine stress effects on *REX1* transcription levels. These could be measured from cells placed under a number of stressors including salt, osmotic stress, oxidative stress and a number of nutrient stress mediums. It would simultaneously be interesting to conduct Rex1 protein analysis on cells under these stressors. Nuclear proteasome granules have been identified in response to oxidative stress (Enenkel *et al*, 2022), it would be worthwhile to fluorescently label proteasome components to address whether the foci observed upon a shift from 30°C to 39°C corresponds to a region of enhanced proteasomal concentration. Our data of GFP-Rex1 mutants expressed within our temperature sensitive *Srp1* mutants corresponds to expected phenotypes that Rex1 import is *Srp1* mediated. However, future work could address the interaction between these proteins further by the use of pull-downs and *in vitro* binding assays. While we have seen a rapid drop in Rex1 levels in response to heat stress, we did not measure a return of Rex1 protein upon a shift from heat-shock to permissive temperatures. Experiments measuring Rex1 protein and transcription levels in cells moved out of heat shock would be interesting to observe how rapidly the cells are able to restore Rex1 activity and whether this is prioritised in a cell trying to return to optimal growth conditions. This would be particularly interesting if *Rrp6/Rrp47* levels were also measured. As *rex1Δ*, *rrp6Δ/rrp47Δ* cells are not viable it would be interesting if a heat-shocked cell, lacking Rex1, prioritize the synthesis of one of these components initially as they share some redundant activity.

Regarding the heterologous expression of the MEL biosynthetic pathway in *S. cerevisiae* there are numerous future steps to optimise its functionality. Initially it is advisable to fluorescently label the biosynthetic enzymes in the genetic context employed in the final production strain. This would allow for imaging of the proteins as they have been expressed together and ensure correct sub-cellular localisation in the final context. Alternatively, cell fractionation and proteomics of the fractions could be performed to ensure that the MEL heterologous enzymes correctly localise. The use of more sensitive analytical techniques for MEL identification could be employed such as GC-MS to validate a complete lack of production in our strains. *U. maydis* peroxisomes are larger and more complex than those of *S. cerevisiae* if transporters for the flux of precursors in and out of the native peroxisome were identified these could be expressed in the production strain to reduce potential bottlenecks.

References

- Achstetter, T. *et al.* (1984) 'Proteolysis in eukaryotic cells. Proteinase yscE, a new yeast peptidase', *Journal of Biological Chemistry*, 259(21), pp. 13344–13348. doi: 10.1016/s0021-9258(18)90700-3.
- Acker, J., Conesa, C. and Lefebvre, O. (2013) 'Yeast RNA polymerase III transcription factors and effectors', *Biochimica et Biophysica Acta - Gene Regulatory Mechanisms*. Elsevier B.V., 1829(3–4), pp. 283–295. doi: 10.1016/j.bbagr.2012.10.002.
- Adams, B. G. (1972) 'Induction of galactokinase in *Saccharomyces cerevisiae*: kinetics of induction and glucose effects.', *Journal of Bacteriology*, 111(2), pp. 308–315. doi: 10.1128/jb.111.2.308-315.1972.
- Aguilar, L. R., Pardo, J. P., Lomelí, M. M., Bocardo, O. I. L., Juárez Oropeza, M. A., & Guerra Sánchez, G. (2017). Lipid droplets accumulation and other biochemical changes induced in the fungal pathogen *Ustilago maydis* under nitrogen-starvation. *Archives of microbiology*, 199, 1195-1209. DOI: 10.1007/s00203-017-1388-8
- Akey, C. W. *et al.* (2022) 'Comprehensive structure and functional adaptations of the yeast nuclear pore complex', *Cell*. Elsevier, 185(2), pp. 361-378.e25. doi: 10.1016/j.cell.2021.12.015.
- Akkermans, V. *et al.* (2020) 'Mannosylerythritol Lipid Production from Oleaginous Yeast Cell Lysate by *Moesziomyces aphidis*', *Industrial Biotechnology*, 16(4), pp. 222–232. doi: 10.1089/ind.2019.0040.
- Alings, F. *et al.* (2015) 'An evolutionary approach uncovers a diverse response of tRNA 2-thiolation to elevated temperatures in yeast', *Rna*, 21(2), pp. 202–212. doi: 10.1261/rna.048199.114.
- Alper, H. *et al.* (2005) 'Tuning genetic control through promoter engineering', *Proceedings of the National Academy of Sciences of the United States of America*, 102(36), pp. 12678–12683. doi: 10.1073/pnas.0504604102.
- Al-Zain, A. *et al.* (2015) 'Cdc6 degradation requires phosphodegron created by GSK-3 and Cdk1 for SCFCdc4 recognition in *Saccharomyces cerevisiae*', *Molecular Biology of the Cell*, 26(14), pp. 2609–2619. doi: 10.1091/mbc.E14-07-1213.
- Andrade, C. J. de *et al.* (2017) 'A novel approach for the production and purification of mannosylerythritol lipids (MEL) by *Pseudozyma tsukubaensis* using cassava wastewater as substrate', *Separation and Purification Technology*, 180, pp. 157–167. doi: 10.1016/j.seppur.2017.02.045.
- Ardito, F. *et al.* (2017) 'The crucial role of protein phosphorylation in cell signaling and its use as targeted therapy (Review)', *International Journal of Molecular Medicine*, 40(2), pp. 271–280. doi: 10.3892/ijmm.2017.3036.
- Bahia, F. M. *et al.* (2018) 'Rhamnolipids production from sucrose by engineered *Saccharomyces cerevisiae*', *Scientific Reports*, 8(1), pp. 1–10. doi: 10.1038/s41598-018-21230-2.
- Beck, A. *et al.* (2021) 'Novel mannosylerythritol lipid biosurfactant structures from castor oil revealed by advanced structure analysis', *Journal of Industrial Microbiology and Biotechnology*, 48(7–8). doi: 10.1093/jimb/kuab042.
- Berger, A. B. *et al.* (2007) 'Hmo1 Is Required for TOR-Dependent Regulation of Ribosomal Protein Gene Transcription', *Molecular and Cellular Biology*, 27(22), pp. 8015–8026. doi: 10.1128/mcb.01102-07.

- Bergeron, D., Faucher-Giguère, L., Emmerichs, A. K., Choquet, K., Song, K. S., Deschamps-Francoeur, G., ... & Scott, M. S. (2023). Intronic small nucleolar RNAs regulate host gene splicing through base pairing with their adjacent intronic sequences. *Genome Biology*, 24(1), 160. DOI: 10.1186/s13059-023-03002-y
- Besada-Lombana, P. B., McTaggart, T. L. and Da Silva, N. A. (2018) 'Molecular tools for pathway engineering in *Saccharomyces cerevisiae*', *Current Opinion in Biotechnology*. Elsevier Ltd, 53, pp. 39–49. doi: 10.1016/j.copbio.2017.12.002.
- Betat, H., & Mörl, M. (2015). The CCA-adding enzyme: a central scrutinizer in tRNA quality control. *Bioessays*, 37(9), 975-982. DOI: 10.1002/bies.201500043
- Bilbrough, T., Piemontese, E. and Seitz, O. (2022) 'Dissecting the role of protein phosphorylation: a chemical biology toolbox', *Chemical Society Reviews*. Royal Society of Chemistry, 51(13), pp. 5691–5730. doi: 10.1039/d1cs00991e.
- Bleichert, F., Granneman, S., Osheim, Y. N., Beyer, A. L., & Baserga, S. J. (2006). The PINc domain protein Utp24, a putative nuclease, is required for the early cleavage steps in 18S rRNA maturation. *Proceedings of the National Academy of Sciences*, 103(25), 9464-9469. DOI: 10.1073/pnas.0603673103
- Boeke, J. D. *et al.* (1987) '[10] 5-Fluoroorotic acid as a selective agent in yeast molecular genetics', *Methods in Enzymology*, 154(C), pp. 164–175. doi: 10.1016/0076-6879(87)54076-9. Boguta, M. (2013) 'Maf1, a general negative regulator of RNA polymerase III in yeast', *Biochimica et Biophysica Acta - Gene Regulatory Mechanisms*. Elsevier B.V., 1829(3–4), pp. 376–384. doi: 10.1016/j.bbagr.2012.11.004.
- Boisnard, S. *et al.* (2009) 'H₂O₂ activates the nuclear localization of Msn2 and Maf1 through thioredoxins in *Saccharomyces cerevisiae*', *Eukaryotic Cell*, 8(9), pp. 1429–1438. doi: 10.1128/EC.00106-09.
- Bölker, M., Basse, C. W. and Schirawski, J. (2008) 'Ustilago maydis secondary metabolism-From genomics to biochemistry', *Fungal Genetics and Biology*, 45(SUPPL. 1), pp. 88–93. doi: 10.1016/j.fgb.2008.05.007.
- Bozaykut, P., Ozer, N. K., & Karademir, B. (2014). Regulation of protein turnover by heat shock proteins. *Free Radical Biology and Medicine*, 77, 195-209. DOI: 10.1016/j.freeradbiomed.2014.08.012
- Brakhage, A. A. and Schroeckh, V. (2011) 'Fungal secondary metabolites - Strategies to activate silent gene clusters', *Fungal Genetics and Biology*. Elsevier Inc., 48(1), pp. 15–22. doi: 10.1016/j.fgb.2010.04.004.
- Campos, J. M. *et al.* (2013) 'Microbial biosurfactants as additives for food industries', *Biotechnology Progress*, 29(5), pp. 1097–1108. doi: 10.1002/btpr.1796.
- Clarke, L. and Carbon, J., 1980. Isolation of a yeast centromere and construction of functional small circular chromosomes. *Nature*, 287(5782), pp.504-509.
- Chamberlain, J. R. *et al.* (1998) 'Purification and characterization of the nuclear RNase P holoenzyme complex reveals extensive subunit overlap with RNase MRP', *Genes and Development*, 12(11), pp. 1678–1690. doi: 10.1101/gad.12.11.1678.

- Chan, C. T. Y. *et al.* (2010) 'A quantitative systems approach reveals dynamic control of tRNA modifications during cellular stress', *PLoS Genetics*, 6(12), pp. 1–9. doi: 10.1371/journal.pgen.1001247.
- Chatterjee, K. *et al.* (2018) 'tRNA dynamics between the nucleus, cytoplasm and mitochondrial surface: Location, location, location', *Biochimica et Biophysica Acta - Gene Regulatory Mechanisms*. Elsevier, 1861(4), pp. 373–386. doi: 10.1016/j.bbagr.2017.11.007.
- Chen, D. C., Yang, B. C. and Kuo, T. T. (1992) 'One-step transformation of yeast in stationary phase', *Current Genetics*, 21(1), pp. 83–84. doi: 10.1007/BF00318659.
- Chen, L., Zhang, J., & Chen, W. N. (2014). Engineering the *Saccharomyces cerevisiae* β -oxidation pathway to increase medium chain fatty acid production as potential biofuel. *PloS one*, 9(1), e84853. doi: 10.1371/journal.pone.0084853
- Chen, L. and Madura, K. (2014) 'Yeast Importin- α (Srp1) performs distinct roles in the import of nuclear proteins and in targeting proteasomes to the nucleus', *Journal of Biological Chemistry*, 289(46), pp. 32339–32352. doi: 10.1074/jbc.M114.582023.
- Chen, W. *et al.* (2017) 'Alternative Polyadenylation: Methods, Findings, and Impacts Methods and Findings of Alternative Polyadenylation', *Genomics, Proteomics and Bioinformatics*. Beijing Institute of Genomics, Chinese Academy of Sciences and Genetics Society of China, 15(5), pp. 287–300. doi: 10.1016/j.gpb.2017.06.001.
- Chernyakov, I. *et al.* (2008) 'Degradation of several hypomodified mature tRNA species in *Saccharomyces cerevisiae* is mediated by Met22 and the 5'-3' exonucleases Rat1 and Xrn1', *Genes and Development*, 22(10), pp. 1369–1380. doi: 10.1101/gad.1654308.
- Cieřla, M. *et al.* (2007) 'Maf1 Is Involved in Coupling Carbon Metabolism to RNA Polymerase III Transcription', *Molecular and Cellular Biology*, 27(21), pp. 7693–7702. doi: 10.1128/mcb.01051-07.
- Ciganda, M. and Williams, N. (2011) 'Eukaryotic 5S rRNA biogenesis', *Wiley Interdisciplinary Reviews: RNA*, 2(4), pp. 523–533. doi: 10.1002/wrna.74.
- Cipollina, C. *et al.* (2008) 'Saccharomyces cerevisiae SFP1: At the crossroads of central metabolism and ribosome biogenesis', *Microbiology*, 154(6), pp. 1686–1699. doi: 10.1099/mic.0.2008/017392-0.
- Conti, E. *et al.* (1998) 'Crystallographic analysis of the recognition of a nuclear localization signal by the nuclear import factor karyopherin α ', *Cell*, 94(2), pp. 193–204. doi: 10.1016/S0092-8674(00)81419-1.
- Copela, L. A., Chakshusmathi, G., Sherrer, R. L., & Wolin, S. L. (2006). The La protein functions redundantly with tRNA modification enzymes to ensure tRNA structural stability. *Rna*, 12(4), 644-654. doi: 10.1261/rna.2307206
- Curran, K. A. *et al.* (2015) 'Short Synthetic Terminators for Improved Heterologous Gene Expression in Yeast', *ACS Synthetic Biology*, 4(7), pp. 824–832. doi: 10.1021/sb5003357.
- Czech, A. *et al.* (2013) 'Reversible and Rapid Transfer-RNA Deactivation as a Mechanism of Translational Repression in Stress', *PLoS Genetics*, 9(8). doi: 10.1371/journal.pgen.1003767.
- Da Silva, N. A. and Srikrishnan, S. (2012) 'Introduction and expression of genes for metabolic engineering applications in *Saccharomyces cerevisiae*', *FEMS Yeast Research*, 12(2), pp. 197–214. doi: 10.1111/j.1567-1364.2011.00769.x.

- Daniels, P. W. *et al.* (2022) 'Contribution of domain structure to the function of the yeast DEDD family exoribonuclease and RNase T functional homolog, Rex1', *Rna*, 28(4), pp. 493–507. doi: 10.1261/rna.078939.121.
- Darst, S. A. (2001) 'Bacterial RNA polymerase', *Current Opinion in Structural Biology*, 11(2), pp. 155–162. doi: 10.1016/S0959-440X(00)00185-8.
- de Estrada, N. M. C. D., Thoms, M., Flemming, D., Hammaren, H. M., Buschauer, R., Ameismeier, M., ... & Hurt, E. (2023). Structure of nascent 5S RNPs at the crossroad between ribosome assembly and MDM2–p53 pathways. *Nature Structural & Molecular Biology*, 30(8), 1119. DOI: 10.1128/EC.1.2.163-173.2002
- DeLoache, W. C., Russ, Z. N. and Dueber, J. E. (2016) 'Towards repurposing the yeast peroxisome for compartmentalizing heterologous metabolic pathways', *Nature Communications*. Nature Publishing Group, 7. doi: 10.1038/ncomms11152.
- Deshaies, R. J. (1997). Phosphorylation and proteolysis: partners in the regulation of cell division in budding yeast. *Current opinion in genetics & development*, 7(1), 7-16. DOI: 10.1016/s0959-437x(97)80103-7
- Dhungel, N. and Hopper, A. K. (2012) 'Beyond tRNA cleavage: Novel essential function for yeast tRNA splicing endonuclease unrelated to tRNA processing', *Genes and Development*, 26(5), pp. 503–514. doi: 10.1101/gad.183004.111.
- Dongmei Bai Flagfeldt, Verena Siewers, Le Huang, and J. N. (2008) 'Characterization of chromosomal integration sites for heterologous gene expression in *Saccharomyces cerevisiae*', *Yeast*, (August), pp. 191–198. doi: 10.1002/yea.
- Dvir, S. *et al.* (2019) 'Erratum: Deciphering the rules by which 5'-UTR sequences affect protein expression in yeast *Proceedings of the National Academy of Sciences of the United States of America*, 116(27), p. 13701. doi: 10.1073/pnas.1909441116.
- Ebersole, T. *et al.* (2005) 'Rapid generation of long synthetic tandem repeats and its application for analysis in human artificial chromosome formation', *Nucleic Acids Research*, 33(15), pp. 1–8. doi: 10.1093/nar/gni129.
- Edwards, A. M., Addo, M. A. and Dos Santos, P. C. (2020) 'Extracurricular functions of tRNA modifications in microorganisms', *Genes*, 11(8), pp. 1–19. doi: 10.3390/genes11080907.
- Enenkel, C., Kang, R. W., Wilfling, F., & Ernst, O. P. (2022). Intracellular localization of the proteasome in response to stress conditions. *Journal of Biological Chemistry*, 298(7), 102083. DOI: 10.1016/j.jbc.2022.102083
- Erhart, E. and Hollenberg, C. P. (1983) 'The presence of a defective LEU2 gene on 2 μ DNA recombinant plasmids of *Saccharomyces cerevisiae* is responsible for curing and high copy number', *Journal of Bacteriology*, 156(2), pp. 625–635. doi: 10.1128/jb.156.2.625-635.1983.
- Ernst, C. M. and Peschel, A. (2011) 'Broad-spectrum antimicrobial peptide resistance by MprF-mediated aminoacylation and flipping of phospholipids', *Molecular Microbiology*, 80(2), pp. 290–299. doi: 10.1111/j.1365-2958.2011.07576.x.
- Fan, L. L. *et al.* (2014) 'Production and identification of mannosylerythritol lipid-A homologs from the ustilaginomycetous yeast *Pseudozyma aphidis* ZJUDM34', *Carbohydrate Research*. Elsevier Ltd, 392, pp. 1–6. doi: 10.1016/j.carres.2014.04.013.

- Fatica, A., Oeffinger, M., Dlakic, M., & Tollervey, D. (2003). Nob1p is required for cleavage of the 3' end of 18S rRNA. *Molecular and cellular biology*. doi: 10.1128/MCB.23.5.1798-1807.2003
- Fang, Fang, et al. "A vector set for systematic metabolic engineering in *Saccharomyces cerevisiae*." *Yeast* 28.2 (2011): 123-136. DOI: 10.1002/yea.1824
- Fingerman, I. et al. (2003) 'Sfp1 plays a key role in yeast ribosome biogenesis', *Eukaryotic Cell*, 2(5), pp. 1061–1068. doi: 10.1128/EC.2.5.1061-1068.2003.
- Fleming, J. A. et al. (2002) 'Complementary whole-genome technologies reveal the cellular response to proteasome inhibition by PS-341', *Proceedings of the National Academy of Sciences of the United States of America*, 99(3), pp. 1461–1466. doi: 10.1073/pnas.032516399.
- Fonvielle, M. et al. (2009) 'Aminoacyl-tRNA recognition by the FemXWv transferase for bacterial cell wall synthesis', *Nucleic Acids Research*, 37(5), pp. 1589–1601. doi: 10.1093/nar/gkn1039.
- Foretek, D. et al. (2016) 'Control of *Saccharomyces cerevisiae* pre-tRNA processing by environmental conditions', *Rna*, 22(3), pp. 339–349. doi: 10.1261/rna.054973.115.
- Frank, P. et al. (1999) 'Purification of *Saccharomyces cerevisiae* RNase H(70) and identification of the corresponding gene', *FEBS Letters*, 450(3), pp. 251–256. doi: 10.1016/S0014-5793(99)00512-8.
- French, S. L. et al. (2008) 'Visual Analysis of the Yeast 5S rRNA Gene Transcriptome: Regulation and Role of La Protein', *Molecular and Cellular Biology*, 28(14), pp. 4576–4587. doi: 10.1128/mcb.00127-08.
- Fu, H. et al. (2009) 'Stress induces tRNA cleavage by angiogenin in mammalian cells', *FEBS Letters*. Federation of European Biochemical Societies, 583(2), pp. 437–442. doi: 10.1016/j.febslet.2008.12.043.
- Fukuoka, T. et al. (2007) 'Structural characterization and surface-active properties of a new glycolipid biosurfactant, mono-acylated mannosylerythritol lipid, produced from glucose by *Pseudozyma antarctica*', *Applied Microbiology and Biotechnology*, 76(4), pp. 801–810. doi: 10.1007/s00253-007-1051-4.
- Furuichi, Y. (2015) 'Discovery of m7G-cap in eukaryotic mRNAs', *Proceedings of the Japan Academy Series B: Physical and Biological Sciences*, 91(8), pp. 394–409. doi: 10.2183/pjab.91.394.
- Furuta, M. et al. (2004) 'Heat-shock induced nuclear retention and recycling inhibition of importin α ', *Genes to Cells*, 9(5), pp. 429–441. doi: 10.1111/j.1356-9597.2004.00734.x.
- Futcher, B. and Carbon, J. (1986) 'Toxic Effects of Excess Cloned Centromeres', *Molecular and Cellular Biology*, 6(6), pp. 2213–2222. doi: 10.1128/mcb.6.6.2213-2222.1986.
- Gaid, M. et al. (2018) 'Biotechnological production of hyperforin for pharmaceutical formulation', *European Journal of Pharmaceutics and Biopharmaceutics*. Elsevier B.V., 126, pp. 10–26. doi: 10.1016/j.ejpb.2017.03.024.
- Galen A. Collins^{1, 2}, Tara Adele Gomez³, R. J. D. and W. P. T. (2008) 'Combined chemical and genetic approach to inhibit proteolysis by the proteasome', *Yeast*, (July), pp. 191–198. doi: 10.1002/yea.
- Garlapati, V. K., Shankar, U. and Budhiraja, A. (2016) 'Bioconversion technologies of crude glycerol to value added industrial products', *Biotechnology Reports*. Elsevier B.V., 9, pp. 9–14. doi: 10.1016/j.btre.2015.11.002.

Gasch, Audrey P., et al. "Genomic expression programs in the response of yeast cells to environmental changes." *Molecular biology of the cell* 11.12 (2000): 4241-4257.

Geetha, S. J., Banat, I. M. and Joshi, S. J. (2018) 'Biosurfactants: Production and potential applications in microbial enhanced oil recovery (MEOR)', *Biocatalysis and Agricultural Biotechnology*. Elsevier Ltd, pp. 23–32. doi: 10.1016/j.bcab.2018.01.010.

Ghavidel, A. *et al.* (2007) 'Impaired tRNA Nuclear Export Links DNA Damage and Cell-Cycle Checkpoint', *Cell*, 131(5), pp. 915–926. doi: 10.1016/j.cell.2007.09.042.

Ghavidel, A. and Schultz, M. C. (2001) 'TATA binding protein-associated CK2 transduces DNA damage signals to the RNA polymerase III transcriptional machinery', *Cell*, 106(5), pp. 575–584. doi: 10.1016/S0092-8674(01)00473-1.

Gibson, D. G. *et al.* (2008) 'Complete chemical synthesis, assembly, and cloning of a *Mycoplasma genitalium* genome', *Science*, 319(5867), pp. 1215–1220. doi: 10.1126/science.1151721.

Gietz, R. D. and Woods, R. A. (2002) 'Transformation of yeast by lithium acetate/single-stranded carrier DNA/polyethylene glycol method', *Methods in Enzymology*, 350(2001), pp. 87–96. doi: 10.1016/S0076-6879(02)50957-5.

Glotzer, M., Murray, A. W. and Kirschner, M. W. (1991) 'Cyclin is degraded by the ubiquitin pathway', *Nature*, 349(6305), pp. 132–138. doi: 10.1038/349132a0.

Goffeau, A. *et al.* (1996) 'Life with 6000 Genes conveniently among the different interna- Old Questions and New Answers The genome . At the beginning of the se- of its more complex relatives in the eukary- cerevisiae has been completely sequenced *Schizosaccharomyces pombe* indicate', *Science*, 274(October), pp. 546–567.

Goldstein, A. L., Pan, X., & McCusker, J. H. (1999). Heterologous URA3MX cassettes for gene replacement in *Saccharomyces cerevisiae*. *Yeast*, 15(6), 507-511. DOI: 10.1002/(SICI)1097-0061(199904)15:6<507::AID-YEA369>3.0.CO;2-P

Goossens, E. *et al.* (2016) 'Enhanced separation and analysis procedure reveals production of triacylated mannosylerythritol lipids by *Pseudozyma aphidis*', *Journal of Industrial Microbiology and Biotechnology*. Springer Berlin Heidelberg, 43(11), pp. 1537–1550. doi: 10.1007/s10295-016-1838-3.

Gu, W. *et al.* (2003) 'tRNA^{His} maturation: An essential yeast protein catalyzes addition of a guanine nucleotide to the 5' end of tRNA^{His}', *Genes and Development*, 17(23), pp. 2889–2901. doi: 10.1101/gad.1148603.

Güldener, Ulrich, et al. "A new efficient gene disruption cassette for repeated use in budding yeast." *Nucleic acids research* 24.13 (1996): 2519-2524. doi: 10.1093/nar/24.13.2519

Han, L., Kon, Y. and Phizicky, E. M. (2015) 'Functional importance of Ψ 38 and Ψ 39 in distinct tRNAs, amplified for tRNA^{Gln}(UUG) by unexpected temperature sensitivity of the s2U modification in yeast', *Rna*, 21(2), pp. 188–201. doi: 10.1261/rna.048173.114.

Hanahan, D. (1983) 'Studies on transformation of *Escherichia coli* with plasmids', *Journal of Molecular Biology*, 166(4), pp. 557–580. doi: 10.1016/S0022-2836(83)80284-8.

Hani, J. and Feldmann, H. (1998) 'tRNA genes and retroelements in the yeast genome', *Nucleic Acids Research*, 26(3), pp. 689–696. doi: 10.1093/nar/26.3.689.

- Harismendy, O. *et al.* (2003) 'Genome-wide location of yeast RNA polymerase III transcription machinery', *EMBO Journal*, 22(18), pp. 4738–4747. doi: 10.1093/emboj/cdg466.
- Hawkins, K. M. and Smolke, C. D. (2008) 'Production of benzylisoquinoline alkaloids in *Saccharomyces cerevisiae*', *Nature Chemical Biology*, 4(9), pp. 564–573. doi: 10.1038/nchembio.105.
- Hess, W. R. and Börner, T. (1999) 'Organellar RNA polymerases of higher plants', *International Review of Cytology*, 190, pp. 1–59. doi: 10.1016/s0074-7696(08)62145-2.
- Hettema, E. H., & Tabak, H. F. (2000). Transport of fatty acids and metabolites across the peroxisomal membrane. *Biochimica et Biophysica Acta (BBA)-Molecular and Cell Biology of Lipids*, 1486(1), 18-27. DOI: 10.1016/s1388-1981(00)00045-7
- Hewald, S., Josephs, K. and Bölker, M. (2005) 'Genetic analysis of biosurfactant production in *Ustilago maydis*', *Applied and Environmental Microbiology*, 71(6), pp. 3033–3040. doi: 10.1128/AEM.71.6.3033-3040.2005.
- Hewald, S. *et al.* (2006) 'Identification of a gene cluster for biosynthesis of mannosylerythritol lipids in the basidiomycetous fungus *Ustilago maydis*', *Applied and Environmental Microbiology*, 72(8), pp. 5469–5477. doi: 10.1128/AEM.00506-06.
- Hilt, W. and Wolf, D. H. (1995) 'Proteasomes of the yeast *S. cerevisiae*: genes, structure and functions', *Molecular Biology Reports*, 21(1), pp. 3–10. doi: 10.1007/BF00990964.
- Holland, J.P. and Holland, M.J., (1980) 'Structural comparison of two nontandemly repeated yeast glyceraldehyde-3-phosphate dehydrogenase genes.' *Journal of Biological Chemistry*, 255(6), pp.2596-2605.
- Holt, L. J. (2012). Regulatory modules: Coupling protein stability to phosphoregulation during cell division. *FEBS letters*, 586(17), 2773-2777. DOI: 10.1016/j.febslet.2012.05.045
- Hood, J.K. and Silver, P.A., (1998) 'Cse1p is required for export of Srp1p/importin- α from the nucleus in *Saccharomyces cerevisiae*'. *Journal of Biological Chemistry*, 273(52), pp.35142-35146.
- Hopper, A.K., (2013) 'Transfer RNA post-transcriptional processing, turnover, and subcellular dynamics in the yeast *Saccharomyces cerevisiae*'. *Genetics*, 194(1), pp.43-67.
- Horecker, B. L. (2002) 'The pentose phosphate pathway.', *The Journal of biological chemistry*. © 2002 ASBMB. Currently published by Elsevier Inc; originally published by American Society for Biochemistry and Molecular Biology., 277(50), pp. 47965–47971. doi: 10.1074/jbc.X200007200.
- Hou, C. *et al.* (2022) 'Systematic prediction of degrons and E3 ubiquitin ligase binding via deep learning', *BMC Biology*. BioMed Central, 20(1), pp. 1–19. doi: 10.1186/s12915-022-01364-6.
- Hoyle, N. P. *et al.* (2007) 'Stress-dependent relocalization of translationally primed mRNPs to cytoplasmic granules that are kinetically and spatially distinct from P-bodies', *Journal of Cell Biology*, 179(1), pp. 65–74. doi: 10.1083/jcb.200707010.
- Huang, S., Aleksashin, N. A., Loveland, A. B., Klepacki, D., Reier, K., Kefi, A., ... & Mankin, A. S. (2020). Ribosome engineering reveals the importance of 5S rRNA autonomy for ribosome assembly. *Nature Communications*, 11(1), 2900. DOI: 10.1038/s41467-020-16694-8

- Izawa, S. *et al.* (2008) 'Heat shock and ethanol stress provoke distinctly different responses in 3'-processing and nuclear export of HSP mRNA in *Saccharomyces cerevisiae*', *Biochemical Journal*, 414(1), pp. 111–119. doi: 10.1042/BJ20071567.
- Jans, D. A. and Hübner, S. (1996) 'Regulation of protein transport to the nucleus: Central role of phosphorylation', *Physiological Reviews*, 76(3), pp. 651–685. doi: 10.1152/physrev.1996.76.3.651.
- Jefferies, H. B. J. *et al.* (1997) 'Rapamycin suppresses 5'TOP mRNA translation through inhibition of p70(s6k)', *EMBO Journal*, 16(12), pp. 3693–3704. doi: 10.1093/emboj/16.12.3693.
- Joan A. Steitz, Celeste Berg, Joseph E Hendrick, Helene La Branche-Chabot, Andres Metspalu, Jutta Rinke, and T. Y. (1988) 'A 5S rRNA/L5 Complex Is a Precursor to Ribosome Assembly in Mammalian Cells', 106(March), pp. 545–556. DOI: 10.1083/jcb.106.3.545
- Jones, E. W., Zubenko, G. S. and Parker, R. R. (1982) 'PEP4 gene function is required for expression of several vacuolar hydrolases in *Saccharomyces cerevisiae*.' , *Genetics*, 102(4), pp. 665–677. doi: 10.1093/genetics/102.4.665.
- Jongedijk, E. *et al.* (2016) 'Biotechnological production of limonene in microorganisms', *Applied Microbiology and Biotechnology*, 100(7), pp. 2927–2938. doi: 10.1007/s00253-016-7337-7.
- Jumper, J., Evans, R., Pritzel, A., Green, T., Figurnov, M., Ronneberger, O., ... & Hassabis, D. (2021). Highly accurate protein structure prediction with AlphaFold. *Nature*, 596(7873), 583-589. DOI: 10.1038/s41586-021-03819-2
- Kadaba, S. *et al.* (2004) 'Nuclear surveillance and degradation of hypomodified initiator tRNA Met in *S. cerevisiae*', *Genes and Development*, 18(11), pp. 1227–1240. doi: 10.1101/gad.1183804.
- Kadaba, S., Wang, X. and Anderson, J. T. (2006) 'Nuclear RNA surveillance in *Saccharomyces cerevisiae*: Trf4p-dependent polyadenylation of nascent hypomethylated tRNA and an aberrant form of 5S rRNA', *Rna*, 12(3), pp. 508–521. doi: 10.1261/rna.2305406.
- Kamada, Y. (2017) 'Novel tRNA function in amino acid sensing of yeast Tor complex1', *Genes to Cells*, 22(2), pp. 135–147. doi: 10.1111/gtc.12462.
- Kasahara, K. *et al.* (2007) ' Assembly of Regulatory Factors on rRNA and Ribosomal Protein Genes in *Saccharomyces cerevisiae* ', *Molecular and Cellular Biology*, 27(19), pp. 6686–6705. doi: 10.1128/mcb.00876-07.
- Kempers-Veenstra, A. E. *et al.* (1986) '3'-End formation of transcripts from the yeast rRNA operon.', *The EMBO journal*, 5(10), pp. 2703–2710. doi: 10.1002/j.1460-2075.1986.tb04554.x.
- Kodiha, M. *et al.* (2008) 'Oxidative stress mislocalizes and retains transport factor importin- α and nucleoporins Nup153 and Nup88 in nuclei where they generate high molecular mass complexes', *Biochimica et Biophysica Acta - Molecular Cell Research*, 1783(3), pp. 405–418. doi: 10.1016/j.bbamcr.2007.10.022.
- Konishi, M., Hatada, Y. and Horiuchi, J. I. (2013) 'Draft genome sequence of the basidiomycetous yeast-like fungus *Pseudozyma hubeiensis* SY62, which produces an abundant amount of the biosurfactant mannosylerythritol lipids', *Genome Announcements*, 1(4). doi: 10.1128/genomeA.00409-13.
- Kos-Braun, I. C., Jung, I. and Koš, M. (2017) 'Tor1 and CK2 kinases control a switch between alternative ribosome biogenesis pathways in a growth-dependent manner', *PLoS Biology*, 15(3). doi: 10.1371/journal.pbio.2000245.

- Kosugi, S., Hasebe, M., Tomita, M., & Yanagawa, H. (2008). Nuclear export signal consensus sequences defined using a localization-based yeast selection system. *Traffic*, 9(12), 2053-2062. DOI: 10.1111/j.1600-0854.2008.00825.x
- Kramer, E. B., & Hopper, A. K. (2013). Retrograde transfer RNA nuclear import provides a new level of tRNA quality control in *Saccharomyces cerevisiae*. *Proceedings of the National Academy of Sciences*, 110(52), 21042-21047. DOI: 10.1073/pnas.1316579110
- Kuechler, E. R. *et al.* (2021) 'Protein feature analysis of heat shock induced ubiquitination sites reveals preferential modification site localization', *Journal of Proteomics*. Elsevier B.V., 239(March), p. 104182. doi: 10.1016/j.jprot.2021.104182.
- Kufel, J., Dichtl, B. and Tollervey, D. (1999) 'Yeast Rnt1p is required for cleavage of the pre-ribosomal RNA in the 3' ETS but not the 5' ETS', *Rna*, 5(7), pp. 909–917. doi: 10.1017/S135583829999026X.
- Kulak, N. A. *et al.* (2014) 'Minimal, encapsulated proteomic-sample processing applied to copy-number estimation in eukaryotic cells', *Nature Methods*, 11(3), pp. 319–324. doi: 10.1038/nmeth.2834.
- Künzler, M. and Hurt, E. C. (1998) 'Cse1p functions as the nuclear export receptor for importin α in yeast', *FEBS Letters*, 433(3), pp. 185–190. doi: 10.1016/S0014-5793(98)00892-8.
- Kutay, U. *et al.* (1997) 'Export of importin α from the nucleus is mediated by a specific nuclear transport factor', *Cell*, 90(6), pp. 1061–1071. doi: 10.1016/S0092-8674(00)80372-4.
- Ladevaia, V. *et al.* (2012) 'MTOR signaling regulates the processing of pre-rRNA in human cells', *Nucleic Acids Research*, 40(6), pp. 2527–2539. doi: 10.1093/nar/gkr1040.
- Landrieux, E. *et al.* (2006) 'A subcomplex of RNA polymerase III subunits involved in transcription termination and reinitiation', *EMBO Journal*, 25(1), pp. 118–128. doi: 10.1038/sj.emboj.7600915.
- Lanford, R. E. and Butel, J. S. (1984) 'Construction and characterization of an SV40 mutant defective in nuclear transport of T antigen', *Cell*, 37(3), pp. 801–813. doi: 10.1016/0092-8674(84)90415-X.
- Lanz, M. C. *et al.* (2021) 'In-depth and 3-dimensional exploration of the budding yeast phosphoproteome', *EMBO reports*, 22(2). doi: 10.15252/embr.202051121.
- Lazarus, C. M., Williams, K. and Bailey, A. M. (2014) 'Reconstructing fungal natural product biosynthetic pathways', *Natural Product Reports*. Royal Society of Chemistry, 31(10), pp. 1339–1347. doi: 10.1039/c4np00084f.
- Lee, D. and Goldberg, A. L. (2022) '26S proteasomes become stably activated upon heat shock when ubiquitination and protein degradation increase', *Proceedings of the National Academy of Sciences of the United States of America*, 119(25), pp. 1–11. doi: 10.1073/pnas.2122482119.
- Lee, J. H., Moir, R. D. and Willis, I. M. (2009) 'Regulation of RNA polymerase III transcription involves SCH9-dependent and SCH9-independent branches of the target of rapamycin (TOR) pathway', *Journal of Biological Chemistry*, 284(19), pp. 12604–12608. doi: 10.1074/jbc.C900020200.
- Lewis, M. A. (1991) 'Chronic and sublethal toxicities of surfactants to aquatic animals: A review and risk assessment', *Water Research*, 25(1), pp. 101–113. doi: 10.1016/0043-1354(91)90105-Y.
- Li, H. *et al.* (2006) 'Nutrient regulates Tor1 nuclear localization and association with rDNA promoter', *Nature*, 442(7106), pp. 1058–1061. doi: 10.1038/nature05020.

- Li, M. Z. and Elledge, S. J. (2007) 'Harnessing homologous recombination in vitro to generate recombinant DNA via SLIC', *Nature Methods*, 4(3), pp. 251–256. doi: 10.1038/nmeth1010.
- Li, X. *et al.* (2018) 'Distribution and diagenetic fate of synthetic surfactants and their metabolites in sewage-impacted estuarine sediments', *Environmental Pollution*. Elsevier Ltd, 242(2018), pp. 209–218. doi: 10.1016/j.envpol.2018.06.064.
- Liam J. Holt, Brian B. Tuch, Judit Villén, Alexander D. Johnson, 2 and Steven P. Gygi, D. O. M. (2009) 'Global Analysis of Cdk1 Substrate Phosphorylation Sites Provides Insights into Evolution', *Science*, 325(September), pp. 1682–1686.
- Lippman, S. I. and Broach, J. R. (2009) 'Protein kinase A and TORC1 activate genes for ribosomal biogenesis by inactivating repressors encoded by Dot6 and its homolog Tod6', *Proceedings of the National Academy of Sciences of the United States of America*, 106(47), pp. 19928–19933. doi: 10.1073/pnas.0907027106.
- Liu, C. *et al.* (2007) 'Proteasome inhibition in wild-type yeast *Saccharomyces cerevisiae* cells', *BioTechniques*, 42(2), pp. 158–162. doi: 10.2144/000112389.
- Liu, Z. *et al.* (2012) 'Different expression systems for production of recombinant proteins in *Saccharomyces cerevisiae*', *Biotechnology and Bioengineering*, 109(5), pp. 1259–1268. doi: 10.1002/bit.24409.
- Liu, Z. *et al.* (2017) 'Systematic comparison of 2A peptides for cloning multi-genes in a polycistronic vector', *Scientific Reports*. Springer US, 7(1), pp. 1–9. doi: 10.1038/s41598-017-02460-2.
- Loewith, R. *et al.* (2002) 'Two TOR complexes, only one of which is rapamycin sensitive, have distinct roles in cell growth control', *Molecular Cell*, 10(3), pp. 457–468. doi: 10.1016/S1097-2765(02)00636-6.
- Longtine, M. S. *et al.* (1998) 'Additional modules for versatile and economical PCR-based gene deletion and modification in *Saccharomyces cerevisiae*', *Yeast*, 14(10), pp. 953–961. doi: 10.1002/(SICI)1097-0061(199807)14:10<953::AID-YEA293>3.0.CO;2-U.
- Lorenz, M. C. *et al.* (1995) 'Gene disruption with PCR products in *Saccharomyces cerevisiae*', *Gene*, 158(1), pp. 113–117. doi: 10.1016/0378-1119(95)00144-U.
- Lorenz, S. *et al.* (2014) 'Genome Sequence of the Basidiomycetous Fungus *Pseudozyma aphidis* DSM70725, an Efficient Producer of Biosurfactant Mannosylerythritol Lipids', *Genome Announcements*, 2(1), pp. 13–14. doi: 10.1128/genomea.00053-14.
- Luan, B. *et al.* (2016) 'Structure of an endogenous yeast 26S proteasome reveals two major conformational states', *Proceedings of the National Academy of Sciences of the United States of America*, 113(10), pp. 2642–2647. doi: 10.1073/pnas.1601561113.
- Ma, J. *et al.* (2012) 'Self-regulated viscous channel in the nuclear pore complex', *Proceedings of the National Academy of Sciences of the United States of America*, 109(19), pp. 7326–7331. doi: 10.1073/pnas.1201724109.
- Madru, C. *et al.* (2015) 'Chaperoning 5S RNA assembly', *Genes and Development*, 29(13), pp. 1432–1446. doi: 10.1101/gad.260349.115.

- Malik, S. *et al.* (2016) 'Biotechnological approaches to the production of shikonins: A critical review with recent updates', *Critical Reviews in Biotechnology*, 36(2), pp. 327–340. doi: 10.3109/07388551.2014.961003.
- Manivasakam, P. *et al.* (1995) 'Micro-homology mediated PCR targeting in *Saccharomyces cerevisiae*', *Nucleic Acids Research*, 23(14), pp. 2799–2800. doi: 10.1093/nar/23.14.2799.
- Maraia, R. J. and Lamichhane, T. N. (2011) '3' processing of eukaryotic precursor tRNAs', *Wiley Interdisciplinary Reviews: RNA*, 2(3), pp. 362–375. doi: 10.1002/wrna.64.
- Maraia, R. J., Mattijssen, S., Cruz-Gallardo, I., & Conte, M. R. (2017). The La and related RNA-binding proteins (LARPs): structures, functions, and evolving perspectives. *Wiley Interdisciplinary Reviews: RNA*, 8(6), e1430. DOI: 10.1002/wrna.1430
- Margottin, F. *et al.* (1991) 'Participation of the TATA factor in transcription of the yeast U6 gene by RNA polymerase C', *Science*, 251(4992), pp. 424–426. doi: 10.1126/science.1989075.
- Mattiroli, F. and Sixma, T. K. (2014) 'Lysine-targeting specificity in ubiquitin and ubiquitin-like modification pathways', *Nature Structural and Molecular Biology*. Nature Publishing Group, 21(4), pp. 308–316. doi: 10.1038/nsmb.2792.
- Maury, J. *et al.* (2016) 'EasyCloneMulti: A set of vectors for simultaneous and multiple genomic integrations in *saccharomyces cerevisiae*', *PLoS ONE*, 11(3), pp. 1–22. doi: 10.1371/journal.pone.0150394.
- Maxwell, B. A., Gwon, Y., Mishra, A., Peng, J., Nakamura, H., Zhang, K., ... & Taylor, J. P. (2021). Ubiquitination is essential for recovery of cellular activities after heat shock. *Science*, 372(6549), eabc3593. DOI: 10.1126/science.abc3593
- Md, F. (2012) 'Biosurfactant: Production and Application', *Journal of Petroleum & Environmental Biotechnology*, 03(04). doi: 10.4172/2157-7463.1000124.
- Michels, A. A. *et al.* (2010) 'mTORC1 Directly Phosphorylates and Regulates Human MAF1', *Molecular and Cellular Biology*, 30(15), pp. 3749–3757. doi: 10.1128/mcb.00319-10.
- Mikkelsen, M. D. *et al.* (2012) 'Microbial production of indolyglucosinolate through engineering of a multi-gene pathway in a versatile yeast expression platform', *Metabolic Engineering*. Elsevier, 14(2), pp. 104–111. doi: 10.1016/j.ymben.2012.01.006.
- Milne, C. A. and Segall, J. (1993) 'Mapping regions of yeast transcription factor IIIA required for DNA binding, interaction with transcription factor IIIC, and transcription activity', *Journal of Biological Chemistry*, 268(15), pp. 11364–11371. doi: 10.1016/s0021-9258(18)82133-0.
- Miyamoto, Y. *et al.* (2004) 'Cellular stresses induce the nuclear accumulation of importin α and cause a conventional nuclear import block', *Journal of Cell Biology*, 165(5), pp. 617–623. doi: 10.1083/jcb.200312008.
- Mnif, I. and Ghribi, D. (2016) 'Glycolipid biosurfactants: main properties and potential applications in agriculture and food industry', *Journal of the science of food and agriculture*, 96(13), pp. 4310–4320. doi: 10.1002/jsfa.7759.
- Mohr, D. *et al.* (2009) 'Characterisation of the passive permeability barrier of nuclear pore complexes', *EMBO Journal*, 28(17), pp. 2541–2553. doi: 10.1038/emboj.2009.200.

- Moir, R. D. *et al.* (2006) 'Protein kinase A regulates RNA polymerase III transcription through the nuclear localization of Maf1', *Proceedings of the National Academy of Sciences of the United States of America*, 103(41), pp. 15044–15049. doi: 10.1073/pnas.0607129103.
- Moore, P. A., Bettany, A. J. E. and Brown, A. J. P. (1990) 'Multiple copies of the pyruvate kinase gene affect yeast cell growth', *Journal of General Microbiology*, 136(12), pp. 2359–2366. doi: 10.1099/00221287-136-12-2359.
- Morita, T. *et al.* (2015) 'Mannosylerythritol lipids: Production and applications', *Journal of Oleo Science*, 64(2), pp. 133–141. doi: 10.5650/jos.ess14185.
- Moser, M. J. *et al.* (1997) 'The proofreading domain of escherichia coli DNA polymerase I and other DNA and/or RNA exonuclease domains', *Nucleic Acids Research*, 25(24), pp. 5110–5118. doi: 10.1093/nar/25.24.5110.
- Motley, A. M., Nuttall, J. M. and Hettema, E. H. (2012) 'Pex3-anchored Atg36 tags peroxisomes for degradation in *Saccharomyces cerevisiae*', *EMBO Journal*. Nature Publishing Group, 31(13), pp. 2852–2868. doi: 10.1038/emboj.2012.151.
- Mühlhofer, M. *et al.* (2019) 'The Heat Shock Response in Yeast Maintains Protein Homeostasis by Chaperoning and Replenishing Proteins', *Cell Reports*, 29(13), pp. 4593-4607.e8. doi: 10.1016/j.celrep.2019.11.109.
- Murray, L. E. *et al.* (1998) 'A yeast glutamine tRNA signals nitrogen status for regulation of dimorphic growth and sporulation', *Proceedings of the National Academy of Sciences of the United States of America*, 95(15), pp. 8619–8624. doi: 10.1073/pnas.95.15.8619.
- Myer, V.E. and Young, R.A., (1998) 'RNA polymerase II holoenzymes and subcomplexes.' *Journal of Biological Chemistry*, 273(43), pp.27757-27760. DOI: 10.1074/jbc.273.43.27757
- Nardozi, J. D., Lott, K. and Cingolani, G. (2010) 'Phosphorylation meets nuclear import: A review', *Cell Communication and Signaling*. BioMed Central Ltd, 8(1), p. 32. doi: 10.1186/1478-811X-8-32.
- Neumeier, J., & Meister, G. (2021). siRNA specificity: RNAi mechanisms and strategies to reduce off-target effects. *Frontiers in Plant Science*, 11, 526455. DOI: 10.3389/fpls.2020.526455
- Nichols, M., Söll, D. and Willis, I. (1988) 'Yeast RNase P: catalytic activity and substrate binding are separate functions.', *Proceedings of the National Academy of Sciences of the United States of America*, 85(5), pp. 1379–1383. doi: 10.1073/pnas.85.5.1379.
- Niosi, J. (2003) 'Alliances are not enough explaining rapid growth in biotechnology firms', *Research Policy*, 32(5), pp. 737–750. doi: 10.1016/S0048-7333(02)00083-5.
- Niu, Y. *et al.* (2019) 'Production and characterization of a new glycolipid, mannosylerythritol lipid, from waste cooking oil biotransformation by *Pseudozyma aphidis* ZJUDM34', *Food Science and Nutrition*, 7(3), pp. 937–948. doi: 10.1002/fsn3.880.
- Northcote, D.H. and Horne, R.W., 1952. The chemical composition and structure of the yeast cell wall. *Biochemical Journal*, 51(2), p.232.
- Ogden, J. E. *et al.* (1986) 'Efficient expression of the *Saccharomyces cerevisiae* PGK gene depends on an upstream activation sequence but does not require TATA sequences.', *Molecular and Cellular Biology*, 6(12), pp. 4335–4343. doi: 10.1128/mcb.6.12.4335.

Oliveira, H. C. D., Bernardes, N. E., Fukuda, C. A., Silva, T. D., Barros, A. C. D., Dreyer, T. R., ... & Bertolini, M. C. Comparative study of the interactions between fungal transcription factor NIT-2 with mammalian and fungal Importin-alpha. DOI: 10.1038/s41598-020-58316-9

Oshima, Y. (1997) 'The phosphatase system in *Saccharomyces cerevisiae*', *Genes and Genetic Systems*, 72(6), pp. 323–334. doi: 10.1266/ggs.72.323.

Otsubo, Y., Kamada, Y. and Yamashita, A. (2020) 'Novel links between TORC1 and traditional non-coding RNA, tRNA', *Genes*, 11(9), pp. 1–11. doi: 10.3390/genes11090956.

Ozanick, S. G. *et al.* (2009) 'Rex1p deficiency leads to accumulation of precursor initiator tRNA^{Met} and polyadenylation of substrate RNAs in *Saccharomyces cerevisiae*', *Nucleic Acids Research*, 37(1), pp. 298–308. doi: 10.1093/nar/gkn925.

Panesar, P. S. *et al.* (2016) 'Bio-processing of agro-industrial wastes for production of food-grade enzymes: Progress and prospects', *Applied Food Biotechnology*, 3(4), pp. 208–227. doi: 10.22037/afb.v3i4.13458.

Pannone, B. K., Xue, D. and Wolin, S. L. (1998) 'A role for the yeast La protein in U6 snRNP assembly: Evidence that the La protein is a molecular chaperone for RNA polymerase III transcripts', *EMBO Journal*, 17(24), pp. 7442–7453. doi: 10.1093/emboj/17.24.7442.

Parker, M. B. and R. (2007) 'Accumulation of Polyadenylated mRNA, Pab1p, eIF4E, and eIF4G with P-Bodies in *Saccharomyces cerevisiae*', *Molecular biology of the cell*, 18(December), pp. 986–994. doi: 10.1091/mbc.E06.

Peng, B. *et al.* (2015) 'Controlling heterologous gene expression in yeast cell factories on different carbon substrates and across the diauxic shift: A comparison of yeast promoter activities', *Microbial Cell Factories*. BioMed Central, 14(1), pp. 1–11. doi: 10.1186/s12934-015-0278-5.

Phillips, E., Ahmad, N., Sun, L., Iben, J., Walkey, C. J., Rusin, A., ... & Johnson, D. L. (2022). MAF1, a repressor of RNA polymerase III-dependent transcription, regulates bone mass. *Elife*, 11, e74740. DOI: 10.7554/eLife.74740

Phizicky, E. M. and Hopper, A. K. (2010) 'tRNA biology charges to the front', *Genes and Development*, 24(17), pp. 1832–1860. doi: 10.1101/gad.1956510.

Pickart, C.M., 2001. Mechanisms underlying ubiquitination. *Annual review of biochemistry*, 70(1), pp.503-533.

Pierce, J. B., van der Merwe, G. and Mangroo, D. (2014) 'Protein kinase a is part of a mechanism that regulates nuclear reimport of the nuclear tRNA export receptors Los1p and Msn5p', *Eukaryotic Cell*, 13(2), pp. 209–230. doi: 10.1128/EC.00214-13.

Piper, P. W., Bellatin, J. A. and Lockheart, A. (1983) 'Altered maturation of sequences at the 3' terminus of 5S gene transcripts in a *Saccharomyces cerevisiae* mutant that lacks a RNA processing endonuclease.', *The EMBO journal*, 2(3), pp. 353–359. doi: 10.1002/j.1460-2075.1983.tb01430.x.

Pluta, K. *et al.* (2001) ' Maf1p, a Negative Effector of RNA Polymerase III in *Saccharomyces cerevisiae* ', *Molecular and Cellular Biology*, 21(15), pp. 5031–5040. doi: 10.1128/mcb.21.15.5031-5040.2001.

Popken, P. *et al.* (2015) 'Size-dependent leak of soluble and membrane proteins through the yeast nuclear pore complex', *Molecular Biology of the Cell*, 26(7), pp. 1386–1394. doi: 10.1091/mbc.E14-07-1175.

- Powers, T. and Walter, P. (1999) 'Regulation of ribosome biogenesis by the rapamycin-sensitive TOR-signaling pathway in *Saccharomyces cerevisiae*', *Molecular Biology of the Cell*, 10(4), pp. 987–1000. doi: 10.1091/mbc.10.4.987.
- Quan, X. X. *et al.* (2007) 'The localization of nuclear exporters of the importin- β family is regulated by Snf1 kinase, nutrient supply and stress', *Biochimica et Biophysica Acta - Molecular Cell Research*, 1773(7), pp. 1052–1061. doi: 10.1016/j.bbamcr.2007.04.014.
- Lemieux, R.U., Thorn, J.A., Brice, C. and Haskins, R.H., 1951. Biochemistry of the ustilaginales: II. Isolation and partial characterization of ustilagic acid. *Canadian Journal of Chemistry*, 29(5), pp.409-414.
- Rau, U. *et al.* (2005) 'Formation and analysis of mannosylerythritol lipids secreted by *Pseudozyma aphidis*', *Applied Microbiology and Biotechnology*, 66(5), pp. 551–559. doi: 10.1007/s00253-004-1672-9.
- Redden, H. and Alper, H. S. (2015) 'The development and characterization of synthetic minimal yeast promoters', *Nature Communications*. Nature Publishing Group, 6, pp. 1–9. doi: 10.1038/ncomms8810.
- Riddick, G. and Macara, I. G. (2005) 'A systems analysis of importin- α - β mediated nuclear protein import', *Journal of Cell Biology*, 168(7), pp. 1027–1038. doi: 10.1083/jcb.200409024.
- Ro, D. K. *et al.* (2008) 'Induction of multiple pleiotropic drug resistance genes in yeast engineered to produce an increased level of anti-malarial drug precursor, artemisinin acid', *BMC Biotechnology*, 8, pp. 1–14. doi: 10.1186/1472-6750-8-83.
- Roberts, D. N. *et al.* (2006) 'Dephosphorylation and Genome-Wide Association of Maf1 with Pol III-Transcribed Genes during Repression', *Molecular Cell*, 22(5), pp. 633–644. doi: 10.1016/j.molcel.2006.04.009.
- Roelants, S. L. K. W. *et al.* (2014) 'Biosurfactant gene clusters in eukaryotes: Regulation and biotechnological potential', *Applied Microbiology and Biotechnology*, 98(8), pp. 3449–3461. doi: 10.1007/s00253-014-5547-4.
- Rokas, A., Mead, M. E., Steenwyk, J. L., Raja, H. A., & Oberlies, N. H. (2020). Biosynthetic gene clusters and the evolution of fungal chemodiversity. *Natural product reports*, 37(7), 868-878. doi: 10.1039/c9np00045c
- Romanos, M.A., Scorer, C.A. and Clare, J.J., 1992. Foreign gene expression in yeast: a review. *Yeast*, 8(6), pp.423-488.
- Rudt, F. and Pieler, T. (1996) 'Cytoplasmic retention and nuclear import of 5S ribosomal RNA containing RNPs', *EMBO Journal*, 15(6), pp. 1383–1391. doi: 10.1002/j.1460-2075.1996.tb00480.x.
- Saheki, T., Matsuda, Y. and Holzer, H., 1974. Purification and characterization of macromolecular inhibitors of proteinase A from yeast. *European Journal of Biochemistry*, 47(2), pp.325-332.
- Saika, A. *et al.* (2016) 'A gene cluster for biosynthesis of mannosylerythritol lipids consisted of 4-O- β -D-Mannopyranosyl-(2R,3S)-Erythritol as the sugar moiety in a basidiomycetous yeast *Pseudozyma tsukubaensis*', *PLoS ONE*, 11(6), pp. 1–16. doi: 10.1371/journal.pone.0157858.
- Saika, A. *et al.* (2018) 'Biosynthesis of mono-acylated mannosylerythritol lipid in an acyltransferase gene-disrupted mutant of *Pseudozyma tsukubaensis*', *Applied Microbiology and Biotechnology*. 102(4), pp. 1759–1767. doi: 10.1007/s00253-017-8698-2.

- Santos, D. K. F. *et al.* (2016) 'Biosurfactants: Multifunctional biomolecules of the 21st century', *International Journal of Molecular Sciences*, 17(3), pp. 1–31. doi: 10.3390/ijms17030401.
- Schillewaert, S., Wacheul, L., Lhomme, F., & Lafontaine, D. L. (2011). The evolutionarily conserved protein Las1 is required for pre-rRNA processing at both ends of ITS2. *Molecular and cellular biology*. doi: 10.1128/MCB.06019-11
- Schmelzle, T. and Hall, M. N. (2000) 'TOR, a central controller of cell growth', *Cell*, 103(2), pp. 253–262. doi: 10.1016/S0092-8674(00)00117-3.
- Schmidt, K. and Butler, J. S. (2013) 'Nuclear RNA surveillance: Role of TRAMP in controlling exosome specificity', *Wiley Interdisciplinary Reviews: RNA*, 4(2), pp. 217–231. doi: 10.1002/wrna.1155.
- Shatkin, A. J. and Manley, J. L. (2000) 'The ends of the affair: Capping and polyadenylation', *Nature Structural Biology*, 7(10), pp. 838–842. doi: 10.1038/79583.
- Shen, L. *et al.* (2019) 'Isolation and purification of biosurfactant mannosylerythritol lipids from fermentation broth with methanol/water/n-hexane', *Separation and Purification Technology*. Elsevier, 219(February), pp. 1–8. doi: 10.1016/j.seppur.2019.03.009.
- Shenton, D. *et al.* (2006) 'Global translational responses to oxidative stress impact upon multiple levels of protein synthesis', *Journal of Biological Chemistry*. © 2006 ASBMB. Currently published by Elsevier Inc; originally published by American Society for Biochemistry and Molecular Biology., 281(39), pp. 29011–29021. doi: 10.1074/jbc.M601545200.
- Shore, D., Zencir, S. and Albert, B. (2021) 'Transcriptional control of ribosome biogenesis in yeast: Links to growth and stress signals', *Biochemical Society Transactions*, 49(4), pp. 1589–1599. doi: 10.1042/BST20201136.
- Shore, D. and Albert, B. (2022) 'Ribosome biogenesis and the cellular energy economy', *Current Biology*. Elsevier, 32(12), pp. R611–R617. doi: 10.1016/j.cub.2022.04.083.
- Siddiqui, M. S. *et al.* (2012) 'Advancing secondary metabolite biosynthesis in yeast with synthetic biology tools', *FEMS Yeast Research*, 12(2), pp. 144–170. doi: 10.1111/j.1567-1364.2011.00774.x.
- Sidorova, J. M., Mikesell, G. E. and Breeden, L. L. (1995) 'Cell cycle-regulated phosphorylation of Swi6 controls its nuclear localization', *Molecular Biology of the Cell*, 6(12), pp. 1641–1658. doi: 10.1091/mbc.6.12.1641.
- Silva, R. de C. F. S. *et al.* (2014) 'Applications of biosurfactants in the petroleum industry and the remediation of oil spills', *International Journal of Molecular Sciences*, 15(7), pp. 12523–12542. doi: 10.3390/ijms150712523.
- Skowronek, Ewa, *et al.* "tRNA 3' processing in yeast involves tRNase Z, Rex1, and Rrp6." *Rna* 20.1 (2013): 115-130.
- Skowronek, E. *et al.* (2014) 'TRNA 3' processing in yeast involves tRNase Z, Rex1, and Rrp6', *Rna*, 20(1), pp. 115–130. doi: 10.1261/rna.041467.113.
- Smirnov, A. *et al.* (2008) 'Two distinct structural elements of 5S rRNA are needed for its import into human mitochondria', *Rna*, 14(4), pp. 749–759. doi: 10.1261/rna.952208.
- Solsbacher, J. *et al.* (1998) 'Cse1p Is Involved in Export of Yeast Importin α from the Nucleus', *Molecular and Cellular Biology*, 18(11), pp. 6805–6815. doi: 10.1128/mcb.18.11.6805.

- Souza-Moreira, T. M. *et al.* (2018) 'Screening of 2A peptides for polycistronic gene expression in yeast', *FEMS Yeast Research*, 18(5), pp. 1–9. doi: 10.1093/femsyr/foy036.
- Spoeckner, S. *et al.* (1999) 'Glycolipids of the smut fungus *Ustilago maydis* from cultivation on renewable resources', *Applied Microbiology and Biotechnology*, 51(1), pp. 33–39. doi: 10.1007/s002530051359.
- Stochaj, U., Rassadi, R. and Chiu, J. (2000) 'Stress-mediated inhibition of the classical nuclear protein import pathway and nuclear accumulation of the small GTPase Gsp1p', *The FASEB Journal*, 14(14), pp. 2130–2132. doi: 10.1096/fj.99-0751fje.
- Suzuki, T. (2021). The expanding world of tRNA modifications and their disease relevance. *Nature Reviews Molecular Cell Biology*, 22(6), 375–392. DOI: 10.1038/s41580-021-00342-0
- Szymański, M. *et al.* (2003) '5 S rRNA: Structure and interactions', *Biochemical Journal*, 371(3), pp. 641–651. doi: 10.1042/BJ20020872.
- Tabb, M. M. *et al.* (2000) 'Evidence for Separable Functions of Srp1p, the Yeast Homolog of Importin α (Karyopherin α): Role for Srp1p and Sts1p in Protein Degradation', *Molecular and Cellular Biology*, 20(16), pp. 6062–6073. doi: 10.1128/mcb.20.16.6062-6073.2000.
- Takaku, H. *et al.* (2003) 'A candidate prostate cancer susceptibility gene encodes tRNA 3' processing endoribonuclease', *Nucleic Acids Research*, 31(9), pp. 2272–2278. doi: 10.1093/nar/gkg337.
- Takemura, R., Inoue, Y. and Izawa, S. (2004) 'Stress response in yeast mRNA export factor: Reversible changes in Rat8p localization are caused by ethanol stress but not heat shock', *Journal of Cell Science*, 117(18), pp. 4189–4197. doi: 10.1242/jcs.01296.
- Tamura, K. (1994) 'The role of the CCA sequence of tRNA in the peptidyl transfer reaction', *FEBS Letters*, 353(2), pp. 173–176. doi: 10.1016/0014-5793(94)01038-2.
- Teichmann, B. *et al.* (2011) 'Identification of a biosynthesis gene cluster for flocculosin a cellobiose lipid produced by the biocontrol agent *Pseudozyma flocculosa*', *Molecular Microbiology*, 79(6), pp. 1483–1495. doi: 10.1111/j.1365-2958.2010.07533.x.
- Teichmann, B. *et al.* (2007) 'A biosynthetic gene cluster for a secreted cellobiose lipid with antifungal activity from *Ustilago maydis*', *Molecular Microbiology*, 66(2), pp. 525–533. doi: 10.1111/j.1365-2958.2007.05941.x.
- Teichmann, B. *et al.* (2010) 'Activation of the ustilagic acid biosynthesis gene cluster in *Ustilago maydis* by the C2H2 zinc finger transcription factor *rual* ∇ ', *Applied and Environmental Microbiology*, 76(8), pp. 2633–2640. doi: 10.1128/AEM.02211-09.
- Thiaville, P. C., Legendre, R., Rojas-Benítez, D., Baudin-Baillieu, A., Hatin, I., Chalancon, G., ... & de Crécy-Lagard, V. (2016). Global translational impacts of the loss of the tRNA modification t6A in yeast. *Microbial cell*, 3(1), 29. doi: 10.15698/mic2016.01.473
- Thomson, E., & Tollervey, D. (2010). The final step in 5.8 S rRNA processing is cytoplasmic in *Saccharomyces cerevisiae*. *Molecular and cellular biology*, 30(4), 976–984. doi: 10.1128/MCB.01359-09
- Thongdee, N., Jaroensuk, J., Atichartpongkul, S., Chittrakanwong, J., Chooyoung, K., Srimahaeak, T., ... & Fuangthong, M. (2019). TrmB, a tRNA m7G46 methyltransferase, plays a role in hydrogen peroxide

resistance and positively modulates the translation of *katA* and *katB* mRNAs in *Pseudomonas aeruginosa*. *Nucleic acids research*, 47(17), 9271-9281. DOI: 10.1093/nar/gkz702

Thumm, M. and Wolf, D. H. (1998) 'From Proteasome to Lysosome: Studies on Yeast Demonstrate the Principles Of Protein Degradation in the Eukaryote Cell', *Advances in Molecular and Cell Biology*, 27(C), pp. 43–70. doi: 10.1016/S1569-2558(08)60457-9.

Torchet, C. and Hermann-Le Denmat, S. (2000) 'Bypassing the rRNA processing endonucleolytic cleavage at site A2 in *Saccharomyces cerevisiae*', *Rna*, 6(11), pp. 1498–1508. doi: 10.1017/S1355838200000558.

Towpik, Joanna, et al. "Derepression of RNA polymerase III transcription by phosphorylation and nuclear export of its negative regulator, Maf1." *Journal of Biological Chemistry* 283.25 (2008): 17168-17174.

Tracy, R. L. and Stern, D. B. (1995) 'Mitochondrial transcription initiation: promoter structures and RNA polymerases', *Current Genetics*, 28(3), pp. 205–216. doi: 10.1007/BF00309779.

Ullman, K. S., Powers, M. A. and Forbes, D. J. (1997) 'Nuclear export receptors: From importin to exportin', *Cell*, 90(6), pp. 967–970. doi: 10.1016/S0092-8674(00)80361-X.

Van Bogaert, I. N. A. *et al.* (2013) 'The biosynthetic gene cluster for sophorolipids: A biotechnological interesting biosurfactant produced by *Starmerella bombicola*', *Molecular Microbiology*, 88(3), pp. 501–509. doi: 10.1111/mmi.12200.

Van Hoof, A., Lennertz, P. and Parker, R. (2000) 'Three conserved members of the RNase D family have unique and overlapping functions in the processing of 5S, 5.8S, U4, U5. RNase MRP and RNase P RNAs in yeast', *EMBO Journal*, 19(6), pp. 1357–1365. doi: 10.1093/emboj/19.6.1357.

Verwaal, R. *et al.* (2007) 'High-level production of beta-carotene in *Saccharomyces cerevisiae* by successive transformation with carotenogenic genes from *Xanthophyllomyces dendrorhous*', *Applied and Environmental Microbiology*, 73(13), pp. 4342–4350. doi: 10.1128/AEM.02759-06.

Voges, D., Zwickl, P. and Baumeister, W., 1999. The 26S proteasome: a molecular machine designed for controlled proteolysis. *Annual review of biochemistry*, 68(1), pp.1015-1068. doi: 10.1146/annurev.biochem.68.1.1015

Vorländer, M. K., Khatter, H., Wetzl, R., Hagen, W. J., & Müller, C. W. (2018). Molecular mechanism of promoter opening by RNA polymerase III. *Nature*, 553(7688), 295-300. DOI: 10.1038/nature25440

Vorländer, M. K., Baudin, F., Moir, R. D., Wetzl, R., Hagen, W. J., Willis, I. M., & Müller, C. W. (2020). Structural basis for RNA polymerase III transcription repression by Maf1. *Nature structural & molecular biology*, 27(3), 229-232. DOI: 10.1038/s41594-020-0383-y

Waite KA, Roelofs J. Proteasome granule formation is regulated through mitochondrial respiration and kinase signaling. *J Cell Sci*. 2022 Sep 1;135(17):jcs259778. doi: 10.1242/jcs.259778. Epub 2022 Sep 7. PMID: 35975718; PMCID: PMC9482347. doi: 10.1242/jcs.259778

Wallace, E. W., Kear-Scott, J. L., Pilipenko, E. V., Schwartz, M. H., Laskowski, P. R., Rojek, A. E., ... & Drummond, D. A. (2015). Reversible, specific, active aggregates of endogenous proteins assemble upon heat stress. *Cell*, 162(6), 1286-1298.

Warner JR (1999) 'The economics of ribosome biosynthesis in yeast', *Trends in Biochemical Sciences*, 24(11), pp. 437–440. Available at: [https://doi.org/10.1016/S0968-0004\(99\)01460-7](https://doi.org/10.1016/S0968-0004(99)01460-7).

- Wei, Y., Tsang, C. K. and Zheng, X. F. S. (2009) 'Mechanisms of regulation of RNA polymerase III-dependent transcription by TORC1', *EMBO Journal*. Nature Publishing Group, 28(15), pp. 2220–2230. doi: 10.1038/emboj.2009.179.
- Wei, Y. and Zheng, X. F. S. (2009) 'Sch9 partially mediates TORC1 signaling to control ribosomal RNA synthesis', *Cell Cycle*, 8(24), pp. 4085–4090. doi: 10.4161/cc.8.24.10170.
- Wells, S. E. *et al.* (1998) 'Circularization of mRNA by eukaryotic translation initiation factors', *Molecular Cell*, 2(1), pp. 135–140. doi: 10.1016/S1097-2765(00)80122-7.
- Wells, G. R., Weichmann, F., Colvin, D., Sloan, K. E., Kudla, G., Tollervey, D., ... & Schneider, C. (2016). The PIN domain endonuclease Utp24 cleaves pre-ribosomal RNA at two coupled sites in yeast and humans. *Nucleic acids research*, 44(11), 5399-5409. DOI: 10.1093/nar/gkw645
- Whitney, M.L., Hurto, R.L., Shaheen, H.H. and Hopper, A.K., 2007. Rapid and reversible nuclear accumulation of cytoplasmic tRNA in response to nutrient availability. *Molecular biology of the cell*, 18(7), pp.2678-2686.
- Wilusz, J. E. *et al.* (2011) 'tRNAs marked with CCACCA are targeted for degradation', *Science*, 334(6057), pp. 817–821. doi: 10.1126/science.1213671.
- Winkler, A., Arkind, C., Mattison, C. P., Burkholder, A., Knoche, K., & Ota, I. (2002). Heat stress activates the yeast high-osmolarity glycerol mitogen-activated protein kinase pathway, and protein tyrosine phosphatases are essential under heat stress. *Eukaryotic cell*, 1(2), 163-173.
- Wittrup, K. D. *et al.* (1994) 'Existence of an optimum expression level for secretion of foreign proteins in yeast', *Annals of the New York Academy of Sciences*, 745, pp. 321–330. doi: 10.1111/j.1749-6632.1994.tb44385.x.
- Wolin, S. L. and Cedervall, T. (2002) 'The La Protein', pp. 375–403. doi: 10.1146/annurev.biochem.Copyright.
- Wood, D. J. and Endicott, J. A. (2018) 'Structural insights into the functional diversity of the CDK–cyclin family', *Open Biology*, 8(9). doi: 10.1098/rsob.180112.
- Woolford, J. L. and Baserga, S. J. (2013) 'Ribosome biogenesis in the yeast *Saccharomyces cerevisiae*', *Genetics*, 195(3), pp. 643–681. doi: 10.1534/genetics.113.153197.
- Yamamoto, S. *et al.* (2012) 'The moisturizing effects of glycolipid biosurfactants, mannosylerythritol lipids, on human skin', *Journal of Oleo Science*, 61(7), pp. 407–412. doi: 10.5650/jos.61.407.
- Yamanishi, M. *et al.* (2013) 'A genome-wide activity assessment of terminator regions in *saccharomyces cerevisiae* provides a "terminatome" toolbox', *ACS Synthetic Biology*, 2(6), pp. 337–347. doi: 10.1021/sb300116y.
- Yan, Q., Zhu, C., Guang, S., & Feng, X. (2019). The functions of non-coding RNAs in rRNA regulation. *Frontiers in Genetics*, 10, 290. DOI: 10.3389/fgene.2019.00290
- Yang, J. and Yang, Y. (2012) 'Plasmid size can affect the ability of *Escherichia coli* to produce high-quality plasmids', *Biotechnology Letters*, 34(11), pp. 2017–2022. doi: 10.1007/s10529-012-0994-4.
- Yoo, C. J. and Wolin, S. L. (1997) 'The yeast La protein is required for the 3' endonucleolytic cleavage that matures tRNA precursors', *Cell*, 89(3), pp. 393–402. doi: 10.1016/S0092-8674(00)80220-2.

Zavala-Moreno, Ariana, et al. "Nitrogen source affects glycolipid production and lipid accumulation in the phytopathogen fungus *Ustilago maydis*." *Advances in Microbiology* 4.13 (2014): 934. DOI: 10.4236/aim.2014.413104

Zhou, X., Li, W., Liu, Y., & Amon, A. (2021). Cross-compartment signal propagation in the mitotic exit network. *Elife*, 10, e63645. DOI: 10.7554/eLife.63645

Zuo, Y. and Deutscher, M. P. (2001) 'Exoribonuclease superfamilies: Structural analysis and phylogenetic distribution', *Nucleic Acids Research*, 29(5), pp. 1017–1026. doi: 10.1093/nar/29.5.1017.